

**Palaeoecological and palaeoclimatological  
implications of the Eocene Northern Hemisphere  
*Azolla* phenomenon**

**Judith Barke**

LPP Foundation 2010

Judith Barke  
Palaeoecology and Biomarine Sciences  
Institute of Environmental Biology (IEB)  
Faculty of Science  
Utrecht University

Laboratory of Palaeobotany and Palynology  
Budapestlaan 4  
3584 CD Utrecht  
The Netherlands

J.Barke@uu.nl  
judithbarke@gmail.com

ISBN: 978-90-393-5466-7  
NSG publication No. 20101101  
LPP Contributions Series No. 32

Cover design by Leonard Bik  
Printed by Wöhrmann Print Service, Zutphen

**Palaeoecological and palaeoclimatological  
implications of the Eocene Northern Hemisphere  
*Azolla* phenomenon**

Palaeoecologische en palaeoclimatologische implicaties  
van het Eocene *Azolla* fenomeen op het noordelijk  
halfmond

(met een samenvatting in het Nederlands)

**Proefschrift**

ter verkrijging van de graad van doctor aan de Universiteit Utrecht op gezag van  
de rector magnificus, prof. dr. J.C. Stoof, ingevolge het besluit van het college  
voor promoties in het openbaar te verdedigen op woensdag 1 december 2010  
des middags te 12.45 uur

*door*

**Judith Barke**

geboren op 28 April 1979 te Mayen (Duitsland)

**Promotoren:** Prof. dr. A. F. Lotter  
Prof. dr. H. Brinkhuis

**Co-promotoren:** Dr. J.H.A. van Konijnenburg- van Cittert  
Dr. J. van der Burgh

The research presented in this thesis was carried out at the Laboratory of Palaeobotany and Palynology, in the groups of Biomarine Sciences en Palaeoecology within the Institute of Environmental Biology (IEB), Utrecht University, The Netherlands. The Research was funded by the Darwin Centre for Biogeosciences and financially supported by the LPP Foundation. Additional financial support was provided by Statoil.



**Members of the dissertation committee:**

Prof. dr. Margaret Collinson  
Department of Earth Sciences  
Royal Holloway University of London  
United Kingdom

Prof. dr. Jack Middelburg  
Department of Earth Sciences  
Utrecht University  
The Netherlands

Prof. dr. ir. Jaap Sinninghe Damsté  
Department of Marine Organic Biogeochemistry  
Royal Netherlands Institute for Sea Research  
The Netherlands

Prof. dr. Jan Roelofs  
Department of Aquatic Ecology and Environmental Biology,  
Institute for Water and Wetland Research,  
Radboud University Nijmegen.  
The Netherlands

Prof. dr. Ellen van Donk  
Department of Biology  
Utrecht University  
The Netherlands

# Contents

Chapter 1	General introduction and synopsis	9
Chapter 2	<b>The Eocene Arctic <i>Azolla</i> bloom: environmental conditions, productivity and carbon drawdown</b>	21
	Speelman, E.N., van Kempen, M.M.L., Barke, J., Brinkhuis, H., Reichart, G.J., Smolders, F.J., Roelofs, J.G.M., Sangiorgi, F., de Leeuw, J.W., Lotter, A.F., Sinninghe Damsté, J.S.	
	<i>Geobiology 7, 155-170, 2009</i>	
Chapter 3	<b>Orbitally-forced <i>Azolla</i> blooms and middle Eocene Arctic hydrology: clues from palynology</b>	47
	Barke, J., Abels, H.A., Sangiorgi, F., Greenwood, D.R., Sweet, A.R., Donders, T., Reichart, G.J., Lotter, A.F., and Brinkhuis, H.	
	<i>Geology, accepted manuscript</i>	
Chapter 4	<b>Obliquity-forced middle Eocene Arctic hydrology – A micropaleontological and cyclostratigraphical approach</b>	59
	Barke, J., Sangiorgi, F., Abels, H.A., Stickley, C.E., Reichart, G.J., Lotter, A.F., and Brinkhuis, H.	
	<i>To be submitted</i>	
Chapter 5	<b>A new species of the freshwater fern <i>Azolla</i> (Azollaceae) from the Eocene Arctic Ocean</b>	83
	Collinson, M.E., Barke, J., van der Burgh, J., and van Konijnenburg-van Cittert, J.H.A.	
	<i>Review of Palaeobotany and Palynology 155, 1-14, 2009</i>	
Chapter 6	<b>Did a single species of Eocene <i>Azolla</i> spread from the Arctic Basin to the southern North Sea?</b>	107
	Collinson, M.E., Barke, J., van der Burgh, J., van Konijnenburg-van Cittert, J.H.A., Heilmann-Clausen, C., Howard, L.E., and Brinkhuis, H.	
	<i>Review of Palaeobotany and Palynology 159, 152-165, 2010</i>	
Chapter 7	<b>Coeval Eocene blooms of multiple species of the fresh water fern <i>Azolla</i> in and around the Arctic and Nordic Seas</b>	137
	Barke, J., van der Burgh, J., van Konijnenburg-van Cittert, J.H.A., Collinson, M.E., Pearce, M.A., Bujak, J., Heilmann-Clausen, C., Speelman, E.N., van Kempen, M.M.L., Reichart, G.J., Lotter, A.F., and Brinkhuis, H.	
	<i>To be submitted</i>	

References	159
Algemene inleiding en samenvatting	171
Acknowledgments	181
Curriculum Vitae	185



# Chapter 1

## **General introduction and synopsis**

Enormous numbers of remains of the free-floating freshwater fern *Azolla* were recovered from early middle Eocene (~49 Ma) central Arctic Ocean sediments drilled at the Lomonosov Ridge during the Arctic coring expedition (ACEX; or Integrated Ocean Drilling Program, IODP, Expedition 302; Backman et al., 2006; Brinkhuis et al., 2006). The co-occurrence of different life stages and reproductive parts of *Azolla* and the absence of land plant detritus in the ACEX sediments, suggests that this floating fern grew and reproduced *in situ* on the Arctic Ocean surface (Brinkhuis et al., 2006). These and associated findings imply the episodic presence of sustained fresh surface waters, strong stratification, and bottom water anoxia (Brinkhuis et al., 2006; Onodera et al., 2008; Stein et al., 2006; Stickley et al., 2008; Waddell and Moore, 2008). In addition, early middle Eocene *Azolla* occurrences were reported from marine sediments in wide-ranging areas of the Arctic Ocean, Labrador Sea and Norwegian-Greenland Sea to North Sea (Brinkhuis et al., 2006). Despite the knowledge of these widespread *Azolla* occurrences in marine deposits, no particular attention has been given to the extent, cause and implications of this unique phenomenon.

## 1.1 What is *Azolla*?

*Azolla*, also known as water fern, mosquito fern, duckweed fern or fairy moss, is a small aquatic fern that has a worldwide distribution from temperate to tropical climates (van Hove and Lejeune, 2002). *Azolla* belongs to the division of Pteridophyta and is the only genus in the family Azollaceae. Seven extant species of *Azolla* are known, which are allocated in two taxonomic sections: the section Euazolla includes the species *A. filiculoides*, *A. rubra*, *A. mexicana*, *A. caroliniana*, and *A. microphylla*, while the section Rhizosperma includes the species *A. pinnata* and *A. nilotica* (Saunders and Fowler, 1993; van Hove and Lejeune, 2002). Over fifty fossil species of *Azolla* are described, the oldest dating back to the mid to late Cretaceous (Collinson, 1980; Collinson, 2001; Collinson, 2002).

### 1.1.1 Morphology

*Azolla* is a free-floating plant, which rarely exceeds 3 to 4 cm in size (except for the species *A. nilotica*, which can grow up to 15 cm or more). This plant consists of pinnately branched, horizontally floating stems, which bear long adventitious roots along the underside. On the upper side they bear small, alternately arranged, overlapping leaves (Fig. 1). Each leaf is divided into two lobes; the thicker dorsal lobe is aerial and chlorophyllous, whereas the thinner ventral lobe is partially submerged, colorless and cup-shaped and provides buoyancy (van Hove and Lejeune, 2002; Wagner, 1997). Under certain conditions, including phosphorus deficiency, very high insolation, or low winter temperature, the color of the leaves change from green to red caused by the production of anthocyanins (red plant pigment) within the

photosynthetic tissue. Reddening of the leaves enables the plant to avoid light damage to the photosynthetic tissue (Janes, 1998a).

The morphology and physiology of *Azolla* is plastic, which enables this fresh water plant to compete in a wider range of habitats. Three phenotypes are identified (Janes, 1998a):

i) The *survival form* is typical of red winter plants. Plants are small, barely branching and very slow-growing.

ii) The *colonizing form* grows most rapidly and is found under spring and summer conditions. This form is typical of plants in open water where space is not limiting. Plants are, green, compact and grow flat on the water surface (up to a monolayer).

iii) The *mat form*. This form is found in thick, well-established mats (greater than a monolayer) from mid to late summer. Plants are green and interlocking. In these mats growth rates are lower than for the colonizing form, but extensive sporulation is common.

These three phenotypes can rapidly interchange within a few weeks if the external environment is altered (Janes, 1998a).



**Fig. 1.** a) monolayer of *Azolla filiculoides* with reddened leaves (picture courtesy A. F. Lotter). b) multiple-layer mat of *A. filiculoides* (picture courtesy M. M. L. van Kempen).

### 1.1.2 Growth and reproduction

The small size of *Azolla* plants enables rapid growth and colonization of water bodies by means of vegetative reproduction (Saunders and Fowler, 1993), reaching doubling times of as little as 5 days (Janes, 1998a). Vegetative reproduction is by far the most common means of reproduction and consists of multiplication by simple fragmentation of the fronds (Wagner, 1997). The sexual reproductive cycle is somewhat more complex (Fig. 2). *Azolla* is a heterosporous fern, meaning that it produces two kinds of spores, micro- and megaspores, which develop in micro- and megasporangia. These sporangia are developed in separate micro- and megasporocarps, both developing at the same individual plant (Saunders and Fowler, 1993). The megasporocarps each produce a single megasporangium, bearing a single megaspore apparatus, which consists of one megaspore (distal) and proximal a number of so-called floats (they were thought to let function as a swimming apparatus for the megaspore, but this is not the case). The megaspore apparatus is usually covered with tangled filaments (filosum). The microsporocarps produce up to 130 microsporangia, each containing 32 or 64 microspores aggregated into 3-10 spongy fragments called massulae (van Hove and Lejeune, 2002; Wagner, 1997). At maturity the microsporangia break open and release the massulae into the water. By means of their hair-like appendages (glochidia), they entangle with the filosum on the megasporocarps. Together they sink to the bottom of the water body, where they remain until germination (Janes, 1998b). It is not yet well-understood which environmental conditions induce *Azolla* to reproduce sexually. However, increased plant density, enhanced phosphate concentrations, and adverse winter temperatures are factors believed to be involved in stimulating sexual reproduction in *Azolla* (Janes, 1998a, b).

### 1.1.3 The *Azolla*-*Anabaena*-Bacteria association

*Azolla* contains a permanent endosymbiotic prokaryotic community (cyanobacteria and bacteria) living inside the cavity of the leaf dorsal lobe of the plant (Carrapiço, 1991; Peters and Mayne, 1974). During the life-cycle of *Azolla* the symbionts are transferred from the parent plant to the new sporophyte. This symbiotic association is thought to be a co-evolved system (Carrapiço, 2006). *Anabaena azollae* supplies *Azolla* with sufficient organic nitrogen for its growth. In exchange, *Azolla* provides the *Anabaena* with a protected environment and a fixed source of carbon (Wagner, 1997). Therefore, nitrogen limitation is not likely to occur.

### 1.1.4 Environmental factors affecting the growth of the *Azolla*

Albeit independent of external resources of organic nitrogen, *Azolla* needs all other essential nutrients that are required by plants. Phosphorous is the most important and often limiting nutrient for its growth. The threshold level of phosphorous for *Azolla* growth is 0.03 mmol l<sup>-1</sup>



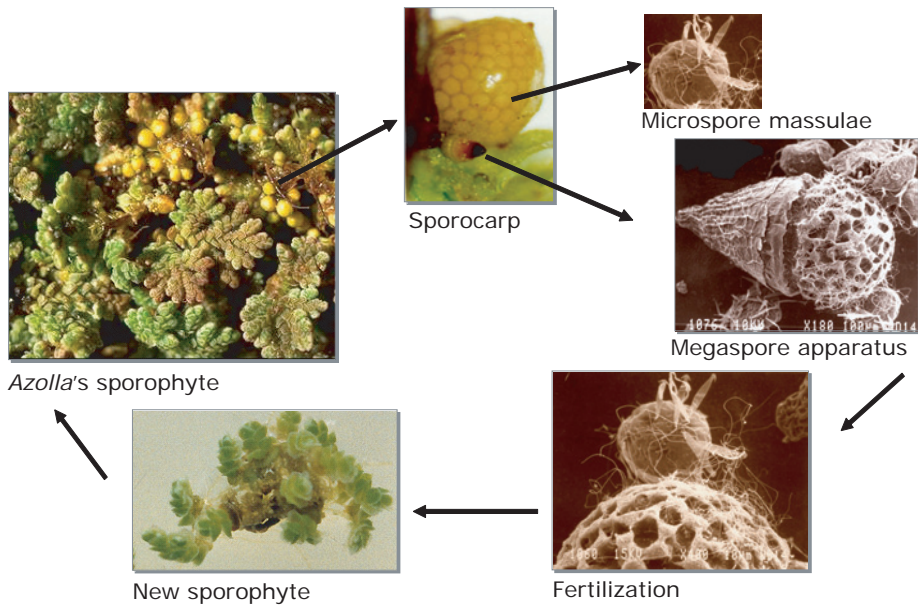


**Fig. 2.** The heterosporous reproductive cycle (courtesy of F. Carrapiço).

(Wagner, 1997). High phosphorous concentrations in the water can initiate extensive blooms of *Azolla* (Carrapiço et al., 1996).

The optimum growth air temperature for *Azolla* spp. ranges between 18°C and 28°C. Some species, however, can survive in a very wide air temperature range of about -5°C to 35°C. The optimum photoperiod is estimated at 20 hours (Wagner, 1997). With respect to temperature and day length, the minimum temperature was found to be the most significant factor influencing relative growth rates of *Azolla*.

CO<sub>2</sub> has a positive effect on the amount of *Azolla* biomass produced (Allen et al., 1988; Idso et al., 1989). Idso et al. (1989) demonstrated that enrichment of atmospheric CO<sub>2</sub> from mean ambient concentration of 340 ppm to 640 ppm allows *Azolla* plants to withstand, and sometimes even flourish, at temperatures above 30°C, which normally would have a debilitating effect.

The optimum pH range for *Azolla* growth is between 4.5 and 7, but it can survive within a range of 3.5-10 pH. The response of *Azolla* to pH is, however, greatly affected by other environmental factors such as light intensity, temperature, and soluble iron (Wagner, 1997).

*Azolla* is a fresh water fern, and increased salinity consequently decreases biomass production considerably. Extant species of *Azolla* have been shown to tolerate salinities up to ~5‰ (van Kempen et al., in review). At higher salinities, the root growth and consequently water and nutrient uptake is severely negatively affected resulting eventually in the death of the plants (van Kempen et al., under review).

## 1.2 The Eocene Arctic '*Azolla* phase'

*Azolla* fossils are known from the mid to late Cretaceous onwards from complete fertile plants and numerous dispersed megaspore apparatuses, single megaspores and massulae. Associated facies with these *Azolla* fossils are in complete support of their growth in freshwater settings including lakes and ponds (Collinson, 2001; Collinson, 2002).

Curiously, mass occurrences of remains of *Azolla* characterize early middle Eocene marine deposits around the sub-Arctic and Nordic seas, mainly recognized in commercial oil and gas exploration wells. A few published palynological studies have shown that this *Azolla* horizon is possibly synchronous in all Nordic Sea locations (Bujak and Mudge, 1994; Pearson and Palmer, 2000; Eldrett et al., 2004). Notably, the termination of this horizon is widely used as stratigraphic marker in industrial boreholes and outcrops, and has recently been calibrated against magnetochron C21r (~49 Ma; Eldrett et al., 2004) offshore Greenland. Despite the knowledge of this marker horizon, no particular attention has been given to the extent, cause and implications of this unique phenomenon.

Only in 2004, when enormous numbers of *Azolla* remains were recovered from coeval micro-laminated central Arctic Ocean sediments (Fig. 3) during the Arctic coring expedition (ACEX; IODP Expedition 302), attention was drawn to the palaeoecological and oceanographical implication of this phenomenon (Backman et al., 2006; Brinkhuis et al., 2006). The presence of mature megaspores with and without attached massulae, single, small groups and large clusters of massulae, and probable aborted megaspores of *Azolla* all indicate that it is highly unlikely that this reflects a transported assemblage. This is strongly supported by the relative scarcity of terrestrial palynomorphs (pollen and spores) and extremely low (<0.1) values of the BIT (branched and isoprenoid tetraether) index, a measure for the amount of river-derived terrestrial organic matter relative to marine organic matter. Hence, there are strong indications that *Azolla* grew and reproduced in situ in the Arctic Ocean, suggesting that surface waters of the central Arctic Ocean were fresh enough

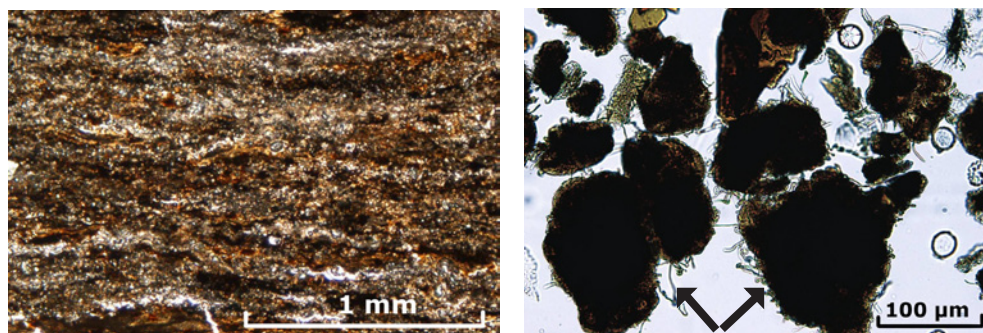


**Fig. 3.** a) Microlaminated central Arctic Ocean early middle Eocene sediments (image courtesy of M.E. Collinson) recovered during the Arctic coring expedition (ACEX; IODP Expedition 302). b) Micropaleontological slide showing amongst others *Azolla* microspore massulae (indicated with arrows; image courtesy H. Brinkhuis).

to allow in situ growth and reproduction of *Azolla*. Widespread coeval *Azolla* occurrences in the Nordic seas were hypothesized to represent transported assemblages from the Arctic Ocean, carried by periodic outflows of freshwater to the Nordic Seas (Brinkhuis et al., 2006).

## 1.3 The Eocene Arctic setting

### 1.3.1 Palaeoceanography

During the early middle Eocene the Arctic Ocean was a nearly entirely landlocked basin (Fig. 4). The exchange between the Arctic Ocean and the global oceans was likely limited to the Norway-Greenland seaway since the connection to the Tethyan Ocean via the Turgay strait ceased to exist in the early middle Eocene (Akhmetiev and Beniamovski, 2009; Radionova and Khokhlova, 2000). Moreover, the exchange between the Arctic and North Atlantic Oceans through the Greenland–Norway Seaway was probably limited to the ocean surface at this time (Jakobsson et al., 2007). The Norwegian-Greenland Sea consisted of a number of isolated sub-basins separated by a mid ocean ridge and the Jan Mayen and Greenland–Senja fracture zones. Furthermore, the Norwegian-Greenland Sea was separated from the

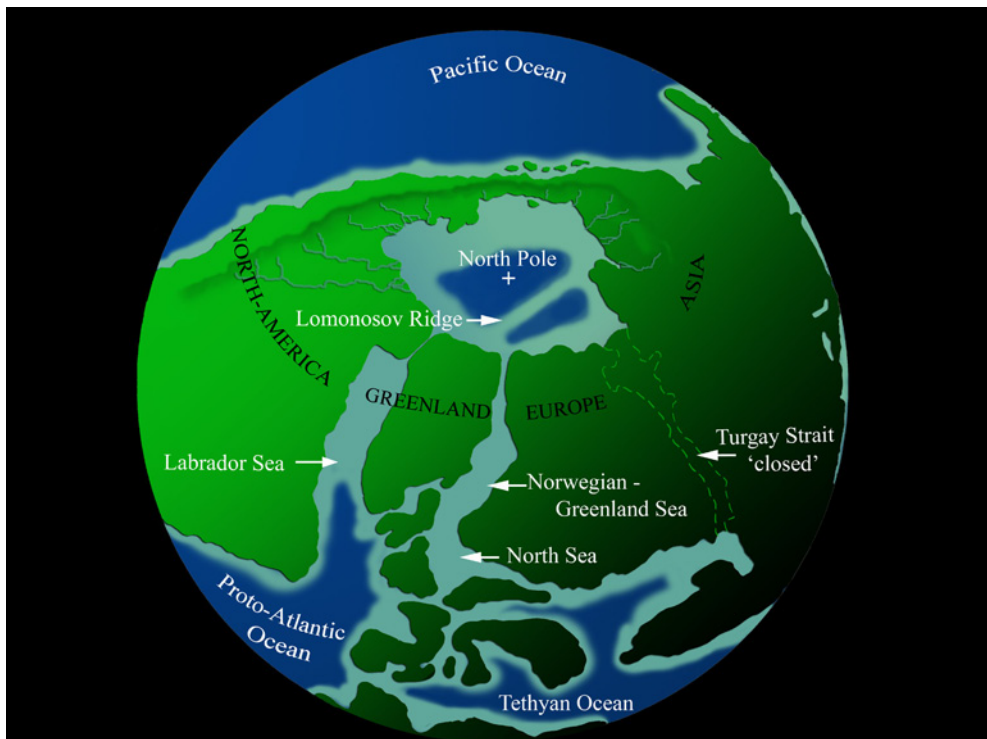


**Fig. 4.** Palaeogeographic reconstruction (early middle Eocene; ~49 Ma; modified from Brinkhuis et al., 2006).

North Atlantic by the Greenland-Scotland Ridge. As a result, intermediate and deep water ventilation was restricted and regional surface water exchange was poor (Eldholm et al., 1994).

### 1.3.2 Eocene Arctic environment and climate

During the early Eocene the Earth was in a Greenhouse state with atmospheric CO<sub>2</sub> concentrations exceeding 2,000 ppm (Pearson and Palmer, 2000). Warm temperatures extended up to higher latitudes and the high Arctic was forested up to a palaeolatitude of 75-80°N (McIver and Basinger, 1999). A mosaic of plant communities characterized the landscape in the Canadian High Arctic, dominated by swamps and woodlands (Francis, 1988; Greenwood and Basinger, 1994; McIntyre, 1991; McIver and Basinger, 1999). Water-logged sites of the swamps were commonly occupied by a climax forest of deciduous conifers, in which *Metasequoia* and/or *Glyptostrobus* were the dominant taxa. The better-drained sites in-between the swamps were covered by hardwood angiosperm forests (Greenwood and Basinger, 1993; Greenwood and Basinger, 1994), dominated by *Carya* (McIver and Basinger, 1999). Upland sites were likely mainly covered by a mix of hardwood angiosperms and evergreen conifers, dominated by *Picea* (McIntyre, 1991; McIver and Basinger, 1999; Richter and LePage, 2004).

The dominance of deciduous vegetation indicates mild and moist summer conditions, and might also explain the tolerance to the lack of sunlight during several months of winter darkness at these high latitudes (Basinger et al., 1994). Field observations and growth ring measurements of the Strathcona Fiord Eocene fossil forest (Eocene age, approximately 50 Ma) on Ellesmere Island indicate that the climate was markedly seasonal and warm and high rainfall prevailed at least during the growing season (Francis, 1988). The composition of the early Palaeogene fossil forest assemblage of the Canadian High Arctic suggests a mean annual temperature of 12-15°C, warmest month mean temperatures of >25 °C, and coldest month mean temperatures of 0-4°C (Basinger et al., 1994; Greenwood et al., 2010).

Global temperatures reached a long-term maximum during the Early Eocene Climatic Optimum (EECO) between 51 and 53 Ma. The EECO was followed by a 17 Myrs long trend to colder conditions, which is known as the transition from a greenhouse towards the modern icehouse Earth (Zachos et al., 2001). The timing of the '*Azolla* phase' (~49 Ma) coincides with the onset of this transition.

## 1.4 Scope and framework of this thesis

This thesis is part of a multi-disciplinary research project, which is entitled the DARWIN *Azolla* project. The overarching goal of this project is to provide the necessary information constraining the potential role of *Azolla* as a moderator of global nutrient cycles and if and how that role, in combination with the geological and oceanographical evolution of the Arctic Ocean, was instrumental in the context of Earth's greenhouse to icehouse transition. This

thesis focuses on the palaeobotanical, palaeoecological, and palaeoceanographical aspects of the *Azolla* phenomenon.

In **Chapter 2** we investigate the potential impact of the abundant and widespread early middle Eocene *Azolla* blooms on the regional and global nutrient cycles. Furthermore, we assess the potential impact of the sustained *Azolla* blooms on the atmospheric  $p\text{CO}_2$ . Flux calculations suggest a carbon storage of  $\sim 0.9 - 3.5 \cdot 10^3$  gigatons of carbon in the Arctic during the *Azolla* interval, which could have resulted in a 55 to 470 ppm drawdown of atmospheric  $p\text{CO}_2$  under Eocene conditions. This indicates that the Arctic *Azolla* blooms could have had a significant effect on global atmospheric  $p\text{CO}_2$  levels through enhanced burial of organic matter.

The abundances of *Azolla* remains in early middle Eocene sediments recovered from the central Arctic Ocean (Integrated Ocean Drilling Program Expedition 302, Core M0004A-11X) show a cyclic distribution that previously have been related to episodic surface water freshening, which was speculated to be orbitally modulated. In **Chapter 3 and 4** we apply an integrated micropaleontological and cyclostratigraphical approach to evaluate the potentially underlying forcing mechanisms for these freshwater cycles and the final demise of *Azolla* at  $\sim 48.1$  Ma. Our results reveal robust cyclic changes in the absolute and relative abundances of all major aquatic and terrestrial palynomorph groups with two clear periodicities: a dominant  $\sim 1.2$  m cyclicity, which we relate to changes in obliquity ( $\sim 40$  ka) and a weaker  $\sim 0.7$  m cyclicity, which we link to precession ( $\sim 21$  ka). In **Chapter 3** we show that cycles in the *Azolla* abundances fluctuate at the obliquity frequency. Peak abundances are associated with periods of enhanced rainfall and runoff, presumably linked to increased local summer temperatures during obliquity maxima. In **Chapter 4** additional examination of the entire organic-walled dinoflagellate cyst (dinocyst) assemblages in combination with siliceous microfossil analysis from the same core implies that throughout the entire obliquity cycle waters were stratified during the growing season with a freshwater surface layer atop. However, during obliquity minima, a slight increase in surface water salinity, shallowing of the halocline, and/or less stable hydrodynamic conditions may have strongly reduced *Azolla* abundances. The precession signal in this high-latitude record is thought to reflect continental runoff from more remote source areas and a stronger seasonal contrast. Runoff (cycles) were shown to continue to influence the central Arctic at decreased intensity following the sudden demise of *Azolla* at  $\sim 48.1$  Ma, though at decreased intensity. A slight change in salinity is suggested to have caused the termination of the '*Azolla* phase'.

Coeval *Azolla* occurrences in middle Eocene deposits of all the Nordic seas have been suggested to represent transported assemblages from the Arctic Ocean by freshwater spills. In order to test this hypothesis it was essential to determine if the Arctic and Nordic Sea *Azolla* occurrences represent a single species. Therefore, in **Chapter 5** we present a full and detailed description of the material of *Azolla* from the middle Eocene central Arctic Ocean. We show that the Arctic Ocean *Azolla* material can be differentiated from all other fossil *Azolla* and is therefore described as a new species: *Azolla arctica*. *Azolla arctica* is represented by fully developed megaspore apparatuses with attached microspore massulae

## Chapter 1

as well as clustered and dispersed microspore massulae.

In **Chapter 6** we examine the coeval *Azolla* assemblage from one of the most southerly sites of *Azolla* records in the North Sea, the Lillebælt Clay Formation, represented in the Danish outcrop (Heilmann-Clausen et al., 1985). This Danish stratum has an excellent biostratigraphy, which enable correlation to global stages and time scales. Furthermore, it yields abundant well-preserved *Azolla* material, including megaspore apparatus, microspore massulae, and the two interconnected, which permits detailed comparison with all characteristics of *Azolla arctica*. Surprisingly, multiple morphological and ultrastructural characters distinguish the Danish *Azolla* species from *Azolla arctica* and it is here described as *Azolla jutlandica* sp. nov. Therefore, contrary to expectations based on the overlapping age of these assemblages, it appears that not a single *Azolla* species has spread from the Arctic to the Southern North Sea either through freshwater spills from the Arctic Ocean or as a result of rapid spread due to highly invasive biology.

Having established the characteristics and variation of the spatially separated Arctic and Danish *Azolla* from these abundant and well-preserved assemblages, further investigations of more fragmentary and less abundant material from multiple borehole cores from intermediate sites were possible. In **Chapter 7** we selected thirteen sites along a north-to-south gradient, between the Arctic Ocean and southern North Sea, and four sites in the western Arctic Ocean that incorporate the early middle Eocene *Azolla*-bearing interval. Our results show that at least five different species of the fast growing *Azolla* bloomed in and around the Arctic to Nordic seas during the same time interval. Warm climates, high precipitation and related runoff, combined with the distinct Arctic and Norwegian-Greenland Sea semi-enclosed palaeogeographic setting likely invoked at least episodically extremely low-salinity surface water layers and concomitant strong stratification of the water column. At some locations evidence suggest *in situ* growth of *Azolla*, at other sites the assemblages are likely the result of transport from nearby continents. The spatial extent (~ 30 million km<sup>2</sup>), duration (~1,2 Myrs), and associated phenomena including carbon-burial potential suggest *Azolla* to may have played an important role in global carbon cycling.

The raw data of this research can be obtained upon request.







# Chapter 2

## **The Eocene Arctic *Azolla* bloom: environmental conditions, productivity and carbon drawdown**

Speelman, E.N., van Kempen, M.M.L., Barke, J., Brinkhuis, H.,  
Reichart, G.J., Smolders, A.J.P., Roelofs, J.G.M., Sangiorgi, F., de  
Leeuw, J.W., Lotter, A.F., Sinninghe Damsté, J.S.

*Published in Geobiology 7, 155-170, 2009*

## Abstract

**Enormous quantities of the free floating freshwater fern *Azolla* grew and reproduced *in situ* in the Arctic Ocean during the middle Eocene, as was demonstrated by microscopic analysis of microlaminated sediments recovered from the Lomonosov Ridge during Integrated Ocean Drilling Program (IODP) Expedition 302. The timing of the *Azolla* phase (~48.5 Ma) coincides with the earliest signs of onset of the transition from a greenhouse towards the modern icehouse Earth. The sustained growth of *Azolla*, currently ranking amongst the fastest growing plants on Earth, in a major anoxic oceanic basin may have contributed to decreasing atmospheric  $p\text{CO}_2$ -levels via burial of *Azolla*-derived organic matter. The consequences of these enormous *Azolla* blooms for regional and global nutrient and carbon cycles are still largely unknown. Cultivation experiments have been set up to investigate the influence of elevated  $p\text{CO}_2$  on *Azolla* growth, showing a marked increase in *Azolla* productivity under elevated (760 and 1910 ppm)  $p\text{CO}_2$  conditions. The combined results of organic carbon, sulphur, nitrogen content and  $^{15}\text{N}$  and  $^{13}\text{C}$  measurements of sediments from the *Azolla* interval illustrate the potential contribution of nitrogen fixation in a euxinic stratified Eocene Arctic. Flux calculations were used to quantitatively reconstruct the potential storage of carbon ( $0.9 - 3.5 \cdot 10^{18}$  gC) in the Arctic during the *Azolla* interval. It is estimated that storing  $0.9 \cdot 10^{18}$  to  $3.5 \cdot 10^{18}$  g carbon would result in a 55 to 470 ppm drawdown of  $p\text{CO}_2$  under Eocene conditions, indicating that the Arctic *Azolla* blooms may have had a significant effect on global atmospheric  $p\text{CO}_2$  levels through enhanced burial of organic matter.**

## 2.1 Introduction

Exceptionally high concentrations of intact microspore massulae and megaspores of the aquatic floating fern *Azolla* have been found in sediments recovered from the Lomonosov Ridge during Integrated Ocean Drilling Program (IODP) Expedition 302, indicating that this freshwater fern grew and reproduced *in situ* in the mid Eocene (~48.5 Ma) Arctic Ocean (Moran et al., 2006; Brinkhuis et al., 2006) (Fig. 1). Sporadically, mass abundances of *Azolla* remains have previously been recognized in the Eocene Arctic and Nordic Seas (e.g., Manum et al., 1989; many confidential oil- and gas exploration studies; Eldrett et al., 2004). Yet, concentrations of *Azolla* microspore massulae recovered at the Lomonosov Ridge Site are several orders of magnitude higher than those found elsewhere (Brinkhuis et al., 2006). Sustained growth of *Azolla* throughout the Arctic provides important constraints on the Eocene Arctic environment. The presence of the freshwater fern *Azolla*, both within the Arctic Basin and in all Nordic seas suggests that at least the surface waters were frequently fresh or brackish during the *Azolla* interval (Brinkhuis et al., 2006). The occurrence of such a fresh surface layer in combination with more saline deeper waters, as indicated by the presence of marine diatoms (Stickley et al., 2008), suggests that the Eocene Arctic Basin was highly

stratified. Salinity stratification, in combination with high riverine input of nutrients, and hence increased surface water productivity and the associated enhanced export of organic matter, are most likely responsible for the development of euxinic conditions in the lower part of the water column, comparable to the present-day Black Sea setting (Stein et al., 2006). Interestingly, the *Azolla* phase approximately coincided with the onset of a global shift towards heavier deep sea benthic foraminifera  $\delta^{13}\text{C}$  values (Zachos et al., 2001) and an overall global cooling trend. In effect, around this time (~48.5 Ma) the transition from a global greenhouse climate towards the modern icehouse started (Zachos et al., 2008; Tripathi et al., 2005), possibly heralded by decreasing atmospheric  $\text{CO}_2$  concentrations (Pearson and Palmer 2000; Pagani et al., 2005). Together these notions suggest that sustained growth of *Azolla* in a major anoxic oceanic basin may have contributed substantially to decreasing atmospheric  $p\text{CO}_2$ -levels.

Here we discuss the potential role of *Azolla* as a modifier of nutrient cycles and evaluate if and how that role, in combination with the geological and oceanographical evolution of the Arctic Ocean, was instrumental for Earth's greenhouse to icehouse transition. We also present the first results from a multidisciplinary research project, combining results from microfossil assemblages, biomarker and geochemical analyses performed on sediments obtained from the Arctic Coring Expedition (ACEX) and *Azolla* cultivation experiments. The latter experiments were set up to elucidate the potential impact of elevated  $p\text{CO}_2$  levels on the growth of *Azolla*. Results of these experiments are used to further constrain knowledge of *Azolla* growth rates, productivity and potential carbon drawdown in the context of reconstructed Eocene Arctic environmental conditions.

## **2.2 Review of existing information**

### **2.2.1 Extant *Azolla***

*Azolla* is a genus of floating aquatic ferns with seven extant species, distributed throughout tropical and temperate regions (Saunders and Fowler, 1993). Extant *Azolla* ranks among the fastest growing plants on Earth, capable of fixing large amounts of carbon and producing vast amounts of organic nitrogen (Wagner, 1997). Dinitrogen fixing bacterial symbionts are known to inhabit a special cavity within the dorsal leaf lobe of *Azolla*. These cyanobacteria, e.g. *Anabaena azollae*, fix atmospheric nitrogen and subsequently release it to *Azolla*, satisfying both its own requirement for combined nitrogen and that of its host. In exchange, the fern provides the endosymbiont with a protected environment and supplies it with a carbon source in the form of sucrose (Peters and Meeks, 1989). Through this symbiosis the aquatic fern *Azolla* is not limited by fixed nitrogen availability (Braun-Howland and Nierzwicki-Baer, 1990) and under favourable conditions may outcompete other macrophytes, bloom fast, and form thick mats. Extant *Azolla* is known as a freshwater fern. Cultivation experiments with *Azolla filiculoides* show that *Azolla* grows well in water with maximum salinity levels of ~5‰ (van Kempen et al., under review).

## 2.2.2 The Eocene Arctic setting

### 2.2.2.1 Palaeoceanography and age assessment of the *Azolla* interval

The ACEX core was recovered from the Lomonosov Ridge, which is a fragment of continental crust that rifted from the Eurasian continental margin during the Late Palaeocene (~57 Ma ago) (Glebovsky et al., 2006). In the late-middle Eocene, the Arctic Ocean was almost completely enclosed as the Norwegian Greenland Sea was not fully open yet (Scotese, 1988). The, at that time, probably still shallow Fram Strait (Jakobsson et al., 2007) possibly formed a deeper, intermittent, connection between the shallow Arctic Basin and the open ocean.

The age model for the ACEX core was established using biostratigraphical and cosmogenic isotope data, as usage of palaeomagnetic polarity data are problematic for this core (Backman et al., 2008). In the Palaeogene, the dinoflagellate cysts (dinocysts)

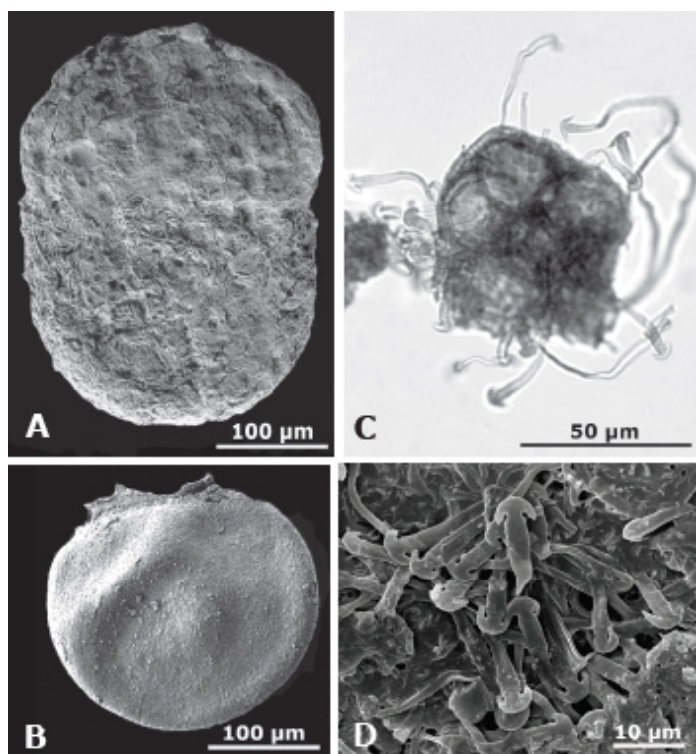


**Fig. 1.** *Azolla* mega- and microspore massula from Hole 302-4A-11x

- A. SEM image of megaspore apparatus showing the distal megaspore and the proximal float zone.
- B. SEM image of dissected megaspore.
- C. LM image of microspore massula showing the embedded microspores and attached glochidia.
- D. SEM image of glochidia on microspore massula showing anchor-shaped tips.

are abundant and occur fairly continuous throughout the record. Therefore, numerous dinocyst events could be calibrated against ODP Leg 151 Site 913B, located in the adjacent Norwegian-Greenland Sea, for which a good magnetostratigraphy is available (Eldrett et al., 2004). Moreover, the *Azolla* horizon, being a widespread and well-calibrated acme event in the entire Arctic Basin and the adjacent Nordic Seas (Fig. 2), can also be used as a stratigraphic marker horizon itself (Brinkhuis et al., 2006; Bujak, Brinkhuis, unpublished exploration data). Based on the observation that the Last Occurrence (LO) of *Azolla* for this interval coincides with the LO of *Eatonicysta ursulae* (Eldrett et al., 2004), the top of the *Azolla* phase is dated at 48.1 Ma (magnetic polarity chronozone C21r), based on Gradstein et al. (2004). However, due to incomplete core recovery, the onset of the *Azolla* interval is missing in the ACEX core (Fig. 3). Also in Core 913B the *Azolla* interval is not fully represented as some spores, though in small numbers, are already present at the base of the core. So at this stage, only an estimate of the minimum duration of the entire *Azolla* interval can be given. In Core 913B *Azolla* is still present near or at the base of Chron 22n. Using the timescale by Gradstein et al. (2004), the beginning of the *Azolla* phase is dated at approximately 49.3 Ma, giving a total duration of 1.2 Ma for the entire *Azolla* interval.

#### *2.2.2.2 Arctic Eocene environmental conditions*

Vertebrate fauna recovered from Ellesmere Island in the 1970s provided some of the first evidence that temperatures in the early Eocene Arctic were substantially warmer than today. The discovery of early Eocene remains of a varanid lizard, the tortoise *Geochelone*, and the alligator *Allognathosuchus* suggested that winter temperatures rarely dipped below freezing (Estes and Hutchinson, 1980). Recently, Arctic sea surface temperatures (SSTs) have been estimated by applying the TEX<sub>86</sub> index, an organic palaeothermometer that is independent of salinity (Schouten et al., 2002; Powers et al., 2004) and calibrated to mean annual SST. TEX<sub>86</sub> values suggest SSTs of ~10°C during, and 13-14°C immediately following, the *Azolla* phase (Brinkhuis et al., 2006). These values are similar to, or slightly higher than, other late Paleocene and Eocene floral, faunal and isotopic proxy evidence for mean annual temperatures in the Arctic (Greenwood and Wing, 1995; Jahren and Sternberg, 2003). Stable oxygen isotope analyses of cellulose from middle Eocene *Metasequoia* wood at Axel Heiberg Island indicates that Arctic climate was not only warm (mean annual temperature of 13.2 ± 2.0 °C), but also quite humid, with an atmospheric water content approximately twice that of today (Jahren and Sternberg, 2003). Based on modern hydrology and fully coupled palaeoclimate simulations, it has been suggested that the warm greenhouse conditions characteristic of the Paleogene period probably induced an intensified hydrological cycle with precipitation exceeding evaporation at high latitudes (Manabe, 1997; Huber et al., 2003). Increased precipitation and reduced exchange of surface water between the Arctic and the open ocean would thus result in low salinity surface water in the Arctic.

*Azolla* megasporos, with or without attached microspore massulae and clusters of dispersed microspore massulae, were found in the ACEX sediments at abundances comparable to those documented in Palaeogene microlaminated freshwater pond facies (Collinson,

2002). The *in situ* growth and reproduction of *Azolla* in the Arctic Ocean, in combination with high abundances of chrysophyte cysts (the endogenously formed resting stage of these freshwater algae), indicate that fresh- or brackish waters frequently dominated the surface water layer (Stickley et al., 2008). Based on qualitative data of endemic assemblages of marine diatoms and ebridians along with very high abundances of chrysophyte cysts, Stickley et al. (2008) confirmed the concomitant occurrence of lower surface water salinities and higher deeper water salinities, also suggesting episodic changes in salinity, stratification

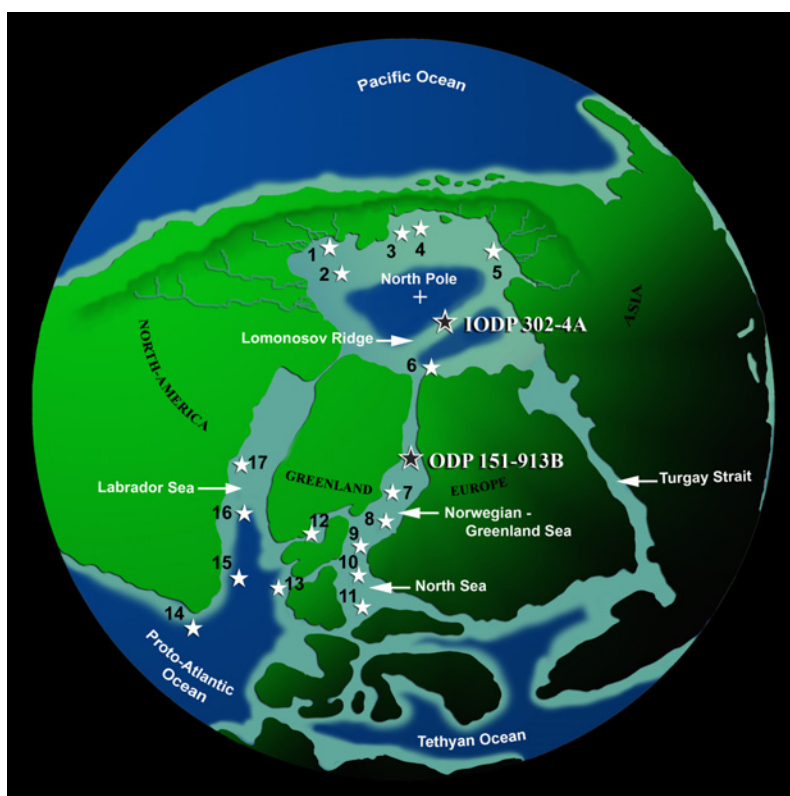
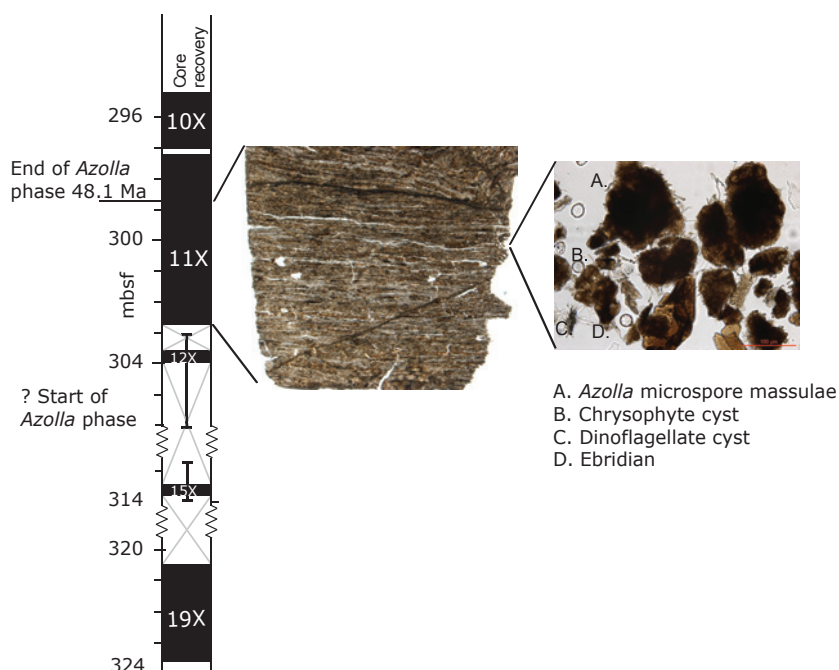


**Fig. 2.** Sites including the earliest middle Eocene *Azolla* acme in various regions of the Nordic Seas. Revision of Table S-1 and Figure S-3 in Brinkhuis et al., 2006 (supplementary information). Complementary sites are given in brackets. **Region 1-2** Mackenzie Delta & Beaufort Basin; **Region 3-4** North slop Alaska & Chukchi Sea (Crackerjack 1 OCS-Y-1320; Popcorn 1 OCS-Y-1275); **Region 5** Siberian Shelf; **Region 6** Barentsz Sea; **Region 7-8** Norwegian - Greenland Sea (6302/6-1, 6406/2-2, 6506/11-6, 6507/8-4, 6608/10-10, 6610/2-1 S, 7316/5-1, DSDP 343, ODP 643A); **Region 9-11** North Sea Basin (16/4-4, 24/12-1, 30/2-1, 34/4-2, M2/A02, M2Z/A02S1, M2Y/A02S2); **Region 12** Faeroe-Shetland Basin; **Region 13** Atlantic, Rockall Bank; **Region 14** Grand Banks, Scotian Shelf; **Region 15** Labrador, Hopedale Basin (South Labrador N-79); **Region 16** Labrador, South Saglek Basin (Gilbert F-53); **Region 17** Labrador, North Saglek Basin (Gjoa G-37, Hekja O-71, Ralegh N-18).

and thus trophic state. The, albeit incomplete, isolation of the Arctic from the worlds' oceans

on sediment lamination (Fig. 3), the absence of fossil benthic organisms, high concentrations of reduced sulphur (pyrite), and organic geochemical biomarker evidence, previous reports on the Arctic region concluded that bottom waters were at least temporally devoid of oxygen (Backman et al., 2006; Brinkhuis et al., 2006; Sluijs et al., 2006; Stein et al., 2006), also at the time of the *Azolla* interval. Considering the estimated duration of the *Azolla* phase (1.2 Ma), it is remarkable that the deeper saline waters did not become increasingly diluted over time to the point that it would be too fresh to sustain pyrite formation. The fact that it did not progressively freshened in itself provides evidence for the existence of a seaway

been a prerequisite for the development of massive *Azolla* occurrences. Given the found salinity intolerance of extant *Azolla* (van Kempen et al., under review), admixing of much more saline water from greater depth would render the surface waters too saline for *Azolla*. In the ACEX sediments no intact vegetative *Azolla* material has been recovered (Brinkhuis et al., 2006), indicating that most of the plant tissue was decomposed in the water column or



ACEX Core recovery. Close up of laminated sediment (courtesy of M. Collinson) and image of fossil content, showing *Azolla*

with the atmosphere, partly related to the dense vegetation cover, usually renders water below *Azolla* mats dysoxic. If the presence of a floating mat of *Azolla* was a prerequisite for surface water stratification, mixing to some degree may have occurred during the long dark winter period. So at least during the growing season, the six months light period, a stratified water column existed with a strong halocline and anoxia at depth.

### 2.2.2.3 Atmospheric Carbon Dioxide levels

A reconstructed mean annual sea surface temperature of  $\sim 10^{\circ}\text{C}$  in the Eocene Arctic during the *Azolla* phase prevailed in absence of oceanic heat transport (Brinkhuis et al., 2006). This implies that increased greenhouse gas concentrations and associated feedbacks must have been the dominant factor in keeping high latitudes warm (Huber et al., 2003). Changes in the carbon dioxide concentrations in the atmosphere are commonly regarded as likely forcing mechanism of global climate on geological time scales because of the large and predictable effect of  $\text{CO}_2$  on temperature (Pearson and Palmer, 2000). The exact relation between atmospheric  $\text{CO}_2$  concentration and the greenhouse climate of the early Eocene is uncertain because proxy measurements from palaeosols (Yapp, 2004; Royer et al., 2001), marine boron isotopes (Pearson and Palmer 2000) and leaf stomatal indices (Royer et al., 2001) give extremely variable estimates of atmospheric  $\text{CO}_2$  concentrations between 400 and 3500 ppmv. In the middle Eocene  $p\text{CO}_2$  is assumed to be up to ten times preindustrial values (Pearson and Palmer, 2000). It is well known that high  $p\text{CO}_2$  may stimulate growth of *Azolla* species (Allen et al., 1988; Idso et al., 1989; Koizumi et al., 2001). Moreover, there are indications that at higher  $\text{CO}_2$  concentrations plants generally cope better with environmental stresses such as high salinity levels (Reuveni et al., 1997).

The *Azolla* phase in the Eocene Arctic, during which the organic carbon content of the sediment reaches a maximum (Moran et al., 2006), coincides with a global shift towards heavier  $\delta^{13}\text{C}$  values in benthic foraminifera (e.g., Zachos et al., 2001), suggesting enhanced global sequestration of organic matter. Waddell and Moore (2008) also found a positive  $\delta^{13}\text{C}$  excursion in fish bone remains and speculated that during a period of extreme primary productivity the Arctic surface waters became depleted in  $^{12}\text{C}$ , which subsequently resulted in burial of the fish bones with  $^{13}\text{C}$  enriched organic matter. The combination of extremely high primary production by *Azolla* on a fresh water surface, together with the anoxic and saline nature of Eocene Arctic deep waters makes the Arctic Basin ideally suited as an important carbon sink. Sustained growth of *Azolla* in a major anoxic oceanic basin may have contributed significantly to reducing atmospheric  $\text{CO}_2$  levels, either directly by the storage of large amounts of organic carbon or/and indirectly through enhanced nitrogen fixation. Nitrogen-fixing bacteria play a key role in global biogeochemical cycles as availability of fixed nitrogen and dissolved phosphorus together limit primary productivity and thus  $\text{CO}_2$  fixation. In anoxic environments a substantial loss of fixed nitrogen occurs through denitrification or anaerobic ammonia oxidation activity (Kuypers et al., 2003) and on shorter timescales fixed nitrogen is often a limiting nutrient. During growth of *Azolla*, however, this loss of fixed nitrogen may be compensated by symbiotic nitrogen fixing bacteria.



## 2.3 Materials and Methods

### 2.3.1 Sample material: extant *Azolla*

*Azolla filiculoides* was collected from an arable land ditch in the surroundings of Elst, The Netherlands (N51°55'48"; E5°50'6"). Two fresh *Azolla* samples were used for biomarker and compound-specific isotope analysis. Bulk *Azolla* and manually picked megaspores were analysed for their  $\delta^{13}\text{C}$  and  $\delta^{15}\text{N}$  isotopic composition.

### 2.3.2 Sample material: IODP 302 (ACEX) sediments

During the IODP 302 ACEX expedition, cores were taken at 1288 m water depth at the Lomonosov Ridge, Expedition 302, Hole M0004A, 87.87 °N, 136.18 °E (Backman et al., 2006). In this study we used sediments from lithological Unit 2, Core M0004A-11X 297.31 to 302.63 mbsf covering the *Azolla* interval as encountered in the core (Brinkhuis et al., 2006). This unit is dominated by very dark clay mud-bearing biosiliceous ooze. Palaeowater depths are estimated to be shallow, perhaps on the order of ~200 m (Moran et al., 2006). The entire core 11X has pale-grey dark-grey laminations. The *Azolla* remains are associated with the light layer in the SEM pictures (Brinkhuis et al., 2006). The recovery within section 11X was good, including the end of the *Azolla* interval. Fifty-four samples were used for palynological analyses, giving a sample resolution of one sample every 10 cm. In total, 90 samples were used for bulk geochemical analyses and two for biomarker and compound-specific isotope analyses. *Azolla* megaspores from the ACEX core were manually picked for the determination of  $\delta^{13}\text{C}$  values.

### 2.3.3 Pilot experiment: Growth of *Azolla* at elevated atmospheric CO<sub>2</sub> concentrations

To study the influence of different atmospheric carbon dioxide concentrations on *Azolla* growth, *Azolla filiculoides* was grown in glass aquaria with a water volume of 15.6 l and headspace of 3.4 l. The aquaria were made air-tight except for a gas overflow outlet. The aquaria were placed in a water bath with a controlled mean temperature of 15°C. At the start of the experiment 4 g of fresh *Azolla* was introduced in each aquarium. Three different treatments with specific atmospheric CO<sub>2</sub> concentrations were completed, with eight replicates per treatment (Fig. 4). At the start of the experiments the measured CO<sub>2</sub> concentrations in the headspaces of the different aquaria amounted to 340, 760 and 1910 ppm, respectively. Appropriate atmospheric CO<sub>2</sub> concentrations were attained by mixing compressed air with custom-made mixtures of various concentrations of CO<sub>2</sub> in synthetic air (Air Liquide, Eindhoven, the Netherlands), using mass flow controllers and gas blenders (Bronkhorst Hi-Tec, Veenendaal, the Netherlands). Per treatment the gas mixture was uniformly distributed between the headspaces of the eight aquaria, refreshing the air volume within each aquarium every 5 min. The nutrient solution in the aquaria contained 1.75 mmol/l NaHCO<sub>3</sub>, 1.75 mmol/l CaCl<sub>2</sub> · 2H<sub>2</sub>O, 0.025 mmol/l NaH<sub>2</sub>PO<sub>4</sub> · H<sub>2</sub>O, 1 mmol/l K<sub>2</sub>SO<sub>4</sub>, 1 mmol/l MgSO<sub>4</sub> · 7H<sub>2</sub>O, 0.01 mmol/l Fe-EDTA, 0.001 mmol/l CuSO<sub>4</sub> · 5H<sub>2</sub>O, 0.02 mmol/l MnCl<sub>2</sub>

## Chapter 2

· 4H<sub>2</sub>O, 0.01 mmol/l ZnSO<sub>4</sub> · 7H<sub>2</sub>O, 0.003 mmol/l Na<sub>2</sub>MoO<sub>4</sub> · 2H<sub>2</sub>O, 0.02 mmol/l H<sub>3</sub>BO<sub>3</sub> and 0.004 mmol/l CoCl<sub>2</sub> · 6H<sub>2</sub>O and was adjusted to a pH of 7.5 using 30% HCl. Fresh nutrient solution was supplied at a rate of 0.2 l/h from containers using peristaltic pumps, the water level being held at a constant level by means of an overflow outlet (Fig. 4). Since no nitrogen was added to the nutrient solution, *Azolla* completely depend on its cyanobacterial symbionts for nitrogen supply. The experiments were performed in a greenhouse where the light flux amounted to at least 150 µmol/m/s at vegetation level, supplemented by 600 watt HDN lamps set to a day: night rhythm of 16:8 h.

The CO<sub>2</sub> concentrations in the headspaces above each aquarium were monitored. Air samples were taken with a syringe at the gas overflow outlet and CO<sub>2</sub> concentrations were measured directly using an Infrared Gas Analyzer (IRGA, type ABB Advance Optima). Nutrient solutions of all aquaria were sampled weekly for nutrient analyses with the aid of rhizons. The solutions were analysed for pH, total inorganic carbon using an Infrared Gas Analyzer (IRGA, type ABB Advance Optima), and total concentrations of Al, Ca, Fe, K, Mg, Mn, Na, P, S, Si and Zn using inductively coupled plasma emission spectrometry (ICP-OES). To avoid contamination all used glassware was immersed in acid (30% HCL) for 24 hours after which it was rinsed three times with demineralised water. Total inorganic carbon content in the nutrient solution was measured by injection of 0.2 ml of the nutrient solution into a concentrated H<sub>2</sub>PO<sub>4</sub> solution of 2.1% in a glass reservoir that was directly coupled to an infrared gas analyser to ensure direct measurement of released dissolved carbon. Plants were harvested on day 0, 10, 17 and 23. At harvest total fresh weight of the *Azolla* was determined for each aquarium after which 4 g of fresh *Azolla* was put back into the aquaria while the rest was dried at 70°C for 48 h to determine the element composition of the biomass. The total dry weight at a specific sampling time was calculated using the dry weight to fresh weight ratio from the sub-sample. Cumulative dry weights were based on using these dry weight ratios, adding them up to the total dry weight calculated for the previous time intervals. To analyse nutrient contents of plant tissue, dried samples were ground in liquid nitrogen. Nitrogen and carbon were subsequently measured with a CNS analyzer (type Fisons NA1500). 200 µg plant material was digested using a acid mixture (4 ml HNO<sub>3</sub> (65%) and 1 ml H<sub>2</sub>O<sub>2</sub> (30%)) (Kingston and Haswell, 1997) in Teflon vessels heated in a Milestone microwave oven. Total concentrations of Al, Ca, Fe, K, Mg, Mn, Na, P, S, Si, and Zn were measured in diluted digestates.

### 2.3.4 Palynology

Sub-samples were first cleaned by removing the top part and oven dried at 60°C overnight. Agepon (Agfa-Gevaert, art Nr AKX2P) wetting agent was added. Precisely weighted sediment samples were then treated with HCl and HF in standard palynological treatment. Residues were sieved retaining the fraction size between 15 and 250 µm. *Lycopodium clavatum* tablets containing a known amount of spores were added to the samples to calculate the concentrations of *Azolla* massulae per gram of sediment. The samples were then examined under a binocular microscope at a magnification of 400x.

### 2.3.5 Bulk TOC, N, S, and isotope measurements

Extant *Azolla* samples were oven dried at 70°C for 24 hours. Total organic carbon (TOC),  $\delta^{13}\text{C}_{\text{TOC}}$ , total nitrogen content (Ntot) and bulk  $\delta^{15}\text{N}$  were measured using an elemental analyser (Fison NA 1500 CNS), connected to a mass spectrometer (Finnigan Delta Plus).  $\delta^{13}\text{C}_{\text{TOC}}$  values are reported against VPDB.  $\delta^{15}\text{N}$  values are calculated as per mille excess above their natural abundance in air. Analytical precision and accuracy were determined by replicate analyses and by comparison with international and in-house standards. Precision was better than 0.1% for TOC, Ntot, and  $\delta^{13}\text{C}_{\text{TOC}}$  and 0.15‰  $\delta^{15}\text{N}$ .

### 2.3.6 Sediment bulk TOC, N, S, and isotope measurements

Total organic carbon (TOC), total nitrogen content (Ntot), total nitrogen isotopic composition ( $\delta^{15}\text{N}$ ) and total sulphur content of bulk sediment samples were determined, with a sampling spacing of 10 cm for the *Azolla* interval. All sediment samples were freeze-dried and subsequently grounded in an agate mortar. Prior to the determination of organic carbon content and  $\delta^{13}\text{C}_{\text{TOC}}$  inorganic carbon was removed. Samples were treated with 10% HCl, rinsed with demineralized water to remove  $\text{CaCl}_2$ , and dried. TOC,  $\delta^{13}\text{C}_{\text{TOC}}$ , Ntot and  $\delta^{15}\text{N}$  were measured using the same procedure, with similar precision and accuracy, as described above in par 3.5. Total concentrations of S were determined after digestion in a mixture of HF,  $\text{HNO}_3$ , and  $\text{HClO}_4$  and final solution in 1M HCl via ICP-OES (Perkin-Elmer Optima 3000). The accuracy and precision of the measurements were monitored by including international and laboratory standards and were better than 3%.

### 2.3.7 Compound-specific isotope analyses ACEX sediments and extant *Azolla*

Both ACEX sediments and extant *Azolla* specimens were freeze-dried, powdered and subsequently extracted with an Accelerated Solvent Extractor (Dionex) using a dichloromethane (DCM) – methanol (MeOH) mixture (9:1, v/v). To separate the compounds of interest an aliquot (ca. 15 mg) of the total extract was methylated with  $\text{BF}_3/\text{MeOH}$  at 60°C for 10 min and subsequently separated by preparative thin layer chromatography (TLC) on kieselgel 60 (Merck, 0.25mm) as described by Skipski et al. (1965). The lower, more polar, bands were silylated with BSTFA in pyridine to convert the alcohols into the corresponding TMS-ethers. Components were identified by GC/MS (Thermo Trace GC Ultra). Samples were on-column injected at 70 °C, on a CP-Sil 5CB fused silica column (30 m x 0.32 mm i.d, film thickness 0.1 µm) with Helium as carrier gas set at constant pressure (100 KPa). The oven was programmed to 130 °C at 20 °C/min and then to 320 °C at 4 °C/min, followed by an isothermal hold for 20 min. Compound specific  $\delta^{13}\text{C}$  values were determined using isotope ratio monitoring gas chromatography-mass spectrometry (GC-IRMS), using a ThermoFinnigan Delta-Plus XP mass spectrometer. A similar column and oven program were used as described above, though with a constant flow of 1.2 ml/min. Co-injected squalane, with a known, offline determined, isotopic composition was used as internal standard. Carbon isotopic compositions are reported relative to the VPDB standard and are based on duplicate



**Fig. 4.** The experimental set up in the greenhouse.

analyses of well-resolved peaks and represent averaged values. In the case of alcohol moieties, the  $\delta^{13}\text{C}$  value of the BSTFA used for silylation was determined by derivatization of an authentic alcohol (myo-inositol) standard with a known  $\delta^{13}\text{C}$  composition.

Standard deviation of co-injected squalane was 0.2‰. Duplicates had a standard deviation better than 0.5‰.

## 2.4 Results and Discussion

In order to further constrain the exact environmental conditions facilitating the Eocene Arctic *Azolla* blooms a suite of geochemical and palynological analyses are performed. Furthermore, the influence of these Eocene conditions is investigated using *Azolla* cultivation experiments, focusing on elevated  $p\text{CO}_2$  conditions. Finally, the combined results will shed light on *Azolla* occurrence, productivity and potential atmospheric  $\text{CO}_2$  drawdown.

### 2.4.1 Pilot cultivation experiments with extant *Azolla*: a key to the past

During the middle Eocene atmospheric CO<sub>2</sub> levels were much higher than today (Pearson and Palmer, 2000). To investigate the influence of elevated atmospheric CO<sub>2</sub> concentrations on *Azolla* growth rates, CO<sub>2</sub> concentrations in the headspaces of the cultivation aquaria were set to values of 340 ppm (control), 760 ppm and 1910 ppm, respectively. Distinct increases in biomass production in response to elevated carbon dioxide concentrations were evident (Fig. 5). After 23 days the total dry biomass amounted to 3.92±0.37, 5.98±0.47 and 7.87±1.04 g cumulative dry weight, respectively. The amount of biomass produced in the high (1910 ppm) CO<sub>2</sub> treatment was twice that of the biomass produced in the control treatment at 340 ppm. The experiment using an intermediate CO<sub>2</sub> concentration (760 ppm) yielded 1.5 times more biomass (Fig. 5). During growth in the light period (16h/d) the preset CO<sub>2</sub> concentrations within the headspaces dropped appreciably. Lowest CO<sub>2</sub> concentrations in headspaces were measured just before harvest, when *Azolla* densities were highest, during the light period. On average pCO<sub>2</sub> values dropped from their preset concentrations to values of 170±100 ppm, 330±140 ppm, and 1080±190 ppm respectively. Flushing the headspaces every 5 minutes thus did not suffice to maintain constant pCO<sub>2</sub> levels. Both pH (7.53±0.27, 7.47±0.17 and 7.43±0.18 in the treatments with 340, 760 and 1910 ppm atmospheric CO<sub>2</sub>, respectively) and total inorganic carbon (TIC) (819±76, 857±94 and 800±175 in the respective treatments) of the culture medium remained constant throughout the experiment with no differences at different levels of CO<sub>2</sub> concentrations. Given the low diffusion rate of CO<sub>2</sub> into water (0.21 m/d or 2.4 µm/s) (Zeebe and Wolf-Gladrow 2001) and the observed stability of pH and TIC in the culture medium, the rapid decreasing CO<sub>2</sub> concentrations in headspace can only be attributed to high CO<sub>2</sub> (g) uptake rates of *Azolla*.

Analyses of the chemical composition of the culture medium showed that the supply rate of fresh medium of 0.2 l/h was not high enough to keep the phosphorus concentration at a constant level (P concentrations dropped from 20 µmol/l to 6 µmol/l). The concentrations of the other elements in the culture medium remained constant. The measured nutrient concentrations in *Azolla* all fall within the range of average concentrations of mineral nutrients in plant dry material matter (Marschner 1995). The decreasing nutrient and N concentrations probably reflect diluting effects. Given the preserved linear growth rates during the experiments (Fig. 5), this dilution did not adversely influence *Azolla* biomass production.

These experiments indicate that at elevated CO<sub>2</sub> (g) concentrations the carbon dioxide uptake of *Azolla filiculoides* increases and that biomass is produced at higher rates at higher pCO<sub>2</sub> concentrations, suggesting that CO<sub>2</sub> might be a limiting factor for *Azolla* growth. Hence, *Azolla* could potentially grow at significantly higher rates under the elevated Eocene pCO<sub>2</sub> conditions than under present-day circumstances. However, it should be noted that other environmental conditions like salinity (Rai et al., 2001), pH (Moretti and Gigliano, 1988; Cary and Weerts, 1992) or nutrient availability (Sah et al., 1989) also affect *Azolla* biomass production.

## 2.4.2 Sedimentary signals of the Eocene Arctic *Azolla* bloom

### 2.4.2.1 Bulk parameters of ACEX sediments

Our high-resolution ACEX TOC profile reveals values ranging between 3.1 and 6.0 wt% (Fig. 6). After the *Azolla* phase (above 289.7 mbsf) TOC decreased to lower levels, around 2 wt%. The high-resolution record of *Azolla* spore counts (Fig. 6) confirms the cyclic nature of the abundance pattern in the *Azolla* record as previously described in Brinkhuis et al. (2006). These cycles have a spacing of just over 1 meter and are positively correlated with the TOC content (Fig. 6). Sangiorgi et al. (2008) applied a Blackman-Tuckey power spectral analysis to palynological and siliceous microfossil data for the middle Eocene (~46 Ma) core section between ~236 to 241 mcd (meters composite depth) and also found a 1 meter periodicity. The available age model for the ACEX core (Backman et al., 2008), and the derived sedimentation rate of 24.3 meters per Ma during the middle Eocene (~46 Ma), suggest that the 1 meter cyclicity is compatible with a Milankovitch-type orbital forcing, representing obliquity. Based on the high latitudinal setting, an obliquity signal is expected to be present. However, since for the *Azolla* phase the age model suggests an overall sedimentation rate of 12.7 m/Ma (Backman et al., 2008), the 1 m cyclicity would correspond to ~80 kyrs. Yet, given that the onset of *Azolla* is missing due to failure in core recovery (Fig. 3), it could be possible that the observed cyclicity in the *Azolla* record still represents obliquity. If these cycles indeed respond to obliquity the amount of time included in the entire *Azolla* event, represented in the recovered sections of the ACEX core, can be calculated. In this case, the estimated minimum duration would only be 160 kyr, based on the observed four obliquity cycles within the recovered part from the *Azolla* interval in the ACEX core (Fig. 6). However, as described before, it is possible that a major part of the *Azolla* phase has not been retrieved in the ACEX core. The recovered *Azolla* interval in the ACEX core thus represents 160 kyrs, with a 24.3 m/Ma sedimentation rate. The duration of the entire *Azolla* interval is 1.2 Ma as inferred from dating of the *Azolla* phase in ODP Leg 151 Hole 913B (Eldrett et al., 2004) (with a 12.7 m/Ma sedimentation rate based on the overall age model (Backman et al., 2008)).

Sulphur concentrations are high throughout the interval, varying between 47 and 72 mg/g dry sediment. C/S ratios show an atomic  $C_{org}/S$  ratio of 1-2 during and after the *Azolla* interval (Fig. 7a). The correlation between Fe and S indicates that most of the S is present in the form of pyrite (Fig. 7b). The black dots represent samples from the *Azolla* interval and all plot above the pyrite line (excess S). This indicates that S must be present as greigite or organically bound S as well. The four points in grey plotting under the pyrite line represent samples from after the *Azolla* interval (above 298.8 mbsf). The accumulation of large quantities of organic matter in an euxinic environment is consistent with the findings of Kurtz et al. (2003) who showed a global minimum in  $C_{org}/S$  pyrite ( $C_{org}/S$  ratio of 2-4) during the early Eocene. The presence of sulphate-rich waters in the deeper parts of the Arctic Basin provides additional evidence for the salinity stratification of the basin described above.

In view of the inferred marine setting of the site during the Eocene an extensive riverine influx of fixed nitrogen seems unlikely. Regeneration or atmospheric nitrogen fixation, therefore, must have played a major role in nitrogen supply. Bulk sedimentary nitrogen isotope ratios are persistently low, between -0.7 and -2.4‰ throughout the *Azolla* phase (Fig. 6) and drop to even lower values (<-2‰) afterwards. Variations in  $\delta^{15}\text{N}$  in surface sediments generally reflect differences in relative nutrient utilization (Schubert and Calvert, 2001) and denitrification or anammox (Altabet and Francois, 1994; Montoya et al., 2004), but can also be influenced by exchange with open-ocean water or runoff. Under oxygen depleted conditions, the reduction of nitrate leads to enrichment of the residual nitrate in  $^{15}\text{N}$  relative to the mean value because  $^{14}\text{NO}_3$  is more readily reduced by bacteria. Under the prevailing anoxic conditions in the Eocene Arctic relatively enriched  $^{15}\text{N}$  values are thus expected as upwelling of nitrate deficit waters generated in the dysoxic deeper parts of the water column by denitrification or anammox bacteria (Cline and Kaplan, 1975; Kuypers et al., 2003) followed by Redfield-type nutrient drawdown should result in nitrate limitation in the photic zone, which would result in a positive  $^{15}\text{N}$  excursion. The small and constant offset (mean 0.9 ‰) between the  $\delta^{15}\text{N}_{\text{tot}}$  and  $\delta^{15}\text{N}_{\text{org}}$  found earlier by Knies et al. (2008) confirms that there is little net influence of  $\text{NH}_4^+$  generation or vertical diffusion on the sedimentary  $^{15}\text{N}$  values. Hence we use bulk  $\delta^{15}\text{N}$  values for reconstruction of the marine nitrogen cycle. The low  $\delta^{15}\text{N}$  values encountered in the Arctic sediments point towards the presence of  $\text{N}_2$ -fixing organisms, which are present in extant *Azolla* species as symbionts. The cultured *Azolla filiculoides* biomass had a similarly low average  $\delta^{15}\text{N}$  of -1.5‰, also consistent with  $^{15}\text{N}$  values reported for other biomass produced by  $\text{N}_2$  fixation (between -1 ‰ and -2‰) (Minagawa and Wada, 1986; Kuypers et al., 2004). Whereas the oxygen depleted water condition resulted in the large scale loss of biologically available nitrogen, phosphorus might have been regenerated more efficiently under such conditions (Gächter et al., 1988; Van Cappellen and Ingall, 1994). Organisms with nitrogen fixating symbionts, like *Azolla*, would have had an ecological advantage. However, direct evidence for the presence of *Anabaena azollae* or other symbiotic nitrogen-fixing cyanobacteria in the Eocene Arctic, either in the form of biomarkers or morphological evidence, has not been found yet.

In extant *Azolla* C/N ratios vary between 9 and 15.  $\text{C}_{\text{org}}/\text{N}_{\text{tot}}$  ratios in the ACEX core were adjusted for the contribution of inorganic nitrogen by subtracting a fixed amount of inorganic nitrogen (47  $\mu\text{mol/g}$ ). This amount is based on extrapolation of the linear relation between  $\text{C}_{\text{org}}$  and  $\text{N}_{\text{tot}}$  content. This concentration is similar to the amount used for subtraction as determined by Knies et al. (2008) using  $\delta^{15}\text{N}$  values. The  $\text{C}_{\text{org}}/\text{N}_{\text{tot}}$  ratios in the ACEX sediments vary from 27 to 46. The calculated  $\text{C}_{\text{org}}/\text{N}_{\text{org}}$  ratios vary from 40 to 80 (Fig. 6) and are significantly higher than those of extant *Azolla*. These higher  $\text{C}_{\text{org}}/\text{N}_{\text{org}}$  ratios point towards extensive selective degradation of nitrogen-rich organic compounds (e.g. amino acids), despite the continuous anoxic bottom waters as evidenced by the presence of laminations in the sediment. After each *Azolla* massulæ abundance peak, a marked decrease in C/N ratio can be observed, which coincides with a drop in  $\delta^{15}\text{N}$  (Fig. 6). Changes



in C/N ratios, therefore, could be linked to changes in source organisms (*Azolla* vs marine plankton) or changes in N preservation. Compositional changes, on the other hand, are not reflected in the observed bulk  $^{13}\text{C}$  values, which vary around  $-27.7\text{‰}$  throughout the interval (Fig. 6). The decrease in  $\delta^{15}\text{N}$  probably indicates that after periods of extensive *Azolla* growth, the water column became slightly more oxygenated, decreasing the impact of denitrification/anammox until the next *Azolla* bloom.

#### 2.4.2.2 Compound specific isotope analyses

In addition to the existing palynological data, a recent study provided molecular evidence for the pervasive past presence of *Azolla* in a freshwater Eocene Arctic setting (Speelman et al., 2009a). It was shown that the total lipid fraction of extant *Azolla* ferns contains a series of mid-chain  $\omega 20$  alkanols,  $1,\omega 20$  diols and  $\omega 20$  hydroxy fatty acids with carbon chain lengths ranging from  $\text{C}_{27} - \text{C}_{36}$ . Selective extraction of extant *Azolla* leaf surface lipids revealed that these compounds most likely originate from *Azolla* leaf waxes. The ACEX sediments from the *Azolla* interval contained most of the described  $\omega 20$  compounds. Especially relatively high quantities of compounds identified as  $1,\omega 20 \text{ C}_{30} - \text{C}_{36}$  diols were detected in both extant *Azolla* species and in sediments from the ACEX core. Based on the uniqueness of the  $\omega 20$  hydroxy compound series and their relative stability, these compounds can be considered to be excellent biomarkers for *Azolla*, can thus be used for compound specific isotope ( $\delta^{13}\text{C}$ ) analyses, and therefore serve as palaeo-environmental indicators for *Azolla*.

Compound specific  $\delta^{13}\text{C}$  values can provide insight into Eocene  $\delta^{13}\text{CO}_2$ . As  $\beta$ -sitosterol is the most abundant sterol present in extracts from *Azolla* (Speelman et al., 2009a), the  $^{13}\text{C}$  of  $\beta$ -sitosterol was measured both for extant *Azolla* and ACEX sediments (Table 1). Here

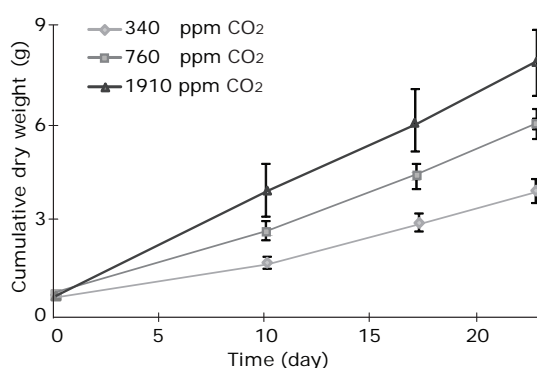


**Fig. 5.** Plot of cumulative biomass against time. Cumulative biomass was calculated by using the fresh weight/dry weight ratio of the sub samples that were taken each harvest for dry weight measurements. Using this ratio the total biomass per week was calculated and this was added to the total dry weight of the week before.



**Table 1.**  $\delta^{13}\text{C}$  compound specific isotopes (‰ vs PDB) for selected compounds and  $\delta^{13}\text{C}$  for bulk organic matter and manually picked *Azolla* megaspores encountered in extant *Azolla* and ACEX sediment extracts.

Diols extant <i>Azolla</i>	$\delta^{13}\text{C}$ (‰)	Diols ACEX	$\delta^{13}\text{C}$ (‰)	Extant <i>Azolla</i>	$\delta^{13}\text{C}$ (‰)	ACEX	$\delta^{13}\text{C}$ (‰)
1,11 C <sub>30</sub> diol	-39.1	1,11 C <sub>30</sub> diol	-	$\beta$ -sitosterol	-32.6	$\beta$ -sitosterol	-29.1
1,13 C <sub>32</sub> diol	-38.0	1,13 C <sub>32</sub> diol	-30.1	$\delta^{13}\text{C}_{\text{TOC}}$	-30.3	$\delta^{13}\text{C}_{\text{TOC}}$	-27.6
1,15 C <sub>34</sub> diol	-38.7	1,15 C <sub>34</sub> diol	-31.3	Megaspores	-30.5	Megaspores	-27.7
1,17 C <sub>36</sub> diol	-39.9	1,17 C <sub>36</sub> diol	-29.7				

we compare stable carbon isotopic compositions of TOC, spores and specific biomarkers of extant *Azolla* and ACEX sediments from the *Azolla* phase to gain insight into differences in the present-day and Eocene environmental conditions at which *Azolla* fixed carbon.

Bulk  $\delta^{13}\text{C}$  values for recent *Azolla* of  $\sim -30$  ‰ (Table 1) are consistent with the findings by Bunn and Boon (1993) for ferns (Pterophyta) in general and in line with their use of the C3 pathway of carbon fixation (Hayes, 2001). The  $\delta^{13}\text{C}$  of the megaspores of extant *Azolla* is also  $\sim -30$ ‰, indicating that there is no significant difference in  $^{13}\text{C}$  content between *Azolla* biomass and spores. However, the  $\delta^{13}\text{C}$  ratios of the lipids extracted from *Azolla* are substantially depleted: the 1, $\omega$ 20 C<sub>30</sub> – C<sub>36</sub> diols have  $\delta^{13}\text{C}$  values of -38.0 to -39.9‰ and the  $\delta^{13}\text{C}$  values for  $\beta$ -sitosterol is -32.6 ‰ (Speelman et al., 2009a). Such differences are generally observed in biomass (Hayes, 2001) and lipids are typically 4-8‰ depleted in  $^{13}\text{C}$  values relative to total cell material. The TOC and the *Azolla* megaspores contain isotopically heavy sugars and proteins and, therefore, their  $\delta^{13}\text{C}$  are higher than those of the individual lipids. The difference in  $\delta^{13}\text{C}$  values between the  $\beta$ -sitosterol and the diols is ca. 6.5‰. Differences in the biosynthetic pathways of isoprenoids (including  $\beta$ -sitosterol) and the compounds with straight chain carbon skeletons (i.e.  $\omega$ 20 diols) will influence the  $^{13}\text{C}$  composition of the individual compounds. These differences may, possibly as a result of the alternative pyruvate/glyceraldehyde-3-phosphate pathway, differ by up to 8‰ (Schouten et al., 1998), which is sufficient to explain the observed 6.5‰ difference between the isoprenoid  $\beta$ -sitosterol and the straight chain  $\omega$ 20 diols in extant *Azolla*.

Of all measured parameters (Table 1) the  $\delta^{13}\text{C}$  values of the diols probably give the most reliable insight into differences in the present-day and Eocene environmental conditions at which *Azolla* fixed carbon. The *Azolla*-specific diols in the ACEX sediments show an enrichment of at least 8 ‰ relative to values observed in extant *Azolla*, between -29.7 to -31.3‰ (Table 1).  $\beta$ -sitosterol is also enriched in  $^{13}\text{C}$  in the Eocene material but only by  $\sim 3$ ‰, a similar enrichment as observed for  $\delta^{13}\text{C}_{\text{TOC}}$  and  $\delta^{13}\text{C}$  of the megaspores (Table 1). The difference between the  $\beta$ -sitosterol and the  $\omega$ 20 diols is only  $\sim 1$  ‰ in the sediment instead of 6.5‰ in extant *Azolla*. This could be due to a mixed origin for the Eocene  $\beta$ -sitosterol. This sterol is not specific for *Azolla* and is probably also produced by algae growing in the water column in the Eocene Arctic, producing  $\beta$ -sitosterol with a different  $^{13}\text{C}$  content. Alternatively, the different offsets could be explained by a difference

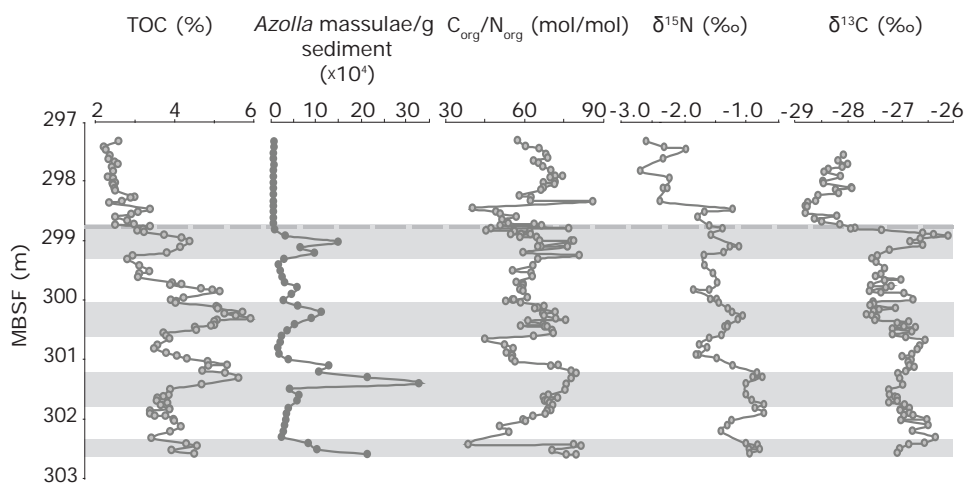


**Fig. 6.** Palynological and geochemical data of high resolution analyses of ACEX sediment, including *Azolla* megaspore counts, TOC (%),  $\delta^{13}\text{C}_{\text{TOC}}$  (‰),  $\delta^{15}\text{N}$  (‰) and  $\text{C}_{\text{org}}/\text{N}_{\text{org}}$  ratio.

in biosynthetic pathways between Eocene *Azolla* and extant *Azolla*, resulting in a much smaller difference between isoprenoidal and acetogenic lipids. Based on the similarity of the distribution of the  $\omega 20$  diols in extant and Eocene *Azolla* this seems unlikely. Sedimentary TOC does not solely contain *Azolla* remains so it also represents mixed contributions. The difference between the  $\delta^{13}\text{C}$  values of the extant and Eocene *Azolla* megaspores is also only 3‰. This could be caused by diagenesis. Extant *Azolla* megaspores still contain a shell mainly consisting of both sugars and protein components, which are typically substantially enriched in  $\delta^{13}\text{C}$  (Hayes, 2001). During diagenesis, sugar and protein carbon degrades more easily, leaving the megaspores increasingly isotopically depleted. The  $\delta^{13}\text{C}$  values of the *Azolla*-specific  $\omega 20$  diols indicate the largest and probably most accurate difference (8‰) in isotopic composition between the present and the Eocene.

Based on reconstructions of Eocene atmospheric  $p\text{CO}_2$  levels, suggesting higher concentrations, and the observation that *Azolla* also takes up atmospheric  $\text{CO}_2$ , and grows faster at elevated  $p\text{CO}_2$  levels, at first sight, lighter rather than heavier  $\delta^{13}\text{C}$  values (Hayes et al., 1999) for *Azolla* biomarkers in ACEX sediment compared to extant *Azolla* are expected. Additionally, the cultured *Azolla* does not seem to fractionate to the full extent during carbon fixation (i.e. bulk values of ca. -33‰ would be expected).  $\delta^{13}\text{C}$  of atmospheric  $\text{CO}_2$  taken up by *Azolla* was probably different in the Eocene and could thus also influence the  $\delta^{13}\text{C}$  ratios. In fact, based on  $\delta^{13}\text{C}$  analyses on foraminifera, the atmospheric  $\text{CO}_2$   $\delta^{13}\text{C}$  was 3 ‰ enriched in the Eocene relative to the present-day atmospheric  $\text{CO}_2$   $\delta^{13}\text{C}$  (Hayes et al., 1999; Pearson et al., 2001; Zachos et al., 2001). A similar enrichment of Eocene *Azolla* biomass and lipids would be expected if they would grow under identical conditions as the extant *Azolla*. This explains part of the 8‰ enrichment. Secondly, elevated  $\text{CO}_2$  levels substantially

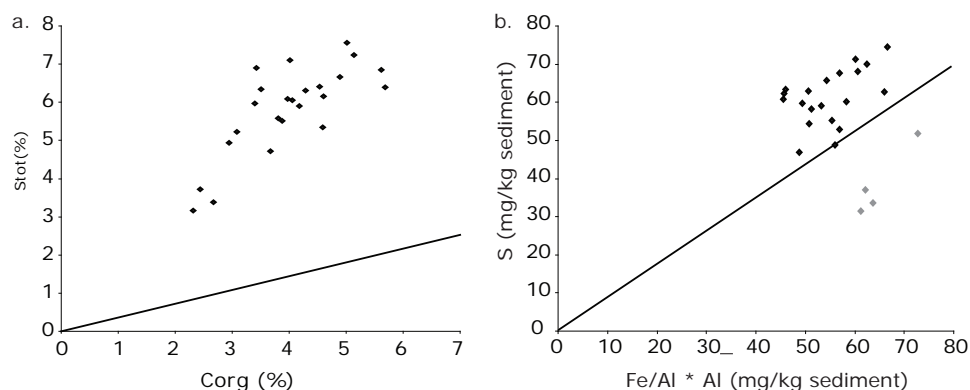


**Fig. 7.** a) Plot of weight percent organic carbon (wt %) versus weight percent total sulphur concentration (wt%). The black line indicates the modern normal marine (non-euxinic) sediments (Berner 1984). b) Fe normalized over aluminum concentration (mg/kg sediment) versus total sulphur content (mg/kg sediment). The S/Fe weight ratio of pyrite (1.15) is plotted. Black dots represent samples from the *Azolla* interval, grey dots represent samples from after the interval.

enhance *Azolla* growth rates, as has been shown in the cultivation experiments (see par 4.1.1). Increased growth rates decreases isotopic fractionation (Hayes et al., 1999), possibly explaining the higher  $\delta^{13}\text{C}$  values for the  $\omega 20$  diols in the ACEX sediments, and counteracting the effect of higher  $\text{CO}_2$  levels. Based on *Azolla* microspore massulae abundances in the core ( $\sim 50,000$  /g dry sediment), or  $5.2 \cdot 10^6$  spores / $\text{m}^2/\text{yr}$ , high Eocene Arctic production rates are inferred. For comparison, it was estimated that a thick mat of  $8 \text{ kg}/\text{m}^2$  fresh biomass is needed to produce 380,000 microsporocarps and 85,000 megasporocarps per  $\text{m}^2$  (Janes 1998). The high  $^{13}\text{C}$  values found here are also consistent with the high  $^{13}\text{C}$  encountered in fish apatite by Waddell and Moore (2008). These were found to reflect extremely high primary production, which resulted in enhanced growth rates and decreased isotopic fractionation, followed by burial of fish bones with  $^{13}\text{C}$  enriched organic matter.

### 2.4.3 Impact of the Arctic *Azolla* bloom on $\text{CO}_2$ drawdown

Using sedimentary TOC content and sedimentation rates the potential  $\text{CO}_2$  drawdown during the *Azolla* interval can be estimated. Combining TOC values of 4 wt% (Fig. 6) with a mass accumulation rate (MAR) of  $35 \text{ g}/\text{m}^2/\text{yr}$  results in a net carbon burial rate of  $1.4 \text{ gC}/\text{m}^2/\text{yr}$ . Recently, Knies et al. (2008) estimated a maximum primary palaeoproductivity during the *Azolla* phase of  $120 \text{ gC}/\text{m}^2/\text{yr}$ , using sedimentary organic carbon content, correcting for decomposition in the water column, burial efficiency, and dilution by inorganic sediment (Knies and Mann, 2002). Our experiments show average production rates for extant *Azolla* under ambient conditions:  $4.5\text{--}5 \text{ g dry weight per m}^2/\text{d}$  or  $2 \text{ g C}/\text{m}^2/\text{d}$ . A production rate of

## Chapter 2

2 g C/m<sup>2</sup>/d would have yielded 120 g C/m<sup>2</sup> within 2 months, a primary production estimate of 120 gC/m<sup>2</sup>/yr thus seems reasonable, albeit a bit on the low side given Eocene  $p\text{CO}_2$  levels and associated enhanced *Azolla* growth. Also the prolonged photoperiod during the Arctic summer would have stimulated higher *Azolla* production. Estimated primary productivity of 120 g C/m<sup>2</sup>/yr in combination with a net carbon burial rate of 1.4 g C/m<sup>2</sup>/yr, demonstrates a fairly low burial efficiency of 1.2%. Hence, despite the water column anoxia extensive biodegradation must have occurred either during transport in the water column or at the sediment-water interface, or over time within the sediments.

The preservation of diols is better than that of for instance fatty acids, neutral lipids, sterols, n-alkanols, and n-alkanes (Sun and Wakeham, 1994), but these compounds are probably more susceptible to degradation than spores. If the preservation of diols reflects the average degree of preservation of *Azolla*-derived organic matter, comparison of the Eocene Arctic diol fluxes with current *Azolla* diol production rates will give a minimum estimate of *Azolla* growth. Diol ( $\omega 20 \text{ C}_{30} - \text{C}_{36}$ ) concentrations in the ACEX core sum up to 4.5  $\mu\text{g/g}$  sediment, or 80  $\mu\text{g/g}$  TOC. In cultured extant *Azolla* the total diol concentration for fresh *Azolla* amounts to 480  $\mu\text{g/g}$  (dry weight) *Azolla* or 190  $\mu\text{g/gC}$  in *Azolla*. If all organic constituents in *Azolla* would preserve equally well, this would indicate that about 40 % of the Eocene TOC would be derived from *Azolla*. Based on the palynological composition (Brinkhuis et al., 2006), this is an underestimate.

$\text{CO}_2$  fixation by *Azolla* and subsequent burial of *Azolla*-derived organic matter has direct consequences for the carbon inventory of the atmosphere - ocean system. The burial of *Azolla*-derived organic matter is assumed to occur in conjunction with ongoing cycling of carbon. To quantify the effect of enhanced organic carbon storage in the Eocene Arctic Basin on atmospheric  $p\text{CO}_2$  levels and ocean-atmosphere partitioning, equation 1 should be solved.

$$\Delta p\text{CO}_2 = \int_{\Sigma C_1}^{\Sigma C_2} \frac{p\text{CO}_2}{\left( I_A + \frac{I_o}{R_{\text{global}}} \right)} d\Sigma C \quad (1)$$

Where  $\Delta p\text{CO}_2$  is the change in atmospheric partial  $\text{CO}_2$  pressure resulting from a perturbation in the global carbon inventory.  $\Delta \Sigma C$  represents the total carbon perturbation: the amount of carbon added to or removed from the inventory.  $I_A$  is the carbon inventory of the atmosphere,  $I_o$  is the carbon inventory of the ocean and  $R_{\text{global}}$  is the average Revelle buffer factor (Revelle and Suess, 1957). Goodwin et al. (2007) showed that this equation can be solved analytically. Here we apply and compare two analytical methods to solve equation 1. The first analytical method used follows a linear approximation (e.g. Archer, 2005) described by equation 2:

$$\Delta pCO_2 = \frac{1}{M} \left( 1 + \frac{I_O}{R_{global} I_A} \right)^{-1} \Delta \Sigma C \quad (2)$$

Where  $M$  represents the molar volume of the atmosphere.  $I_A$ ,  $I_O$  and  $R_{global}$  are evaluated at a steady-state carbon partitioning between ocean and atmosphere, assuming a mean annual global SST of 20° C, with total air-sea carbon levels corresponding to Eocene values (Table 2). This relation is found to be valid if either the change in carbon inventory is small or as long as the value of  $R_{global}$  increases when charge neutral carbon is extracted from the system.

**Table 2.** Calculated values for  $I_A$ ,  $I_O$ ,  $R_{global}$ , and  $I_B$ , for two sets of Eocene conditions.

	$I_A$ (gC)	$I_O$ (gC)	$I_B$ (gC) <sup>a</sup>	$R_{global}$
Eocene ~800 ppm <sup>b</sup>	1.70 10 <sup>18</sup>	1.491 10 <sup>20</sup>	1.26 10 <sup>19</sup>	13.7
Eocene ~2000 ppm <sup>c</sup>	4.25 10 <sup>18</sup>	1.901 10 <sup>20</sup>	1.49 10 <sup>19</sup>	17.8

<sup>a</sup>  $I_B$  is calculated as  $I_B = I_O / R_{global} + I_A$ , using a mean annual SST of 20 °C and salinity of 35 psu

<sup>b</sup> 800 ppm: sea surface alkalinity of 2800  $\mu\text{mol eq/kg}$ , after Pearson and Palmer (2000)

<sup>c</sup> 2000 ppm : sea surface alkalinity of 3400  $\mu\text{mol eq/kg}$ , after Pearson and Palmer (2000)

The second analytical solution has been found to better approximate carbon emissions up till 5000 GtC (corresponding to a  $pCO_2$  level of 1050 ppm, starting from 280 ppm) (Goodwin et al., 2007). This solution makes use of a total air-sea “buffered” carbon inventory,  $I_B$  (Goodwin et al., 2007). The buffered amount of carbon represents the  $CO_2$  available for redistribution between the atmosphere and the ocean.  $I_B$  is assumed to be constant. This last approximation can also be used for larger emissions as it allows for variation in  $R_{global}$ .

$$pCO_2 = P_i e^{\frac{\Delta \Sigma C}{I_B}} \quad (3)$$

$P_i$  is the initial partial pressure of carbon dioxide. Each of the analytical methods is applied to two different sets of Eocene initial  $p\text{CO}_2$  conditions. Despite the extensive biodegradation, after a period of 160.000 yr still 224 kg/m<sup>2</sup> organic carbon, based on net carbon flux of 1.4 gC/m<sup>2</sup>/yr, accumulated. For the entire Eocene Arctic basin (4.0 10<sup>6</sup> km<sup>2</sup>), provided TOC contents are laterally uniform at 4%, this would amount to 9.0 10<sup>17</sup> gC or 3.3 10<sup>18</sup> gCO<sub>2</sub>. Alternatively the *Azolla* phase also included the unrecovered sections below 11X till 15X, which using an average accumulation rate of 1.27 cm/kyr corresponds to a duration of 1.2 Ma. This maximum extent of the sedimentary sequence corresponds to a carbon storage of 3.5 10<sup>18</sup> gC or 13 10<sup>18</sup> gCO<sub>2</sub>.

Based on Eocene partial CO<sub>2</sub> pressure, and corresponding Eocene alkalinity (Pearson and Palmer, 2000), the atmospheric  $I_A$ , oceanic  $I_O$ , and the Revelle buffer factor can be calculated. The total amount of buffered carbon ( $I_B$ ) is then computed for the Eocene case (Table 2). The first Eocene case uses an initial partial CO<sub>2</sub> pressure of 800 ppm, with an alkalinity of 2800  $\mu\text{mol/kg}$  (Pearson and Palmer et al. (2000) estimate for ~49 Ma). The second case assumes a 2000 ppm  $p\text{CO}_2$  and corresponding alkalinity of 3400  $\mu\text{mol/kg}$  (Pearson and Palmer estimate for ~53 Ma) (Table 2). Both are evaluated for two estimates of organic carbon accumulation in the *Azolla* interval (Table 2). In figure 8 the two analytical solutions are shown for the two different Eocene scenarios. Differences in  $I_B$  lead to differences in decrease in atmospheric  $p\text{CO}_2$ , following equation 3, which explains why the impact of sequestration of similar amounts of carbon burial results in different effects on  $p\text{CO}_2$  levels.

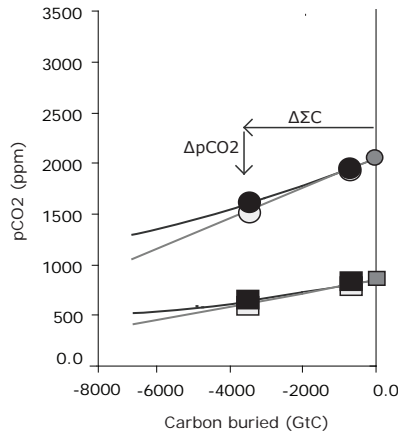


**Fig. 8.** Atmospheric  $p\text{CO}_2$  against emission/drawdown of -6,000 to + 10,000 GtC. Light grey lines:  $p\text{CO}_2$  responds linearly with emissions, as described by equation 2. Dark grey lines:  $p\text{CO}_2$  decreases exponentially with carbon drawdown, following equation 3. Calculated  $p\text{CO}_2$  levels for the different carbon storages (0.9 10<sup>18</sup> and 3.5 10<sup>18</sup> gC respectively) are plotted in white for the linear and in black for the exponential solution. For both analytical solutions  $I_A$ ,  $I_O$ ,  $R_{\text{global}}$ , and  $I_B$  are evaluated at a steady state at the two chosen Eocene  $p\text{CO}_2$  levels of 800 and 2000 ppm. Sea surface salinity is set to 35 psu, global SST to 20 °C, Eocene  $p\text{CO}_2$  and alkalinity are obtained from Pearson and Palmer (2000).

**Table 3.** Response of atmospheric  $p\text{CO}_2$  to calculated burial of organic matter during the *Azolla* interval for two different Eocene initial partial pressure estimates.

	<b>1. linear <math>p\text{CO}_2</math> drawdown (burial of <math>0.9 \cdot 10^{18}</math> gC)</b>	<b>1. linear <math>p\text{CO}_2</math> drawdown (burial of <math>3.5 \cdot 10^{18}</math> gC)</b>	<b>2. exponential <math>p\text{CO}_2</math> drawdown (burial of <math>0.9 \cdot 10^{18}</math> gC)</b>	<b>2. exponential <math>p\text{CO}_2</math> drawdown (burial of <math>3.5 \cdot 10^{18}</math> gC)</b>
Eocene ~800 ppm	57 ppm	220 ppm	55 ppm	195 ppm
Eocene ~2000 ppm	120ppm	470ppm	120 ppm	420 ppm

For both scenarios,  $R_{\text{global}}$  initially decreases as charge neutral  $\text{CO}_2$  is extracted from the air-sea system, making the linear approximation less suitable for the larger perturbations in  $\Delta\Sigma\text{C}$ . Still, the two different analytical approaches (linear and exponential) give very similar results (Table 3; Fig. 8) for the same Eocene scenarios. In absolute amounts,  $\text{CO}_2$  drawdown is higher in the 2000 ppm case than in the 800 ppm. Relatively, however, drawdown falls in the same range: ~7% for  $9.0 \cdot 10^{17}$  gC and ~25% for storage of  $3.5 \cdot 10^{18}$  gC. The close match between the two is explained by the fact that for both the 800 and the 2000 ppm cases a similar ocean carbon inventory ( $I_{\text{o}}/R_{\text{global}}$ ) of  $\sim 1.1 \cdot 10^{19}$  gC was inferred. Based on our calculations sequestration of  $9.0 \cdot 10^{17}$  gC in the Arctic Basin had the potential to lower the concentration of atmospheric  $p\text{CO}_2$  by ca. 55 - 120 ppm. When an estimated total extent of the *Azolla* interval of ~15m is used, an even higher  $\text{CO}_2$  drawdown of 195 - 470 ppm is calculated, based on  $3.5 \cdot 10^{18}$  gC storage. However, the exact magnitude of atmospheric  $\text{CO}_2$  drawdown was also influenced by carbon cycle related feedback mechanisms. For instance, storage of carbon results in an increase in ocean water pH and an increase in  $\text{CO}_3^{2-}$  concentration. This perturbs the  $\text{CaCO}_3$  cycle by increasing global burial rates of  $\text{CaCO}_3$ . Such a perturbation in turn acts to buffer changes in oceanic pH and thus reduces amplitude of atmospheric  $p\text{CO}_2$  changes. On the other hand, a temperature feedback (i.e. cooling) would increase solubility of  $\text{CO}_2$  in the ocean and thus further decrease atmospheric  $p\text{CO}_2$  levels. On longer timescales (~100 kyr), reduced silicate weathering would possibly counteract  $\text{CO}_2$  storage to some extent.

Forty percent of the calculated 55 - 470 ppm  $\text{CO}_2$  drawdown is directly attributable to *Azolla* production, because 40% of TOC consists of *Azolla*-derived carbon. Indirectly, however, nitrogen fixation by organisms associated with *Azolla* could have increased the regional fixed nitrogen availability. The excess fixed nitrogen would have been available for other organisms in the Arctic Basin as well. If transported from the basin this excess fixed nitrogen could have increased productivity in an even larger area. In this way, Arctic *Azolla* blooms could also have enhanced carbon drawdown indirectly in a much larger area potentially contributing even more to decreasing  $\text{CO}_2$  levels in the Eocene.

## 2.5 Summary

Palaeoenvironmental reconstructions of the Middle Eocene Arctic Ocean suggest a warm, humid environment, with aquatic floating *Azolla* inhabiting a fresh water layer capping more saline Arctic bottom waters. *Azolla* microspore massulae counts from sediments recovered during IODP Expedition 302 at the Lomonosov Ridge indicate *in situ* growth. Eocene *Azolla*, by not only profiting from the freshwater input, but also by helping to maintain stratification and thus oxygen depletion, provides its own feedback. Stable isotope analyses ( $\delta^{13}\text{C}$ ) of extracted biomarkers for *Azolla* revealed that values in the Eocene differ from the present day by 3‰ ( $\beta$ -sitosterol) and 8‰ ( $1, \omega$ -20  $\text{C}_{30} - \text{C}_{36}$  diols), respectively. These differences are partly due to the different composition of the Eocene global DIC reservoir but also suggest that *Azolla* primary production rates were much higher in the Eocene than nowadays, leading to less  $^{13}\text{C}$  fractionation.

The first results of culturing experiments of extant *Azolla* mimicking Eocene  $p\text{CO}_2$  conditions show doubling growth rates of *Azolla filiculoides* in the 1910 ppm atmospheric  $p\text{CO}_2$  treatment compared to the control of 340 ppm. Under Eocene  $p\text{CO}_2$  conditions, *Azolla* could thus reproduce at higher rates than under present-day  $\text{CO}_2$  concentrations and could fix carbon at higher rates. Based on bulk sediment analyses, including high organic carbon contents, low C/S ratios, overall, euxinic bottom water conditions are inferred, which is consistent with previous reports (Knies et al., 2008). Bulk  $\delta^{15}\text{N}$  values are persistently low ( $< -1\text{‰}$ ) and mark the importance of nitrogen fixation as a source of fixed N in the stratified basin. The high  $\text{C}_{\text{org}}/\text{N}_{\text{org}}$  ratios point toward extensive selective degradation of nitrogen-rich organic compounds, despite the continuous anoxic bottom waters. Given the low reconstructed burial efficiency of 1.2%, considerable biodegradation must indeed have occurred despite the reconstructed euxinic bottom water conditions.

A minimum and maximum estimate of carbon storage in the Arctic for the *Azolla* interval has been obtained. Calculations are based on extrapolation of the organic carbon accumulation rates over the entire Eocene Arctic basin, leaving out the Nordic Sea areas. The maximum organic carbon storage of  $3.5 \cdot 10^{18} \text{ gC}$  is calculated based on accumulation rates of  $12.7 \text{ cm/kyr}$  and a time interval of 1.2 Ma for the *Azolla* interval. The minimum estimate is based on only the recovered ACEX sediments as age control and an associated accumulation rate of  $2.43 \text{ cm/kyr}$ , in which case still a substantial amount of  $9.0 \cdot 10^{17} \text{ gC}$  stored is computed. Storage of  $3.5 \cdot 10^{18} \text{ g}$  carbon roughly corresponds to a 195 - 470 ppm and  $9.0 \cdot 10^{17} \text{ gC}$  to a 55 - 120 ppm  $\text{CO}_2$  drawdown. It has been estimated that the growth of *Azolla* itself contributed at least 40% to this carbon drawdown via net carbon fixation and subsequent sequestration.

## Acknowledgements

This research used samples and data provided by the Integrated Ocean Drilling Program (IODP). Funding for this research was provided by the DARWIN centre for Biogeology. Authors



would like to thank Statoil for general support and additional samples from exploration wells. We would also like to thank Gijs Nobbe and Rinske Knoop for technical laboratory assistance.



# Chapter 3

## **Orbitally-forced *Azolla* blooms and middle Eocene Arctic hydrology: clues from palynology**

Barke, J., Abels, H.A. Sangiorgi, F., Greenwood, D.R., Sweet, A.R., Donders, T., Reichart, G.J., Lotter, A.F., and Brinkhuis, H.

*Accepted for publication in Geology*

## Abstract

The high abundances and cyclic distribution of remains of the freshwater fern *Azolla* in early middle Eocene sediments from the Arctic Ocean have previously been related to episodic surface water freshening, which was speculated to be orbitally modulated. Our integrated palynological and cyclostratigraphical analysis of the recovered 'Azolla interval' in Integrated Ocean Drilling Program (IODP) Core 302-M0004A-11X resulted in the recognition of two clear periodicities: a dominant ~1.2 m cyclicity, which we relate to changes in obliquity (~40 ka) and a weaker ~0.7 m cyclicity, which we link to precession (~21 ka). Cycles in the abundances of *Azolla*, cysts of freshwater-tolerant dinoflagellates, and swamp-vegetation pollen show co-variability in the obliquity domain. This strong correlation suggests periods of enhanced rainfall and runoff during *Azolla* blooms, presumably linked to increased local summer temperatures during obliquity maxima. *Larix* and bisaccate conifer pollen co-vary at the precession frequency, with peak occurrences corresponding to precession minima, possibly as a result of enhanced continental runoff from a more remote source area and a stronger seasonal contrast. Following the sudden demise of *Azolla* at ~48.1 Ma, runoff (cycles) continued to influence the central Arctic at decreased intensity. This and a concomitant decline in swamp-vegetation pollen suggests edaphically drier conditions on land and decreased runoff into the Arctic Ocean, causing salinity changes, which might have been fatal for *Azolla*. Moreover, a sea-level rise, inferred from overall decreasing total terrestrial palynomorph concentrations, possibly facilitated oceanic connections.

## 3.1 Introduction

The modern Arctic Ocean receives a high volume of river flow, which combined with a positive precipitation-evaporation budget of the local basin itself, results in surface water freshening in this largely enclosed basin (Hay et al., 1993; Serreze et al., 2006). The freshwater balance of the Arctic is greatly influenced by orbitally forced (latitudinal) insolation changes, which affect local precipitation and drives the poleward atmospheric heat and moisture transport (Lawrence et al., 2003; Raymo and Nisancioglu, 2003). In an Eocene climate modeling study, Lawrence et al. (2003) showed that during times of maximum seasonal insolation contrast, which could be due to both changes in precession and/or obliquity, precipitation increases over high northern hemisphere latitudes with rises in the order of 13% in Siberia, 23% in northern Greenland, and 22% in northern North America. Similar changes are simulated when changing high latitude temperatures (Held and Soden, 2006; Shellito et al., 2009).

During the Eocene Greenhouse conditions, the hydrological cycle was intensified (Huber et al., 2003) and the Arctic atmosphere contained ~2 x more water vapor compared to today (Jahren and Sternberg, 2003). A high precipitation regime prevailed in the western

and eastern Arctic, which likely resulted in enhanced freshwater runoff to the Arctic basin (Eldrett et al., 2009; Greenwood et al., 2010) that at this time was nearly entirely enclosed (Jakobsson et al., 2007). High concentrations of megaspores and microspore massulae of the freshwater fern *Azolla arctica* (Collinson et al., 2009; Chapter 5), were recovered from early middle Eocene marine sediments cored at the Lomonosov Ridge in the central Arctic Ocean (Backman et al., 2006; Brinkhuis et al., 2006). The co-occurrence of different life stages and reproductive parts of *Azolla*, and the absence of land plant detritus show that this floating fern grew *in situ* on the ocean surface (Brinkhuis et al., 2006; Collinson et al., 2009; Chapter 5). Over the recovered ~4-m-thick 'Azolla interval', concentrations of *Azolla* remains vary between 50,000 and 300,000 specimens/g dry sediment, showing that the intensity of its growth changed episodically (Brinkhuis et al., 2006). Given that *Azolla* has been restricted to freshwater systems since at least the Paleocene (Collinson, 2002), this suggests the episodic presence of a substantial freshwater cap on the surface ocean (Brinkhuis et al., 2006; Stickley et al., 2008). A stratified water column with freshwater on top of more saline deepwater is supported by siliceous microfossil data and geochemical proxies (Brinkhuis et al., 2006; Onodera et al., 2008; Stein et al., 2006; Stickley et al., 2008; Waddell and Moore, 2008).

The fluctuations in the *Azolla* concentrations are strongly cyclic and have been suggested to be orbitally forced (Brinkhuis et al., 2006). Orbitally-induced insolation changes, driving local climate as well as pole-ward atmospheric heat and moisture transport, likely influenced the amount of precipitation and freshwater discharge into the Arctic Ocean. This suggests that the episodic changes in the freshening of Arctic surface waters and subsequent *Azolla* pulses could be astronomically driven. We hypothesize that orbitally-driven *Azolla* changes are accompanied by in-phase changes in the terrestrial elements sensitive to hydrology (vegetation), and marine phytoplankton changes sensitive to salinity.

In this study, we evaluate the potentially underlying forcing mechanisms for these freshwater cycles and the final demise of *Azolla* at ~48.1 Ma by applying an integrated palynological and cyclostratigraphical approach. Furthermore, we aim to unravel potentially different impacts of individual orbital frequencies.

### 3.2 Materials and methods

The studied material derived from Site M0004A, Core 11X, between 297.31 and 302.63 mbsf, which was cored at the Lomonosov Ridge in the central Arctic Ocean during IODP Expedition 302, or Arctic coring expedition (ACEX) (Backman et al., 2006; Fig.1). Fifty-four samples, earlier investigated in the pilot study of Brinkhuis et al. (2006), were examined in detail for palynology. Here we present three aquatic palynomorph records: *Azolla* and cysts of two freshwater-tolerant dinoflagellate taxa and five pollen-based records: total bisaccate pollen, *Larix* pollen, Taxodiaceae/Cupressaceae/Taxaceae pollen (TCT-pollen), *Alnus* pollen and pollen of warm temperate angiosperms. The palynomorph records were analyzed cyclostratigraphically using spectral analysis and bandpass filtering. For details on these methods see the Supplementary Information.

### 3.3 Results

All samples yield well-preserved, rich palynomorph assemblages showing concentrations of up to 400,000 specimens/g dry sediment. The interval from 298.81 to 302.63 mbsf is dominated by *Azolla massulae* and is referred to as the 'Azolla interval' (Fig. 2A; see also Supplementary Information). Furthermore, the samples yield abundant cysts of freshwater-tolerant dinoflagellate taxa, notably *Senegalinium* spp. (Fig. 2C) and *Phthanoperidinium* spp. (mainly *P. echinatum*) (Fig. 2B) (Pross and Brinkhuis, 2005; Sangiorgi et al., 2008; Sluijs and Brinkhuis, 2009; Sluijs et al., 2005). The terrestrial assemblage is rich in angiosperm pollen, mainly deriving from the warm-temperate tree taxa *Carya*, Fagaceae,

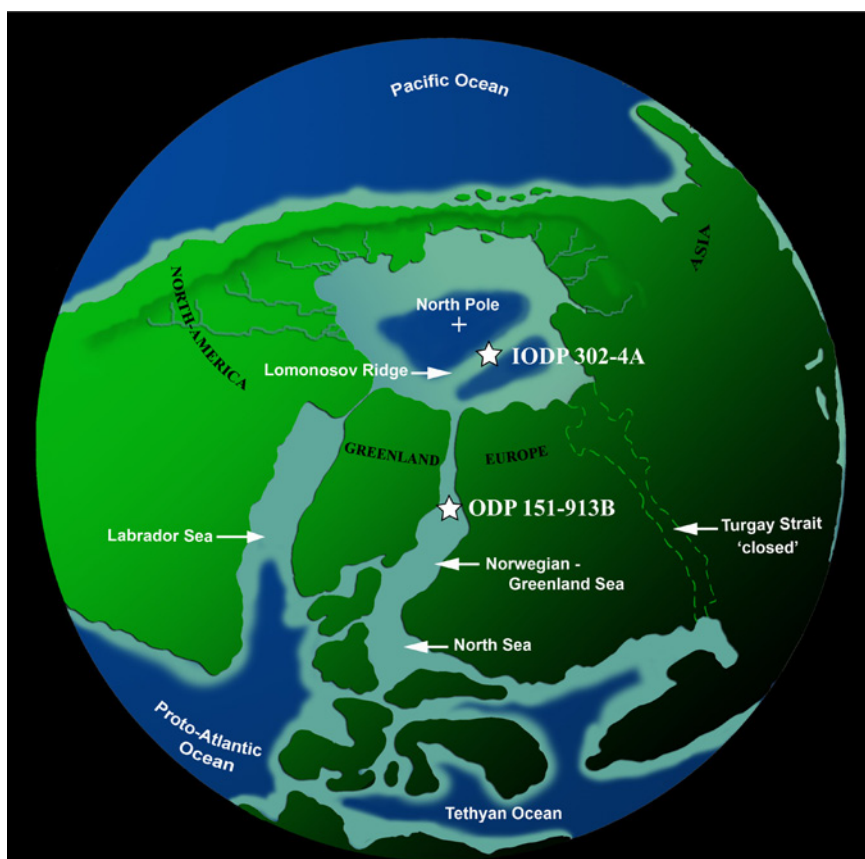


**Fig. 1.** Palaeogeographic reconstruction (middle Eocene; ~50 Ma) showing site locations of the Integrated Ocean Drilling Program (IODP) Expedition 302 (or Arctic coring expedition, ACEX) and Ocean Drilling Program (ODP) Expedition 151.

*Liquidambar*, and *Ulmus* (Fig. 2E), but also pollen of cool-temperate taxa is present, such as *Alnus* (Fig. 2F). Furthermore, the terrestrial assemblage comprises abundant gymnosperm pollen, including *Larix* pollen (Fig. 2G), bisaccate pollen deriving from evergreen conifers such as *Picea* and *Pinus* (Fig. 2H), and Taxodiaceae/Cupressaceae/Taxaceae pollen (TCT-pollen), likely including the swamp-forest genera *Metasequoia* and/or *Glyptostrobus* (Fig. 2D). These genera are common in macro-remain floras throughout the surrounding Arctic, including the middle Eocene Axel Heiberg Island assemblages (Greenwood and Basinger, 1994; Greenwood et al., 2010).

All major aquatic and terrestrial palynomorph groups reveal robust cyclic changes in their absolute and relative abundances. Abundances of *Azolla* and cysts of the freshwater-tolerant dinoflagellate taxa *Senegalinium* spp. (lower part of percentage record; Fig. 2C) and *Phthanoperidinium* spp. (Fig. 2B) co-vary and show a cyclicity with a periodicity of  $\sim 1.2$  m. Abundances of TCT-pollen (Fig. 2D) and pollen abundances of both warm- and cool-temperate angiosperms (Fig. 2E,F, respectively) reveal a similar  $\sim 1.2$  m cyclic pattern. Peaks in TCT-pollen abundances slightly lag *Azolla* peaks and the peaks in both angiosperm pollen records are associated with *Azolla* abundance minima. This opposite phase-relation between *Azolla* and angiosperm pollen abundances is maintained when TCT-pollen abundances are excluded from the pollen percentage sum. This implies that the observed phase relation is robust and independent of the TCT-pollen abundances. Abundances of *Larix* and bisaccate pollen (Fig. 2G,H, respectively), and *Senegalinium* spp. (concentration record and upper part of the percentage record; Fig. 2C) reveal cyclicity with about half the periodicity of *Azolla* cycles ( $\sim 0.7$  m).

At 298.81 mbsf, *Azolla* abundances decrease to just a few specimens/g and numbers do not increase again in the upper 150 cm of the core (Fig. 2A). Simultaneous with the final demise of *Azolla*, TCT-pollen abundances show a sharp decline and remain low in the overlying section (Fig. 2D). The palynological assemblage in the upper 150 cm of the core (297.31–298.81 mbsf) is dominated by cysts of the freshwater-tolerant dinoflagellate taxon *Senegalinium* spp. (Fig. 2C). Cyst abundances of the freshwater-tolerant dinoflagellate taxon *Phthanoperidinium* spp. continue to show a  $\sim 1.2$  m cyclic pattern after the demise of *Azolla*, albeit with a slightly decreased magnitude (Fig. 2B). Total terrestrial palynomorph concentrations gradually decrease throughout the entire core section (Fig. 2I).

### 3.4 Discussion and conclusions

Given the average sedimentation rate of  $\sim 24.3$  m/Ma, calculated for the middle Eocene interval (see Supplementary Information), we derive a duration of  $\sim 49$  ka for the dominant  $\sim 1.2$  m cyclicity and  $\sim 29$  ka for the weaker  $\sim 0.7$  m cyclicity. Taking the uncertainties in the age model (Backman et al., 2008) into account (see Supplementary Information), we are confident in relating these cycles to the astronomical-type cycles of obliquity ( $\sim 40$  ka in the early Middle Eocene; Laskar et al., 2004) and precession ( $\sim 21$  ka) respectively.

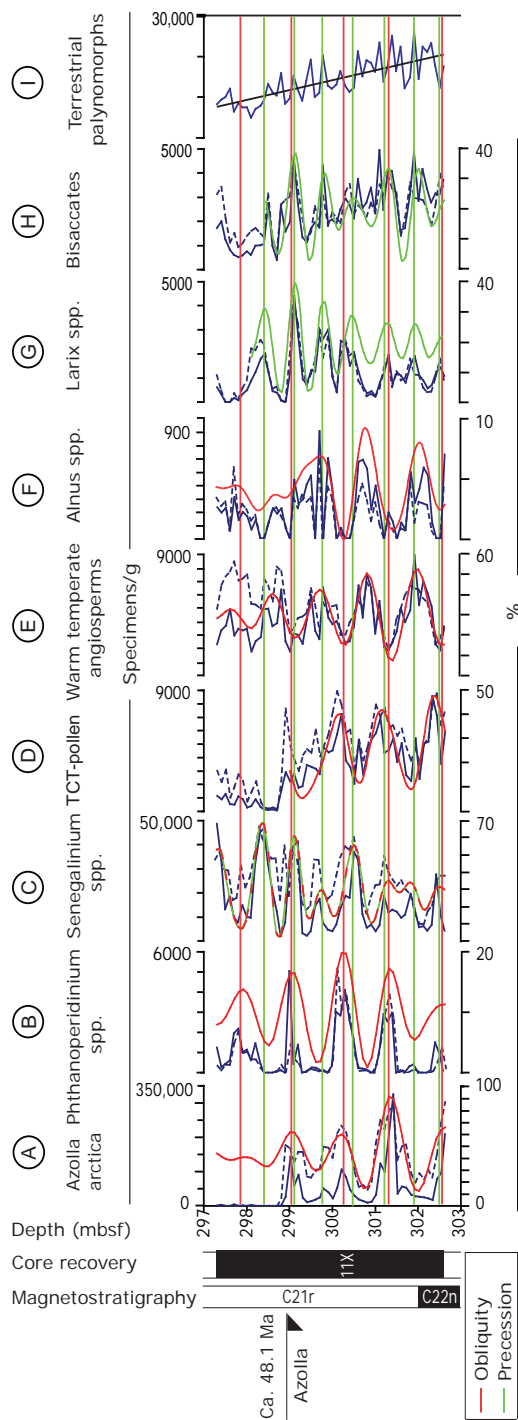


**Fig. 2.** Selection of aquatic and terrestrial palynomorph proxy data from Integrated Ocean Drilling Program (IODP) Core 302-M0004A-11X and interpreted orbital cyclicity. Concentration data (specimens/g) are given in solid blue lines with scale bars on the upper X-axes. Percentages are given in dashed blue lines with scale bars on the lower X-axes. Percentages are calculated relative to: (A) the total aquatic assemblage, (B,C) the total dinocyst assemblage, (D-G) the total of all angiosperm and gymnosperm pollen, excluding bisaccate pollen, (H) the total pollen assemblage (for details see the Supplementary Information). TCT-pollen = Taxodiaceae/Cupressaceae/Taxaceae pollen. The Gaussian bandpass filter is shown in red (Obliquity) and green (Precession). The Y-axes shows depth in meters below sea floor (mbsf), core recovery and magnetostratigraphy.



The fluctuations in the abundances of *Azolla* are positively correlated with variations in the abundances of cysts that derive from freshwater-tolerant dinoflagellates. This implies large variations in surface water salinity over time, which can be caused by local precipitation over the Arctic Ocean itself and/or river discharge. Abundances of terrestrial elements sensitive to hydrology are fluctuating synchronously with *Azolla* abundances: peaks in swamp forest pollen abundances are nearly in-phase with *Azolla* peaks, suggesting coeval swamp expansion on coastal areas surrounding the Arctic Ocean. This suggests that local precipitation changed in-phase with *Azolla*. Moreover, *Azolla* abundance minima are associated with high abundances of pollen deriving from both cool- and warm-temperate angiosperms. This anti-phase relationship of both cool- and warm-temperate angiosperms with *Azolla*, freshwater-tolerant dinoflagellates, and swamp vegetation suggests that these angiosperms are also *primarily* driven by humidity rather than by temperature during the Greenhouse conditions of the Eocene. Hence, peaks in angiosperm pollen are interpreted to indicate edaphically drier conditions on land. Spectral analysis suggests that these fluctuations are linked to obliquity. Increased obliquity leads to higher summer insolation at high latitudes (Milankovitch, 1941), which in turn might enhance total annual precipitation in the Arctic region (Held and Soden, 2006; Lawrence et al., 2003). Extant *Azolla* species are known for their very high growth rates, being able to double their biomass in only a few days (Janes, 1998a, b). Under suitable conditions this aquatic fern rapidly colonizes vast areas on freshwater bodies (Carrapico et al., 1996). Sufficient freshening of the Arctic Ocean surface waters during the growing season may have allowed rapid colonization by *Azolla* of the ocean surface during obliquity maxima. In addition, a longer growing season during an obliquity maximum could enhance the integrated annual *Azolla* flux. Conversely, declines of *Azolla* are likely associated with obliquity minima, causing lower summer insolation at high latitudes, shortening of the growing season, and probably less local precipitation and freshwater runoff. Arctic Ocean surface waters may not have become fresh enough to sustain *Azolla* growth, or only in restricted areas, or only during a limited time of the year, which would have reduced the annual integrated *Azolla* flux.

Surprisingly, a second frequency is observed in the abundances of bisaccate and *Larix* pollen, which corresponds with half the duration of the obliquity cycle. This suggests that this frequency either represents the precession cycle or a non-linear response to obliquity. Since this frequency continues also in the upper part of the record, when the lower frequency signal of obliquity becomes less clear, it most likely reflects a true precession related climate response. Precession influences seasonality and thus intensity of summer insolation at the low to mid latitudes (Milankovitch, 1941). Still, a maximum seasonal insolation difference (during precession minima on the northern hemisphere) has been shown to result in enhanced total annual precipitation in wide-ranging areas of the northern hemisphere including the high latitudes (Lawrence et al., 2003) and increased continental runoff in North America (Sloan and Huber, 2001). Since, bisaccates *primarily* represent long-distance transport (runoff), and also the large *Larix* pollen grains would have mainly been transported by water, the precession signal in these pollen abundances likely reflects

changes in continental runoff. Enhanced local runoff would, however, also have favored *Azolla* and *Phthanoperidinium* abundances, which do not show a precession frequency. Yet, the precession signal in these pollen records might reflect a more distant, somewhat lower latitude source. Runoff from a more remote source area would have carried relatively less water compared to the local freshwater discharge, though likely comprising a higher nutrient level. Hence, runoff from a more remote source area may not have freshened Arctic Ocean surface waters sufficiently to sustain the growth of *Azolla* and *Phthanoperidinium*. The fact that *Senegalinium* co-varies with *Larix* and bisaccate pollen at the precession frequency, notably in the upper part of the record, suggests that this freshwater-tolerant and heterotrophic dinoflagellate was less sensitive to small changes in salinity and may have responded to an enhanced riverine nutrient input during precession minima. Moreover, bisaccates are produced by evergreen conifers, which are expected to be more tolerant to subfreezing rather than to milder winter temperatures at high latitudes. Subfreezing temperatures would have prevented evergreen conifers from staying metabolically active and consuming their resources during the several month of winter darkness, when photosynthesis is inhibited (LePage, 2003; Read and Francis, 1992). Hence, peaks in bisaccate pollen abundances, which go together with peaks in pollen, deriving from the cold-temperate conifer *Larix*, may correspond to times of maximum seasonal contrast during precession minima.

The final demise of *Azolla* may have occurred when surface waters no longer became sufficiently fresh during the growing season. Although the dinocyst assemblage is furthermore dominated by freshwater-tolerant taxa and abundances of normal marine taxa are low, suggesting the continued presence of low-salinity surface waters, it is conceivable that a slight increase in salinity could have crossed the critical threshold of salinity tolerance for *Azolla*. A reduction in the concentrations of *Phthanoperidinium* may be an indication of such a subtle salinity increase. Concomitantly with the *Azolla* demise, TCT-pollen abundances show a marked decline. This may reflect edaphically drier conditions on the surrounding coastal areas that diminished the swamp habitats and favored the growth of angiosperm vegetation. Furthermore, a sea-level rise may be inferred from the overall decrease in total terrestrial palynomorph concentrations. The *Azolla* interval is concomitant with a sea-level low stand correlated to Chron 21r (~49 Ma; Miller et al., 2005). A subsequent sea-level rise could have facilitated oceanic connections, causing a salinity increase that may have become lethal for *Azolla*, while salt-water intrusion onto the coastal areas would have drastically diminished the salt-intolerant swamp forests.

## Acknowledgments

We thank L. Bik, N. Welters and J. van Tongeren for their great support and C. Greenwood, J.H.A. van Konijnenburg-van Cittert and H. Visscher for their pollen analytical assistance. J. van der Burgh and M.E. Collinson are thanked for discussions on the ecology of *Azolla* and F.J. Hilgen and L.J. Lourens for discussions on spectral analysis. Jerry Dickens and two anonymous reviewers are also acknowledged. This research used samples and

data provided by the Integrated Ocean Drilling program (IODP). This is publication number DW-2009-5006 of the Darwin Center for Biogeosciences, which partially funded this project. Furthermore, we thank Statoil for their financial support. DRG's research is supported by the Natural Sciences and Engineering Research Council of Canada.

## Supplementary Information

### Material

IODP Expedition 302 cored site M0004A on the Lomonosov Ridge (87.87°N; 136.18°E) at 1288 meter water depth (Backman et al., 2006). Cores from several lithological units were recovered, including Unit II between 223.56 and 313.61 meter below sea floor (mbsf) (Moran et al., 2006). This Unit is characterized by very dark gray mud-bearing biosiliceous ooze and shows microlaminations on submillimeter-scale with dark, organic-rich laminae alternating with lighter, marine siliceous laminae (Backman et al., 2006; Brinkhuis et al., 2006). Core 11X, between 297.31 and 302.63 mbsf, is unusual in that it contained extreme abundances of remains of the freshwater fern *Azolla* between 298.81 and 302.63 mbsf. For the underlying Core 12X, between 301.35 and 306.35 mbsf, only 0.4% of sediment was recovered from the core catcher, which still contained *Azolla* remains. There was no recovery for cores 13 and 14. Core 15, between 313.35 and 315.35 mbsf, comprised 13% of recovered sediment, which no longer contained *Azolla* remains. Thus, the onset of the *Azolla* interval is uncertain from available information on the Lomonosov Ridge, it is located somewhere between Core 12 and Core 15. The 'Azolla interval' as referred to in this publication, points to the recovered part of this interval from 298.81 to 302.63 mbsf).

### Age assessment

Sedimentation rates for the mid-Eocene section including the *Azolla* interval were initially estimated at 12.7 m/Ma (Backman et al., 2008). However, recently performed wavelet analysis for parts of this interval (Pälike et al., 2008) has shown that sedimentation rates are comparable to the overlying Eocene section (Unit 2, Core 302-M0002A-55X), which are estimated at ~20 m/Ma by Pälike et al. (2008) and 24.3 m/Ma by Backman et al. (2008). Based on a sedimentation rate of 24.3 m/Ma, a minimum duration of 160 ka was estimated for that part of the *Azolla* interval recovered during ACEX (Speelman et al., 2009b; Chapter 2). The absolute age of 48.1 to 49.3 Ma (based on the Gradstein et al., 2004 timescale) and full maximum duration of 1.2 Ma of the *Azolla* interval can be inferred from high latitude sites in the North Atlantic Ocean (e.g., Ocean Drilling Program ODP Leg 151 Site 913; (Eldrett et al., 2004), which received modest amounts of *Azolla*, presumably transported from the Arctic Ocean (Speelman et al., 2009b; Chapter 2).

### Palynological analysis

Fifty-four samples with 10 cm spacing were processed for palynology at the Laboratory of Palaeobotany and Palynology at Utrecht University using HCl (30%) and cold HF (40%) with no oxidation and sieving over a 15 and 250 µm mesh (for details see Wood et al., 1996). Slide-mounted residues were examined under the light microscope. For dinocyst quantification a minimum of 200 dinocysts was counted for most samples. Dinocysts were identified following nomenclature cited in Fensome and Williams (2004); environmental

interpretations followed Pross and Brinkhuis (2005), Sluijs et al.(2005) and Sluijs and Brinkhuis (2009). Other aquatic palynomorphs counted include remains of the freshwater fern *Azolla*, acritarchs, and remains of fresh to brackish water algae like *Cymatiosphaera* spp. and *Tasmanites* spp. Percentages of *Azolla* were calculated based on the total aquatic assemblages. Percentages of individual dinocyst taxa were based on the total dinocyst counts to prevent overprint of the freshwater signal. Also for the terrestrial palynomorph assemblage a minimum count of 200 pollen and spores was aimed for. However, since some samples yielded only little terrestrial palynomorphs, counts were normally between 100 and 245 specimens, with an average of about 180. Pollen and spore identification was based on Moore et al. (1991) and McIntyre (1991). Furthermore, spores were counted. Pollen percentages were calculated on the total of all angiosperm and gymnosperm pollen, excluding bisaccate pollen to prevent bias by long-distance transport. Bisaccate pollen percentages were calculated relative to the total pollen.

### Time series analysis

Time series analysis was performed on the palynomorph records and on selected species records in the depth domain. For this analysis *Analyseries* version 1.1.1 (Paillard et al., 1996) was used, applying the Blackman-Tukey spectral analysis, using compromise settings and a 90% confidence interval. Power spectra were calculated and a Gaussian bandpass filter was reconstructed, which were plotted together with the data (see Fig. 2A-H).



# Chapter 4

## **Obliquity-forced middle Eocene Arctic hydrology – a micropaleontological and cyclostratigraphical approach**

Barke, J., Sangiorgi, F., Abels, H.A., Stickley, C.E., Reichart, G.J.,  
Lotter, A.F., and Brinkhuis, H.

*To be submitted*

## Abstract

The high abundances and cyclic distribution of remains of the freshwater fern *Azolla* in early middle Eocene sediments from the Arctic Ocean (Integrated Ocean Drilling Program Expedition 302, Core M0004A-11X) have previously been related to obliquity-forced episodic surface-water freshening. In order to further test this concept we examined organic-walled dinoflagellate cyst (dinocyst) assemblages from the same core. Abundances of freshwater-tolerant hexaperidinioid dinocysts co-vary with *Azolla* abundances and confirm enhanced surface-water freshening at times of *Azolla* blooms. These periods of increased precipitation and/or runoff are likely linked to enhanced local summer insolation during obliquity maxima. Combined with siliceous microfossil assemblage analysis, performed on the interval of one *Azolla* cycle, this indicates that throughout the entire obliquity cycle waters were stratified during the growing season, with a fresher surface water layer atop. However, during obliquity minima, a slight increase in surface-water salinity, shallowing of the halocline, and/or less stable hydrodynamic conditions (i.e., mixing) may have strongly reduced *Azolla* abundances. Following the sudden demise of *Azolla* at ~48.1 Ma, runoff (cycles) continued to influence the central Arctic at decreased intensity. Changes in the composition of the dinocyst assemblages indicate a slight increase in salinity concurrent with the final demise of *Azolla*, which likely became lethal for *Azolla*.

## 4.1 Introduction

An intensified hydrological cycle characterized the Greenhouse conditions of the early Paleogene (Huber *et al.*, 2003) with the Arctic atmosphere containing approximately twice the amount of water vapor than today (Jahren and Sternberg, 2003). A high precipitation regime prevailed in the western and eastern Arctic that likely resulted in much enhanced freshwater runoff to the semi-enclosed Arctic Basin (Hay *et al.*, 1993; Serreze *et al.*, 2006; Jakobsson *et al.*, 2007; Greenwood *et al.*, 2010). Analysis of central Arctic Ocean sediments, recovered during the Arctic coring expedition (ACEX; Integrated Ocean Drilling Program (IODP) Expedition 302), revealed that low-salinity, stratified surface-water conditions prevailed throughout the latest Paleocene to middle Eocene (e.g., Sluijs *et al.*, 2008; Sangiorgi *et al.*, 2008a,b; Stickley *et al.*, 2008; Onodera *et al.*, 2008). A further increase in surface-water freshening is likely to have occurred in the early middle Eocene for a maximum duration of ~1.2 Myrs (between 48.1 - 49.3 Ma), indicated by the enormous amounts of remains of the freshwater fern *Azolla* recovered from the ACEX sediments (Brinkhuis *et al.*, 2006; Backman *et al.*, 2006; Speelman *et al.*, 2009b; Chapter 2). Through several lines of evidence it has been shown that this freshwater fern (*Azolla arctica*) grew *in situ* within Arctic Ocean surface-waters, implying the sustained presence of a fresh surface-water layer



(Brinkhuis et al., 2006; Collinson et al., 2009; Chapter 5). A stratified water column with fresher water on top of more saline deeper is supported by siliceous microfossil data and an array of geochemical proxies (Brinkhuis et al., 2006; Onodera et al., 2008; Stein et al., 2006; Stickley et al., 2008; Waddell and Moore, 2008).

The lower-middle Eocene ACEX sediments of the *Azolla* interval are finely laminated with alternating dark, organic rich layers and light, biosilica-rich layers at millimeter to submillimeter scale. Within this *Azolla* interval, the dark layers are dominated by *Azolla* remains, whereas the light-colored layers are dominated by siliceous microfossils (Backman et al., 2006; Brinkhuis et al., 2006). These laminae are thought to reflect alternations of early spring brackish phytoplankton blooms followed by a late spring to summer precipitation increase and stable stratified fresh surface waters allowing rapid chrysophyte and *Azolla* growth (Brinkhuis et al., 2006).

Superimposed on these annual laminations, *Azolla* abundances furthermore show cyclic fluctuations at  $\sim 1.2$  m. These cyclic fluctuations indicate that freshening of Arctic surface-waters occurred in major episodes that were suggested to be orbitally forced (Brinkhuis et al., 2006). In an Eocene climate modeling study, Lawrence et al. (2003) showed that during times of maximum seasonal insolation contrast, which could be due to both changes in precession and/or obliquity, precipitation increases over high Northern Hemisphere latitudes with 13% in Siberia, 23% in northern Greenland, and 22% in northern North America. This suggests that the episodic freshening of Arctic surface-waters and subsequent *Azolla* pulses may thus have been astronomically driven. We hypothesize that these orbitally-driven changes in Arctic Ocean hydrology will also be reflected in the assemblage composition of siliceous and organic micro-organisms sensitive to changes in salinity.

In this study, we aim to better constrain the effect of orbital forcing on the Arctic Ocean hydrology at a time when the Arctic was still ice-free by applying an integrated micropaleontological and cyclostratigraphical approach. We aim to gain further insights into the potentially underlying forcing mechanisms for the cyclic fluctuations in the *Azolla* abundances and the eventual demise of *Azolla* at  $\sim 48.1$  Ma. Furthermore, we aim to unravel potentially different impacts of individual orbital frequencies.

## **4.2 Material & Methods**

### **4.2.1 Study site**

IODP Expedition 302, or the Arctic coring expedition (ACEX), cored site M0004A on the Lomonosov Ridge (87.87°N; 136.18°E) at 1288 meter water depth (Backman et al., 2006). Cores from several lithological units were recovered, including Unit II between 223.56 and 313.61 meters below sea floor (mbsf) (Moran et al., 2006). This Unit is characterized by very dark gray mud-bearing biosiliceous ooze and shows fine laminations on submillimeter-scale with dark, organic-rich laminae alternating with lighter, biosiliceous laminae (Backman et al., 2006; Brinkhuis et al., 2006). Core 11X, (297.31 to 302.63 mbsf), is unusual in that

it contains very high abundances of the remains of the freshwater fern *Azolla* between 298.81 and 302.63 mbsf. *Azolla* remains are also found in the core catcher of Core 12X. Between Cores 12X and 15 X there is a coring gap and in Core 15X *Azolla* remains are no longer present. Hence the 'Azolla interval' covers the stratigraphic section between the last (abundant) occurrence of *Azolla* at 298.81 mbsf in Core 11X downward including at least Core 12X, but may extend to somewhere within the coring gap above Core 15X.

### 4.2.2 Age assessment

Sedimentation rates for the lower-middle Eocene section including the *Azolla* interval were initially estimated at 12.7 m/Ma (Backman et al., 2008). However, recently performed wavelet analysis for parts of this interval (Pälike et al., 2008) has shown that sedimentation rates are comparable to the overlying Eocene section (Unit 2, Core 302-M0002A-55X), which are estimated at ~20 m/Myrs by Pälike et al. (2008) and 24.3 m/Ma by Backman et al. (2008). Based on a sedimentation rate of 24.3 m/Ma, a minimum duration of 160 ka was estimated for the part of the *Azolla* interval recovered during ACEX (Speelman et al., 2009b; Chapter 2). The absolute age of 48.1 to 49.3 Ma (based on the Gradstein et al., 2004 timescale) and maximum duration of ~1.2 Myrs of the *Azolla* interval can be inferred by correlation to high latitude sites in the North Atlantic Ocean (e.g., Ocean Drilling Program ODP Leg 151 Site 913; Eldrett et al., 2004), which received modest amounts of *Azolla*, presumably transported from the Arctic Ocean (Speelman et al., 2009b; Chapter 2).

### 4.2.3 Palynological analysis

Fifty-four samples from Core M0004A-11X between 297.31 to 302.63 mbsf, were processed for palynology using HCl (30%) and cold HF (40%) with no oxidation and sieving over a 15 and 250 µm mesh (for details see e.g., Wood et al., 1996). These samples were earlier investigated in the preliminary study of Brinkhuis et al. (2006) and are here examined in detail, particularly focusing on the organic-walled dinoflagellate cysts (dinocysts). Slide-mounted residues were analyzed under the light microscope. For quantitative analysis a minimum of 200 dinocysts were counted for most samples. Besides dinocysts, also other aquatic palynomorphs were included in the quantitative counts such as remains of the freshwater fern *Azolla*, acritarchs, and remains of fresh to brackish water algae like *Cymatiosphaera* spp. and *Tasmanites* spp. Percentages of *Azolla* were calculated based on the total aquatic assemblage. Percentages of individual dinocyst taxa are based on the total dinocyst counts to prevent overprint of the freshwater signal. Dinocysts were identified following nomenclature cited in Fensome and Williams (2004). New species are discussed in the Appendix. Environmental interpretations followed Pross and Brinkhuis (2005), Sluijs and Brinkhuis (2009), Sluijs et al. (2008), and Sluijs et al. (2005). The Peridinioid-Gonyaulacoid ratio (the P/G-ratio) is often used as proxy for palaeoproductivity (cf. Pross and Brinkhuis, 2009; Sluijs et al., 2005; Sluijs and Brinkhuis, 2009). This proxy is based on likely differences in feeding strategy between peridinioid- and gonyaulacoid dinoflagellates; the former being mainly heterotrophic and the latter autotrophic (see also discussion in Sluijs and Brinkhuis,

2009). The ratio is calculated based on the number of individual specimens of peridinioid cysts, divided by the total number of specimens of peridinioid and gonyaulacoid cysts. Co-occurring sporomorphs are discussed in chapter 3.

#### 4.2.4 Time series analysis

Time series analysis was performed on the palynomorph records and on selected species records in the depth domain. For this analysis *Analyseries* version 1.1.1 (Paillard et al., 1996) was used, applying the Blackman-Tukey spectral analysis, using compromise settings and a 90% confidence interval. Power spectra were calculated and a Gaussian bandpass filter was reconstructed, which were plotted together with the data (see Fig. 2A-H).

#### 4.2.5 Siliceous microfossil (silicofossil) assemblage analysis

Six sediment samples were analyzed between 299.02 to 300.12 mbsf for one *Azolla* cycle. For silica-selective processing these organic-rich, carbonate-poor sediments required only oxidation of organic matter (hot 30% hydrogen peroxide) and removal of clays. For quantitative analysis, 1 ml of divinylbenzene microspheres (concentration  $3.28 \times 10^6$  spheres/ml) was added to each of the digested samples prior to slide preparation (Battarbee and Kneen, 1982). Slides were analyzed for their silicofossil content at magnification x1000 using a Zeiss Axioplan microscope with Plan-NEOFLUAR objectives. The following five groups were encountered and tallied: diatoms (both resting spores and vegetative valves), chrysophyte cysts, ebridians, silicoflagellates and siliceous endoskeletal dinoflagellates (e.g., actiniscidians). At least 500 individual silicofossils per sample were tallied. The silicofossil aspect to this study is trialed here to assess the potential for multi-proxy micropaleontology studies throughout the entire *Azolla* interval. Abundances of the 3 most important groups in the ACEX sediments – the diatoms, ebridians and chrysophyte cysts – are indicated in this study.

### 4.3 Results

Dinocysts abundances range between ~9,000 and ~135,000 specimens per gram of sediment. Nineteen dinocyst genera were identified of which seven belong to the Peridinioid lineage (P-cysts) and twelve to the Gonyaulacoid lineage (G-cysts; for illustrations see Plate I-IV). The P-cysts *Deflandrea* sp. A, *Deflandrea* sp. B, *Lentinia* spp., and *Senegalinium* spp. may dominate the dinocyst assemblage in certain intervals. Furthermore, there are frequent to abundant occurrences of the P-cysts *Cerodinium depressum*, *Phthanoperidinium echinatum*, *Phthanoperidinium* sp. A, *Palaeocystodinium* spp., *Wetzeliella articulata*, and *Charlesdowniea clathrata* (Fig. 1). All these P-cysts derive from dinoflagellate genera that are suggested to be low-salinity-tolerant (Pross and Brinkhuis, 2005; Sluijs et al., 2005; Sluijs et al., 2008; Sluijs and Brinkhuis, 2009; Sangiorgi et al., 2008a,b). The most abundant G-cysts are *Cribooperidinium* spp., *Impagidinium* spp., *Operculodinium*

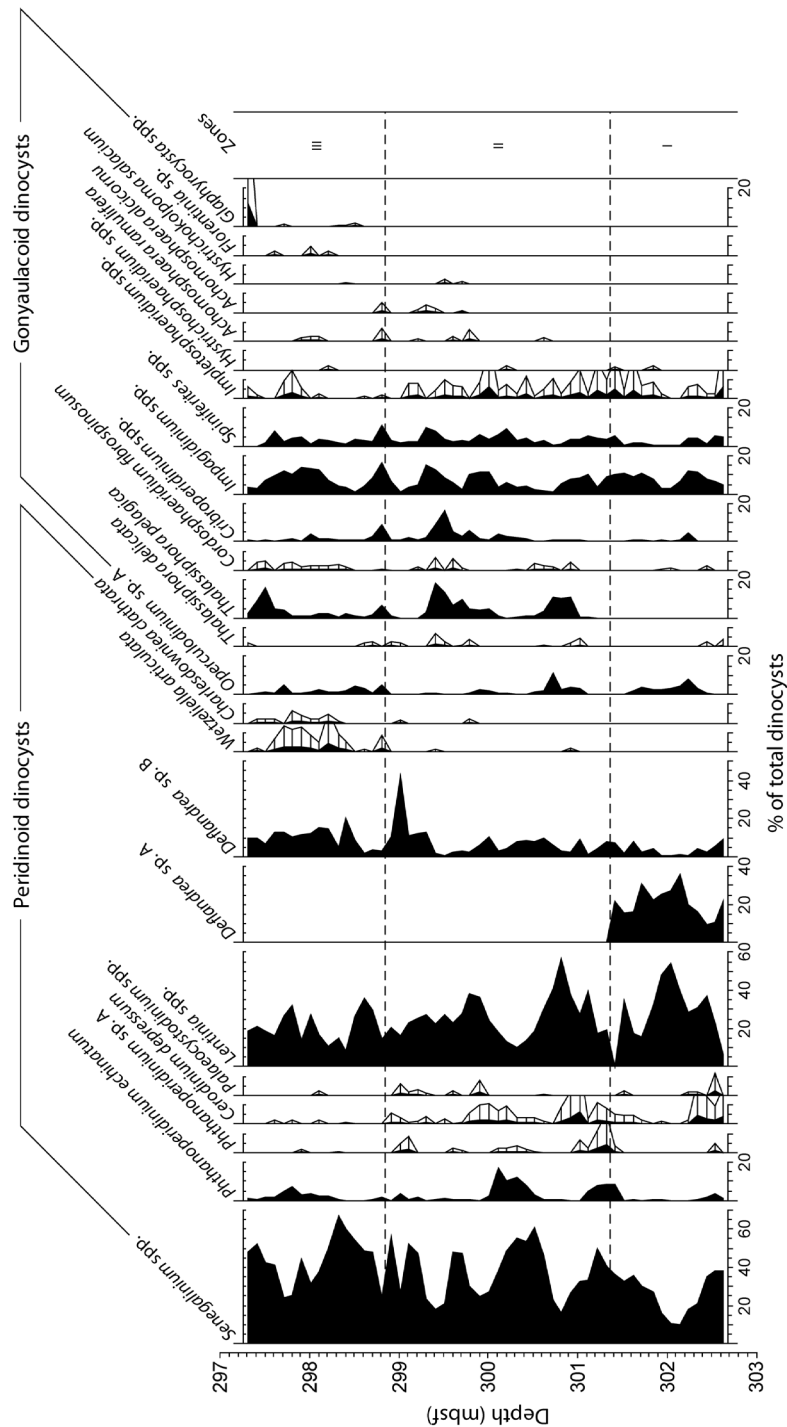


Fig.1 . Relative changes in the dinoflagellate cyst assemblage throughout the studied section of Integrated Ocean Drilling Program (IODP) Core 302-M0004A-11X. For taxa that have relatively low abundances (maximum abundance below 10%), a 5x exaggeration is illustrated.

sp.A, *Spiniferites* spp., and *Thalassiphora pelagica*. *Glaphyrocysta* spp. show a single high abundance at 297.31 mbsf. Furthermore, there are frequent to few occurrences of the G-cysts *Achomoshiaeridium alaicornu*, *Achomosphaeridium ramulifera*, *Cordosphaeridium fibrospinosum*, *Impletosphaeridium* spp., *Florentinia* sp., *Hystrichokolpoma salacium*, *Hystrichosphaeridium* spp., and *Thalassiphora delicata* (Fig. 1). Most of these G-cysts are documented to derive from dinoflagellate genera that are typically reflecting open marine conditions (Pross and Brinkuis, 2005; Sluijs et al., 2005; Sluijs et al., 2008).

There are important compositional changes in the dinocyst assemblage throughout the section. Based on these compositional changes, three zones may be distinguished, (Fig.1); within zone I (301.35 to 302.63 mbsf) representatives of the low-salinity tolerant genera including *Deflandrea* sp. A, *Lentinia* spp., and *Senegalinium* spp. dominate the assemblage. At the boundary from zone I to II *Deflandrea* sp. A disappears. Within zone II (298.81 to 301.35 mbsf), representatives of the low-salinity-tolerant dinoflagellate genera *Cerodinium depressum* and *Lentinia* spp. show an overall decrease, whereas representatives of the dinoflagellate genera restricted to open marine conditions such as *Achomoshiaeridium alaicornu*, *Achomosphaeridium ramulifera*, *Hystrichokolpa salacum*, *Cordosphaeridium fibrospinosum*, and *Thalassiphora pelagica* show their first (consistent) occurrences. The boundary between zone II and III at 298.81 mbsf corresponds to the last occurrence of abundant *Azolla*. Representatives of the low-salinity-tolerant dinoflagellate genera *Cerodinium depressum*, *Phthanoperidinium* sp. A, and *Palaeocystodinium* spp. occur only sporadically within zone III (297.31 to 298.81 mbsf), whereas *Wetzeliiella articulata*, *Charlesdowniea clathrata* and more open marine taxa *Florentinia* sp. and *Glaphyrocysta* spp. have their first consistent occurrences.

The relative and absolute abundances of many of the dinocysts reveal the same ~1.2 m cyclic pattern as apparent in the *Azolla* abundances (Fig. 2). Peaks in the various dinocysts follow successively one another with peaks in cysts of low-salinity-tolerant dinoflagellates *Senegalinium* spp. (lower part of the percentage record; Fig. 2 B) and *Phthanoperidinium* spp. (Fig. 2C) showing in-phase changes with *Azolla arctica* (Fig. 2A), followed by successive peaks in *Cerodinium depressum* (Fig. 2D) and *Lentinia* spp. (Fig. 2E). Thereafter follow peaks in the open marine forms *Operculodinium* sp. A (Fig. 2F), *Thalassiphora* spp. (Fig. 2G), and *Cordosphaeridium fibrospinosum* (Fig. 2H), which are in anti-phase with *Azolla*. The ~1.2 m cyclicity retains in most of these dinocysts after the final demise of *Azolla* at 298.81 mbsf, although for the low-salinity-tolerant taxa *Cerodinium depressum*, *Lentinia* spp. and *Phthanoperidinium* spp. (Fig. 2C-E) at a decreased magnitude. In contrast, *Senegalinium* spp. abundances (Fig. 2B) reveal a ~0.7 m cyclicity in the upper part of the record. Moreover, the ratio between the Peridinioid (P) and Gonyaulacoid (G) cysts (the P/G-ratio) shows a ~ 0.7 m cyclicity (Fig. 2I).

The silicofossil assemblage analysis performed for the interval from 299.02 to 300.12 mbsf, spanning one *Azolla* cycle, shows highest total silicofossil concentrations (~160 x 10<sup>6</sup> specimens/g) concurrent with the *Azolla* abundance minimum at 299.42 mbsf (Fig. 2J). Lowest concentrations (~ 60 x 10<sup>6</sup> specimens/g) correlate with the *Azolla* peaks

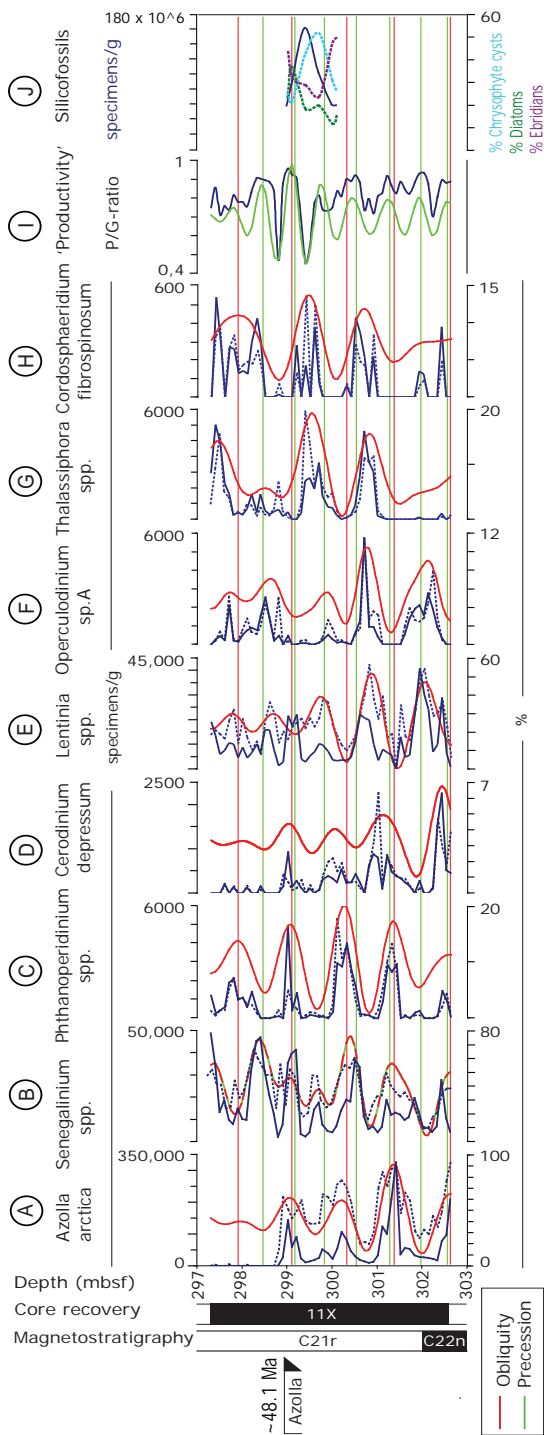


**Fig. 2.** Selection of dinoflagellate cyst proxy data from Integrated Ocean Drilling Program (IODP) Core 302-M0004A-11X and interpreted orbital cyclicity. Concentration data (specimens/g) are given in solid blue lines with scale bars on the upper X-axes. Percentages, calculated relative to the total dinocyst assemblage, are given in dashed blue lines with scale bars on the lower X-axes. The Gaussian bandpass filter is shown in red (Obliquity) and green (Precession). The Y-axes shows depth in meters below sea floor (mbsf), core recovery and magnetostratigraphy.

at 299.02 and 300.12 mbsf. Chrysophyte cysts are the most abundant silicofossils by our counting methods, followed consecutively by ebridians then diatoms (Fig. 2J). Our counting methods give a conservative estimate of the abundance of chrysophyte cysts relative to the other siliceous algal groups in the ACEX sediments. For example, if numbers of cells were reconstructed then diatom abundance would be even lower compared to chrysophyte cysts. While chrysophyte cyst abundances are highest during the *Azolla* abundance minima and lowest during *Azolla* peaks, ebridian abundances are positively correlated with *Azolla* abundances. Diatom abundances show two peaks at 299.12 and 299.72 mbsf, which correspond to peaks in *Senegalinium* spp. abundances (Fig. 2B) and to peaks in the P/G-ratio (Fig. 2I). Abundances of silicoflagellates are relatively low and do not vary significantly within this interval.

## 4.4 Discussion

The dinocyst assemblage is dominated by low-salinity-tolerant hexaperidinioids and also the silicofossil assemblage yields a high abundance of cysts of freshwater chrysophytes, which reflects the overall fresh Arctic surface-water conditions at the time of the *Azolla* interval. Concomitant occurrences of cysts of open marine gonyaulacoid dinoflagellates and the presence of brackish to marine silicofossils such as ebridians, diatoms, and silicoflagellates, suggests the presence of higher salinity waters likely underlying the freshwater surface.

Given the average sedimentation rate of ~24.3 m/Myrs calculated for the middle Eocene interval, we derive a duration of ~49 kyr of the dominant ~1.2 m cyclicity and of ~29 kyr of the weaker ~0.7 m cyclicity. Taking the uncertainties in the age model (Backman et al., 2008) into account, we are confident in relating these cycles to the astronomical-type cycles of obliquity (~40 kyr in the early middle Eocene; Laskar et al., 2004) and precession (~21 kyr), respectively.

Many dinocysts show an obliquity frequency in their relative and absolute abundances. Peak abundances of the various taxa successively follow each other with a small phase-lag. Cysts of freshwater-tolerant peridinioid dinoflagellates, co-varying with *Azolla* abundances, are thought to have peaked during obliquity maxima, when enhanced summer insolation probably escalated rainfall and freshwater runoff to the Arctic Ocean (Chapter 3). The halocline was probably stable and deep throughout the growing seasons and the surface waters were sufficiently fresh, creating suitable conditions for *Azolla* to bloom on widespread areas of the ocean surface. The high peridinioid abundance during *Azolla* peaks furthermore implicates enhanced eutrophic conditions. These peridinioid dinoflagellates likely thrived in the fresh surface-water layer together with *Azolla*. Ebridians, that also show highest relative abundances during *Azolla* peaks, were likely living in the higher salinity suboxic subsurface-waters, where they may have profited from abundant food and reduced competition in this light and oxygen limited waters below the thick *Azolla* mats.

Cyclic changes in the abundance of the low-salinity-tolerant dinoflagellates *Cerodinium depressum* and *Lentinia* spp. follow cycles in the *Azolla* abundances with a small

phase-lag, suggesting that these taxa are less sensitive to slight changes in ocean surface salinity.

Peak abundances of cysts deriving from open marine gonyaulacoid dinoflagellates correlate with *Azolla* abundance minima and are consequently linked to obliquity minima. The abundance of the gonyaulacoid *Thalassiphora pelagica* is indicative of stratified waters (e.g., Sluijs et al., 2005) and the high abundance of cysts of freshwater chrysophytes suggest that a strong halocline existed throughout the growing season during obliquity minima. Whereas chrysophytes were likely living in the fresh surface-water layer above the halocline, open marine gonyaulacoid dinoflagellates likely thrived in the more saline subsurface waters. Chrysophytes, as well as gonyaulacoid dinoflagellates are thought to have been autotrophic as inferred from their extant representatives (Sluijs et al., 2005; Stickley et al., 2008). Their high abundance during obliquity minima suggests that waters were more oligotrophic at these times. During obliquity maxima, a dense *Azolla* cover probably significantly reduced light conditions and restricted the growth of other photosynthetic organisms. The reason that *Azolla* abundances were reduced during obliquity minima, despite the presence of a low-salinity surface-water layer, may be due to a slight increase in surface ocean salinity and a shortening of the growing season. Arctic Ocean surface-waters may only have become sufficiently fresh in restricted areas, or only during a limited time of the year, to sustain *Azolla* growth, which would have reduced the annual integrated *Azolla* flux.

A second, but weaker cyclicity is apparent in the P/G-ratio and in the upper part of the *Senegalinium* record, which we can relate to the precession frequency. The precession signal in this high latitude record is thought to reflect changes in runoff from more distant, somewhat lower latitude sources, resulting from variations in seasonal insolation at low and mid latitudes, affecting the intensity of precipitation and runoff (Chapter 3). In contrast, to the local precipitation and runoff induced by obliquity that likely resulted in high volumes of freshwater entering the Arctic Ocean, runoff from more remote source areas, affected by precession, may have carried higher amounts of nutrients, but relatively less volume of freshwater. This is corroborated by the P/G ratio that shows precession frequency, suggesting changes in productivity in the Arctic Ocean that were likely caused by external nutrient supply. The fact that *Senegalinium* spp. abundances fluctuate at the precession frequency in the upper part of the record suggests that this freshwater-tolerant and heterotrophic dinoflagellate was less sensitive to small changes in salinity and may have responded to increased riverine nutrient input during precession minima. Contrarily, *Phthanoperidinium* spp. continues to show obliquity frequency, suggesting that this taxon was more sensitive to slight changes in salinity and responded primarily to the local freshwater runoff.

The compositional changes in the dinocyst assemblage at the transition from interval I to II likely indicate a slight increase in salinity since the number of genera of representatives of open marine dinoflagellates increases substantially, whereas representatives of low-salinity tolerant dinoflagellates show an overall decrease in abundances. This subtle increase in salinity may explain the overall decreasing trend in *Azolla* abundances within this zone. At the transition from interval II to III, concurrent with the final demise of *Azolla*, a decline



in low-salinity-tolerant dinoflagellates and several first occurrences of representatives of open marine taxa suggest an increase in ocean surface-water salinity. It is conceivable that even slight increases in salinity and mixing could have crossed the critical threshold of salinity tolerance for *Azolla* and may have become fatal for this water fern. Conspicuously, following the *Azolla* demise, runoff cycles continued to influence the Arctic Ocean albeit at decreased magnitude, indicated by the reduced amplitude of cycles in the cyst abundances of the low-salinity-tolerant dinoflagellate *Lentinia* spp. and *Phthanoperidinium* spp. Whether this increase in salinity is a consequence of enhanced oceanic connections as hypothesized by Brinkhuis et al. (2006) or a result of a reduction in local precipitation and freshwater discharge into the Arctic Ocean remains unknown. A climate modeling study by Shellito et al. (2009) suggests that opening the Arctic Ocean results in an increase of regional precipitation by 30-50% through increased ocean and atmospheric heat transport through this region and enhanced convective activity. This implies that the influx of saltier water due to increased oceanic connections and outflow of freshwater from the Arctic will be compensated by enhanced precipitation and runoff into the Arctic Basin. Thus, if enhanced oceanic connections would have caused the salinity increase at the end of the *Azolla* interval, the influx of saltier water had a bigger impact on surface-water salinity than the additional freshwater discharge into the Arctic Basin.

## 4.5 Concluding remarks

Palynological and cyclostratigraphical examination of the changing dinocyst assemblages in the *Azolla* interval of central Arctic Core 302-M0004A-11X reveals cyclic fluctuations in the dinocyst abundances that are dominantly driven by the ~40 ka obliquity cycle. Cysts abundances of freshwater-tolerant dinoflagellates co-vary with *Azolla* abundances and suggest enhanced surface-water freshening at times of *Azolla* blooms, likely corresponding to obliquity maxima. Integrated siliceous microfossil data, performed for the interval of one *Azolla* cycle, indicate that throughout the entire obliquity cycle waters were stratified (during the growing season) with a low-salinity surface layer atop. However during obliquity minima, slightly less precipitation and runoff as well as a shorter growing season likely caused a subtle increase in surface-water salinity and restricted the extension and/or duration of *Azolla* growth and likely reduced the annual integrated *Azolla* flux. A second and weaker frequency is mainly shown in the peridinioid/gonyaulacoid-ratio, which we relate to the ~21 ka precession cycle. A high P/G-ratio, implying enhanced productivity, is likely associated with precession minima and is probably a response to increased external nutrient supply as a result of enhanced continental runoff from more distant, somewhat lower latitude sources. Previously, all hexaperidinioid dinoflagellates were almost indiscriminately considered to be 'low-salinity-tolerant' without distinction (e.g., Sluijs and Brinkhuis, 2009). Using the present results, with apparently subtle changes in the dinoflagellate communities reflecting slightly differing salinities, we are now able to propose a more refined scheme of relative salinity

## Chapter 4

tolerance for typical Eocene hexaperidinoids (see Table 1). Our findings suggest that among organic-walled dinoflagellate cysts, representatives of *Phthanoperidinium* appear to be most tolerant towards freshwater conditions, followed by *Senegalinium* spp. Non hexa-styled peridinoids like *Wetzeliiella* and *Charlesdowniea* spp. appear to be less tolerant towards very low salinities but have an intermediate position (Table 1).

**Table 1.** Interpreted relative salinity tolerance of the dinocyst genera and species encountered in Integrated Ocean Drilling Program (IODP) Core 302-M0004A-11X.

Dinocyst genera	Dinocyst species	Interpreted salinity tolerance
<i>Phthanoperidinium</i>	<i>Phthanoperidinium echinatum</i> <i>Phthanoperidinium</i> sp.A	Freshwater
<i>Senegalinium</i>	<i>Senegalinium</i> spp.	Fresh to brackish water
<i>Cerodinium</i>	<i>Cerodinium depressum</i>	
<i>Lentinia</i>	<i>Lentinia</i> spp.	
<i>Palaeocystodinium</i>	<i>Palaeocystodinium</i> spp.	
<i>Deflandrea</i>	<i>Deflandrea</i> sp.A	
<i>Deflandrea</i>	<i>Deflandrea</i> sp.B	
<i>Wetzeliiella</i>	<i>Wetzeliiella articulata</i> <i>Charlesdowniea clathrata</i>	Brackish water
<i>Thalassiphora</i>	<i>Thalassiphora delicata</i> <i>Thalassiphora pelagica</i>	Stratified conditions with reduced thickness of fresh surface layer
<i>Impletosphaeridium</i>	<i>Impletosphaeridium</i> spp.	Open Marine
<i>Operculodinium</i>	<i>Operculodinium</i> sp.A	
<i>Cordosphaeridium</i>	<i>Cordosphaeridium fibrospinosum</i>	
<i>Achomosphaeridium</i>	<i>Achomosphaeridium alaicornu</i> <i>Achomosphaeridium ramulifera</i>	
<i>Spiniferites</i>	<i>Spiniferites</i> spp.	
<i>Cribroperidinium</i>	<i>Cribroperidinium</i> spp.	
<i>Impagidinium</i>	<i>Impagidinium</i> spp.	
<i>Hystrichosphaeridium</i>	<i>Hystrichosphaeridium</i> spp.	
<i>Hystrichokolpoma</i>	<i>Hystrichokolpoma salacium</i>	
<i>Florentinia</i>	<i>Florentinia mantellii</i>	
<i>Glaphyrocysta</i>	<i>Glaphyrocysta</i> spp.	

Following the sudden demise of *Azolla* at ~48.1 Ma, runoff (cycles) continued to influence the central Arctic at decreased intensity. The compositional changes in the dinocyst assemblage indicate a slight increase in salinity coeval with the final demise of *Azolla*, which likely became lethal for *Azolla*.

## **Acknowledgements**

We thank L. Bik, N. Welters and J. van Tongeren for their great support. F.J. Hilgen and L.J. Lourens are thanked for discussions on spectral analysis. This research used samples and data provided by the Integrated Ocean Drilling program (IODP). The Darwin Center for Biogeosciences partially funded this project. Furthermore, we thank Statoil for their financial support.

Plate I.

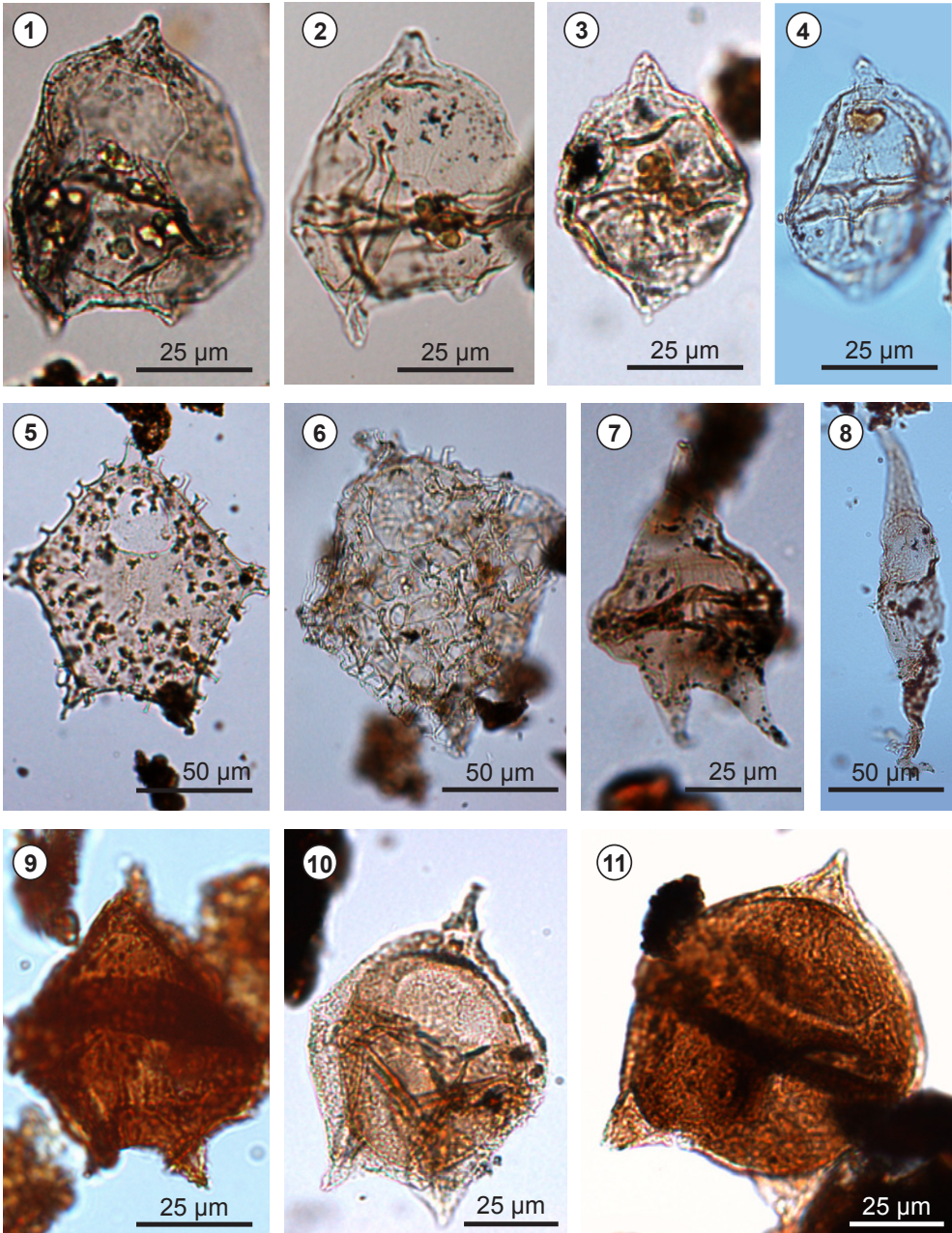


**Plate I.**

- (1) *Senegalinium* spp.; dorsal view; (Sect.:1; Interval: 1-3)
- (2) *Senegalinium* spp. ventral view; (Sect.:1; Interval: 1-3; Coordinates: L18,2-L19,1)
- (3) *Phthanoperidinium* sp. A (Sect.:1; Interval: 103-105 cm; Coordinates: M28,2)
- (4) *Phthanoperidinium echinatum* (Sect.:2; Interval: 21-23 cm; Coordinates: 18-118)
- (5) *Wetzeliiella articulata* (Sect.:1; Interval: 61-63 cm; Coordinates: F17,2)
- (6) *Charlesdowniea clathrata* (Sect.:2; Interval: 21-23 cm; Coordinates: M16,4)
- (7) *Cerodinium depressum* (Sect.:1; Interval: 51-53 cm; Coordinates: J17)
- (8) *Palaeocystodinium* spp. (Sect.:1; Interval:1-3 cm; Coordinates:30.5/118.5)
- (9) *Lentinia* spp.
- (10) *Deflandrea* sp. B (Sect.:2; Interval: 21-23 cm; Coordinates: Q30,1-3)
- (11) *Deflandrea* sp. A (Sect.:3; Interval: 131-133 cm; Coordinates: N31,2)



Plate II.

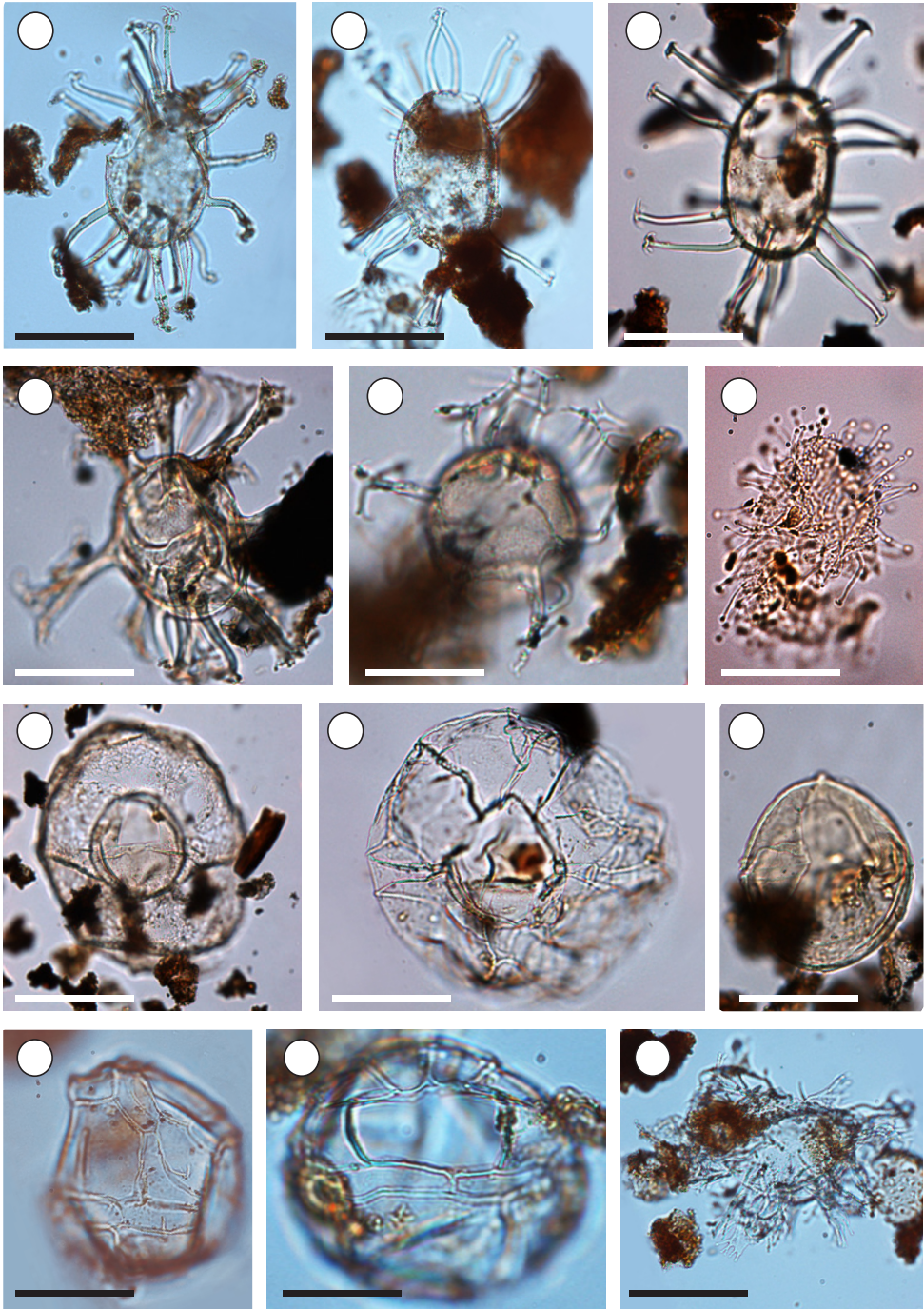


**Plate II.**

- (1) *Operculodinium* sp. A; lateral view; (Sect.:3; Interval: 41-43 cm; Coordinates: 20.5/112.5)
- (2) *Operculodinium* sp. A; dorsal view; (Sect.:3; Interval: 41-43 cm; Coordinates: 24/125)
- (3) *Operculodinium* sp. A; dorsal view; (Sect.:4; Interval: 31-33 cm; Coordinates: K27,1-3)
- (4) *Cordosphaeridium fibrospinosum* (Sect.:1; Interval: 111-113 cm; Coordinates: P19,3)
- (5) *Spiniferites* spp. (Sect.: 2; Interval: 1-3 cm; Coordinates: R25,1-2)
- (6) *Impletosphaeridium* spp. (Sect.:1; Interval: 51-53 cm; Coordinates: N21,4-N22,3)
- (7) *Thalassiphora pelagica* (Sect.:1; Interval: 91-93 cm; Coordinates: M30,2-4)
- (8) *Thalassiphora delicata* (Sect.:3; Interval: 141-143 cm; Coordinates: G27)
- (9) *Cribroperidinium* spp. (Sect.:2; Interval: 1-3 cm; Slide 2; Coordinates: J22,2)
- (10) *Impagidinium* sp. A; (Sect.:1; Interval: 1-3 cm; Slide 1; Coordinates: 27.5/131) note that the sulcal plate 'as' is enlarged in this species
- (11) *Impagidinium* sp. A (Sect.:1; Interval: 1-3 cm; Slide 1; Coordinates: 26/119)
- (12) *Glaphyrocysta* spp. (Sect.:1; Interval: 1-3; Coordinates:23.5/118.5)

Plate III.

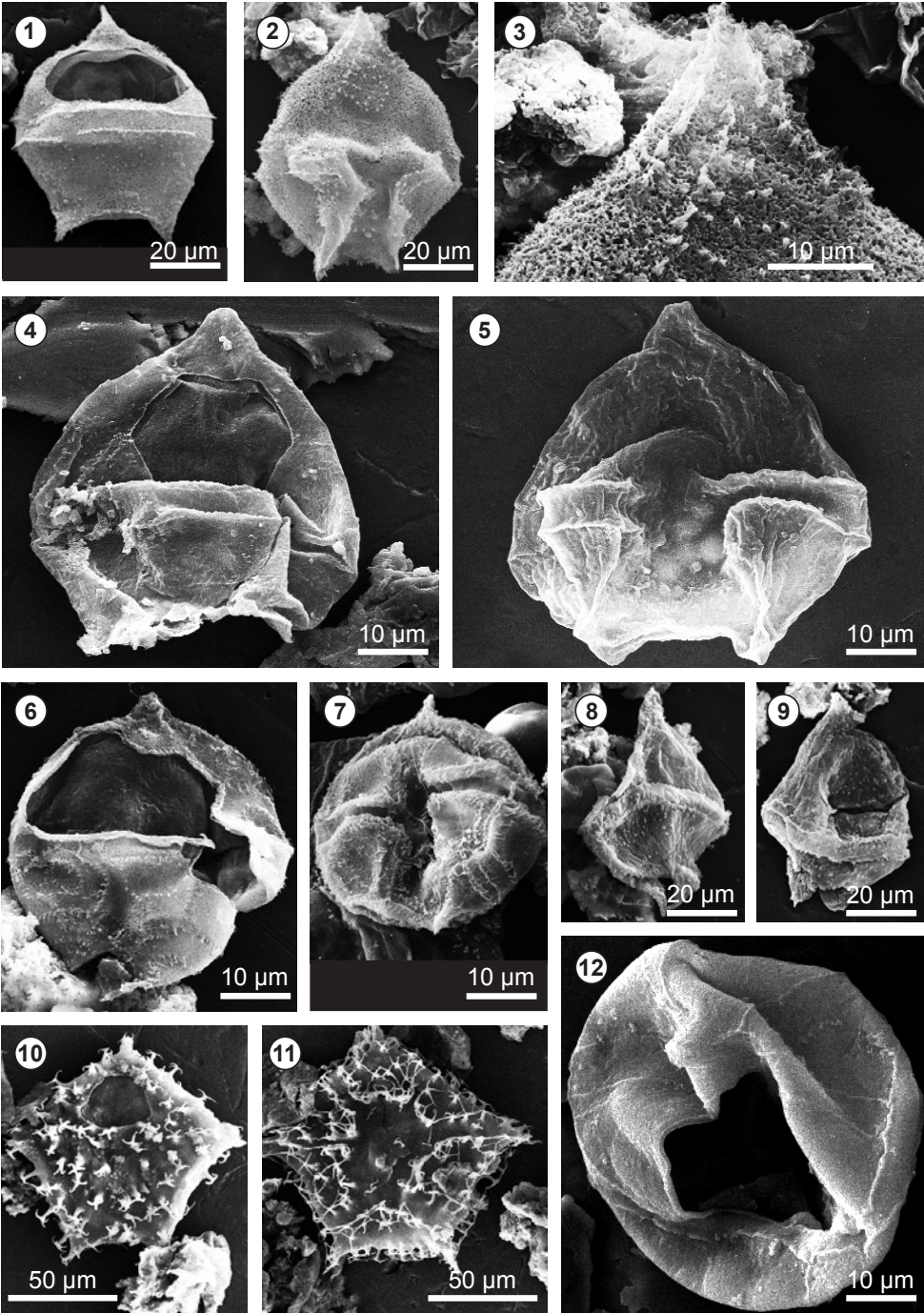




**Plate III.**

- (1) *Deflandrea* sp. B; dorsal view (Sect.:1)
- (2) *Deflandrea* sp. B; ventral view (Sect.:1)
- (3) *Deflandrea* sp. B; detail of (Plate 3, 2); (Sect.:1)
- (4) *Senegalinium* spp.; dorsal view (Sect.:1; Interval: 1-3)
- (5) *Senegalinium* spp.; ventral view (Sect.:1)
- (6) *Phthanoperidinium echinatum*; dorsal view (Sect.:1)
- (7) *Phthanoperidinium echinatum*; ventral view (Sect.:1; Interval: 1-3)
- (8) *Lentinia* spp.; lateral view (Sect.:1; Interval: 1-3)
- (9) *Lentinia* spp.; dorsal view (Sect.:1)
- (10) *Wetzeliella articulata*; dorsal view (Sect.:1)
- (11) *Charlesdowniea clathrata*; ventral view (Sect.:1)
- (12) *Cribroperidinium* spp.; note distorted apical complex and archeopyle representing 3" (Sect.:1)

Plate IV.

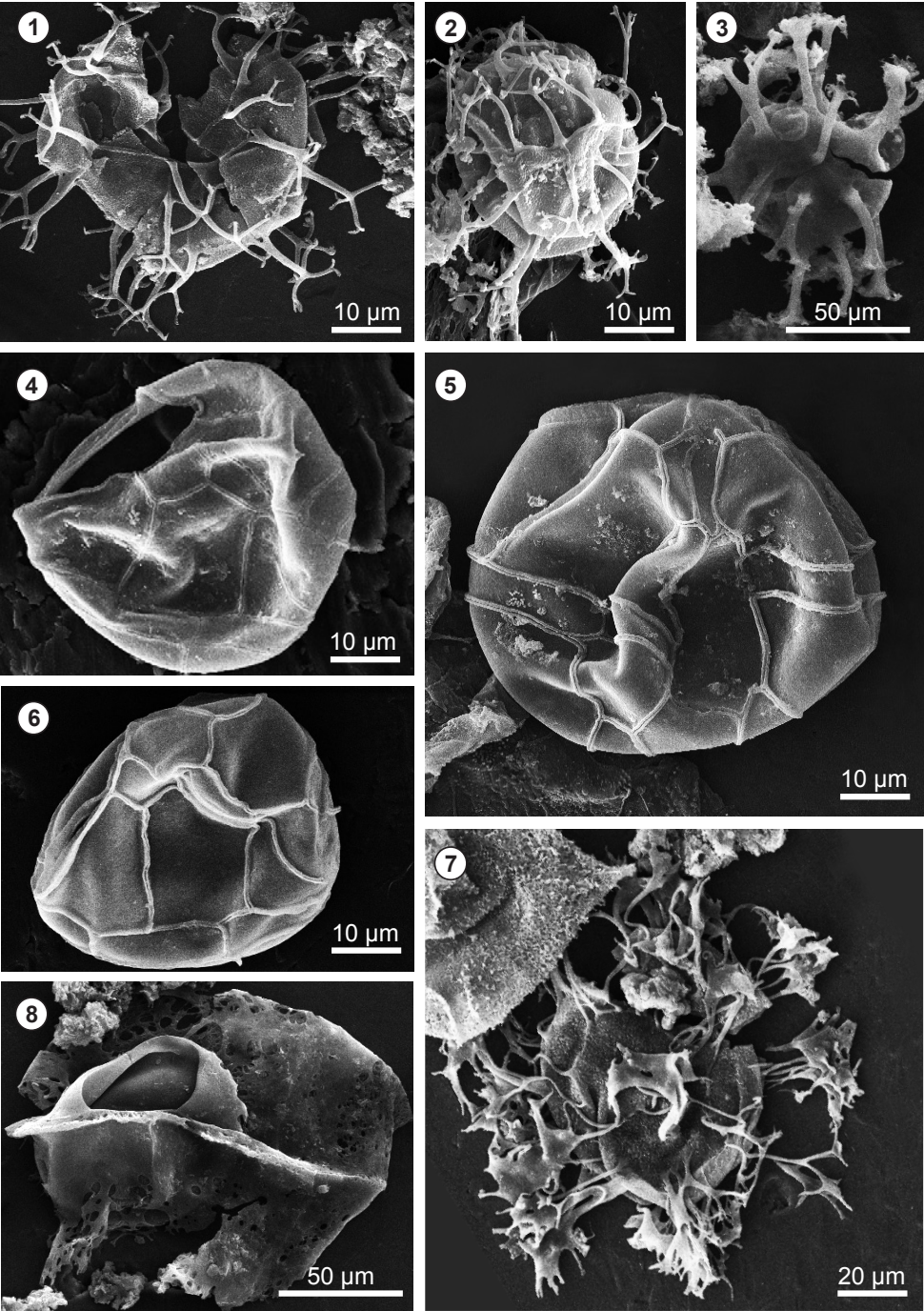


**Plate IV.**

- (1) *Spiniferites* spp. (Sect.:1)
- (2) *Spiniferites* spp. (Sect.:1; Interval: 1-3)
- (3) *Cordosphaeridium fibrospinosum* (Sect.:1)
- (4) *Impagidinium* sp. A (Sect.:1)
- (5) *Impagidinium* sp. A (Sect.:1; Interval: 1-3)
- (6) *Impagidinium* sp. A (Sect.:1; Interval: 1-3)
- (7) *Glaphyrocysta* spp. (Sect.:1; Interval: 1-3)
- (8) *Thalassiphora pelagica* (Sect.:1)

## Appendix

### List of dinocyst taxa and taxonomic remarks

The allocation of taxa into genera and species follows the nomenclature cited in Fensome and Williams (2004). Some new taxa have been recorded and are discussed below and will formally be described elsewhere. Plate references for illustrated taxa are given in brackets.

*Achomoshaeridium alaicornu*

*Achomosphaeridium ramulifera*

*Cerodinium depressum* (Plate I, 7)

*Cribroperidinium* spp. (Plate II, 9; Plate III, 12)

*Cordosphaeridium fibrospinosum* (Plate II, 4)

*Deflandrea* sp. A (Plate I, 11)

**Remarks.** This taxon closely resembles *Deflandrea striata*, but differs by having a less prominent apical horn and lacking the typical connection of both antapical horns by a phragm.

*Deflandrea* sp. B (Plate I, 10; Plate III, 1-3)

**Remarks.** The morphology of this taxon lies in between the genera *Cerodinium* and *Deflandrea*. Most aspects are reminiscent of the broad morphology of *Deflandrea phosphoritica*, but differs in having a more equidimensional archaeopyle (archaeopyle index ~1). The wall structure of *Deflandrea* sp B differs from *D. phosphoritica* by having a microreticulate periphragm with an often partly denticulate ornamentation. Denticles are typically between 1-1,5 µm long and are predominantly present along the apical horn on the ventral side, on the 1' apical plate (intratabular arrangement), and along the longitudinal furrow of the cinulum.

*Florentinia*. sp. (Plate IV, 3)

**Remarks.** This taxon resembles *Florentinia mantellii*, but is smaller, and has more slender processes. The archaeopyle is often difficult to discern, likely involving all apical and one (3'' ?) precingular plate. There is a chance that this taxon represents specimens reworked from Upper Cretaceous strata.

*Glaphyrocysta* spp. (Plate II,12; Plate IV,6)

*Hystrichokolpoma salacium*

*Hystrichosphaeridium* spp.

*Impletosphaeridium* spp. (Plate II,6)

*Impagidinium* spp. (Plate II,10-11; Plate IV,4-5)

*Lentinia* spp. (Plate I, 9; Plate III, 8-9)

*Operculodinium* sp. A (Plate II, 1-3)

**Remarks.** This species of *Operculodinium* is characterized in having a distinctly oval shaped outline of the cyst.

*Palaeocystodinium* spp. (Plate I, 8)

*Phthanoperidinium echinatum* (Plate I, 4; Plate III, 6-7)

*Phthanoperidinium* sp. A (Plate I, 4)

**Remarks.** This species of *Phthanoperidinium* is characterized by having large pustules on the periphragm surface and by having a distinct apical and antapical horn.

*Senegalinium* spp. (Plate I, 1-2; Plate III, 4-5)

*Spiniferites* spp. (Plate II, 5; Plate IV, 1-2)

*Thalassiphora delicata* (Plate II, 8; Plate IV, 7)

*Thalassiphora pelagica*

*Wetzeliella articulata* (Plate I, 5; Plate III, 10)

*Charlesdowniea clathrata* (Plate I, 6; Plate III, 11)



# Chapter 5

## **A new species of the freshwater fern *Azolla* (Azollaceae) from the Eocene Arctic Ocean**

Collinson, M.E., Barke, J., van der Burgh, J., and van Konijnenburg-van Cittert, J.H.A.

*Published in Review Palaeobotany and Palynology, 155, 1-14, 2009*

## Abstract

A new fossil species of the freshwater fern *Azolla* (Azollaceae, Salviniales) is described from an unusual setting of high palaeolatitude in the Arctic Ocean. *Azolla arctica* sp. nov., (lower Middle Eocene, Lomonosov Ridge) is represented by fully developed megaspore apparatuses with attached microspore massulae and clustered and dispersed microspore massulae. These abundant co-occurring fossils, combined with their associated biota, demonstrate that *Azolla* was growing and reproducing on a freshwater surface of the Eocene Arctic Ocean. *Azolla arctica* is compared with other fossil *Azolla* species, especially those from around Arctic and Nordic Seas. It documents new characteristics for the genus. The megaspore apparatus is small with a thin megaspore wall and a distinctive exoperine where nodular exoperinal masses fuse at several levels resulting in a rugulate, undulating, punctate to foveolate exoperine surface. Microspore massulae have two size classes of glochidia, short (<25 µm) and long (>55 µm), the anchor-shaped tips lack recurved flukes. **These distinctive characters provide the potential to recognise *Azolla arctica* as fragmentary remains in palynological preparations from drill cores. Therefore, future comparisons with other fossils will reveal if a single species grew across the Arctic Ocean and if freshwater spills from the Arctic spread into the Nordic Seas.**

## 5.1 Introduction

*Azolla* Lamarck is a free-floating freshwater fern with an excellent fossil record from the Cretaceous onwards (Collinson, 1980, 1991; Vadja and McLoughlin, 2005). There are about 8 species from the Paleocene to Miocene represented by fertile whole plants (summarised in Batten and Collinson, 2001, p. 14), which are very similar in habit and gross morphology to the modern species and which, combined with associated fossils and sedimentological evidence, confirms the existence of the modern genus *Azolla* as a free-floating freshwater plant since at least the Paleocene (Collinson, 2002). Many other fossil species of *Azolla* are represented by the megaspores and microspore massulae of this heterosporous genus (Collinson, 1980, 1991; Batten and Collinson, 2001; Vadja and McLoughlin, 2005) which frequently are found in attachment or co-occurrence. The discovery of *Azolla* megaspores and microspore massulae at very high palaeolatitudes in an oceanic setting, namely in middle Eocene sediments of the Lomonosov Ridge in the Arctic Ocean, led Brinkhuis et al. (2006) to infer an episodic freshening of warm Arctic Ocean surface waters during an approximately 800,000 year interval. Brinkhuis et al. (2006) also noted that there were widespread *Azolla* occurrences in middle Eocene deposits of all the Nordic seas and suggested that these probably resulted from freshwater spills from the Arctic Ocean. In order to further test this hypothesis it will be essential to determine if the Arctic and Nordic Sea occurrences represent a single species of *Azolla*. Therefore, the aim of this paper is to present a full and



detailed description of the Arctic Ocean *Azolla* material. The Arctic Ocean *Azolla* is compared with existing species, as far as is possible with the sometimes limited existing data, and the most similar species are identified for future more detailed comparative study.

## 5.2 Materials and Methods

### 5.2.1 Samples

Some specimens were studied in palynological slides from Integrated Ocean Drilling Program, Arctic Coring Expedition (IODP ACEX) leg 302, Site 4, Hole A, Core 011X (Brinkhuis et al., 2006). The specimens illustrated in this paper, and which form the basis for the diagnosis and description, were studied in mesofossil preparations (see below for methods) from the same core from section 3W at level 133-136 cm (top 301.64 metres below sea floor (mbsf) and 293.1 metres composite depth (mcd)); section 3W at level 132-133 cm (top 301.62 mbsf and 301.62 mcd) and from section 1W at level 111-113 cm (mbsf and mcd 298.41) and 2W at level 111-113 cm (mbsf and mcd 299.91). Polished thin sections, perpendicular to microlaminations, of sediment samples from 1W 111-113 cm and 3W 133-136 cm were made by embedding in epoxy resin (EPO FIX, Struers Ltd., Solihull, UK) and polishing to standard thickness. They were examined by LM and SEM, the latter using an Hitachi (Hitachi High Technologies Corporation, Tokyo, Japan) S-3000N SEM in variable pressure mode at 70Pa with back scatter detector. Material is housed in the Laboratory of Palaeobotany and Palynology (Utrecht).

### 5.2.2 Sample processing and study

For level 111-113 cm dry sediment samples (5gm aliquots) were disaggregated in hot water followed by a short treatment with 30% H<sub>2</sub>O<sub>2</sub>. Residues were sieved retaining everything larger than 125 µm and this material was sorted under a binocular microscope. *Azolla* specimens were picked with fine brushes and then cleaned for 3 days in 30% hydrofluoric acid with a brief HCl treatment first (no reaction) and a brief HCl rinse prior to neutralisation. For scanning electron microscopy (SEM) specimens were mounted using glue (Bostik; Bostik Ltd, Leicester, UK) on a coverglass, sputter coated with gold in a Polaron (Quorum Technologies Ltd., Ringmer, UK) E1500 sputter coater, and examined in either an Hitachi (Hitachi High Technologies Ltd., Tokyo, Japan) S3500N SEM or a FEI (FEI Company, Hillsboro, Oregon, USA) Quanta 200F field emission ESEM.

Specimens for transmission electron microscopy (TEM) were mostly taken from section 1W and 2W at level 111-113 cm with one megaspore apparatus and one microspore massulae cluster from section 3W at 133-136 cm. Specimens were removed from the SEM stubs intact by gently brushing on the adhesive with acetone where necessary. Specimens were embedded in Spurr (Agar Scientific Ltd., Stanstead, UK) resin. Sections 60 nm thick were cut with a Diatome (Diamond AG, Biel, Switzerland) diamond knife using a Riechert Ultracut E ultramicrotome (Leica Microsystems, GmbH, Wetzlar, Germany), and examined unstained using an Hitachi (Hitachi High Technologies Corporation, Tokyo, Japan) H-7600

TEM. All sections of the megaspore apparatus were cut in a near median longitudinal plane from proximal to distal pole (or along their longest axis when the surface hair covering and compaction prevented identification of the poles). The TEM images herein are therefore directly comparable with those in Collinson (1991) and Batten and Collinson (2001). Representative semi-thin sections were dried onto microscope slides and stored without mounting medium or coverslips.

For levels 132-133 cm and 133-136 cm (Utrecht) samples (ca 1cc) were cleaned and oven dried overnight at 60°C. Agepon (Agfa-Gavaert, art Nr AKX2P, Leverkusen, Germany) wetting agent was added and samples were then treated with HCl and HF in standard palynological treatment, the residues sieved through 250 µm mesh and the retained fraction examined under a binocular microscope. Specimens were picked for SEM and rinsed in distilled water before mounting. Specimens were mounted from a droplet of water onto negative film attached to the stub with Araldite (Ciba Speciality Chemicals Holding Inc. distributed by Bostik Ltd, Leicester, UK) (see Moore et al., 1991) coated with gold in a Bal-Tec (Balzers, Liechtenstein) SCD 050 sputter coater and examined with a JEOL (Tokyo, Japan) JSM 5300 SEM (Leiden), or coated with platinum using a Cressington 208hr sputter coater (Cressington Scientific Instruments, Watford, England) and examined under a Philips (Eindhoven, The Netherlands) XL30S FEG SEM (Utrecht). Samples for light microscopy were mounted in glycerine jelly and sealed with permanent laquer (Rambo Panster Jachtlak, Sigma Kalon, Uithoorn, The Netherlands) and these mounts were used for measurements of the megaspore apparatus, microspore massulae, microspores and glochidia sizes. Some specimens (stated in figure legends) were embedded in polyethylene glycol 2000 (Scientific Polymer Products, Inc., Ontario, New York, USA) and hand sectioned and the sections studied by light microscopy (LM). A few specimens (stated in figure legends) were briefly (ca 5 mins) treated with Schulze's solution ( $\text{KClO}_3$  & 30%  $\text{HNO}_3$ ) prior to light microscopy. LM photographs (5MB) were captured with a Konica KD 500Z digital camera. Unless stated in the figure legends digital images (LM, SEM or TEM) have not been manipulated other than to enhance contrast or brightness of the entire image.

### 5.2.3 Descriptive terminology and classification

The diagnosis follows the sequence, style and terminology of those in Batten and Collinson (2001) to enable comparison with *Azolla* species from the North Sea Basin, which have so far been studied in detail with SEM and TEM. The *Azolla* megaspore apparatus is subdivided into a distal megaspore and a proximal float system. The term 'float' is a misnomer as it has been demonstrated conclusively that the floats do not render the megaspore more buoyant (Fowler, 1975; Dunham and Fowler, 1987). *Azolla* microspores are not shed but contained within a perine-derived microspore massula, the outer surface of which is usually ornamented with hairs (glochidia), often barbed, which readily become attached to hairs (filosum) on the surface of the megaspore apparatus. For further details of *Azolla* morphology see Batten and Collinson (2001 and references cited). The classification follows Smith et al. (2006). Exoperine surface terminology follows Punt et al. (2007).

## 5.3 Systematic palaeobotany

### 5.3.1 Taxonomic status

Order—Salviniales Britt.

Family—Azollaceae Wettstein

Genus—*Azolla* Lamarck

Species—*Azolla arctica* Collinson et al., sp. nov.

### 5.3.2 Specific diagnosis

Megaspore apparatus oblong with obtuse poles ca 350-400  $\mu\text{m}$  long, ca 250  $\mu\text{m}$  in maximum width. Megaspore inferred to be spherical to subspherical when uncompressed, 200-250  $\mu\text{m}$  in diameter with a trilete mark at the proximal pole, laesurae extend up to two-thirds of the radius of spore, lips very slightly elevated. Entire megaspore apparatus covered with a thick ( $>8 \mu\text{m}$ ) mat of intertwined hairs (0.3-0.6  $\mu\text{m}$  in diameter) which arise almost entirely from the proximal region of the megaspore (hence suprafilosum). Remnants of megasporocarp wall, one cell layer thick, firmly attached over the proximal pole of the megaspore apparatus. Megaspore wall consisting of an exine ca 1-2  $\mu\text{m}$  thick and a two-layered perine ca 3-4  $\mu\text{m}$  thick. Megaspore surface finely rugulate under the transmitted light microscope. Under SEM and in thin section under TEM the inner surface of the exine forming a more or less continuous membrane beneath a more open structure; small irregular cavities dominating the exine and the endoperine, giving both a spongy, porous appearance; exoperine consisting of contorted nodular or clavate to tabular masses, (1-2  $\mu\text{m}$  in thickness) with a solid exterior but alveolate interior, supported on sparse short narrow columns (usually less than 0.5  $\mu\text{m}$  in width) ; exoperinal masses partially fused at different levels producing a rugulate undulating exoperine surface, finely and irregularly perforate, varying from punctate to foveolate, occasionally fossulate (maximum dimension of perforations 0.2-2.0  $\mu\text{m}$ ) and rugulae typically  $<1 \mu\text{m}$  in width). Occasional rare hairs extend from the exoperine (hence infrafilosum) in the distal parts of the megaspore. Exoperinal excrescences absent. Perine expanded in thickness and becoming spongy in structure near the proximal pole of the spore forming a collar; collar encircling the megaspore and giving rise to numerous hairs of the suprafilosum extending up into the central region of the float zone, and out onto the outer surface of the entire megaspore apparatus.

Float system a compact dome-shaped structure occupying the apical third of the megaspore apparatus, extending over the apical part of the megaspore; floats numerous, 15 to 18, loosely organised in three tiers. Floats spongy, pseudovacuated in structure, discoidal to spherical in shape and enmeshed by hairs of the suprafilosum.

Microspore massulae single or grouped in clusters, irregular in shape with a thin outer wall, internally spongy, vacuolated in structure. Massulae contain up to 15 smooth walled trilete microspores (20-25  $\mu\text{m}$  in diameter), laesurae extending up to two thirds of the radius of the spore. Outer surface of microspore massulae with numerous aseptate glochidia in two size classes, long glochidia  $>55 \mu\text{m}$ , shorter glochidia ( $<25 \mu\text{m}$ ) often in

bundles, each glochidium with a broad basal attachment, narrow lower stalk and broader upper stalk with a distal dilation and constriction below an anchor shaped tip, flukes narrow abruptly and lack recurved hooks.

Holotype—U22874.

Paratypes—Figured material U22875. Other referred material – U22876.

Etymology—from the Arctic Ocean where the material was discovered.

Locality—IODP Leg 302, Hole 4A, Core 011X, Lomonosov Ridge, Arctic Ocean (Brinkhuis et al., 2006).

Stratigraphy—lowermost Middle Eocene, lower part of Chron C21r, from ca 49 to ca 48.3 Myr ago (Brinkhuis et al., 2006).

## 5.4 Additional descriptive notes and discussion of morphology

### 5.4.1 Megaspore apparatus – general organisation

In general the shape is oblong with obtuse ends (Fig. 1, 1, 2; Plate I, 1, 2), but many specimens are somewhat distorted by compaction resulting in foreshortening in the longer dimension (Plate I, 3). The maximum length is ca 400  $\mu\text{m}$ , which is smaller than in many fossil *Azolla* species (e.g. Sweet and Hills, 1976; Batten and Collinson, 2001). A single specimen was found in which the filosum and floats had been displaced revealing the megaspore (Plate I, 4). Dissection revealed the complete megaspore which showed clear trilete laesurae and an encircling collar (Plate I, 5). Further details of the collar are discussed

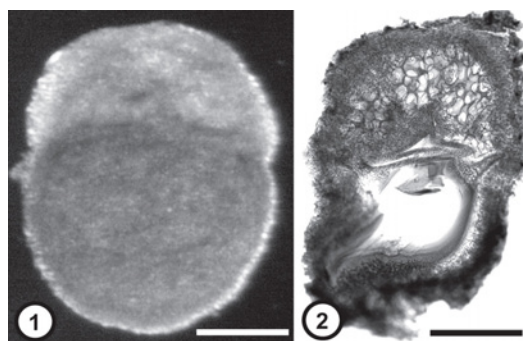


**Fig. 1.** Megaspore apparatuses of *Azolla arctica* sp. nov. from the lower Middle Eocene of the Lomonosov Ridge, Arctic Ocean (part of succession and area applies to all figures in this publication). LM images to show relative proportions and positions of megaspore and float system.

1. Combined reflected and transmitted light of entire megaspore apparatus, float system is in the upper pale area and is demarcated from the megaspore (lower, dark area) by the narrow encircling band of the collar, all enclosed by suprafilosum. U22875A.

2. Hand cut thin section showing upper vacuolated float system and lower empty megaspore, both surrounded by suprafilosum. U22875NO, slide 4393. Scale bars: 100  $\mu\text{m}$ .

with the float zone. Many specimens have attached microspore massulae (Plate I, 1, 2, 4, 6). The proximal end of the megaspore apparatus is covered by an apical cap (remnants of megasporocarp) (Plate I, 7), which overlies the suprafilosum (Plate I, 8) and the entire apparatus is enveloped by suprafilosum, which obscures the underlying structure (Fig. 1, 1; Plate I, 1-3, 6, 8). The extent of the float zone, approximately the upper one third of the megaspore apparatus, is only revealed by a combination of reflected and transmitted light (Fig. 1, 1), and by a thick section studied by LM (Fig. 1, 2) where the vacuolated nature of the floats is also evident. The collar, delimiting the float zone, is also revealed in Fig. 1, 1 but can sometimes be recognised in SEM images (e.g. Plate I, 2 and to a lesser extent Plate I, 3).

#### 5.4.2 Megaspore apparatus – megaspore wall

The megaspore wall is obscured by a thick (8-10  $\mu\text{m}$ ) suprafilosum (Fig. 1, 1, 2; Plate I, 1-3, 6, 8). In section the exine, endoperine and exoperine are together very thin (maximum 6  $\mu\text{m}$ ) and the layers are of similar thickness to one another. The perine is much thinner than is typical for other *Azolla* species e.g. those studied by Batten and Collinson (2001) which were 5-14  $\mu\text{m}$  thick. The thinness of the wall does not seem to be attributable to compression as exoperinal element shape and exoperinal columnar elements are not (or only slightly) distorted and exine and perine retain porosity.

The exoperinal surface is penetrated by small holes, some of which extend down to the endoperine surface whilst others extend only to the next layer of exoperine (Plate I, 9, 10). The small holes vary in size and shape but are very small, typically less than 1  $\mu\text{m}$  and often less than 0.5  $\mu\text{m}$  but occasionally up to 2  $\mu\text{m}$  in maximum dimension (Plate I, 9, 10). Exoperinal hairs (infrafilosum) are extremely rare (Plate I, 9, 10). We considered the possibility that the exoperine might be underdeveloped if immature, but this hypothesis is rejected, because (i) (Plate I, 9) naturally revealed and dissected (Plate I, 10) exoperine has the same structure (see also suprafilosum below) (ii) isolated microspore massulae are found attached to megasporangia indicating that material had been dispersed as part of the natural reproductive cycle (Fig. 1, 1; Plate I, 1, 2, 6) (iii) SEM (Plate I, 11) and TEM (Plate III, 1-4) sections reveal a fully developed, layered, wall organisation and a fully expanded megaspore.

In thin section under TEM the exine has a slightly more dense structure and less electron lucency (appears visually darker), but otherwise it is difficult to distinguish the exine from the endoperine (Plate III, 1-3). Both have a spongy appearance as a result of small cavities in their structure (Plate III, 4) but, as seen in both TEM (Plate III, 4) and SEM (Plate I, 9) the exine has slightly larger sporopollenin units resulting in a less granular appearance. The exoperine consists of variously shaped units that range from nodular to clavate to tabular and which are supported on typically narrow columnar elements so sparsely distributed that some exoperinal masses in any given section seem to be unsupported (Plate III, 1-4). The exoperinal masses are fused at various levels through the thickness of the exoperine (Plate III, 1-3), which results in their very variable shape in section and gives the surface of the

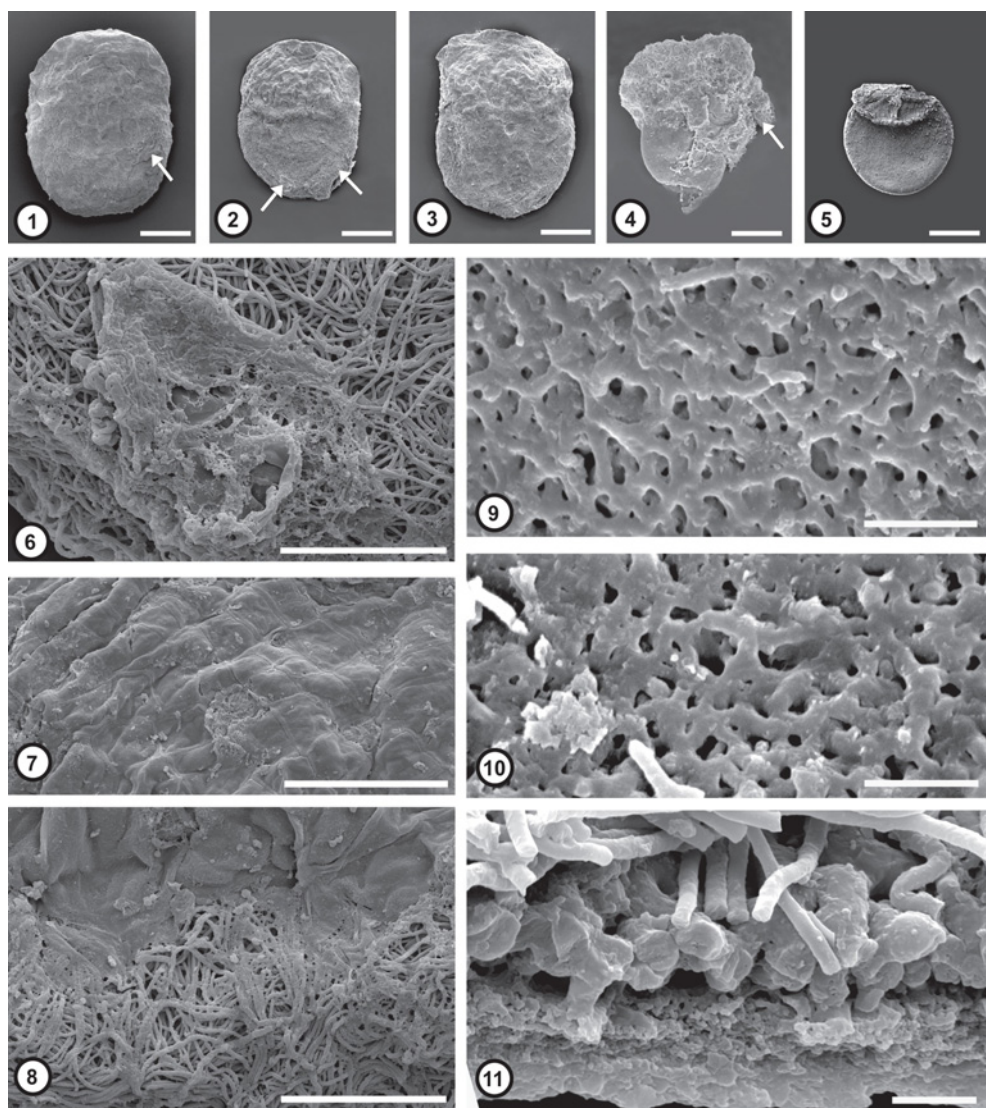


**Plate I.** Megaspore apparatuses and megaspore of *Azolla arctica* sp. nov. All SEM. Scale bars: 1-5: 100 µm; 6, 8: 20 µm; 7: 50 µm 9, 10: 5 µm; 11: 2 µm.

1, 2. Typical megaspore apparatuses, covered with suprafilosum, both with apical cap and both with attached microspore massulae, 2 showing the collar clearly (background debris removed using photoshop). Arrows mark attached microspore massulae.

1. Holotype U22874.

2. Now in TEM block with grids U22875K.

3. Megaspore apparatus slightly distorted by compaction. U22875B.

4. The only megaspore apparatus found where the megaspore wall was revealed through natural displacement of



the suprafilosum (which remains firmly attached all round the float system). Arrow marks an attached microspore massula. U22875C.

5. Dissected megaspore showing encircling collar and trilete laesurae (background blacked out using photoshop). U22875D.

6. Detail from 2, microspore massula attached to suprafilosum near center base of megaspore apparatus.

7. Detail from 2, apical cap showing diamond shapes marking anticlinal walls of cap cells.

8. Detail from 2, external surface of collar covered with suprafilosum at junction with overlying apical cap (upper part of image).

9. Detail from 4 outer surface of exoperine of megaspore wall, naturally revealed.

10. Outer surface of exoperine of megaspore wall revealed by dissection. U22875E.

11. Fracture through megaspore wall (exine at base, endoperine and exoperine) and overlying suprafilosum. U22875F.

exoperine a wavy and undulating rugulate morphology in several planes (Plate I, 9, 10). (The appearance can be visualised as if a thick pile of noodles or spaghetti had partially fused together).

### 5.4.3 Megaspore apparatus - float system

The float system occupies the upper third of the megaspore apparatus (Fig. 1, 1, 2). The float zone is clearly multifloated, without doubt having far more than 9 floats. Float numbers were studied using macerations and sections examined by transmitted light microscopy (Plate IV, 1, 2), in addition to median longitudinal sections (Plate IV, 3) and transverse (Plate IV, 4) sections at three levels examined by TEM. Our observations indicate that the floats are arranged in three tiers (Plate IV, 2, 3) with six floats in each of the lower tiers (Plate IV, 1, 4) and either three or six floats in the upper (most proximal) tier, resulting in either 15 or 18 floats. The compaction of the material and the extensive persistent covering of suprafilosum (up to 17  $\mu\text{m}$  thick) have made it impossible to be certain. In attempting to count floats we counted packages of vacuolated or spongy tissue as seen in LM (Plate IV, 1, 2) and in TEM section readily distinguished from the sectioned solid hairs of the suprafilosum (Plate III, 5; Plate IV, 3, 4). The float zone is delimited at the base by the collar (Fig. 1, 1; Plate III, 5; Plate IV, 3), which is formed from the expanded perine (Plate III, 5) and encircles the megaspore (Plate I, 5).

### 5.4.4 Megaspore apparatus – suprafilosum

The thick and persistent suprafilosum is a striking feature of *A. arctica*. The thickness ranges from 8-10  $\mu\text{m}$  over the megaspore wall to up to 17  $\mu\text{m}$  over the float system. We found only a single specimen (Plate I, 4) where the filsum had been displaced so as to reveal the surface of the megaspore exoperine. Furthermore, it was extremely difficult to remove the filsum by dissection to reveal the exoperine (Plate I, 5, 10). Notably, both the naturally revealed (Plate I, 9) and dissected (Plate I, 10) exoperinal surfaces have the same morphology indicating that dispersed megaspores are fully mature even when totally covered by suprafilosum.

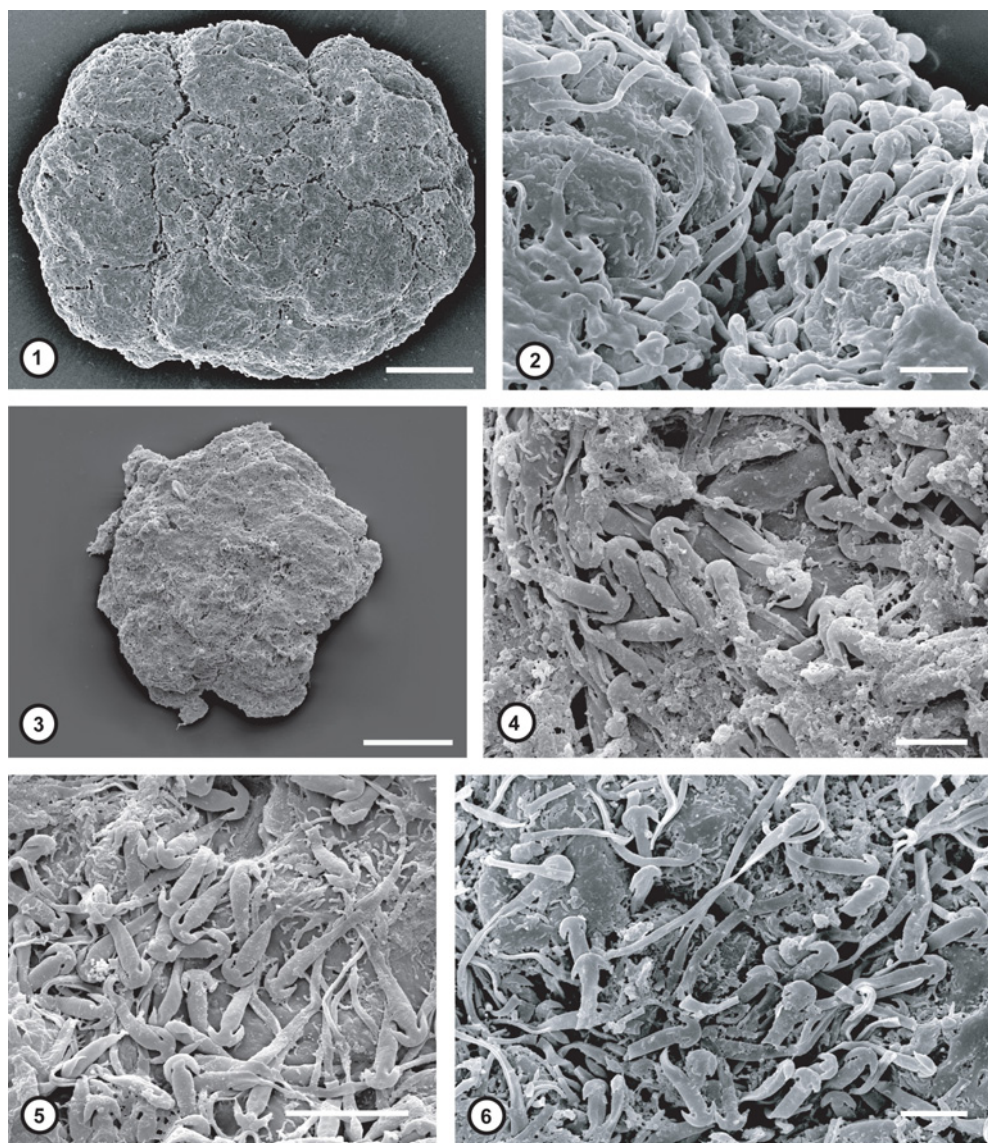


**Plate II.** Compact clusters of microspore massulae of *Azolla arctica* sp. nov. All SEM. Scale bars: 1, 3: 100  $\mu\text{m}$ ; 2, 4: 10  $\mu\text{m}$ ; 5, 6: 10  $\mu\text{m}$ .

1. Compact, clearly defined, grouping of multiple sub units (inferred microsporocarp) each subunit much larger than a single massula, hence each inferred to represent contents of one microsporangium not yet separated into component massulae. U22875G.

2. Detail from 1 showing anchor-tipped glochidia.

3. A typical compact cluster of microspore massulae where no clearly defined external shape is evident (cf. 1) and individual subunits are hard to distinguish. U22875H.



4. Detail from 3 showing anchor-tipped glochidia.

5, 6. Glochidia on microspore massulae of *Azolla arctica* sp. nov., as seen in SEM, from two different sample levels, showing long and short glochidia with narrow shafts broadening in their upper part, with a distal slight expansion and pronounced contraction below the anchor-shaped tips, and lack of recurved flukes. The wall of the microspore massula also has a patchy ornament of very short narrow hair-like structures.

5. Detail from 3.

6. U.228751.

#### 5.4.5 Megaspore apparatus – apical cap and location of symbionts

The apical cap is a surviving remnant of the megasporocarp wall. In *A. arctica* the cellular nature is clear from the external surface where diamond-shaped outlines of anticlinal walls are visible (Plate I, 7) and TEM sections reveal that the layer is one cell thick (Plate III, 5, 6). The organisation is similar to that shown in LM sections of modern *Azolla* by Dunham and Fowler (1987) and Carrapico (1991). In modern *Azolla*, symbiotic bacteria are located beneath this cap and hence transferred through the sexual reproductive phase of the life cycle (Dunham and Fowler, 1987; Carrapico, 1991). However, the bacteria are not preserved in the Arctic material. The apical cap is preserved on only a few other species of fossil *Azolla* megaspore apparatuses (Collinson, 1980) so reflects the high quality of preservation of the *A. arctica* material.

#### 5.4.6 Microsporocarps or microsori

These compound structures (Plate II, 1, 2) are large (350-500 µm in longest dimension) and consist of a large number (7-26) of sub-units with individual sizes from 130-220 µm. This suggests that they are microsporocarps or microsori containing microsporangia, not microsporangia containing microspore massulae. TEM sections showed that no outer wall was preserved, thus we have no direct evidence for the sporocarp. If these structures had reached full maturity it would be expected that the sporangial contents would have begun to separate into massulae. An example of a probable microsorus from the Cretaceous/Paleogene boundary was figured by Van Bergen et al. (1993, fig. 2H, I). In that example multiple units (inferred microsporangia) remained in a cluster but in some sporangial units the segregation of distinct individual massulae could be recognised. The *A. arctica* specimens have not reached this stage of maturity. Even in fertile fossil plants such as *A. stanleyi* (Hoffman and Stockey, 1994), where megasporocarps were preserved in place, the megasporocarp, microsporocarp and sporangial walls were not preserved. Thus the absence of these walls from the Arctic Ocean material is not surprising.

#### 5.4.7 Microsporangia and microspore massulae clusters

Clusters of microspore massulae are very common in the samples (Plate II, 1-4; Plate III, 8, 9; Plate V, 1-3). They can be recognised by the clumping of a number of discoidal units, on which glochidia can be seen by SEM and in high magnification LM. None of these clusters or their components have a recognisable microsporangium wall either in LM (Plate V, 1-3),

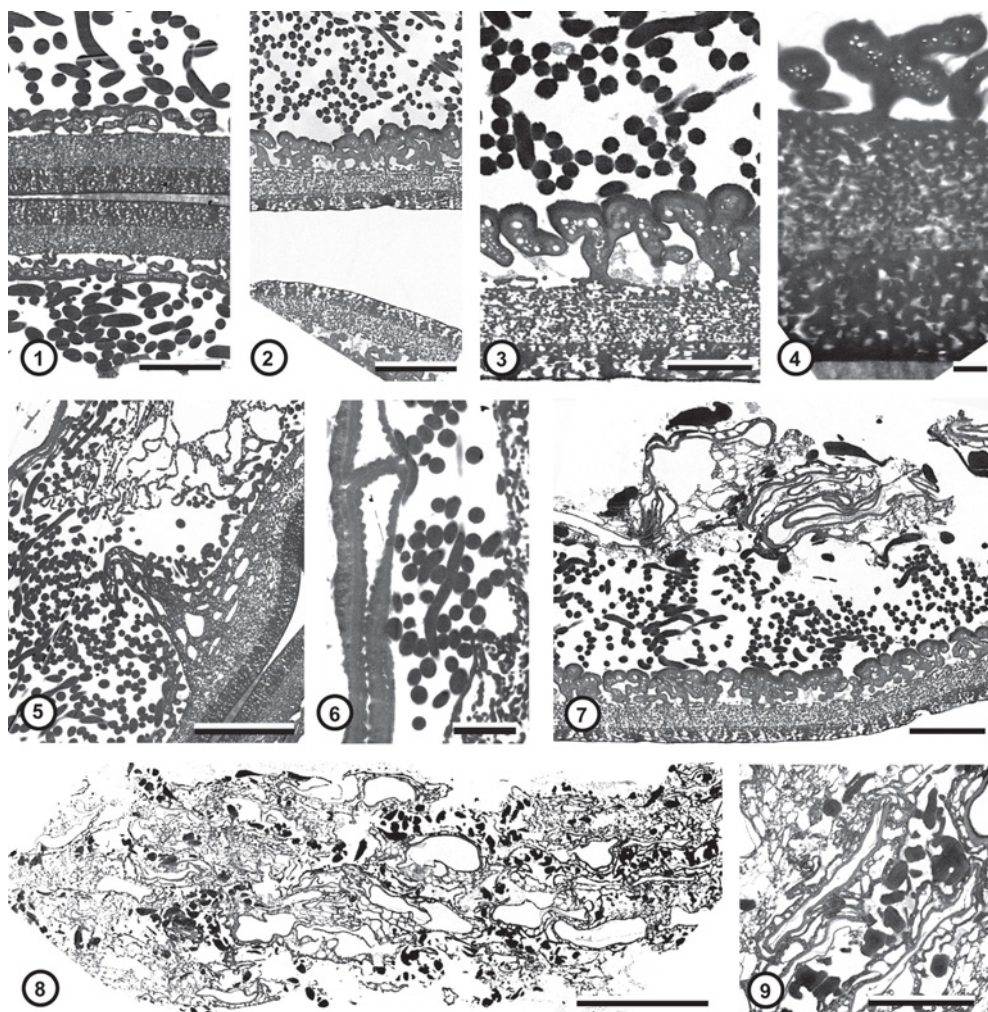


**Plate III.** Megaspore wall of *Azolla arctica* sp. nov. All TEM of ultrathin sections. 2 and 3 are from the megaspore in Plate I, 2, as is Plate III, 7. Plate III, 1 and 4, TEM block and grids, U22875L also shown in 5, 6 and Plate IV, 3. Scale bars: 1-2: 5  $\mu$ m; 3: 2  $\mu$ m; 4: 0.5  $\mu$ m; 5: 10  $\mu$ m; 6: 2  $\mu$ m; 7: 5  $\mu$ m; 8: 20  $\mu$ m; 9: 5  $\mu$ m.

1, 2. Wall of two different megaspores, various planes of section through solid hairs of the supraflosum are seen covering the megaspore wall but no hairs arise from the exoperine (= no infrafilosum), exoperine masses, at several levels, vary from tabular to nodular to clavate, and are supported at their bases by sparse narrow columns; underlying endoperine and exine are of similar thickness to one another, the endoperine is less electron dense than the innermost exine.

3. Higher magnification of wall of same megaspore as 2 with detail of clavate and nodular exoperinal masses.

4. Higher magnification of wall of same megaspore as 1 showing that the exine (base of image) is composed of slightly larger sporopollenin units and hence is less granular than endoperine.

5-6. Apical cap and collar of megaspore apparatus of *Azolla arctica* sp. nov. 5. Detail of collar from left of Plate IV, 3 showing spongy open texture; the vacuolated structure of one float is seen above the collar at top right of

image, both are surrounded by the solid hairs of the suprafilosum and are covered by the single cell thick apical cap (top left of image).

6. Detail of apical cap (left of image) showing one anticlinal wall and single cell thickness, with underlying suprafilosum and float fragment (at right of image). Same specimen as 1, 4 and Plate IV, 3.

7. Microspore massula attached by glochidia to suprafilosum of megaspore apparatus of *Azolla arctica* sp. nov. Same specimen as Plate I, 2; Plate III, 2, 3. Sections through glochidia have the same electron density as suprafilosum hairs but glochidia are much larger diameter.

8-9. Microspore massula cluster of *Azolla arctica* sp. nov.

8. Portion of microspore massulae cluster with sections through glochidia (electron dense) shafts, occasionally through anchor-shaped tips, demarcating individual massulae within the cluster. Larger spaces are microspores within the vacuolated massula tissue. TEM block and grids U22875N.

9. Detail of same specimen as 8 showing sections through glochidia, including one anchor-shaped tip, walls of microspores lacking differentiated layers and vacuolated massula tissue.

SEM (Plate II, 1, 3) or TEM (Plate III, 8) images; therefore, it is difficult to be certain which components represent the entire contents of a single sporangium. In TEM sections the glochidia are more electron dense (darker) and so the dark structures demarcate the boundaries between massulae even in compressed clusters (Plate III, 8, 9).

Compact clusters, inferred to represent microsporangia, may contain from 4-9 microspore massulae situated on the outer sides of the cluster (Plate V, 3). In the compact clusters the outer shorter glochidia are closely adpressed to the massulae and the inner longer glochidia are extended into the central hollow of the cluster (Plate V, 3). In some cases furrows can be seen marking the positions along which massulae will separate on dispersal. Following oxidation disintegrating clusters are held very loosely together by entwined extended glochidia (Plate V, 4) and similar loosely entwined microspore massulae are also seen in the mesofossil and palynological preparations. These clusters are interpreted as different maturation stages, the loose clusters having been dispersed and the compact clusters being immature to mature but preserved prior to dispersal.

#### 5.4.8 Microspore massulae

Microspore massulae are found attached to megaspores (Plate I, 1, 2, 4), and they occur singly (Plate V, 6-10) and in clusters (see above) in the sediment samples. The massulae vary considerably in size with very small specimens (Plate V, 10), large specimens (Plate V, 7, 8) and intermediates (Plate V, 6). Their attachment to megaspores is mediated by the anchor shaped tips of the glochidia (Plate II, 5, 6; Plate V, 6-10), which become entwined in the suprafilosal hairs covering the megaspore apparatus (Plate I, 6; Plate III, 7). Glochidia are numerous on each massula. In TEM sections the glochidia are very electron dense (dark) in contrast to the other massula tissues and the anchor shaped tips can be recognised (Plate III, 7-9) as well as various planes of section through the shaft. The glochidia fall into two size classes. Shorter glochidia are grouped in bundles and are ca 15-25  $\mu\text{m}$  in length (Plate V, 6, 8, 9). Long glochidia are not grouped in bundles and range from ca 55  $\mu\text{m}$  to 85  $\mu\text{m}$  (Plate II, 5, 6; Plate V, 7, 8). The shorter and longer glochidia are on opposite sides of

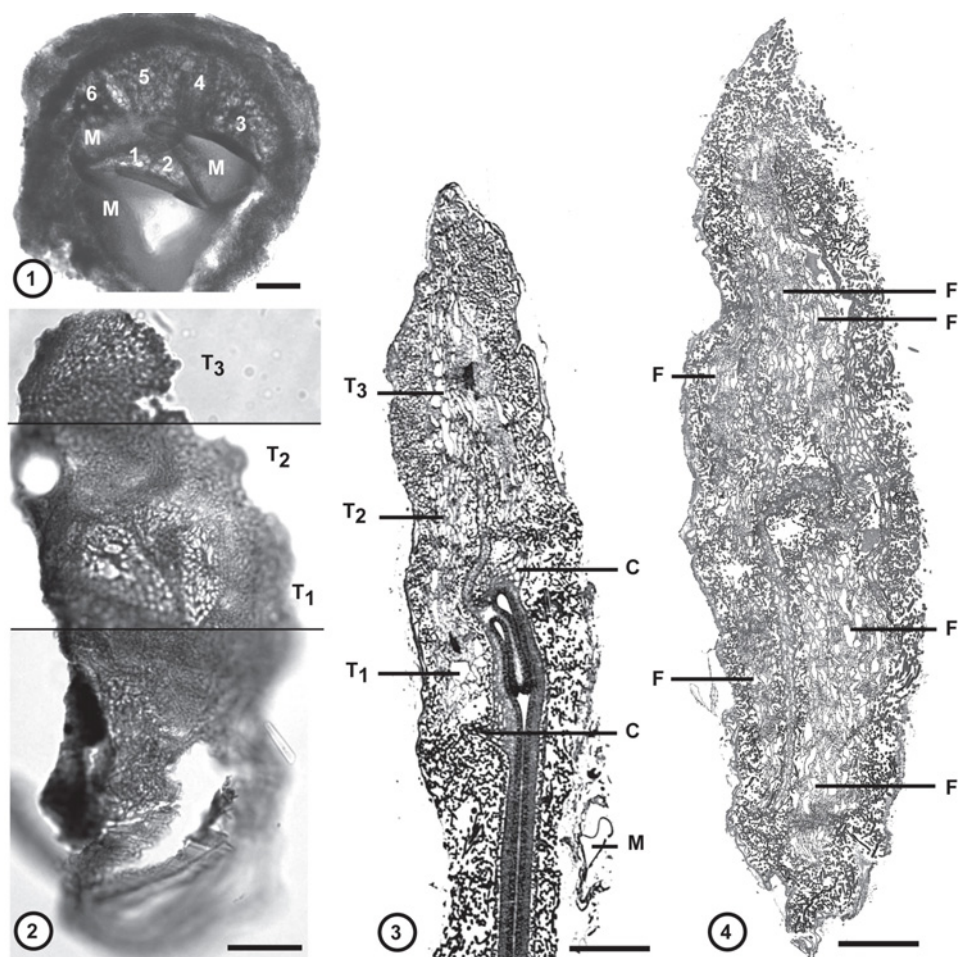


**Plate IV.** The float system of the megaspore apparatus of *Azolla arctica* sp. nov. 1 and 2 LM of hand cut thin sections, 3 and 4 TEM of ultrathin sections. Scale bars: 1, 2: 40 µm; 3, 4: 20 µm.

1. Transverse section through lower part of float system showing one tier of six vacuolated floats and the proximal megaspore surface. U22875P, slide 4396.
2. Longitudinal section through megaspore apparatus showing three tiers of vacuolated floats (T<sub>1</sub>-T<sub>3</sub>) and basal empty megaspore. U22875Q, slide 4365.
3. Longitudinal section through float system and proximal part of megaspore showing three tiers (T<sub>1</sub>-T<sub>3</sub>) of vacuolated floats, sections through the spongy collar (C) (at left and right) and the central column. The megaspore apparatus is slightly distorted by compaction such that the proximal part of the megaspore has been folded and the float system and collar have been pushed up and compacted on the right hand side of the image. Same specimen as Plate III, 1, 4.
4. Transverse section through lower tier of floats and parts of the collar and trilete laesurae. Montage from four separate original images. Six vacuolated floats can be distinguished (F) in this float tier by using the intervening solid electron dense suprafillosal hairs to demarcate float boundaries. Relative positions of floats have been distorted by compaction (the section would be +/- circular in uncompacted material). U22875M.



the massulae (Plate V, 8) but this is often not clear in dispersed specimens (Plate V, 6, 7). Very rarely the glochidia are branched (Plate V, 6). The anchor-shaped tips are up to 4-5  $\mu\text{m}$  wide and the flukes are up to 3  $\mu\text{m}$  long. The lower part of the shaft is up to 1  $\mu\text{m}$  wide and the widest upper part of the shaft is up to 2  $\mu\text{m}$  wide. Near the tip the shaft expands slightly and then constricts to about 1  $\mu\text{m}$  before expanding again into the anchor-shaped tip. All glochidia tips have two flukes and none have other barbs along the shaft. The flukes usually have acute ends. Unusually amongst anchor-tipped glochidia on *Azolla* species those of *A. arctica* do not have recurved flukes. This distinctive feature has been demonstrated on multiple specimens (Plate II, 4-6; Plate V, 10, 11). The outer wall of the massulae has a patchy, variable, ornament of short (<2  $\mu\text{m}$ ) narrow (<0.1  $\mu\text{m}$ ) hair-like structures Plate II, 5, 6). Microspores (up to 15 per massula) are trilete (Plate V, 5), have a smooth wall with no differentiated layers (Plate III, 9) and are 20-25  $\mu\text{m}$  in diameter. They are enclosed within spongy pseudovacuated tissue (Plate III, 9; Plate V, 5).

## 5.5 Differentiation

### 5.5.1 Clearly distinct species

*Azolla arctica* is multifloated and hence distinguished from 3 and 9 floated species (listed in Collinson, 1980, 1991). Of the multifloated species (listed with source references in Sweet and Hills, 1976; Collinson, 1980, 1991; Vajda and McLoughlin, 2005) the following features differ from *A. arctica* - *A. bulbosa* Snead and *A. teschiana* Florschuetz emend Batten and Collinson are distinguished by having exoperinal excrescences on the megaspore wall (Sweet and Hills, 1976; Batten and Collinson, 2001); *Azolla barbata* Snead has coiled glochidia lacking anchor-shaped tips; in *A. extincta* Jain the microspore massulae lack glochidia; *Azolla distincta* Snead, lacks the distal dilation on the glochidia and floats were easily detached from the megaspore; *Azolla boliviensis* Vajda and McLoughlin has up to 30 floats in 3 tiers; *Azolla schopfii* Dijkstra emend Batten and Collinson has very little suprafilosum, almost entirely restricted to the zone between the floats, and the megaspore surface is ornamented with discrete verrucae to clavae, which are grouped around depressions to form a reticulum; *Azolla colwellensis* Collinson has 18 (to 24) clearly defined floats and an extensive infrafilosum derived from a columnar to coarsely rugulate exoperine. *Azolla velus* is superficially similar to *A. arctica* as the megaspore apparatus is totally covered by suprafilosum. However, the exoperine surface is smooth and almost flat with large rounded holes (1-5  $\mu\text{m}$  in diameter) forming a 'reticulum'. In TEM section the exoperine columnar elements are tall and often broad and they expand upwards to form clavae which fuse to produce the smooth flat surface.

### 5.5.2 Species with inadequate data for detailed comparison

The following species cannot be fully compared with *A. arctica*. In *A. simplex* Hall the floats are probably detached (Martin, 1976), but the species can reasonably be distinguished by reticulate exine and small amount of filiosum.

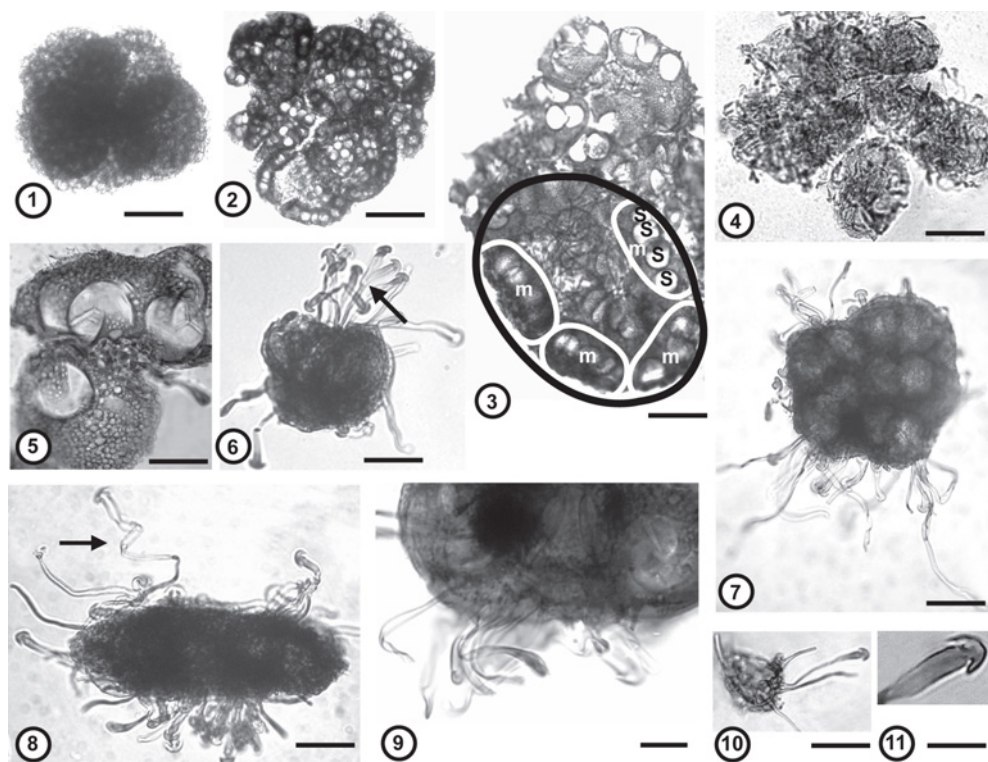


**Plate V.** Microspore massulae (clusters and single) of *Azolla arctica* sp. nov. All LM untreated apart from 4 which was treated with short oxidation (see methods). Scale bars: 1, 2: 100  $\mu$ m; 3, 4: 50  $\mu$ m; 5-8, 10: 20  $\mu$ m; 9, 11: 10  $\mu$ m.

1. Compact cluster of microspore massulae where contents of individual sub-units (inferred microsporangia) cannot be distinguished and microspores are hard to discern. U22875R, slide 4373.
2. Compact cluster of microspore massulae where microspores are much more obvious than in 1, inferred later developmental stage. U22875S, slide 4398.
3. Portion of compact cluster of microspore massulae where the contents of a single microsporangium (black circle) can be recognised with four massulae (m, white circles) clearly arranged around the margins of the sporangium. Microspores (s) are clearly seen. U22875T, slide 4398.
4. Microspore massulae partially released from compact cluster by oxidation treatment and showing glochidia. U22875GU slide 4378.
5. Trilete microspores within vacuolated tissue of the microspore massula. U22875V, slide 4398.
- 6-8, 10. Various naturally dispersed single microspore massulae to show the wide variety of sizes.
6. also shows the single example of a forked glochidium (arrow). U22875W, slide 1.
7. shows two size classes of glochidia length but with glochidia spreading out around the massula as is typical in palynological preparations where their precise point of origin cannot be seen. U22875X, slide 7.
8. Side view of a massula showing that the shorter glochidia are grouped in bundles on one side whilst the longer glochidia (e.g. arrow) are scattered on the opposite side. U22875Y, slide 2.
9. Part of a microspore massula showing attachment of a bundle of short glochidia. U22875W, slide 1.
10. An extremely small massula. U22875W, slide 1.
11. Detail of anchor-shaped tip of glochidium demonstrating absence of recurved flukes. U22875W, slide 1.

Three Cretaceous-Paleocene species listed by Collinson (1980) are represented only by megaspore apparatuses studied in LM mounts where float number is said to be numerous but not known (*Azolla conspicua* Snead, *A. lauta* Snead, *A. filosa* Snead, all described by Snead (1969)). The exine surfaces were described as finely punctate or infragranulate, finely granular or finely granulate respectively (Snead, 1969) all different from *A. arctica*, which is finely rugulate in our LM preparations of the entire megaspore apparatus. *Azolla elegans* Jain and Hall (Paleocene) had lost the floats, the exine was described by LM as finely reticulate so differs from *A. arctica*.

Five Cretaceous species listed by Collinson (1980), one *Azolla* sp. (late Albian, India) listed by Vajda and McLoughlin (2005) and one *Azolla* sp. described and figured by Kvaček and Manum (1993) from the Paleogene of Spitsbergen, were known only from microspore massulae. Only three of these, *A. cretacea* Stanley and *A. gigantea* Bergad and Hall and *Azolla* sp. (Kvaček and Manum, 1993) have anchor-tipped glochidia of similar morphology to *A. arctica*. *Azolla cretacea* morphology was the same as that of massulae attached to and associated with megaspores of *Azolla montana* Hall and Swanson emend Jain and Hall (see below). The megaspore apparatuses belonging to *A. gigantea* and *Azolla* sp. are unknown preventing further comparison, but *Azolla* sp. differs from *A. arctica* in having glochidia with recurved flukes.

### 5.5.3 Closely similar species – Outside the Arctic

All the species discussed in this section have microspore massulae with glochidia with anchor-shaped tips and a distal dilation plus constriction and are thus similar to *A. arctica*. *A. anglica* Martin has septate glochidia, which differs from *A. arctica* but it is difficult to assess the importance of septae (Collinson, 1980) as both septate and non-septate glochidia are sometimes found on the same massula in modern *Azolla*.

*Azolla montana* Hall and Swanson emend Jain and Hall has 15-20 small floats (exceptionally, there are 10) in two tiers and descriptions in Hall and Swanson (1968) and Jain and Hall (1969) indicate that the filosum is sometimes completely missing. In *A. arctica* the floats seem to be in three tiers. In *A. arctica* the filosum is very persistent, even being present though displaced in the single specimen we found where the megaspore surface was revealed naturally (Plate I, 4). The megaspore surface of *A. montana* is rugulo-reticulate formed of variously fused clavae, areolae of reticulum 1-3 µm wide. This also differs from *A. arctica*, where the wall is rugulate-perforate not reticulate and the perforations are of smaller scale.

*Azolla stanleyi* Jain and Hall was described in detail with SEM and TEM observations by Hoffman and Stockey (1994). The megaspores are very similar to those of *A. arctica* having an extensive persistent suprafilosum and more than 15 floats roughly organized in three tiers. Hoffman and Stockey (1994) stated that the megaspore apparatus also has an infrafilosum arising from the exoperine. If correct this would differ from *A. arctica*, but the SEM illustrations do not demonstrate an extensive infrafilosum, so we do not consider this characteristic appropriate for differentiation. Hoffman and Stockey (1994) described the

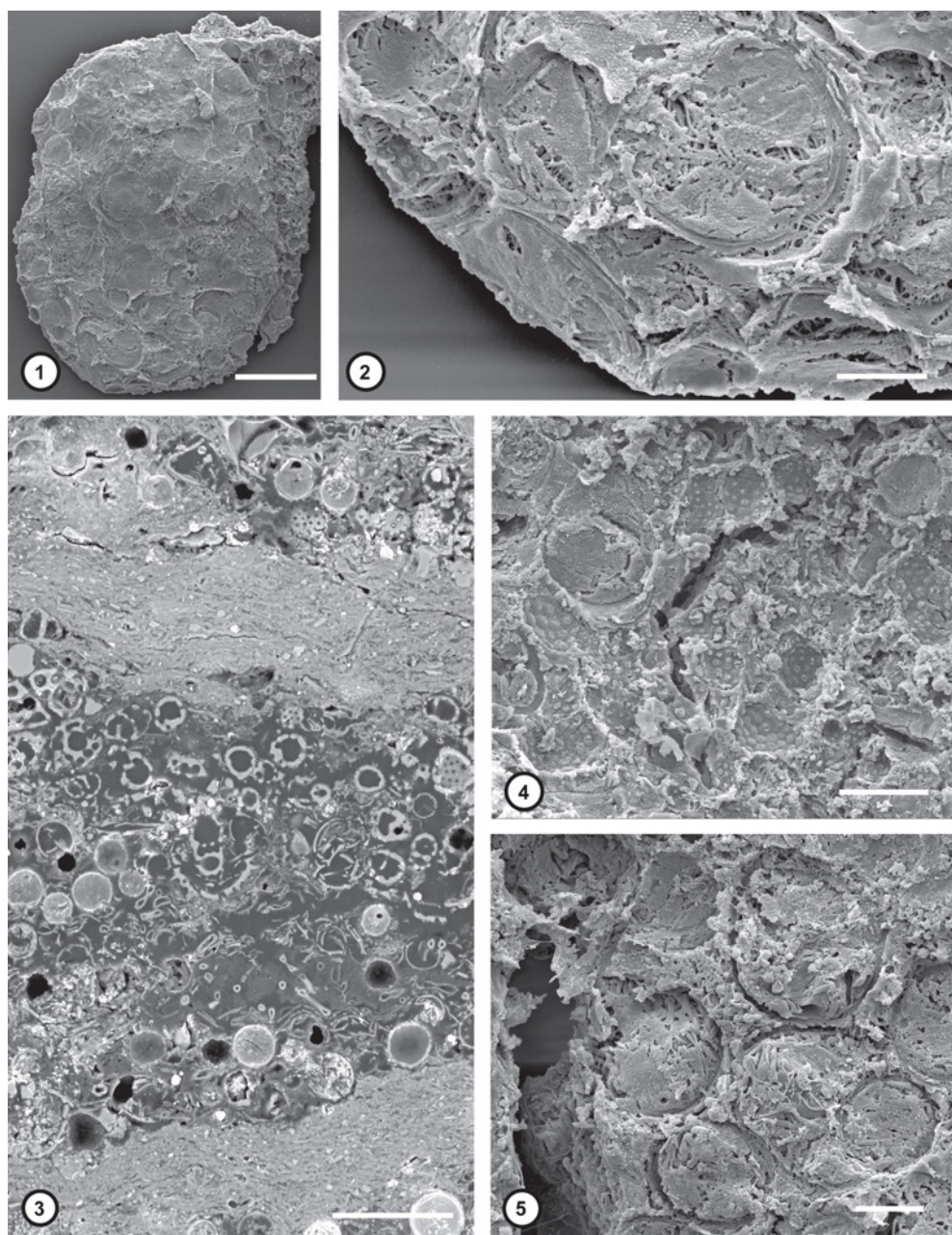


**Plate VI.** 1, 2, 4, 5. Impressions of microplankton on the surfaces of megaspore apparatus and microspore massula clusters and the organic-rich sediment lamina on which these are lying, from Section 1W level 111-113 cm. Scale bars: 1: 100  $\mu\text{m}$ ; 2, 4, 5: 20  $\mu\text{m}$ ; 3: 50  $\mu\text{m}$ .



1. Megaspore apparatus covered in microplankton impressions and lying on an organic rich lamina (which continues to right of specimen but has been trimmed in this illustration). U.22875J.
2. Detail from lower left of 1 showing details of diatom and chrysophyte impressions and underlying suprafilum.
3. Polished thin section of sediment from Section 1W level 111-113 cm of the Azolla interval. SEM image with back scatter detector. Paler layers are clay rich and contain organic material (including Azolla) whilst darker layers are biosilica rich with numerous siliceous microplankton (including chrysophyte cysts (large circular in cross section) and ebridians (spindles and tiny circular cross sections)). U.22877.
4. Detail of a portion of the organic-rich lamina to right of 1, i.e. the surface on which the megaspore apparatus is resting, showing a covering of chrysophyte cysts.
5. Detail of surface of a microspore massula cluster showing microplankton impressions and underlying glochidia. Specimen now in TEM block, same specimen as Plate III, 8 and 9.

exoperine surface as rugulo-reticulate. In our opinion a more appropriate description would be rugulate and foveolate to fossulate, because the distance between the holes is much greater than their breadth (rugulae up to 7  $\mu\text{m}$  in width), the holes are 1  $\mu\text{m}$  or more in diameter and some are elongate (e.g. 1  $\mu\text{m}$  x 5  $\mu\text{m}$ ). Irrespective of the terminology used the holes are irregularly arranged, vary in size from 1-5  $\mu\text{m}$  in longest dimension and are set in a rugulate surface. In *A. arctica* the holes are much closer together and mostly smaller (0.2-2  $\mu\text{m}$ ) and the rugulae are much narrower and in several planes. In thin section under TEM the exoperine of *A. stanleyi* consists of broad, thick fused baculae and in this respect differs strongly from *A. arctica* and is more similar to *A. anglica* (see below).

*Azolla anglica* Martin has up to 24 floats in three tiers similar to *A. arctica*. However, in strong contrast to *A. arctica* it has very limited filum such that the exoperine is always revealed and many specimens had lost their float apparatus (Martin, 1976). The exoperine is very different from that of *A. arctica*. *Azolla anglica* has a foveolate exoperine surface with lumina of foveolae 1-2.5  $\mu\text{m}$  diameter and the surrounding rounded muri 3-5  $\mu\text{m}$  in width. In section the exoperine is composed of broad thick baculae supported by frequent short columns, which differs strongly from *A. arctica*.

#### 5.5.4 Closely similar species – Arctic and Nordic Seas

One microspore massula from the Eocene in DSDP site 343 off the coast of central Norway was figured and described, as *Azolla* sp., by Kvaček and Manum (1993, plate 2, figs. 4, 5). It is very similar to Plate V, 8 in showing two size classes of glochidia including some at least 70  $\mu\text{m}$  in length and shorter ones in bundles. The microspores are of the same size and morphology and the anchor tipped glochidia lack recurved flukes. As far as can be judged from microspore massulae only this specimen, of all the fossil *Azolla* with which we have made comparisons, is the same as the *A. arctica*. According to Kvaček and Manum (1993) Boulter and Manum (1989) recorded similar massulae in Eocene cores of ODP site 643 in much the same area.

*Azolla areolata* Sweet and Hills is the most similar species to the Arctic Ocean *Azolla*. However, there are the following differences. The megaspore apparatus of *A. areolata* is larger (mean 479  $\mu\text{m}$ ) than that of *A. arctica*, the floats range from 18-27, usually 24,

in number, more than *A. arctica*. *Azolla areolata* usually lacks exoperinal excrescences but they do occur rarely (Sweet and Hills, 1976, fig. 62) (they are lacking in *A. arctica*) and the exoperine surface of *A. areolata* has more uniform and larger perforations (ca twice the size of those in *A. arctica*) with a slight tendency to form a reticulum, the outer surface of which is more in a single plane than the surface in *A. arctica*. The exine (mean 2.8  $\mu\text{m}$ ) and perine (mean 13  $\mu\text{m}$ ) thicknesses are much greater than in *A. arctica*. The suprafilosum is less extensive in *A. areolata* so that the floats can sometimes be seen and the megaspore exoperine surface is revealed in patches; both these features are unlike *A. arctica*. The original description of *A. areolata* states that a collar is absent, although fig. 50 in Sweet and Hills (1976) suggests the possible presence of a small collar; *Azolla arctica* has a distinct collar. Some glochidia of the microspore massulae in *A. areolata* have recurved hooks (fig. 74 in Sweet and Hills, 1976) whilst those of *A. arctica* do not. Glochidia of *A. areolata* range from 27 -(mean 38  $\mu\text{m}$ )- 55  $\mu\text{m}$ , thus lacking both the smaller size class and the very long glochidia of *A. arctica*. Glochidia of *A. areolata* show a more gradual change in width along their length and a narrower distal dilation than those of *A. arctica*.

### 5.5.5 Undescribed material

There are many occurrences of *Azolla* in the Arctic and Nordic Seas recorded in palynological preparations (pers. comm. with Dr. Bujak; Brinkhuis et al. 2006 including supplementary material). At least one of these (Heilman-Clausen, 1996) includes co-occurring megaspore apparatuses and microspore massulae (Heilman-Clausen, pers. comm. 2005) and hence provides potential for a full and detailed future comparison with all of the characteristics of *Azolla arctica* described in this paper. Preliminary research shows that this *Azolla* species (Heilman-Clausen, 1996) is not con-specific with *Azolla arctica*.

### 5.5.6 Summary

Using current species concepts from literature, the Arctic Ocean *Azolla* can be distinguished from all other previously described species. The Arctic Ocean *Azolla* is therefore described here as a new species.

There is one previously described species, *A. areolata* Sweet and Hills (1976) which, according to its description, is most similar to the Arctic Ocean *Azolla*. Nevertheless, there are numerous characters (see above), which distinguish *A. arctica*. *A. areolata* occurs in a monotypic assemblage in Banks Island, Arctic Canada (Sweet and Hills, 1976) in sediments dated as Paleocene or Eocene. Therefore, it will be important to reinvestigate *A. areolata*. Especially a more detailed study of the megaspore wall using TEM and glochidia using SEM is necessary in order to make a more detailed assessment of the distinguishing features.

## 5.6 Discussion and wider implications

### 5.6.1 Environmental Implications

The *Azolla* material occurs in finely laminated sediments with sub-millimetre scale microlaminations (Plate VI, 3). The laminations are paired light-coloured biosilica-rich layers and dark organic rich layers with clay. The biosilica rich layers contain three-dimensionally preserved siliceous microplankton (Plate VI, 3) including freshwater chrysophyte cysts, and brackish-marine diatoms, silicoflagellates and ebridians whilst the organic-rich layers contain *Azolla* material (Brinkhuis et al. 2006). Brinkhuis et al. (2006) interpreted these microlaminations as possibly reflecting early spring growth of brackish water microplankton blooms, followed by a spring to summer precipitation increase leading to blooms of chrysophytes and of *Azolla* over a stratified freshwater surface layer.

Our SEM images of *Azolla* megaspores (Plate VI, 1, 2, 4) and microspore massula clusters (Plate VI, 5) sometimes reveal chrysophyte and rarely diatom impressions, proving the close juxtaposition of the *Azolla*-rich and microplankton-rich layers and the close association of the *Azolla* with freshwater chrysophyte plankton. Our sieved residues do not contain any land derived material such as cuticle fragments (either with or without stomata) or small seeds, and we saw only extremely rare and very poorly preserved tiny wood fragments.

Our data demonstrate the frequent attachment of microspore massulae to megaspores, indicating that both reproductive components had been shed, dispersed and then recombined as part of the natural reproductive cycle of *Azolla*. In addition there are fully mature megaspores and microspore massulae but also various developmental stages of microspore massulae.

All of this information gives additional support to that provided in Brinkhuis et al. (2006) to prove that the *Azolla* were growing and reproducing in situ in the Arctic Ocean. *Azolla* is known to have been a free floating freshwater plant since at least the Paleocene, based on ecology of associated fossils, sedimentological context and fossil fertile whole plants whose habit and functional biology is almost indistinguishable from the living genus (Collinson, 2002). Furthermore, modern *Azolla* is only tolerant of a few parts per thousand salinity, even when preconditioned experimentally by gradual increase in salt content (Rai and Rai, 1998). *Azolla arctica* occurs in greater abundance (2-8 megaspore apparatuses per gram of sediment) than fossil *Azolla* from freshwater sediments with similar microlaminations (Collinson, 1983). These facts require that a freshwater surface layer existed on the Arctic Ocean during the *Azolla* interval of the lowermost Middle Eocene.

### 5.6.2 Developmental implications and new characteristics for *Azolla*

As a fairly small freshwater plant, easily buried in lacustrine sediments, *Azolla* has a good fossil record and is one of the few plant fossil taxa represented by a number of whole plants. There are some eight fossil species of *Azolla* known from fertile whole plants, ranging

from the Paleocene to Miocene (Batten and Collinson, 2001). Some 20 additional species are known from megaspore apparatuses and attached microspore massulae, which also provide a very full range of reproductive characters. However, few of these species have been examined in detail using LM, SEM and TEM. Our combined investigation of *A. arctica* has yielded some new information for Eocene fossil *Azolla*, particularly on developmental stages of microspore massulae and additional characters not previously recorded for *Azolla*.

The *A. arctica* material demonstrates that the massulae form around the outside of a cluster (Plate V, 3) equivalent to the contents of one microsporangium. The central part of the cluster is hollow with the long glochidia extending into it. Short glochidia are on the outside of the massula, grouped in bundles addressed to the massula surface. On dispersal all glochidia protrude from the surface (Plate V, 6-8) and can become entwined in the suprafilousum of the megaspore apparatus (Plate I, 6; Plate III, 7).

It is consistent with most other early Paleogene *Azolla* that *A. arctica* has a large number of floats. However, no other multifloated *Azolla* species possesses two size classes of glochidia, very long glochidia, bundles of short glochidia or glochidia whose anchor-shaped tips lack recurved flukes. The *A. arctica* megaspores are also distinctly smaller and have a much thinner megaspore wall than previously recorded multifloated species.

### 5.6.3 Recognising the Arctic Ocean *Azolla* interval from fragmentary material

It is important for geologists, palaeobiologists and palaeoclimatologists to be able to recognise stratigraphically and palaeoenvironmentally important events in the small sample sizes provided by drill cores. Palynology samples rarely contain *Azolla* megaspore apparatuses due to small sample sizes and/or removal of larger size fractions by sieving. However, fragments of *Azolla* microspore massulae, especially glochidia, are fairly common in palynology preparations. Comparison with literature indicates that two features of *A. arctica* glochidia are unique to this species. No other species has such long glochidia, 55-85  $\mu\text{m}$  as *A. arctica*, and the lack of recurved hooks on the glochidia tips also seems to be unique to the Arctic Ocean *Azolla*. Furthermore, a single published specimen in a palynological preparation from the Nordic Seas (Kvaček and Manum, 1993) does indeed show these characteristics. These features therefore offer potential for identification of the *Azolla* interval (sensu Brinkhuis et al., 2006) across the Arctic and Nordic Seas where the termination is an important stratigraphic markers and the interval itself marks an episodic freshening of Arctic Ocean surface waters (Brinkhuis et al., 2006).

## 5.7 Conclusions

Material of *Azolla* from the middle Eocene of the Lomonosov Ridge, Arctic Ocean, can be differentiated from all other fossil *Azolla* and is therefore described as a new species *Azolla arctica* Collinson et al. This study reveals significant new characteristics for the genus

*Azolla* that have not previously been reported in the fossil record, as well as demonstrating developmental stages of fossil microspore massulae.

*Azolla arctica* is abundant in the Arctic Ocean sediments. It occurs over an 800,000 year interval as microspore massulae represented in palynological slides, which co-occur with reduced abundances of marine microplankton, increased abundances of freshwater microplankton, in the absence of land derived plant material (Brinkhuis et al., 2006). In a narrower interval, spanning at least 25 cm thickness of microlaminated sediments, *Azolla* is represented by large numbers of megaspore apparatuses many with attached microspore massulae, by clusters of microspore massulae representing microsporangial and microsporocarp contents and by isolated microspore massulae. These co-occurring fossils include different developmental stages as well as material naturally dispersed as part of the reproductive cycle. Furthermore there are no other determinable plant mesofossils and no land-derived plant debris (such as cuticles with stomata) associated with the *Azolla*. All of these facts confirm and strengthen the arguments of Brinkhuis et al. (2006) that the *Azolla* was growing in situ on a freshwater surface of the Arctic Ocean.

*Azolla areolata* Sweet and Hills (1976) from the Paleocene or Eocene of Arctic Canada is recognised as the most similar previously described species to *A. arctica* sp. nov.. Material of *A. areolata* should be re-examined in detail to obtain a fuller understanding of the differences between these two Arctic species.

Two key features are evident on *A. arctica* that might be determinable in palynological preparations, namely long glochidia (>55 µm) and anchor-shaped tips to glochidia, which lack recurved flukes. Therefore, palynologists, including those working in industry, may be able to recognise the stratigraphically and environmentally important lower Middle Eocene *Azolla* interval through careful study of glochidia in palynological preparations.

## Acknowledgements

The authors thank T. Brain in Kings College London for embedding and sectioning the specimens illustrated by TEM and for his extensive support for both TEM and SEM during this study and B. J. van Heuven in Leiden and J. van Tongeren in Utrecht for technical support for the SEM work. The samples, and accompanying data, were provided by the Integrated Ocean Drilling Program (IODP). The cores were obtained by the Arctic Coring Expedition (ACEX), Leg 302 expedition scientists, who are listed in Brinkhuis et al. (2006). Without their efforts this study would not have been possible. We thank the Darwin Centre, Utrecht and Statoil for their financial support.



# Chapter 6

## **Did a single species of Eocene *Azolla* spread from the Arctic Basin to the southern North Sea?**

Collinson, M.E., Barke, J., van der Burgh, J., van Konijnenburg-  
van Cittert, J.H.A., Heilmann-Clausen, C., Howard, L.E., and  
Brinkhuis, H.

*Published in Review Palaeobotany and Palynology, 159, 152-165, 2010*

## Abstract

Recent Arctic drilling has revealed that the freshwater surface-floating heterosporous fern *Azolla arctica* Collinson et al. (Azollaceae, Salviniiales) bloomed and reproduced in the Arctic Ocean on a massive scale during the early Middle Eocene. These blooms have been suggested to have been capable of significant drawdown of atmospheric CO<sub>2</sub> paving the way to Cenozoic climatic cooling. Sites of similar age across the Arctic and Nordic Seas also contain *Azolla* fossils suggestive of an area much larger than the Arctic Ocean being affected by *Azolla* blooms, as far south as Denmark. Here we investigate the Danish occurrences known from the Lillebælt Clay Formation, transitional Ypresian/Lutetian in age (latest Early Eocene to earliest Middle Eocene). The Lillebælt Clay is a marine deposit rich in diverse organic-walled dinoflagellate cysts yet conspicuously characterized by abundant co-occurring and interconnected fully mature *Azolla* megaspores and microspore massulae. Perhaps surprisingly, we find that multiple morphological and ultrastructural characters distinguish the Danish *Azolla* species from *Azolla arctica* and it is here described as *Azolla jutlandica* sp. nov. Therefore, contrary to expectations given the overlapping age of these assemblages, it appears that not a single *Azolla* species has spread from the Arctic to the Southern North Sea either through freshwater spills from the Arctic Ocean or as a result of rapid spread due to highly invasive biology. Apparently Northern Hemisphere middle and high latitude conditions near the termination of a period known as the Early Eocene Climatic Optimum (EECO) were suitable for proliferation of two different *Azolla* species, one in the Arctic Ocean and one in the southern North Sea.

## 6.1 Introduction

The freshwater surface-floating heterosporous fern *Azolla* bloomed and reproduced in the Arctic Ocean during the early Middle Eocene (Brinkhuis et al., 2006; Collinson et al., 2009). These blooms are implicated in the drawdown of CO<sub>2</sub> (Speelman et al., 2009b) with potential consequences for climate change. Sites of similar age across the Arctic and Nordic Seas also contain *Azolla* fossils (Brinkhuis et al., 2006; Speelman et al., 2009b) indicating that an area much larger than the Arctic Ocean could have been affected by *Azolla* blooms.

Amongst the c. 412 genera of aquatic macrophytes in freshwaters (Chambers et al., 2008) *Salvinia* (sister taxon to *Azolla*) is ranked with *Eichornia* (Pontederiaceae, flowering plant) as two of the world's worst aquatic pests (Chambers et al., 2008). *Azolla* is also an invasive species (Wagner, 1997; Garcia-Murillo et al., 2007) and one of the worlds fastest growing aquatic macrophytes, with a doubling time of 2-5 days (Peters et al., 1980; Lumpkin and Plunkett, 1982; Zimmerman, 1985). For example, *Azolla filiculoides* has spread, between 1920 and 2005, across most of the western half of the Iberian Peninsula (Garcia-Murillo et



al., 2007). In Donana National Park (SW Spain) *Azolla filiculoides* L. has spread from a first collection in 2000 to wetland sites across most of the area of the park (c. 65000 hectares) by 2004 (Garcia-Murillo et al., 2007). This invasive biology implies that, given suitable conditions, a single species of *Azolla* could easily have spread across the area of the Arctic and Nordic Seas within a few thousand years. Although some modern *Azolla* species have relatively restricted distribution, *A. filiculoides* is native to a wide geographic area, including through South and North America (Lumpkin and Plucknett, 1980). Speelman et al. (2009b) have shown that *Azolla* biomass production increases at elevated CO<sub>2</sub> levels (such as may have pertained during the late Early and early Middle Eocene) thus increasing the ease with which an *Azolla* species could have spread across the Eocene Arctic and Nordic Seas.

An alternative possibility, suggested by Brinkhuis et al. (2006), is that Arctic Basin *Azolla* mats were transported through huge Arctic freshwater spills, to as far south as the southern North Sea. This possibility is supported by the fact that sediments in the Norwegian-Greenland Sea contain ten times less *Azolla* than those in the Arctic Basin and contain both *Azolla* and fully marine organic walled dinoflagellate cysts (dinocysts), the latter arguing against surface freshwaters like those inferred for the Arctic Basin.

A third explanation for the occurrence of the same species of *Azolla* at two distant sites would be long distance dispersal. The late Pleistocene to early Holocene fossil occurrences of two extant *Azolla* species on the Galapagos Islands, one of which survives there today, imply dispersal over 600 miles of ocean (Schofield and Colinvaux, 1969).

There are up to 7 species of *Azolla* today (Saunders and Fowler, 1993) occurring naturally in all major biogeographic areas except the Pacific Islands and Antarctica (Chambers et al., 2008). Two species occur today in the Palaearctic and Afrotropical regions (Chambers et al., 2008); two or three in the Nearctic (Chambers et al., 2008; Evrard and Hove, 2004) with the largest number per geographic area of four in the Neotropical region (Chambers et al., 2008). Saunders and Fowler (1992) noted that the two modern species *A. nilotica* and *A. pinnata* overlap in distribution in tropical Africa. Therefore it is perfectly likely that more than one *Azolla* species could have existed at any given time interval in the area encompassed by the Arctic and Nordic Seas. Collinson (2002) noted that *A. schopfii* and *A. velus* (clearly distinct fossil species) co-occurred in the Paleocene Ravenscrag Formation whilst Batten and Collinson (2001) noted the same two species at the same depth in a borehole in the South Dakota Paleocene. Sweet and Hills (1976, p.335) noted that *A. bulbosa* and *A. stanleyi* co-occurred in a corehole in the Paleocene Paskapoo Formation. Co-occurrence of *A. filiculoides* Lam. and *A. tegeliensis* Florsch. is described for the quaternary flora of Baanhoek in the Netherlands (Florschütz, 1938). These examples demonstrate that more than one *Azolla* species did co-exist in the past.

Fundamental to testing the relevance of these hypotheses is determining if the same *Azolla* species occurs across the Arctic and Nordic Seas and this requires the detailed study of *Azolla* assemblages outside the Arctic Basin. Study of an assemblage of *Azolla* from Denmark is appropriate as the first step in this work for three reasons. Firstly, the assemblage is from the most southerly site of *Azolla* records in the North Sea (Brinkhuis et al., 2006, fig.

S-3, table S-1 Danish outcrops; Speelman et al., 2009b, fig 2) so, if conspecific with that from the Arctic, this will demonstrate wide geographic spread. Secondly, the assemblage comes from strata where one of us (CH-C) has undertaken extensive and detailed analysis of dinoflagellate assemblages. These dinoflagellates provide an excellent biostratigraphy (multiple zonal markers are present) and enable correlation to global stages and time scales. Thirdly, the Danish strata have yielded abundant well-preserved *Azolla* material, including megaspore apparatus, microspore massulae and the two interconnected. The quality of the assemblage will permit detailed comparison with all characteristics of *Azolla arctica* Collinson et al. and will also establish levels of variation in the Danish material. Having established the characteristics and variation of the spatially separated Arctic and Danish *Azolla*, from these abundant and character-rich assemblages, it will then be possible to further test the various hypotheses in the future using more fragmentary and less abundant material from multiple borehole cores from intermediate sites.

In this paper correlation between the Arctic and Danish sites will be established using dinoflagellates and magnetostratigraphy via Ocean Drilling Program (ODP) Hole 913B in the Norwegian-Greenland Sea. The Danish transitional Ypresian/Lutetian *Azolla* assemblage will be described and compared in detail to *Azolla arctica* from the Arctic Basin to determine if the two assemblages are conspecific.

## 6.2 Materials and methods

*Azolla arctica* has been fully documented in Collinson et al. (2009). This material was recovered from the Lomonosov Ridge during the Arctic Coring Expedition (ACEX) or Integrated Ocean Drilling Program (IODP) Expedition 302, Site 4, Hole A, Core 011X) and specimens were studied in palynological slides and mesofossil preparations.

The Danish *Azolla* is known from just a single horizon, up to 2.8 m thick, and was first observed and described in an unpublished master thesis (Heilmann-Clausen, 1978). This occurrence has only been briefly mentioned since then (Heilmann-Clausen, 1993, 1996; Heilmann-Clausen et al., 2008) and the material has not been fully described. The *Azolla*-bearing horizon occurs in all localities in exactly the same lithostratigraphical position, namely in the middle of Bed L2 of the Lillebælt Clay Formation, defined in Heilmann-Clausen et al. (1985). The material studied in detail here comes from Heilmann-Clausen sample 2904 from Kirstinebjerg, northern Lillebælt area in central Denmark, and is derived from processing 29 grams dry weight of sediment, and sieving retaining material above 40µm. The sample is rich in dinoflagellates as well as *Azolla* megaspore apparatus and microspore massula clusters.

19 megaspore apparatus (three with attached microspore massulae) and two microsporocarps were studied by SEM (Collinson). The megaspore apparatus were specifically picked to represent the range of morphologies seen in the sample. Two of these megaspore apparatus and one of the microsporocarps were studied by TEM (Collinson). Specimens

contain varying amounts of iron pyrite crystals, especially in the float zone of the megaspore apparatus, which limited TEM work and has affected the preservation of the exoperine and microspore massula surface in some cases.

Samples were independently studied at Utrecht University; 5 megaspore apparatus and 5 microspore massula clusters were studied by SEM; 50 megaspore apparatus, 5 microspore massula clusters and 32 prepared massulae were studied by LM. Samples were processed following the method described in Collinson et al. (2009). One of the megaspore apparatus (Plate I,3) was treated with Schulze's solution ( $\text{KClO}_3$  & 30%  $\text{HNO}_3$ ) for c. 5 min prior to light microscopy. LM photographs are taken with a Pentax Camera Optio L30. LM, SEM and TEM photographs have not been manipulated other than to enhance contrast and brightness of the entire photograph unless stated in the figure legends.

A single specimen of the Danish *Azolla* was also studied (by LH) using the Gatan X-ray Ultramicroscope (XuM), which is a nano-computed tomography (nano-CT) system hosted on an XL30 FEG SEM at The Natural History Museum, London. The XuM uses the electron beam of the SEM to produce a microfocus x-ray source on a metal target. The generated x-rays are transmitted through the sample and projected onto a high performance direct detection low noise CCD detector to form an image (Mayo et al., 2005, Mainwaring, 2008). Projected images are acquired at 1 degree rotation increments over 190 degrees and reconstructed to generate a 3D volume. This volume can be virtually dissected to produce digital sections at any orientation throughout the sample.

For XuM the specimen was mounted onto a brass pin stub, using Bostik diluted with acetone, and coated with 20 nm of gold-palladium, using a Cressington sputter coater. The x-ray source was generated by focusing a 10 kV electron beam, spot size 4 with a 200µm aperture onto a Vanadium target. The images were acquired with a 400s exposure (total acquisition time of 21 hours) and a LoG Deconvolution filter (kernel width 0.578) applied to reduce the noise. The reconstructions were carried out using Gatan's cone-beam algorithms in DigitalMicrograph. The digital slices were generated using VG Studio Max 2.0.

## 6.3 Biostratigraphy and correlation

### 6.3.1 Danish *Azolla*

The lower beds of the Lillebælt Clay, including the L2 Bed, are non-calcareous and entirely barren of calcareous micro- and nannofossils. However, a high-resolution dinoflagellate zonation (Heilmann-Clausen, 1988) serves as a biostratigraphical framework. The *Azolla*-bearing horizon spans the boundary between the *Areosphaeridium diktyoplokum* Zone and the *Dracodinium pachydermum* Zone (zones of Heilmann-Clausen, 1988). Currently, *Dracodinium pachydermum* Caro 1973 is considered as a junior synonym of *Wetzeliella eocaenica* Agelopoulos 1967, a view followed here, so in the following the name *Wetzeliella eocaenica* will be used for the species instead of *Dracodinium pachydermum*. The zonal boundary is defined by the first occurrence of *W. eocaenica* and is associated with the

simultaneous last occurrence of *Charlesdowniea columna* as well as other dinocyst events discussed in Heilmann-Clausen (1993 and in prep.).

Other dinocyst events relevant for the age of the *Azolla* horizon include the first occurrence of *Areosphaeridium diktyoplokum* at the base of the *Areosphaeridium diktyoplokum* Zone in the topmost Røsnæs Clay Formation (Bed R6), the last occurrence of *Eatonicysta ursulae* within the *D. pachydermum* Zone (in lower part of Bed L4), and the last occurrence of *Wetzeliiella eoacaenica* at the top of the *D. pachydermum* Zone (upper part of Bed L4).

### 6.3.2 Arctic *Azolla*

Unfortunately, due to the unusual freshwater conditions, the index dinoflagellate species of the Danish (and North Sea Basin) sequence are all absent from the Arctic ACEX IODP 302 cores (Brinkhuis et al., 2006). Furthermore there is no palaeomagnetic record from the ACEX sediments (Backman et al., 2008). However, three ODP cores in the nearby Norwegian-Greenland Sea, contain both the *Azolla* interval and the age diagnostic dinoflagellates that are also present in the Danish succession as well as having paleomagnetic data (Eldrett et al., 2004). ODP Hole 913B contains a substantial quantity of *Azolla* glochidia and microspore massulae in palynological preparations (Eldrett et al., 2004) allowing the abundance and stratigraphic distribution to be documented (Brinkhuis et al., 2006, fig. 2). The last occurrence of abundant *Azolla* in ODP Hole 913B coincides with the last consistent occurrence of *Eatonicysta ursulae* and is above the LO of *Charlesdowniea columna* (Eldrett et al., 2004, supplementary online information; Brinkhuis et al., 2006; HB personal observations) and is directly calibrated against mid Chron C21r (Eldrett et al., 2004). Furthermore, Brinkhuis et al. (2006, fig 2) noted the last occurrence of abundant *Eatonicysta ursulae* within Chron C22n within ODP 913B, at a level where only small numbers of *Azolla* were recorded, hence possibly near the onset of the *Azolla* interval. The LO of *Charlesdowniea columna* occurs within the interval with abundant *Azolla*, well below the LO of *Eatonicysta ursulae*, and is directly correlated to near the top of Chron C22n according to Eldrett et al. (2004) and Brinkhuis et al. (2006). The age of the top of Chron C22n is 48.6 Ma according to Ogg et al. (2008).

### 6.3.3 Age comparison of *Azolla* occurrences

The *Azolla* interval was thought to maximally span c. 800,000 years c. 49.1 to 48.3Ma according to Brinkhuis et al. (2006, fig 2) or 600,000 yrs (c. 49.2 to 48.6Ma, based on the latest age model of Backman et al. (2008, fig 7)) whilst Speelman et al. (2009b) now estimate the maximal duration of the *Azolla* interval in the Arctic and Nordic Seas to be in the order of 1.2Ma from 48.1 to 49.3Ma based on the Gradstein et al. (2004) timescale.

As shown above the Danish and the Norwegian-Greenland Sea *Azolla* intervals both span the LO of *Charlesdowniea columna*. In the offshore North Sea an Eocene dinocyst zonation, mainly based on ditch cutting samples and therefore based on last occurrences, was published by Bujak and Mudge (1994). Bujak and Mudge (1994) noted the occurrence of

*Azolla* in Subzone E3b, the top of which is defined by the LO of *Charlesdowniea columna*. The top of the overlying subzone 3c is defined by the last consistent occurrence of *Eatonicysta ursulae* and the top of the subsequent subzone 3d is defined by the LO of *Eatonicysta ursulae*. In Denmark the LO of *Eatonicysta ursulae* is also above the abundant *Azolla* occurrence (in Lillebælt Clay Bed L4) whilst in the Norwegian-Greenland Sea LO of abundant *Azolla* is coincident with last consistent occurrence of *Eatonicysta ursulae* (Eldrett et al., 2004; HB personal observations) (note that LO *Eatonicysta ursulae* was not plotted in Brinkhuis et al. (2006)). The proposed correlation of the LO of abundant *Azolla* in the Arctic with the LO of abundant *Azolla* in ODP Hole 913B (Brinkhuis et al. 2006; HB personal observations) is consistent with the current ACEX age model of Backman et al. (2008) but remains an assumption.

Summarizing the above, several biostratigraphical markers clearly indicate that the Danish *Azolla* is of the same age as the abundant *Azolla* interval in the Norwegian-Greenland Sea. Although in the Arctic Ocean there is very little direct evidence of the age relationships, within the confines of the available evidence the Arctic *Azolla* appears to be of at least overlapping age.

## 6.4 Descriptive terminology and classification

The diagnosis follows the sequence, style and terminology of those in Batten and Collinson (2001) and Collinson et al. (2009) to enable comparison with *Azolla* species from the North Sea and Arctic Ocean Basins, which have so far been studied in detail with SEM and TEM. The *Azolla* megaspore apparatus is subdivided into a distal megaspore and a proximal float system. The term 'float' is a misnomer as it has been demonstrated conclusively that the floats do not render the megaspore more buoyant (Fowler, 1975; Dunham and Fowler, 1987). *Azolla* microspores are not shed but contained within a perine-derived microspore massula, the outer surface of which is usually ornamented with hairs (glochidia), often barbed, which readily become attached to hairs (filosum) on the surface of the megaspore apparatus. For further details of *Azolla* morphology see Batten and Collinson (2001) and Collinson et al. (2009). The classification follows Smith et al. (2006). Exoperine surface terminology follows Punt et al. (2007).

## 6.5 Systematic Palaeobotany

### 6.5.1 Taxonomic status

Order Salviniales

Family Azollaceae

Genus *Azolla* Lamarck

Species *Azolla jutlandica* Collinson et al., sp. nov.

### 6.5.2 Specific diagnosis

Megaspore apparatus ovoid to pear-shaped, c. 350-410  $\mu\text{m}$  long, c. 300  $\mu\text{m}$  wide. Megaspore inferred to be spherical to sub-spherical with a flattened apical part when uncompressed, diameter c. 300  $\mu\text{m}$ , trilete mark on the proximal pole, leasurae relatively short, extending up to one third of the spore radius. Leasurae slightly elevated, up to 5  $\mu\text{m}$  high. Entire megaspore apparatus covered by a c. 5  $\mu\text{m}$  thick mat of intertwined hairs (filosum). Hairs always arise from the proximal region of the megaspore (hence suprafilosum) but also, to a much lesser degree, from the exoperine of the megaspore wall (hence infrafilosum). Remnants of megasporocarp wall, one cell layer thick, firmly attached over the proximal pole of the megaspore apparatus.

Megaspore wall consisting of an exine c. 4  $\mu\text{m}$  thick and a two layered perine c. 7-8  $\mu\text{m}$  thick extending to at least 15  $\mu\text{m}$  with excrescences. Megaspore surface scabrate under the transmitted light microscope. In thin section under TEM the inner surface of the exine forming a more or less continuous membrane, beneath a more open structure, small irregular cavities dominating the exine and the endoperine, giving both a spongy porous appearance. In thin section in TEM exoperine consisting of nodular to clavate masses (1 to 4  $\mu\text{m}$  in thickness), with a solid exterior but an alveolate interior, supported on sparse short narrow columns (usually less than 1  $\mu\text{m}$  in width). Exoperinal masses producing a surface which, under SEM, is scabrate, to granulate to baculate or clavate (units c. 1  $\mu\text{m}$  in diameter and up to 2  $\mu\text{m}$  high), to almost rugulate in places (units up to 3  $\mu\text{m}$  in length). Sometimes hairs arise from the exoperine (hence infrafilosum) all over the megaspore. Megaspore perinal excrescences variable, ranging from 15 to 30  $\mu\text{m}$  high, at irregular intervals over the spore, sometimes coalescing laterally; megaspores sometimes tuberculate. Perinal excrescences formed from proliferation of the endoperine and surmounted by exoperine. Perine expanded in thickness and becoming spongy in structure near the proximal pole of the spore forming a collar, collar encircling the megaspore and giving rise to numerous hairs extending up into the central region of the float zone and out onto the outer surface of the entire megaspore apparatus.

Float system a compact pyramidal structure with rounded apex, occupying at least the upper two fifths of the megaspore apparatus, slightly overlapping the proximal part of the megaspore. Floats probably 6, arranged in one tier, spongy, pseudovacuated, wedge-shaped and enmeshed in the hairs of the filosum, organised in groups of two between partitions of a well distinguished columella. Collar and columella originating from the exoperine in the apical part of the megaspore.

Microspore massulae single or grouped in clusters, irregular in shape, internally spongy, vacuolated in structure. Massulae contain 6-20 smooth-walled trilete microspores (20-25  $\mu\text{m}$  in diameter), laesurae extend up to one third of the radius of the spore. Outer surface of microspore massulae with numerous aseptate glochidia, from 25 – 40  $\mu\text{m}$  long, with a broad basal attachment, narrower lower stalk, wider upper stalk with a distal dilation and a distinct constriction below an anchor shaped tip. Flukes narrow gradually and lack recurved hooks.

Holotype - Collinson Plate I,1; U23047

Paratypes - Figured material U23048A-P; other referred material U23049. Light microscope slides Prep.4483-4507.

Locality - Kirstinebjerg, Trelde Næs, northern Lillebælt area, central Denmark

Stratigraphy - Bed L2, Lillebælt Clay Formation, northern Lillebælt area, Albækhoved, Ølst and Hinge

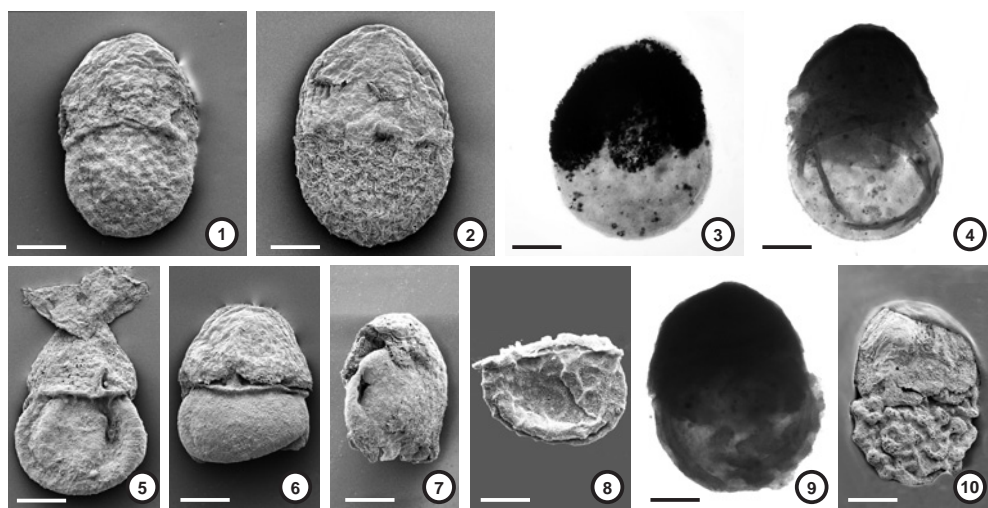


**Plate I.** 1,2,5-8,10 SEM; 3,4,9 LM. Scale bars: 1-10: 100 µm.

1. Megaspore apparatus with intact apical cap and entire covering of filosum, underlying collar and exoperinal excrescences are visible. Surface shows damage (Plate III, 5) common in this material. Holotype: U23047.
2. Megaspore apparatus with intact apical cap and entire covering of filosum, collar obscured, swirling of filosal hairs (detail Plate II,12) reveals presence of underlying excrescences. U23048G. Specimen now in TEM block.
3. Megaspore apparatus with covering of filosum, float zone (dark) is revealed by dense pyrite accumulation and the curved bases of three (out of six) floats can be clearly distinguished. This specimen has undergone oxidation (see method section). Prep. 4494.
4. Megaspore apparatus with darker float zone and lighter megaspore zone, megaspore wall partially folded due to compaction. Prep. 4495.
5. Megaspore apparatus in which part of the filosum and apical cap have naturally folded back revealing underlying float zone, collar and megaspore. U23048M.
6. Megaspore apparatus where the filosum has been lost over the megaspore but is retained over the float zone, the collar and basal part of one arm of the columella are revealed with parts of floats either side of the columella. Base of megaspore is folded due to compaction. U23048O.
7. Megaspore apparatus where filosum has been partially lost over the megaspore but megaspore surface is not damaged. U23048K.
8. Isolated megaspore, badly damaged but with fragments of attached filosum (background blacked out using Photoshop). U23048E.
9. Megaspore apparatus with large, columnar, partially coalescing excrescences. Prep. 4493.
10. Megaspore apparatus with large, columnar, partially coalescing excrescences background blacked out using Photoshop). U23048J.



## 6.6 Additional descriptive notes and comparison with *Azolla arctica*

### 6.6.1 Megaspore apparatus - general organisation and filosum

In general the shape of the megaspore apparatus in *Azolla jutlandica* is ovoid to pear-shaped with more pointed proximal end (Plate I, 1-6, 9, 10) in contrast to the obtuse ends in *A. arctica*. Maximum length is small like *A. arctica*. In *A. arctica* the suprafilosum was persistent on all except one specimen studied (Collinson et al., 2009, plate I, 4). In *A. jutlandica* many specimens (at least 33) are completely covered with filosum as in *A. arctica*. However, in one specimen the cap and most filosum had folded back away from the spore (Plate I, 5) and in c. 6 specimens the filosum was partly (Plate I, 7) or totally lost over the megaspore (Plate I, 6, 10). Also c. 5 isolated megaspores were found (Plate I, 8). These specimens indicate that the filosum was much less persistent and much more readily detached in *A. jutlandica* than in *A. arctica*. The apical cap (Plate II, 1, 2, 4) is similar to the apical cap of *A. arctica*. In some specimens (Plate II, 4) of *A. jutlandica* the effects of decomposition and pyrite crystal growth can be clearly seen where the cap layer is only partially preserved, revealing the underlying filosum near the cap base and where the outer periclinal cell wall of the cap layer has been lost to reveal the gemmate inner surface of the inner periclinal cell wall, the structure of which is exactly like that in *A. arctica*. The float zone occupies more of the megaspore apparatus, two-fifths to one half in *A. jutlandica* (Plate I, 1-5, 9, 10) but only one third in *A. arctica*. The collar (Plate I, 1, 5, 6; Plate II, 5) in *A. jutlandica* is very similar to *A. arctica* but the columella is more distinct in *A. jutlandica* (Plate II, 5).

### 6.6.2 Megaspore apparatus – megaspore wall

The undamaged megaspore wall is revealed by specimens with partial loss of filosum (Plate I, 7) and by broken specimens (Plate II, 6). Typically the megaspore wall is obscured by a filosum, which is thinner in *Azolla jutlandica* (up to 5  $\mu\text{m}$ ) than in *A. arctica* (8-10  $\mu\text{m}$ ). The filosal hairs are c. 1  $\mu\text{m}$  in diameter, wider than in *A. arctica*, and typically randomly arranged (Plate II, 7) (exception see below). In section (Plate II, 8-11) the exine, endoperine and exoperine are together 10-12  $\mu\text{m}$  thick (excluding excrescences), twice the thickness of *A. arctica*. In *A. arctica* there are no perinal excrescences. None of the *A. arctica* specimens showed any topography or distinctive arrangement of filosal hairs such as might indicate underlying perinal excrescences. None of the TEM sections of *A. arctica* (n=4) revealed excrescences and all showed very similar megaspore wall organisation. In *A. jutlandica* three specimens (including Plate I, 9, 10) have very pronounced excrescences (tuberculate to columnar), others clearly show topography of excrescences (Plate I, 1; Plate II, 15) underlying the filosum, whilst in some specimens there is no external indication of excrescences (Plate I, 2). However, when these are sectioned (Plate II, 10) even these reveal that excrescences are present. Also the arrangement of the filosum, when pristine, has a swirling fingerprint



like pattern where it is folded around the excrescences (Plate II,12), which can also be seen under LM when focussing through the layers (e.g. in specimen shown in Plate II,13). The central part and the main topography of the excrescence is formed from proliferation of the endoperine (Plate II,10,11). Exoperine is of a similar thickness over the excrescence as over the rest of the megaspore wall (Plate II,10,11). Excrescences are dome-shaped (Plate I,1; Plate II,15) to columnar (Plate II,14), showing some degree of coalescence (Plate II,13,14) but never link up to form a regular reticulum. Their undamaged surface is the same as that over the main megaspore wall (Plate II,14). When damaged the central part of large excrescences is spongy, vacuolated (Plate II,16) and this relates to holes in the endoperine seen in TEM sections.

The exoperinal surface under SEM is scabrate to granulate to baculate or clavate with rounded units c. 1  $\mu\text{m}$  in diameter and up to 2  $\mu\text{m}$  high (Plate III,1,2). Surface in places is almost rugulate (Plate III,2,3,4) as a result of exoperinal masses fusing in a single plane. The short rugulae reach up to 3  $\mu\text{m}$  in length. The pattern is very variable with some short straight rugulae and some sharply angled (Plate III,2,4). In a number of specimens the surface is altered (probably due to a combination of decomposition and diagenetic factors including extensive pyrite crystal growth). The damaged surface of the megaspore apparatus overlying the megaspore can be so different from the undamaged surface such that it could be misinterpreted as a different exoperine morphology (Plate III,5). The exoperine surface itself is also often damaged and may appear as a fine irregular reticulum (lumina 1-3  $\mu\text{m}$ ) (Plate III,3,6) or it may be perforate (parts of Plate III,2,4). These appearances relate to the underlying alveolate structure of the exoperinal masses as seen in TEM sections (Plate II,10,11) and also to damage by pyrite crystal growth. By light microscopy the fine reticulum is sometimes very distinct (Plate III,6) when focussing through the megaspore wall and sometimes the small perforations are also visible. In contrast, in *A. arctica* the exoperinal masses are fused at various levels through the thickness of the exoperine resulting in a wavy and undulating rugulate morphology in several planes. In *A. jutlandica* infrafilosum hairs arise from the exoperine surface. These are very scarce (Plate III,7).

In thin section under TEM (Plate II,9-11) the exine has a slightly more dense structure and less electron lucency (appears visually darker) but otherwise is difficult to distinguish from the endoperine. Both have a spongy appearance as a result of small cavities in their structure. In the exine these show a tendency to be elongate perpendicular to the surface giving a slightly radially striate appearance which is not present in the endoperine or in the exine of *A. arctica*. In *A. jutlandica* the surface of the endoperine is irregular with small protrusions (Plate II,9) that extend up to 2  $\mu\text{m}$  into the spaces between the columnar units of the exoperine. These endoperinal protrusions are lacking in *A. arctica* and we consider this a species diagnostic character. The endoperine in some areas contains small holes (Plate II,10,11), ranging from 1-4  $\mu\text{m}$  in maximum length, these occur in various positions but have a tendency to be elongate parallel to the surface of the endoperine, except in the excrescences where they are more isodiametric (Plate II,10). These holes are lacking in *A. arctica*.

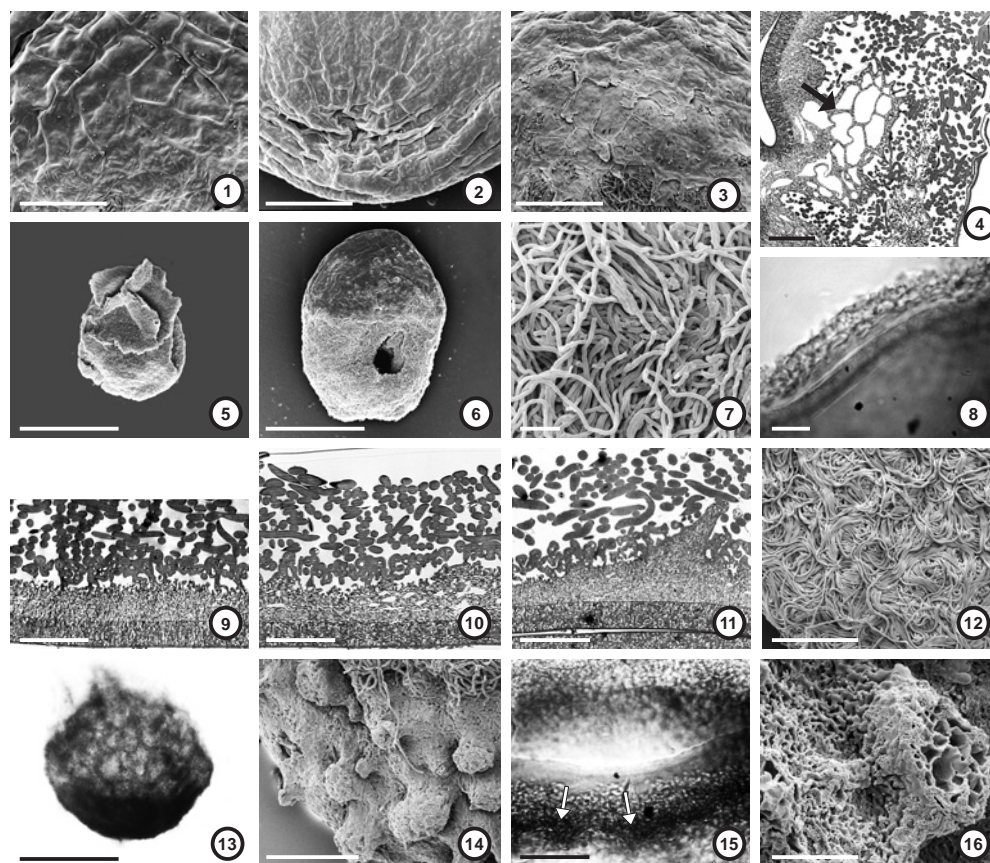


**Plate II.** 1-3,5-7,12,14,16 SEM; 4,9-11 TEM; 8,13,15 LM. Scale bars: 1-3,12,14,15: 50  $\mu$ m; 4,7-11: 10 $\mu$ m; 5,6,13: 200  $\mu$ m; 16: 20  $\mu$ m

1. Cell pattern of apical cap near base, topography of underlying filousum can be seen at the base of the image. U23048F.
2. Apical cap looking onto the apex of the megaspore apparatus. U23048D.
3. Damaged apical cap, base of image reveals filousum where cap has been lost, mid-part of image has cap cells which have lost their outer periclinal wall, upper part of image has intact cap. U23048H.
4. Ultrathin section of part of a megaspore apparatus (same specimen as Plate II, 11) showing (from top left of image downwards to base right) the megaspore wall, the spongy collar derived from exoperine, the filousum (most electron dense) surrounding the collar, part of a float and the single cell layer of the cap (arrow) covering the filousum. U23048L.
5. Naturally damaged specimen lacking filousum and floats and thus revealing the collar and columella (background blacked out using Photoshop). U23048E.
6. Slightly damaged megaspore apparatus covered in filousum but revealing underlying megaspore wall surface (Plate III,1) beneath small hole in the filousum. U23048D.
7. Filousum overlying surface of megaspore typically showing irregular intertwining of hairs. U23048D.
8. Thick section showing megaspore wall overlain by filousum. Prep. 4493.
9. Ultrathin section showing megaspore wall and overlying filousum from Plate 1,2. Innermost exine at base of image slightly more electron dense and more radially striate than overlying endoperine; endoperine surface with

small irregular protrusions between sparse columnar elements of the exoperine; exoperine consists of nodular to clavate masses supported on the sparse columnar elements. U23048G.

10. Ultrathin section showing megaspore wall and overlying filsum, from Plate I,2. Characteristics as in Plate II,9 except that endoperine contains small holes and there are partial sections through two excrescences at left and right of image. The presence of excrescences was not obvious in all sections (Plate II,9) nor prior to sectioning except from the swirling pattern of filsum (Plate II,12). U23048G.

11. Ultrathin section (same specimen as Plate II,4) showing megaspore wall and overlying filsum. Characteristics as in Plate II,9 except for the large excrescence formed from proliferation of endoperine. U23048L.

12. Filsum over megaspore surface (detail of Plate I,2) with swirling hairs indicating presence of underlying excrescences (see in TEM section Plate II,10). U23048G.

13. Megaspore apparatus compressed longitudinally, partial coalescence of excrescences shown by darker bands. Float zone detached; part of columella and filsum protruding in upper part of image. Prep. 4485.

14. Detail of megaspore wall of specimen with mostly undamaged pronounced columnar excrescences which vary considerably in size. Filsum still present over float zone and seen at top of image. U23048P.

15. Thick section showing dome-shaped excrescences (arrows) on megaspore wall. Prep. 4492.

16. Surface of damaged megaspore wall (from Plate I,10) revealing underlying spongy texture of large excrescence. U23048J.

The exoperine as seen in TEM section (Plate II, 9-11) consists of nodular to clavate masses (1-4  $\mu\text{m}$  in thickness and up to 4  $\mu\text{m}$  high) with a solid exterior but an alveolate interior; supported on sparse, short, narrow columns (usually less than 1  $\mu\text{m}$  in width and typically c. 2  $\mu\text{m}$  high). *A. arctica* has tabular masses in addition which are lacking in *A. jutlandica*. The surface of the exoperine as seen in section is more or less in a single plane in *A. arctica* whilst in *A. jutlandica* it is irregular (Plate II,9). Where the exoperinal masses are fused in *A. jutlandica* this occurs more or less at a single level leaving clear spaces between the columns (Plate II,9), in contrast in *A. arctica* there are several levels of fusion resulting in very discontinuous and irregular spaces.

### 6.6.3 Megaspore apparatus – float system

The float system occupies at least two fifths of the proximal part of the megaspore apparatus (Plate I,1-6,9,10) slightly more than in *Azolla arctica*. In *A. jutlandica* the float system is a compact pyramidal structure with rounded apex (Plate I,1-4,6,9) whilst in *A. arctica* it is dome-shaped. The float zone in *A. jutlandica* is clearly not multifloated, in contrast to *A. arctica* which was estimated to have 15-18 floats in three tiers and undoubtedly more than 9 floats. In *A. jutlandica*, there is one tier of floats (Plate I,5; Plate III,8,9), their spongy structure can be seen in LM (Plate III,9) and in damaged specimens by SEM (Plate I,6; Plate III,11). The floats are arranged in groups of two (Plate I,5) between partitions of a well-distinguished columella (Plate II,5). In contrast in *A. arctica* the columella was thinner in all parts and hence much less distinct. In one specimen of *A. jutlandica* a possible very small third float (or float partition) is present in one visible compartment (Plate I,5), which suggests that the maximum possible float number is nine, but we consider that a float number of six is likely to typify *A. jutlandica*.

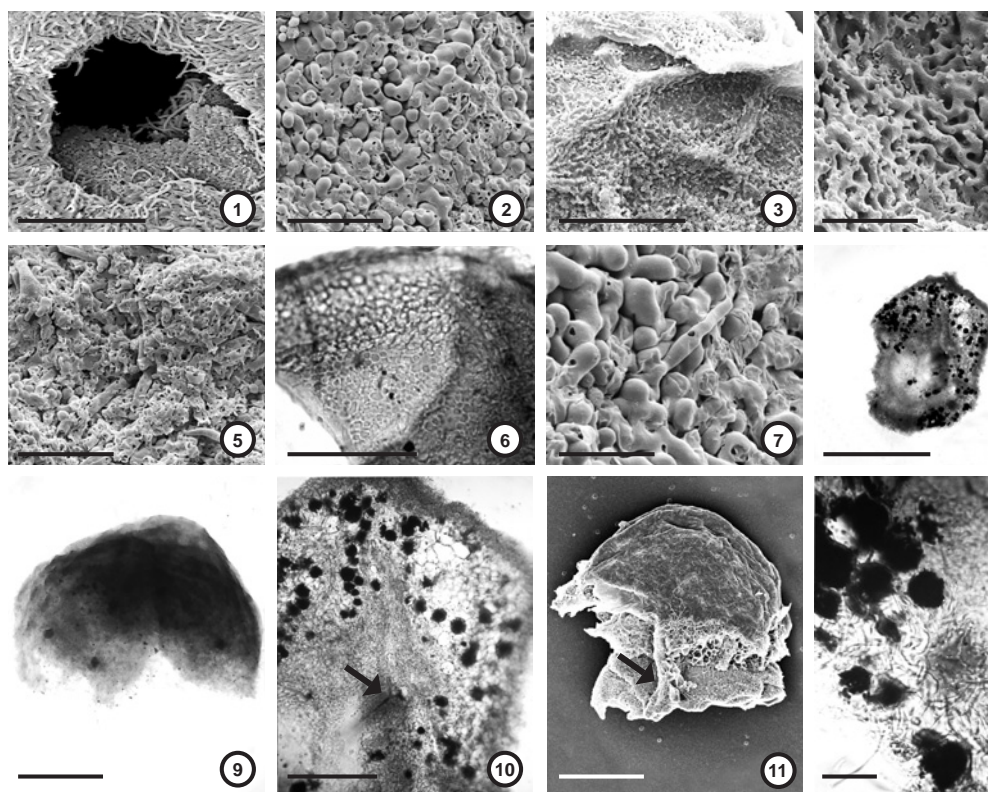


**Plate III.** 1-5,7,11 SEM; 8-10,12 LM. Scale bars: 1,3,6,10: 50  $\mu$ m; 2,4,5,12: 10  $\mu$ m; 7: 5  $\mu$ m; 8: 200  $\mu$ m; 9,11: 100  $\mu$ m

1. Broken megaspore apparatus (detail of Plate II,6) revealing surface of megaspore exoperine where filiosum has broken away. U23048D.
2. Largely undamaged surface of megaspore exoperine where filiosum has been lost (detail of Plate I,7). Small holes are the result of pyrite crystal growth. U23048K.
3. Surface of megaspore exoperine on an isolated megaspore (Plate I,8) showing rugulate to reticulate surface as a result of alteration. U23048E.
4. Surface of megaspore exoperine (detail of Plate I,10 between excrescences) with rugulate pattern, partly damaged by pyrite growth (small holes) and decomposition or abrasion. U23048J.
5. Surface of megaspore apparatus from Plate I, 1 (holotype). Much of the surface is severely altered and could potentially be misinterpreted as a granular exoperine, especially if studied by LM. However, some filiosum hairs are clearly evident and a small patch of true exoperine surface has been revealed in the lower left of the image. U23047.
6. Dissected megaspore wall showing appearance of fine reticulum when focussing through the wall layers. Prep. 4492.
7. Detail of Plate III,2; Plate I,7 showing rare infrafiliosum hair. U23048K.
8. Thick section of megaspore apparatus showing float zone. Prep. 4490.
9. Float zone dissected from megaspore apparatus focussing on two large floats each of which occupies the entire length of the float zone. Prep. 4487.

10. Detail of Plate III,8 showing spongy nature of float, central column of suprafilosum, and trilete mark of megaspore. Prep. 4490.

11. Dissection of upper part of megaspore apparatus showing collar, one branch of the columella (arrow) and adjacent spongy tissue of the floats. U23048B.

12. Detail of Plate III,8; Thick section of megaspore apparatus with aborted megaspore within float tissue. Prep. 4490.

In one LM section (Plate III,8,10) of a megaspore apparatus the megaspore with the trilete mark, a clear columella, a central column of suprafilosum and the single tier of floats were distinguishable. On the distal part of the megaspore apparatus an abortive megaspore (measuring ca 13µm diameter) with a distinct trilete mark was found (Plate III,12) within spongy float-like tissue.

#### 6.6.4 Microsporocarps, microsori or microsporangia

These compound structures are compressed round to ovoid and range in longest dimension from 150-250 µm. A specimen seen by LM (Plate IV, 1) suggests a minimum of four sub-units and four sub-units can also be seen in a LM (Plate IV, 2) section. Under SEM three specimens (Plate IV, 3-5) show 7-11 sub-units on one side suggesting up to c. 20 sub-units in total. Each sub-unit is c. 50-60 µm in diameter as seen under LM and SEM. In one specimen (Plate IV, 5) and in the LM section (Plate IV, 2) the structure shows evidence of separation of the sub-units. The sub-units are covered in glochidia and show ornamentation (Plate IV, 6), both identical with those of dispersed microspore massulae or massula clusters (see below). The structures are tentatively interpreted as microsporocarps or microsori containing microsporangia, but it is possible that they may represent the contents of a single microsporangium containing microspore massulae and the size of the sub-units is more consistent with the latter.

#### 6.6.5 Microspore massulae

Microspore massulae are occasionally found attached to megaspores (Plate IV, 7), rarely occur in clusters (Plate IV, 8) and occur singly (Plate IV, 9,13) in the sediment samples. As in *A. arctica* the massulae are variable in shape and flattened discoidally, they vary considerably in size although the smallest specimens of *A. jutlandica* may have been lost through the 40 µm sieve. Measured isolated massulae range from 50-100 µm in longest dimension. Their attachment to the megaspores is mediated by the anchor-shaped tips of the glochidia that become enmeshed in the filousum hairs covering the megaspore apparatus (Plate IV, 7). In *A. jutlandica* numerous spiny dinoflagellates also attach to the megaspores and some are attached amongst the microspore massulae (Plate IV, +7, object at lowest right). In TEM section the glochidia can be distinguished as solid structures (Plate IV, 11) whilst the main body of the massula is spongy vacuolated and encloses the microspores (Plate IV, 11,12).



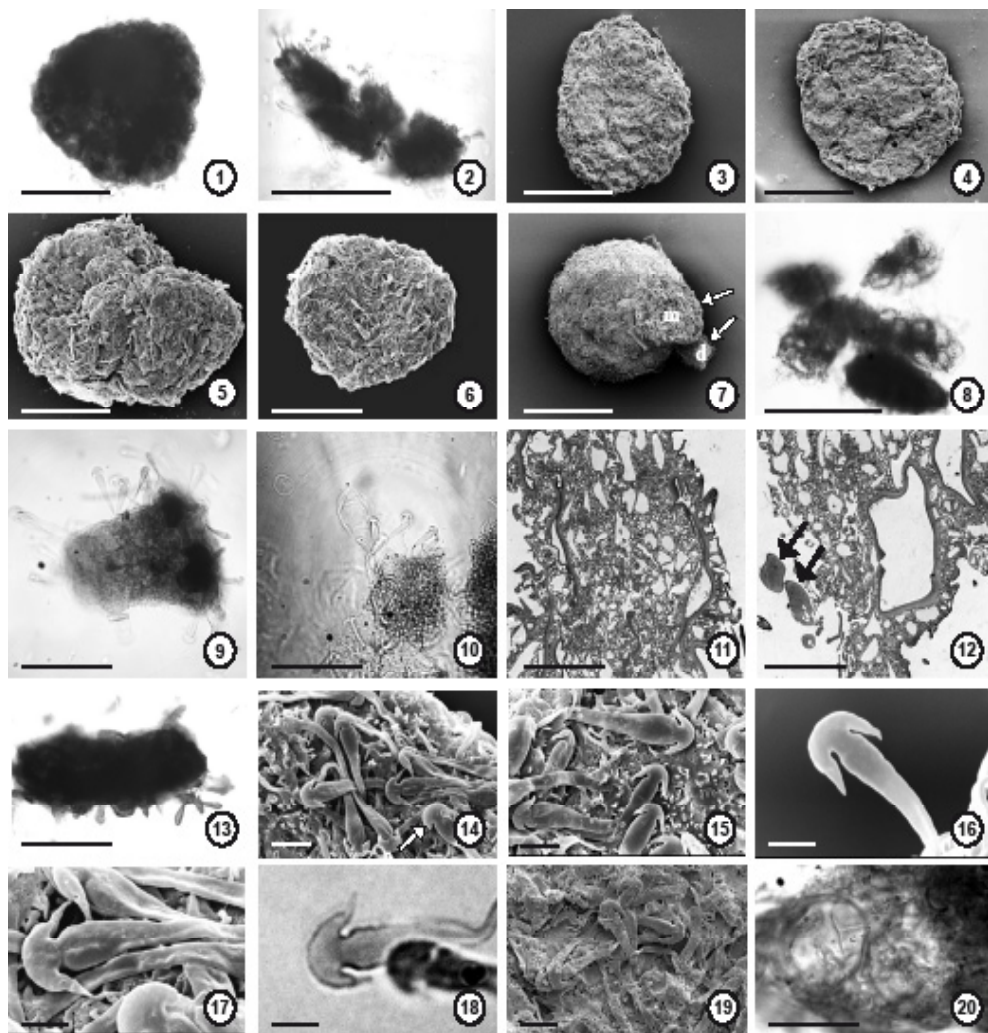


**Plate IV.** 1,2,8-10,13,18 LM; 3-7,14-17,19,20 SEM; 11,12 TEM. Scale bars: 1-6,8: 100  $\mu$ m; 7: 200  $\mu$ m; 9,10,13: 50  $\mu$ m; 11,12,14,16,19: 10  $\mu$ m; 15, 17, 18: 5  $\mu$ m; 20: 20  $\mu$ m. 1-6. Compact groups of microspore massulae (microsporocarps, microsori or microsporangial contents).

1. Complete group showing at least four subunits. Prep. 4483.
2. Thick section showing at least four subunits. Prep. 4483.
3. 4. 5. Groups showing various numbers of subunits (7-11) on exposed side implying at least 20 in total. 3-5. U23048N. U23048R. U23048C. Specimen 3 now in TEM block.
6. Group where subunits are not clear but size indicates that it cannot be a single microspore massula. Glochidia are clearly seen (background blacked out using Photoshop). U23048A.
7. Megaspore apparatus compressed base to apex, with attached microspore massula (arrow m) and dinoflagellate (arrow d). U23048I.
8. Cluster of microspore massulae showing microspore contents. Prep. 4483.

9. Single microspore massula with single size category of anchor-tipped glochidia and a rare example of grouped glochidia at lower right.
10. Small microspore massula with anchor-tipped glochidia. Massulae loosely attached to filousum of megaspore apparatus. Prep. 4486.
11. Ultrathin section of microspore massula showing spongy vacuolated tissue and microspores. U23048N.
12. Detail of single microspore, spongy tissue and glochidia in section at left. U23048N.
13. Single microspore massula showing discoidal shape. Prep. 4483.
14. Glochidia showing single size class, basal broad attachment (upper left), middle narrow stalk, expansion in upper stalk, and an example of a rounded tip of fluke when fluke extensions have been lost (arrow). U23048A.
15. Glochidia, (one with very wide upper stalk (top of image)) and massula surface showing perforations and short, narrow hair-like ornamentation. U23048A.
16. Single glochidium showing expansion in upper stalk, distal dilation, anchor shaped tip and flukes with short terminations and lacking recurved hooks. U23048I.
17. Detail of Plate IV,14; Single glochidium showing features as in Plate IV,16 but with long fluke terminations. U23048A.
18. Single glochidium as in Plate IV,17 to demonstrate that these diagnostic features can be seen in LM, for example when glochidia are observed in a palynology preparation. Prep. 4483.
19. Microspore massula surface damaged mainly by pyrite growth. U23048N.
20. Microspores with laesurae extending up to one third of the spore radius. Prep. 4488.

Outer surface of microspore massulae with numerous aseptate glochidia (Plate IV, 9,10). Glochidia are of only a single size class, ranging from 25-40  $\mu\text{m}$  in length, (Plate IV, 9,14,) in contrast to *A. arctica* which has two size classes of glochidia, 15-25 and 55-85  $\mu\text{m}$ . There are only occasional suggestions of glochidia groupings (Plate IV,9 bottom right) and the overall arrangement cannot be clearly discerned in *A. jutlandica*. Glochidia in *A. jutlandica* have a basal attachment up to 5  $\mu\text{m}$  wide (Plate IV, 14,15), slightly narrowed to a very thin and flattened (up to 1 $\mu\text{m}$  thick and 2-3  $\mu\text{m}$  wide) lower stalk (Plate IV, 14,15) which widens again in the upper stalk (Plate IV, 14-18) which can be crumpled (Plate IV, 17). Upper stalk reaches a maximum width (up to 8  $\mu\text{m}$ ) at the distal dilation (Plate IV, 15-18) followed by a distinct constriction below the anchor shaped tip (Plate IV, 15-18). In contrast, in *A. arctica* the maximum stalk width is up to 3  $\mu\text{m}$ . The upper widest part of the stalk of a glochidium can be considered functionally to act as the stiff shaft of an anchor. The width of the anchor shaped tip (=termination width in Sweet and Hills, 1976) is 8-10  $\mu\text{m}$  in *A. jutlandica* in contrast to 4-5  $\mu\text{m}$  in *A. arctica*. Flukes were measured according to the definition in Sweet and Hills (1976). The flukes in *A. jutlandica* are up to 6  $\mu\text{m}$  long (in total) (Plate IV, 17) in contrast to those of *A. arctica* which are c. 3  $\mu\text{m}$  long. In *A. jutlandica* the flukes terminate in a tapering end c. 2  $\mu\text{m}$  in length (Plate IV, 17). A much shorter tapering end (c. 0.5  $\mu\text{m}$ ) is present in *A. arctica* but was not noted as a discrete structure by Collinson et al. (2009). When the tapering ends are lost the fluke termination is rounded in *A. jutlandica* (Plate IV, 14 arrow). As in *A. arctica* fluke swellings are absent, and all glochidia tips have two flukes and none have other barbs along the shaft. As in *A. arctica* there are no recurved hooks on the flukes. The microspore massula surface between the glochidia is perforate and ornamented by short narrow hair-like structures 2-4  $\mu\text{m}$  long

## Chapter 6

and less than 1  $\mu\text{m}$  wide (Plate IV, 15). *A. arctica* has the same surface ornamentation but the hair like structures are smaller (up to 2  $\mu\text{m}$  long and 0.1  $\mu\text{m}$  wide). The surface ornamentation in *A. jutlandica* is often altered by the same processes that have affected the megaspore exoperine. The damaged surface is more perforate and the small hairs are lost (Plate IV, 19). On the damaged massulae, glochidia have small holes and pyrite crystals are often seen on the surface. Massulae contain 6-20 smooth-walled trilete microspores (20-25  $\mu\text{m}$  in diameter) (Plate IV, 8), laesurae extend up to one third of the radius of the spore (Plate IV, 20) in contrast to *A. arctica* where the laesurae are longer, c. two thirds of the radius.

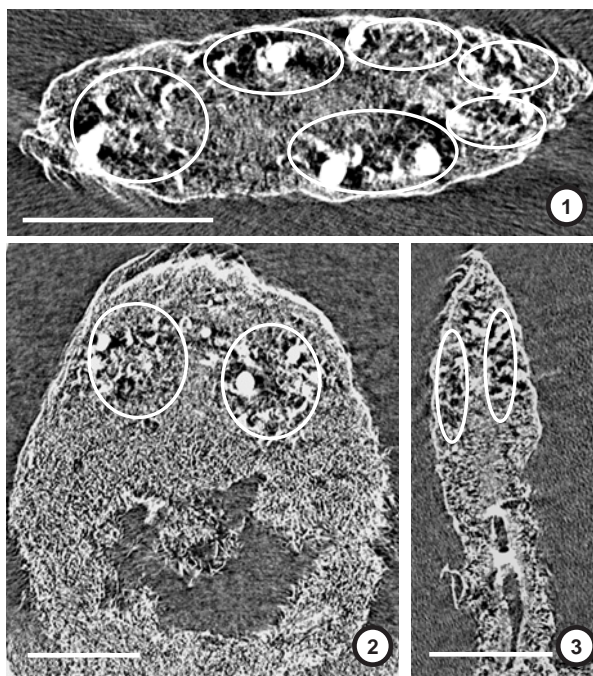


**Plate V.** Scale bars: 1-3: 100  $\mu\text{m}$ .

All XuM, digital sections. Bright white patches are pyrite. White circles outline approximate positions of the individual floats (open spongy structure of floats seen as larger dark spaces), compression has caused some displacement from float position in life.

1. Transverse section of megaspore apparatus near the base of the float system showing all six floats.
2. Longitudinal section perpendicular to plane of compaction, section passing through two floats, one either side of the columella.
3. Longitudinal section parallel to plane of compaction, section passing through two floats, one either side of the columella.



## **6.7 Distinctive characteristics which are common to *Azolla arctica* and *Azolla jutlandica***

- 1) Small megaspore apparatus.
- 2) Retention of proximal 'cap' remnants of megasporocarp wall.
- 3) General organisation of exine, endoperine and exoperine as seen in section by TEM
- 4) Filosum covering obscuring underlying structure in at least some specimens.
- 5) Presence of collar.
- 6) Aseptate glochidia with two flukes and no other barbs.
- 7) Flukes on glochidia have anchor-shaped tips that lack recurved hooks.

## **6.8 Distinctive characteristics which differ between *Azolla arctica* and *Azolla jutlandica***

Table 1 shows the distinctive characters which distinguish *Azolla jutlandica* from *Azolla arctica*. Filosum hairs and anchor-shaped tips to glochidia are both much larger in size in *A. jutlandica* compared to *A. arctica*. However these characters are interdependent for functional reasons as the anchors hook onto the filosum hairs. Equally, for morphological reasons of space occupation, the float number and float tier number to some extent controls shape of float system. Therefore there are eight independent characters that can be used to distinguish *A. arctica* from *A. jutlandica*.

The differences in these characters between *A. jutlandica* and *A. arctica* fall outside the range of variation known in modern species or fossil populations, as far as can be judged from the published literature and the available studies of intraspecific variation (see section 9).

## **6.9 Known intraspecific variation in key characteristics of *Azolla***

When considering if the Danish and Arctic *Azolla* are conspecific it is essential to have a framework of understanding of variation in natural populations of *Azolla*. Here we discuss examples from modern species and from assemblages of fossil species collected from a single stratigraphic unit.

### **6.9.1 Megaspore apparatus**

Perkins et al. (1985) argued that megaspore wall structure and surface ornament was diagnostic at species level. This was supported by Fowler and Stennett-Wilson (1978). Evrard and Hove (2004) showed that *A. filiculoides* had constant wall surface structure (perine surface type described as warty) over a wide geographic area whilst *A. cristata* (= *A. caroliniana*) was more variable. However, *A. filiculoides* and *A. cristata* could be

distinguished as the latter has non-warty perines. Gardenal et al. (2007) also report that studies of *A. filiculoides* have revealed constant structure over a wide geographic area (Argentina, Asia, Hawaii, France and Brazil). *A. filiculoides* has a wide distribution in the Americas and in Australia and New Zealand. The Australian and New Zealand material is distinguished by megaspore wall ultrastructure in section (granulate in *A. filiculoides* var *rubra* in contrast to alveolate in *A. filiculoides* s.s.) as well as the presence of filsum on the collar of the megaspore apparatus and can be given varietal status as *A. f. var rubra* (Large and Braggins, 1993), subspecific status (Fowler and Stennett-Wilson, 1978) or species status as *A. rubra* R. Br (Saunders and Fowler 1993) an ongoing taxonomic problem (Evrard and Hove, 2004).

Zhou (1983) undertook a comprehensive study of the megaspore wall of *Azolla pinnata* R. Brown using modern populations from China, India, Africa and Australia as well as a fossil assemblage from China. Zhou noted that *A. pinnata* was readily distinguishable from the only other species then grouped in section Rhizosperma, *A. nilotica* Decaisne, where the exoperine consists of broad clavae with regularly spaced foveolae giving a coarse granular surface and there are long spiny perinal excrescences. This contrasted with regularly branched anastomosing bacula and elongated, rounded, tubercular or irregular excrescences in *A. pinnata*. In the populations of *A. pinnata* the exoperine varied little with minor variations in shape and size of bacula and shape, size and number of perinal excrescences. Occasionally, in the Australian populations, the exoperinal bacula were extended and connected with each other to form filaments, also involved in composition of the excrescences. In the African material the bacula were more elongate and slender by comparison with other samples. Two types of endoperine were recognized, one (Chinese and Australia megaspores) with rod to thread like elements usually densely aggregated throughout and the other (African material) with many minute cavities. Zhou also noticed minor variations in the appearance of megaspore wall ultrastructure depending on whether the section studied was transverse or longitudinal. In this study (and previous work by the current authors) TEM sections of megaspore apparatus are median longitudinal thus eliminating any variation due to plane of section of megaspore wall such as documented by Zhou (1983). Overall Zhou (1983) concluded "that the ultrastructure of the sporoderm is essentially constant in the megaspores of *A. pinnata* except in the African specimens which are regarded by some authors as a variety .... or even a distinct species". Spaces in endoperine, like those seen in African *Azolla pinnata* but not in other populations of same species (Zhou 1983), although present in Danish material, are not used herein as a species character because of the uncertain status of African *Azolla pinnata*. Saunders and Fowler (1992) distinguished three geographic subspecies of *A. pinnata* using the differences between elongate excrescences and short tuberculate excrescences to distinguish between Asian and African subspecies. Teixeira et al. (2000) showed that *A. pinnata* ssp *asiatica* and *A. pinnata* ssp *africana* both occur in Africa. The two species then in *Azolla* section Rhizosperma (*A. nilotica* and *A. pinnata*) both have perinal excrescences and overlap in distribution in tropical Africa (Saunders and Fowler, 1992). However, the cladistic analysis

by Saunders and Fowler (1993) showed no synapomorphies for this section which was paraphyletic. Section Rhizosperma was restricted to *A. pinnata* in the revised classification by Saunders and Fowler (1993). Variation in the presence or absence of spaces in the endoperine was also noted in New Zealand *A. filiculoides* ssp *rubra* by Fowler and Stennett-Wilson (1978) similar to that noted above observed by Zhou (1983) in *Azolla pinnata* from different geographic areas.

Field (1999) studied variation in *Azolla filiculoides* from three modern populations (introduced) and one fossil population in the UK. Variation was found in size, shape, and external morphology of the megaspore apparatus including in the number of depressions in megaspore surface, the pitted or warty appearance of the surface (possibly linked to partial preservation of megasporocarp or megasporangial walls over the pits), the number of infrafilosum filaments and the width of the collar. Field (1999) concluded that, because of this variation, it would be unwise to create new fossil species of *Azolla* on the basis of small or subtle variations in the megaspore apparatus alone.

Float number, especially in fossil multifloated species, can be very variable (see tables in Collinson, 1980 and Vадja and McLoughlin, 2005). Batten and Collinson (2001) noted that floats could be subdivided in fossil *A. teschiana* and Collinson (1980) figured a specimen of 9-floated *A. prisca* with the lower tier of subdivided floats giving a total float number of 15. In 3 and 9 floated forms float number in fossil species is usually more constant (table in Collinson, 1980). Teixeira et al. (2000) showed that float number could vary up to 11 and 14 in the typically 9-floated species *Azolla pinnata* and quoted Teixeira (1999) as having made similar observations of float numbers greater than the usual three in *Azolla filiculoides* and Saunders (unpublished) to consider that variations in float number were common but rarely reported in the literature.

### 6.9.2 Microspore massulae

Hills and Weiner (1965 Text-figure 1) illustrated the variation in the shape of glochidia tips in two assemblages of fossil *Azolla* species, *A. geneseana* Hills and Weiner and *A. primaeva* (Penhallow) Arnold. The anchor shaped tips of glochidia in *A. geneseana* usually had two flukes but sometimes exhibited three or four; all of these lacked any constriction below the flukes. In contrast those of *A. primaeva* only had two flukes and the stalk expanded followed by a constriction below the flukes.

In some cases the degree of septation in glochidia has been noted as a distinctive specific character (e.g. for *Azolla cristata* and *Azolla filiculoides* Gardenal et al., 2007) but observations such as those of Godfrey et al. (1961), where septate and non-septate glochidia were found typically on a single massula, have led authors to argue against its usefulness. Evrard and Hove (2004) revisited the question by re-examining the herbarium material of *A. filiculoides* that Godfrey et al. (1961) studied. They recorded that of 503 glochidia observed in *A. filiculoides* (on 36 massulae derived from 5 microsporocarps) 427 were unseptate, 63 possessed one septum and 13 were biseptate. As a result they used glochidia septation as one characteristic to distinguish *A. filiculoides* (mostly 0-1septate) from *A. cristata* (mostly 2-pluriseptate).

### 6.9.3 Summary

Future work is needed combining molecular, morphological and ultrastructural work on modern *Azolla* populations to fully establish the levels of intraspecific and interspecific variation and apply this understanding to species delimitation in fossils. On the basis of the available information the difference between the Danish and Arctic *Azolla* assemblages far exceeds the range of variation encompassed in the current concept of any modern species.

## 6.10 Comparison with other fossil *Azolla* species

### 6.10.1 Introduction

Many fossil species are clearly different from *Azolla jutlandica*. This includes all species lacking filose over the megaspore wall, all species lacking glochidia or lacking anchor-shaped tips on the glochidia, or with septate glochidia, all species with recurved hooks on the flukes of the glochidia and all multifloated species (*A. teschiana* and *A. bulbosa* are discussed below as they show clear excrescences on the megaspore wall). Lists and references to fossil *Azolla* species maybe found in Sweet and Hills (1976), Collinson (1980, 1991) and Vajda and McLoughlin (2005).

Uniquely in *Azolla* species *A. jutlandica* is interpreted as having six floats. In contrast to *A. arctica* (Collinson et al. 2009) we have been unable to illustrate the float zone of *A. jutlandica* with TEM due to the presence of abundant pyrite. We have therefore applied XuM (X-ray Ultra-microscopy; nano-scale 3D computed tomography (CT) within a Scanning Electron Microscope) a new technique that permits digital sections to be obtained at high resolution through a sample. The results (Plate V) support our interpretation of six floats but we do not feel that they are absolutely conclusive because we are clearly at the limits of resolution for this kind of sample in XuM. Therefore, because the float number of six could conceivably be a misinterpretation, or it might be an aberrant aspect of the Danish population, we provide a comparison with other fossil species having small numbers of floats (three or nine). These comparisons are made with Early Tertiary species, and with those from other time periods if they are similar in a number of other characters.

Comparisons are also made with all fossil *Azolla* species with clear excrescences, and also with those with the same type of aseptate glochidia with anchor-shaped tips and lacking recurved hooks.

### 6.10.2 Fossil species with 3 floats

*Azolla intertrappea* Sahni and Rao 1934 from the Eocene of India has massulae and glochidia that are similar to those of *A. jutlandica*, but the megaspore is smaller (diameter 215  $\mu\text{m}$  versus 300  $\mu\text{m}$  in *A. jutlandica*) and does not show excrescences, just as *A. pyrenaica* Florschütz et Amor 1960 from the Pliocene and Pleistocene of France.

*Azolla indica* Trivedi and Verma 1971, also from the Eocene of India, differs in having septate glochidia and the megaspores lack excrescences.

*Azolla geneseana* Hills and Weiner 1965 has glochidia with usually two flukes but occasionally three to four and these have recurved hooks. The megaspores are larger than in *A. jutlandica* (c. 400-500 µm in diameter).

*Azolla tomentosa* Nikitin 1948 (see also Dorofeev, 1963) has a cap that covers only the top part of the floats. The filosum appears to be thin and there are no excrescences. The description and illustrations do not enable more detailed comparison.

*Azolla tunganensis* Dorofeev 1963 from the Oligocene of Russia lacks a diagnosis. The illustrations show medially swollen glochidia with recurved flukes and the species differs from *A. jutlandica* in this respect without any doubt. Moreover, the cap only covers the upper part of the float system (see also Friis, 1977).

### 6.10.3 Fossil species with 9 floats

All these species have an upper tier of 3 floats and a lower one of 6 floats.

*Azolla tegeliensis* Florschütz emend Bertelsen 1972 lacks glochidia and is thus very different from *A. jutlandica*, just as *A. aspera* Dorofeev 1963.

*Azolla nana* Dorofeev 1959 differs in its lack of a collar and glochidia, and is thus very different from *A. jutlandica*. Furthermore, its megaspores are relatively small (only c. 160 µm in diameter) and have a granulose perispore.

*Azolla prisca* Reid and Chandler emend Fowler 1975 has a cap that covers only the upper tier of floats in the megaspore apparatus, the lower float tier is always visible; the same applies for *Azolla turgaica* Dorofeev 1959, *A. pseudopinnata* Nikitin 1957 and *A. suchorukovii* Dorofeev 1968. In *A. jutlandica* the cap covers the whole of the floats.

*Azolla sibirica* Dorofeev 1959 has a cap that is often turned upwards, just as we have observed in one megaspore apparatus of *A. jutlandica*. Excrescences might be present but are not clearly indicated in the illustrations and not mentioned in the diagnosis. Although a filosum is clearly present around the collar, it seems to be more or less absent from the megaspore unlike *A. jutlandica*. No massulae have been described.

*Azolla turgaica* Dorofeev 1959 has a small cap that covers only the upper tier of floats. Excrescences might be present on the megaspores but they are not clearly illustrated nor mentioned in the diagnosis. The massulae lack glochidia unlike *A. jutlandica*.

*Azolla ventricosa* Nikitin 1965 has been recorded from Oligocene and Miocene floras in Siberia and Europe. It resembles *A. tegeliensis* but is smaller: it has, as do all the Russian species with nine floats, a relatively small cap differing in this aspect from *A. jutlandica* (see also Friis, 1977).

The Oligocene-Miocene *Azolla nikitini* Dorofeev 1955 has slightly smaller megaspores (diameter c. 200 µm) than *A. jutlandica*, with a distinct collar and excrescences only on the distal part of the megaspore (tubercles in Friis, 1977). The usual sculpture of the megaspore wall consists of verrucae and/or rugulae. The cap is much smaller than in *A. jutlandica* and covers only the upper tier of three floats. No massulae have been described. *Azolla roemoensis* Bertelsen 1974, from the late Upper Miocene of Denmark, has larger megaspore apparatuses (445-572 µm versus 350-410 µm in *A. jutlandica*) and megaspores

(292-368  $\mu\text{m}$  versus c. 300  $\mu\text{m}$  in *A. jutlandica*), and a baculate megaspore sculpture. Moreover, the cap covers only the upper tier of floats.

For comparison of *Azolla antiqua* Dorofeev 1959 see below as this species is the most similar in the group of 9-floated *Azolla* species.

### 6.10.4 Other fossil species with a few similar characters

*Azolla teschiana* Florschütz emend Batten & Collinson 2001, *A. bulbosa* Snead emend Sweet & Hills 1976, and *A. antiqua* Dorofeev 1959, share some characters with *A. jutlandica*, in particular all have megaspores with perinal excrescences (described as 'rather large nodes' in *A. antiqua*).

The surface of the endoperine has not been studied in *A. antiqua* (no sections were studied), or for *A. bulbosa*. In *A. teschiana* the endoperine surface does have protrusions but they are broader and more nodular (Batten and Collinson, 2001 plate V, 11) than those in *A. jutlandica*. The exoperine surface is stated to be smooth in *A. antiqua* but no SEM was undertaken and there are no high magnification LM illustrations. *A. bulbosa* has irregular rugulae fusing to form an irregular reticulate-like surface, whilst *A. teschiana* has a rugulate tuberculate foveolate sculpture. All these differ from *A. jutlandica*. In *A. antiqua* no filosum is mentioned or present on illustrations, *A. teschiana* has many hairs of infrafilosum which cover much of the spore but do not completely obscure the surface, and there are fewer hairs on the distal face. Many other hairs of suprafilosum arise from the proximal pole of the spore and intermesh with infrafilosum. *A. bulbosa* has a filamentous portion of columella, probably equivalent to suprafilosum, and filsum is absent from the distal surface or represented by a scattering of filaments, Sweet and Hills (1976, fig 10) shows a covering of filsum but not totally obscuring the exoperine surface. A filsum, which obscures the exoperine and floats, is present in many specimens of *A. jutlandica* although others lack filsum over the megaspore surface. In *A. bulbosa* filsum hairs are 0.5 $\mu\text{m}$  in diameter and in *A. teschiana* 0.5-1  $\mu\text{m}$ , the latter similar to *A. jutlandica*.

The *A. teschiana* megaspore apparatus is ovate, the float zone is compact, dome-shaped to elongate and covers about one half of the proximal part of the megaspore. The *A. antiqua* megaspore (apparently meaning megaspore apparatus) is described (in the official translation) as ellipsoidal or egg-shaped and horizontally cut off or blunt at the top. From the illustrations (Dorofeev, 1959, fig III, 2-5) the float zone is a flattened dome shape. In *A. bulbosa* the megaspore complex (= megaspore apparatus) is described as ovate in outline and the supraspore (= float zone) as rounded. However, illustrations in Sweet and Hills (1976, figs 4, 6, 8, 9) show a slightly obtuse apex.

*A. teschiana* has 24 floats arranged in three tiers of nine, nine and six from base to apex. One or more of these floats may be divided into smaller units.

*A. antiqua* has nine floats in two tiers, three upper larger and six lower smaller. The number of lower floats in individual specimens ranges from eight to nine but in a typical assemblage there are six. Collinson (1980) incorrectly quoted the total float numbers as 6-9. *A. bulbosa* usually has 24 floats (range 21-27) in three tiers, the lower tier usually nine

(range 5-12); middle tier usually nine (range 8-12) and the upper tier three to six.

In *A. antiqua* microspore massulae were not observed. In *A. teschiana* glochidia have anchor-shaped tips, are aseptate and distally dilated, numerous, typically 20-35  $\mu\text{m}$  long. In *A. bulbosa* glochidia have anchor-shaped tips (figs 23, 24), are aseptate, occur over the entire surface of the massulae though tending to be concentrated to one side, mean 32  $\mu\text{m}$  long (range 23-42  $\mu\text{m}$ ). Both species lack long (>55  $\mu\text{m}$ ) glochidia. Glochidia in *A. bulbosa* have a maximum stalk width 2.85  $\mu\text{m}$  (range 2-4  $\mu\text{m}$ ), anchor tip (termination) mean width 7.3  $\mu\text{m}$  (range 5.5-9); fluke mean length mean 6.57  $\mu\text{m}$  (range 5.5 –8.5  $\mu\text{m}$ ). Glochidia in *A. teschiana* (from Batten and Collinson, 2001, plate IV, 6) have maximum stalk width about 3  $\mu\text{m}$ , anchor-tip maximum width about 5  $\mu\text{m}$ ; fluke length about 5  $\mu\text{m}$ . *A. teschiana* glochidia possess recurved hooks but *A. bulbosa* glochidia do not.

### 6.10.5 Distinction of *A. jutlandica*

None of the fossil species with three or nine floats is similar to *Azolla jutlandica* in their other characteristics. Therefore, *A. jutlandica* is a distinct species, even if the unique character of six floats were to be ignored.

The only distinctive character shared between *A. teschiana* and *A. jutlandica* is the presence of excrescences. Otherwise the two are very different. *A. antiqua* megaspores have excrescences but their derivation from the megaspore wall is not known nor is there any detail of their structure. This species cannot be compared for microspore massulae. There are no details known of the exoperine surface or the endoperine surface, the former is described as smooth but probably based only on LM observations. On other available characters *A. antiqua* differs from *A. jutlandica*. *A. nikitinii* also has excrescences but is otherwise different from *A. jutlandica*.

There are a number of characters shared between *A. jutlandica* and *A. bulbosa*. In both glochidia are aseptate, with wide anchor-shaped tips, long flukes and no recurved hooks, filusum is present over the megaspore apparatus (however both the exoperine surface and the individual floats in the float zone are visible i.e. not obscured by filusum, in strong contrast to *A. jutlandica*). The exoperine surface has some similarity to *A. jutlandica* but the muri of the irregular reticulum seen in LM are much wider in *A. bulbosa*. Unfortunately the exoperine surface between the excrescences is not clear from the SEM illustration by Sweet and Hills (1976, fig 10) and therefore exact comparison is not possible. In *A. bulbosa* the exoperine is composed of baculae elongated parallel to the surface (experine 2 sensu Sweet and Hills, 1976) supported on a columellate structure (=experine 1). This was described by light microscopy and it is difficult to compare exactly with our TEM work but there are no major differences. In *A. bulbosa* the experine (=exoperine) is mean 9.5  $\mu\text{m}$  (range 5.5-12.5  $\mu\text{m}$ ) thick; the inperine (= endoperine) is 3.5  $\mu\text{m}$  thick (range 2.0 to 5.5  $\mu\text{m}$ ) and granular to finely vacuolated. The overall thickness of the perine, exoperine and endoperine overlap in *A. jutlandica* and *A. bulbosa*. Like *A. jutlandica*, *A. bulbosa* has excrescences. However, in *A. bulbosa* these are formed from the exoperine (=experinal prolongations) whilst in *A. jutlandica* they are formed from endoperine. They are up to 28  $\mu\text{m}$  long (=high) and 7-12



$\mu\text{m}$  in diameter in *A. bulbosa* and formed from fusion and elongation of several rugulae from the exoperine; excrescences range from abundant at the distal end to absent at the proximal pole and reach maximum length at the distal end. In contrast in *A. jutlandica* excrescences are up to 14  $\mu\text{m}$  high, randomly arranged and formed from proliferation of the endoperine with a covering of exoperine that does not differ from that between the excrescences.

Therefore, although *A. bulbosa* seems to be most similar of currently described fossil species to *A. jutlandica*, there are major differences. *A. bulbosa* has numerous floats, mean of 24 in three tiers, whilst in *A. jutlandica* there are only 6 in one tier. Although float number is known to be variable (see section above) there is no example of any variation which encompasses such a range of float number. *A. bulbosa* also has a more sparse filosum revealing underlying structures and perinal excrescences formed from exoperine by elongation of perinal rugulae. In addition in *A. bulbosa* the collar is absent and the size of the megaspore apparatus ranges from 385 to 555  $\mu\text{m}$  long with a mean of 455  $\mu\text{m}$ .

## 6.11 Comparison with modern species

Modern *Azolla* species have three or nine floats on the megaspore apparatus. Therefore comparison with *A. jutlandica* is necessary as argued for fossil species with three and nine floats (see above). Saunders and Fowler (1993) divided the genus *Azolla* into two subgenera *Azolla* and *Tetrasporocarpia*. Species in Subgenus *Azolla* sect *Rhizosperma* (*A. pinnata* R.Br.) and the monotypic Subgenus *Tetrasporocarpia* (*A. nilotica* Decne ex Mett) have nine floats, lack an infrafilosum and the massulae lack anchor-shaped tips to the glochidia. They are thus quite different from *A. jutlandica*. The remaining five species were placed in Subgenus *Azolla* section *Azolla*.

Evrard and Hove (2004) revised the taxonomy of the New World species of *Azolla* Subgenus *Azolla*, Section *Azolla* and provided an extensive bibliography of work on the species. They retained just two species: *Azolla filiculoides* Lam and *Azolla cristata* Kaulf (the latter name having priority and including in synonymy *A. caroliniana* auct non Wild.; *A. microphylla* auct non Kaulf. and *A. mexicana* K. Presl). These two main groupings are present in molecular phylogenies although there is disagreement on numbers of species in the latter (Reid et al 2006, Metzgar et al 2007). The perine of *A. cristata* lacks excrescences and is unlike *A. jutlandica*. Additional differences include the presence of recurved flukes on the anchor-tips of glochidia, presence of only three floats and presence of a large collar in *A. cristata* (Saunders and Fowler, 1993; Martin, 1976; (under former species nomenclature) Gardenal et al., 2007).

The perine surface of *A. filiculoides* has pronounced excrescences (=warty sensu Evrard and Hove, 2004) derived from endoperine (Martin, 1976) like *A. jutlandica*. However, these are closely packed, frequently coalescing and similar in size so that the outer appearance of the megaspore often forms a negative reticulum; this outer surface is not (or only slightly) obscured by infrafilosum (Fowler and Stennett-Willson, 1978; Field, 1999; Large and Braggins, 1993; Gardenal et al., 2007) so the megaspore is quite unlike



*A. jutlandica*. *A. filiculoides* has anchor-tipped glochidia on the microspore massulae like *A. jutlandica*, however they have recurved flukes (Saunders and Fowler, 1993; Gardenal et al., 2007), unlike *A. jutlandica*. *Azolla filiculoides* has three floats and a large collar which is glabrous (Saunders and Fowler, 1993; Martin, 1976; Gardenal et al., 2007; Large and Braggins, 1993; Field, 1999) again unlike *A. jutlandica*.

The remaining species of *Azolla* Subgenus *Azolla* Section *Azolla* is native to New Zealand and Australia and is sometimes known as *A. rubra* R. Br or as *A. filiculoides* Lam. var *rubra* (R. Br.) Strasburger (Large and Braggins, 1993). Molecular phylogenies link *rubra* and *filiculoides* in the same lineage (Metzgar et al 2007) and consider them distinct species (Reid et al 2006). *A. rubra* differs from New World *A. filiculoides* in having filusum arising from the collar and an alveolate endoperine ultrastructure (Large and Braggins, 1993; Martin, 1976; Fowler and Stennett-Willson, 1978), two characteristics like *A. jutlandica* (although the latter is uncommon (Plate 2, 10). All the other characters cited above for *A. filiculoides* still distinguish *A. jutlandica*.

## 6.12 Conclusions

Fossil remains of *Azolla* (megaspores, microspore massulae clusters, isolated microspore massulae and microspore massulae attached to megaspores) is abundant in the middle of Bed L2 of the Lillebælt Clay Formation in Denmark. The Danish *Azolla* abundance is of transitional Ypresian/Lutetian age which likely overlaps with the age of *Azolla arctica* Collinson et al. (2009) known from the Lomonosov Ridge in the Arctic Ocean. The Danish *Azolla* shares some characteristics with *Azolla arctica*, including aseptate glochida with anchor-tips lacking recurved flukes. However, the Danish *Azolla* differs in having pear-shaped megaspores with rounded pyramidal float zone; six floats in one tier, arranged in three groups of two; excrescences, formed of endoperine, on the megaspore wall; exoperine surface scabrate to clavate with masses fused in a single plane; ornamented endoperine surface; filusum with wider hairs (up to 1 µm) and more readily detached over the megaspore; a single size class of glochidia length with none longer than 40 µm and larger glochidia tips (up to 10 µm wide) and flukes (up to 6 µm long). Filusum hair size and glochidia tip size are functionally linked and the float system shape is linked to the float number, but the number of independent character differences remains greater than that documented between populations of single modern *Azolla* species or fossil *Azolla* populations as recorded in the literature. Therefore, the Danish *Azolla* is described as *Azolla jutlandica* sp. nov. Moreover, our study demonstrates that a single *Azolla* species did not spread from the Arctic to the southernmost North Sea in Denmark. In incomplete material or palynological preparations a fragment of megaspore wall studied on an SEM strew mount, or a population analysis of glochidia tip sizes studied by light microscopy, should enable the distinction of *A. arctica* from *A. jutlandica*. Therefore, studies of less abundant and more fragmentary *Azolla* from intervening sites can potentially determine the distribution of the two species and establish if they co-occurred or occupied different sites in intervening areas between the Eocene Arctic and southern North Sea Basin.

## Acknowledgements

We would like to thank R. van der Ham for access to specialist literature; T. Brain in Kings College London for embedding and sectioning the specimens illustrated by TEM and for his extensive support for both TEM and SEM work during this study; B.J. van Heuven in Leiden and J. van Tongeren in Utrecht for technical support for the SEM work. The samples and accompanying data for *Azolla arctica* (Collinson et al 2009) with which *A. jutlandica* sp nov is compared in detail, were provided by the Integrated Ocean Drilling Programme (IODP). We thank the Darwin Centre, Utrecht and Statoil for their financial support.





# Chapter 7

## **Coeval Eocene blooms of multiple species of the fresh water fern *Azolla* in and around the Arctic and Nordic Seas**

Barke, J., van der Burgh, J., van Konijnenburg-van Cittert, J.H.A.,  
Collinson, M.E., Pearce, M.A., Bujak, J., Heilmann-Clausen, C.,  
Speelman, E.N., van Kempen, M.M.L., Reichart, G.J., Lotter, A.F.,  
and Brinkhuis, H.

*To be submitted*

During the early middle Eocene (~49 Ma), the central Arctic Ocean was episodically densely covered by the fast growing freshwater fern *Azolla*, implying sustained freshening of surface waters and strong stratification. Coeval *Azolla* fossils in neighboring Nordic seas were thought to have been sourced from the Arctic Basin. The recognition of two different *Azolla* species, one Arctic and one North Sea, raised doubts about this hypothesis. Here we show that not merely two, but five, different species of *Azolla* had coeval blooms and spread across different areas, both on and around the Arctic and Nordic Seas. Warm climates, high precipitation and related runoff, combined with the semi-closed palaeogeographic setting of the Arctic Ocean and Norwegian-Greenland Sea, probably led, at least episodically, to in situ *Azolla* blooms on extraordinarily low-salinity ocean surfaces. Climatic conditions also enabled *Azolla* to bloom in extensive wetlands on adjacent continents from where its remains were transported to oceanic settings. The spatial extent (~30 million km<sup>2</sup>), duration (~1.2 Myrs), and associated phenomena (including carbon burial potential) suggest that *Azolla* played an important role in global carbon cycling.

High concentrations of megaspores and microspore massulae of the free-floating freshwater fern *Azolla arctica* were recovered from basal middle Eocene (~49 Ma) central Arctic Ocean sediments drilled at the Lomonosov Ridge during the Arctic coring expedition (ACEX; or Integrated Ocean Drilling Program, IODP, Expedition 302; Brinkhuis et al., 2006; Collinson et al., 2009; Chapter 5). Nowadays, *Azolla* requires standing freshwater bodies, such as ponds and lakes in tropical, subtropical, and warm temperate regions. Extant species of *Azolla* have been shown to tolerate salinities up to 5‰ (van Kempen, under review). Even when experimentally pre-conditioned to gradual increases of salt concentrations, *Azolla* tolerates salinities only up to 5.5‰ (Rai and Rai, 1998). *Azolla* fossils are known from the mid-late Cretaceous onwards and occupied freshwater habitats, as reconstructed from a number of widely distributed complete fertile plants of several fossil species (Collinson, 2001; Collinson, 2002).

The co-occurrence of different life stages and reproductive parts of *Azolla arctica* and the absence of land plant detritus suggests that this floating fern grew and reproduced *in situ* on the Arctic Ocean surface (Brinkhuis et al., 2006; Collinson et al., 2009; Chapter 5), waxing and waning with the obliquity (~40 kyr) cycle for some 1.2 Myrs (Speelman et al., 2009b; Chapter 2, 3). These and associated findings imply the episodic (~40 kyr) presence of sustained fresh surface waters, strong stratification, and bottom water anoxia (Brinkhuis et al., 2006; Onodera et al., 2008; Stein et al., 2006; Stickley et al., 2008; Waddell and Moore, 2008; Chapter 3, 4). Additional basal middle Eocene *Azolla* occurrences were reported from marine sediments in wide-ranging areas of the Arctic Ocean, Labrador Sea and Norwegian-Greenland Sea to North Sea (Brinkhuis et al., 2006; Speelman et al., 2009b; Chapter 2). Coeval occurrences of *Azolla* remains in sediments of the Nordic seas were previously suggested to represent transported assemblages of *A. arctica* from the Arctic Ocean by freshwater spills (Brinkhuis et al., 2006). Recently, however, examination

of assemblages from a site in Denmark revealed the presence of a second *Azolla* species (*A. jutlandica*; Collinson et al., 2010; Chapter 6). *A. jutlandica* is absent from the Arctic assemblage, raising doubts about the hypothesis that Nordic sea *Azolla* assemblages were transported from the Arctic Ocean. In contrast, it intriguingly suggests that *Azolla* blooms, involving at least two species, occurred ~synchronously over a wide area and along a large latitudinal gradient. To test this and other options, and their implications, we selected thirteen sites along a north-to-south transect, between the Arctic Ocean and southern North Sea, plus four sites from the western Arctic Ocean that incorporate the basal middle Eocene *Azolla*-bearing interval (Supplementary Fig.S-1; Table S-1). We investigate the time equivalence of this interval between locations and determine the *Azolla* species composition and abundance per site. In addition, the entire palynomorph assemblages were analysed, and the proportion of terrestrially derived mesofossils (wood, fusain, and cuticles >250µm) is estimated to better understand the depositional processes and environmental conditions.

The basal middle Eocene *Azolla* occurrences in the Nordic seas are consistently associated with the subsequent last occurrences of two marine dinoflagellate-cyst (dinocyst) species (*Charlesdowniea columna* and *Eatonicysta ursulae*), confirming that they are geologically synchronous (Supplementary Information – Note 1). In the Eocene Arctic Ocean, these marine dinoflagellates are not recorded, probably due to an intolerance of brackish conditions, which hampers direct correlation between the Nordic seas to the Arctic Ocean. However, available evidence suggests that the *Azolla* blooms are at least of overlapping age (Figure 1; Supplementary Information – Note 1).

Surprisingly, our examinations of the various *Azolla* assemblages reveal that no less than five different *Azolla* species were present in the Arctic Ocean and Nordic Seas during the Eocene 'Azolla phase'. In addition to the previously documented *Azolla arctica* (Collinson et al., 2009; Chapter 5) and *A. jutlandica* (Collinson et al., 2010; Chapter 6), three additional *Azolla* species have been identified that are here referred to as *Azolla* sp. 1, *Azolla* sp. 2 and *Azolla* sp. 3. Species identification is based on distinctive morphological features of their microspore clusters (massulae), with their hair-like appendages (glochidia) (Plate I; Supplementary Figure S-2), and the megaspore apparatuses (Plate II). *Azolla* sp. 3 is an exception, the identification being based exclusively on its very distinctive megaspore apparatuses (9 floats in two tiers, lowermost tier always visible, very little filusum; see Plate II, 14). Microspore massulae of *Azolla* sp. 3 were either unidentifiable or not present in the sample. The key morphological features that distinguish the various species are summarized in Supplementary Table S-2. The geographical distribution of the five species is illustrated in Figure 2 and their relative abundances are given in Supplementary Table S-3 (for material and methods see Supplementary Information – Note 2).

The remainder of the palynomorph assemblage composition at the Arctic sites (sites 1-5) and at the Norwegian-Greenland site (site 6) supports the inference that surface waters were fresh to brackish, as indicated by the high abundance of peridinioid dinocysts (up to 73% of palynomorphs) comprising a high proportion of freshwater-tolerant taxa such as *Senegalinium* spp. (see Sangiorgi et al., 2008; Sluijs and Brinkhuis, 2009). In addition,

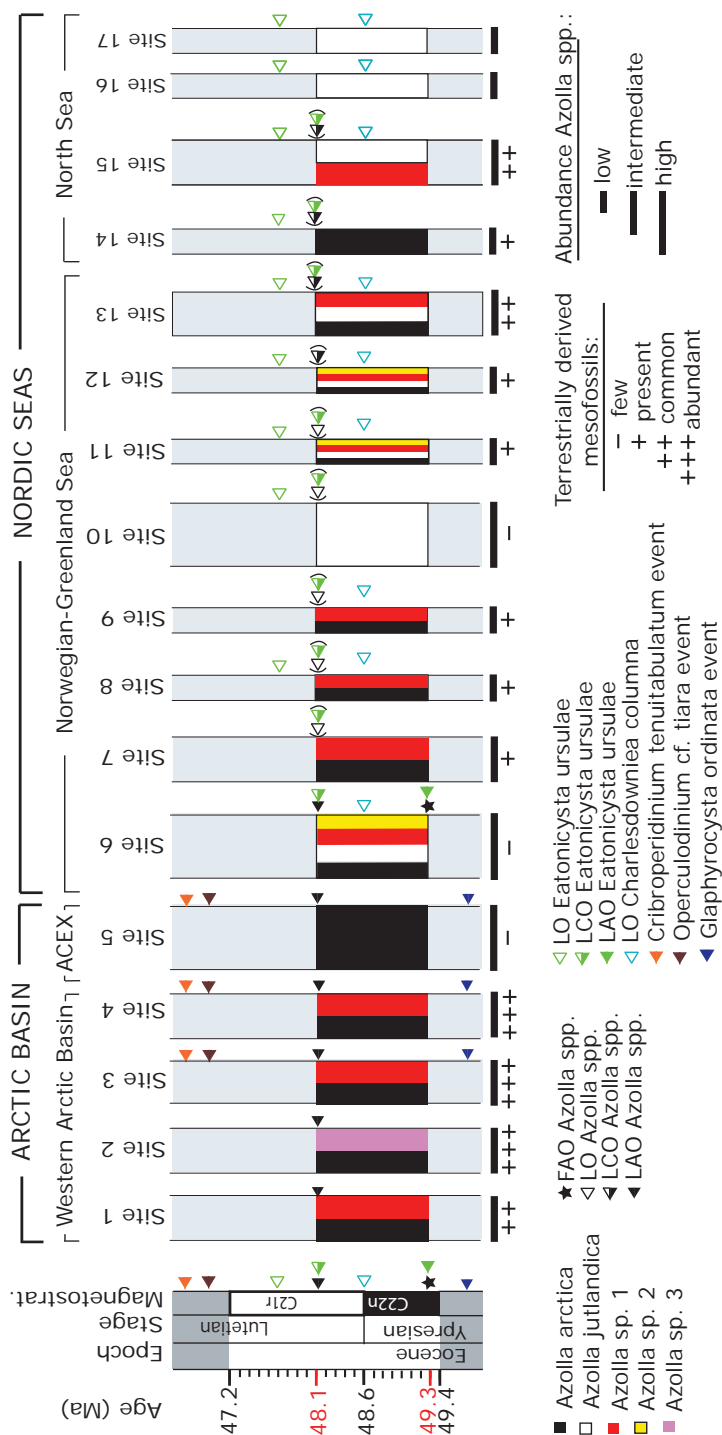


**Fig. 1.** Correlation panel illustrating the position of the Azolla interval relative to available chrono- and biostratigraphy at the various study sites. Calibration against the timescale of Gradstein et al. (2004) is obtained from Site 6, ODP Site 913B. Events shown between brackets imply extrapolation from cutting samples (see Supplementary Information— Note 1 for further explanations). The abundance of *Azolla* spp. is shown relative to the total palynomorph assemblage and the presence/absence of the various species of *Azolla* is indicated. The raw data are provided in Supplementary Table S3.



gonyaulacoid dinocysts, including typical open marine taxa such as *Achomosphaera* spp., *Hystrichokolpoma* spp., *Impagidinium* spp. and *Spiniferites* spp. (see Pross and Brinkhuis, 2005; Sluijs et al., 2008 for review) occur in relatively low abundances (0-15% of palynomorphs). The high abundance of *Azolla arctica* (up to 90% of palynomorphs) in the monospecific assemblage at the central Arctic Ocean ACEX site (site 5) and the high abundance of *Azolla* spp. at the Norwegian-Greenland sea site (site 6; up to 71% of palynomorphs) together with the low amount of terrestrially-derived mesofossils (present to rare), strongly suggest the *in situ* growth of *Azolla* spp. At site 7 there is also good evidence for surface water freshening (the palynomorphs assemblage consists of up to 28% of peridinoid dinocysts with a high proportion of freshwater-tolerant taxa such as *Phthanoperidinium* spp.; see Sluijs and Brinkhuis, 2009 for review) and rare occurrences of terrestrially-derived mesofossils

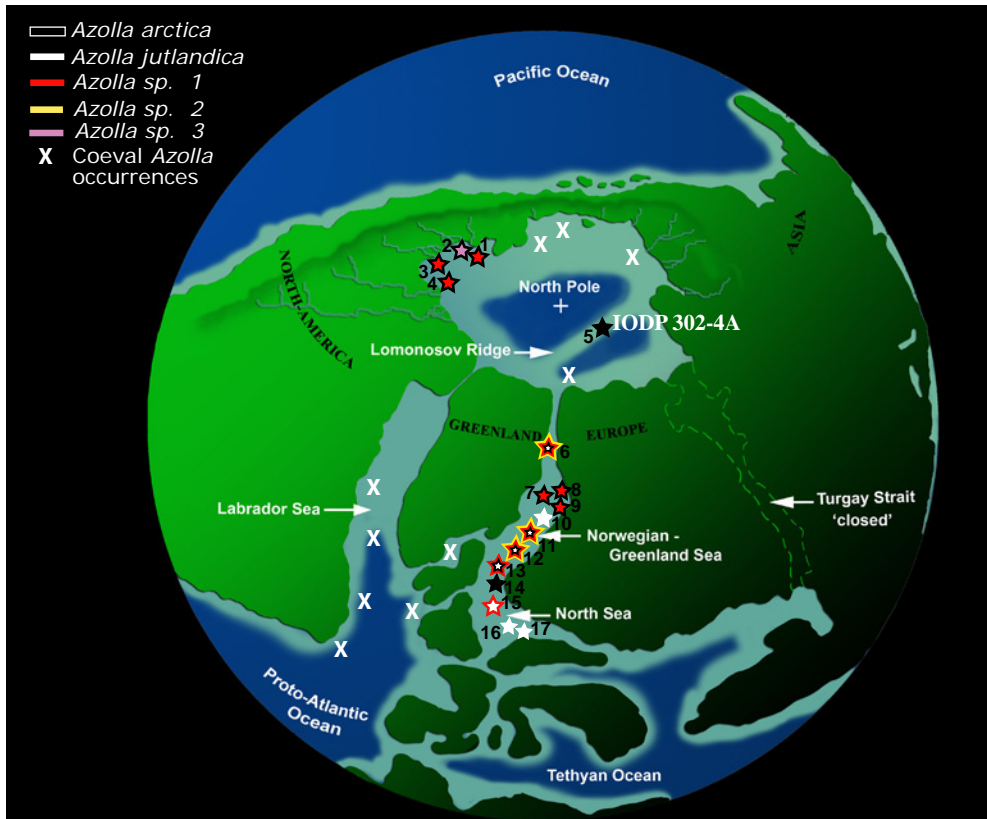


**Fig. 2.** Palaeogeographic reconstruction (early middle Eocene; ~49 Ma; modified from Brinkhuis et al., 2006) showing the geographical distribution of the five *Azolla* species in the Arctic Ocean and Nordic Seas based on their microspore massulae and megaspore occurrences. Coeval *Azolla* occurrences (as indicated by white crosses) relate to additional basal middle Eocene *Azolla* occurrences reported in Brinkhuis et al. (2006).

suggest that *Azolla* spp. (up to 20% of palynomorphs) were growing *in situ* at this site. In contrast, much higher amounts of terrestrially-derived mesofossils (frequent to common) and the relatively low proportion of *Azolla* spp. remains (12 to 27% of palynomorphs) at the western Arctic sites (sites 1-4) suggests that *Azolla* spp. remains here were washed in from nearby landmasses. At sites in the Norwegian-Greenland Sea to North Sea (8-17) high abundances of gonyaulacoid dinocysts (40 to 90% of palynomorphs), excluding low-salinity-tolerant forms such as *Spiniferites cruciformis* (Kouli et al., 2001) and low abundances of freshwater-tolerant (peridinioid) cysts such as *Senegalinium* spp. and *Phthanoperidinium* spp. suggest relatively higher salinities. The conditions at these sites were presumably not favorable for the *in situ* growth of *Azolla*. *Azolla* spp. abundances range between low to intermediate at these sites (1 to 30% of palynomorphs), with higher amounts of terrestrially-derived mesofossils at sites with relatively higher *Azolla* spp. abundances. This distribution pattern is likely a result of runoff and transportation from the nearby continents. Site 10, in the southern Norwegian-Greenland Sea, is an exception having high abundances of *Azolla jutlandica* remains (52% of palynomorphs), but hardly any terrestrially-derived mesofossils. This implies that *A. jutlandica* remains were transported from other Nordic sea areas, e.g. from the northern Norwegian-Greenland Sea, where they were likely growing *in situ*.

Decreasing absolute and relative abundances of *A. arctica* with increasing distance from the Arctic Ocean (see Supplementary Information – Note 3 and Supplementary Table S-3), do however suggest that *Azolla arctica* remains were indeed transported from the Arctic Ocean to the Norwegian-Greenland Sea and North Sea.

Our results thus indicate that *in situ* *Azolla* blooming is likely to explain the occurrences of *Azolla* at sites in the central Arctic Ocean and at sites in the northern Norwegian-Greenland Sea, sites where there is every indication for fresh surface waters, a high abundance of *Azolla*, and low abundance of terrestrially derived mesofossils. At all other sites, the *Azolla* assemblages reflect washed-in materials from adjacent landmasses or from the central Arctic Ocean (in case of *A. arctica*).

During the generally warm early Eocene, the hydrological cycle was intensified (Huber et al., 2003; Speelman, 2010a) and a high precipitation regime prevailed at high and mid latitudes, with mean annual precipitation values of >1200 mm/yr as e.g. estimated for Axel Heiberg Island and Greenland (Greenwood et al., 2010; Eldrett et al 2009). This resulted in high volumes of freshwater entering the Arctic Ocean and Norwegian-Greenland Sea (Andreasson et al., 1996; Greenwood et al., 2010). Net runoff and precipitation entering the Arctic Ocean possibly amounted to  $1.5 \times 10^{13} \text{ m}^3/\text{yr}$ , which is equivalent of ~ 1700 mm/yr (Speelman, 2010b). The onset of the *Azolla* interval is shortly after the Early Eocene Climatic Optimum (EECO; 51–53 Ma), when  $p\text{CO}_2$  was high (>2000 ppm) and global temperatures reached a long-term maximum (~12°C global deep-sea temperature) (Pearson and Palmer, 2000; Zachos et al., 2008). Per °C temperature rise, climate modelling simulations suggests an increase in global mean precipitation by about 2 to 3% (Held and Soden, 2006). This implies that superimposed on the overall wet conditions prevailing during the early Eocene, a further increase in precipitation is likely to have occurred during the EECO.

During the early middle Eocene the Arctic Ocean was a nearly entirely landlocked basin and the connection to global oceans was restricted to a shallow surface water exchange via the Norwegian-Greenland Seas (Akhmetiev and Beniamovski, 2009; Jakobsson et al., 2007; Radionova and Khokhlova, 2000; Roberts et al., 2009). Closing the seaway connections to the Arctic Basin has been simulated to result in mean Arctic surface salinities as low as ~ 6 psu (Roberts et al., 2009). This is corroborated by integrated modelling and compound-specific  $\delta D$  results, which suggest significant freshening of Arctic Ocean surface waters (0-6 psu) during the '*Azolla* phase' (Speelman, 2010b). These values overlap with the reported maximum salinity tolerance of modern *Azolla* of ~5‰ (van Kempen, under review). At the same time, the Norwegian-Greenland Sea consisted of a number of isolated sub-basins, separated by the mid-ocean ridge and the Jan Mayen and Greenland-Senja fracture zones (Eldholm et al., 1994). In the eastern Greenland Sea, the Vøring Plateau acted as a barrier, influencing the Cenozoic evolution of water mass circulation (Laberg et al., 2005). Furthermore, the Norwegian-Greenland Sea was separated from the Arctic and North Atlantic by the two major Cenozoic water mass barriers: the Yermak Plateau-Morris Jesup Rise and the Greenland-Scotland Ridge, respectively. As a result, intermediate and deep water ventilation was restricted and regional surface water exchange was poor (Eldholm et al., 1994). A sea-level low stand at ~49 Ma during Chron 21r (Miller et al., 2005) may have further isolated the Arctic Ocean and Norwegian-Greenland Sea basins, leading to additional freshening of ocean surface waters.

From our results we can conclude that extensive *Azolla* blooms occurred during the same early middle Eocene time interval on a very wide (~30 million km<sup>2</sup>) geographical scale. This implies the existence of wide-ranging continental wetlands on bordering landmasses, at least in western Canada, Alaska, and Europe, combined with sustained, unprecedented discharge of freshwater into the semi-closed Arctic and Norwegian-Greenland Sea basins, creating widespread fresh surface waters. The overarching environmental factor that affected all these locations simultaneously is precipitation. During the early middle Eocene, globally high temperatures prevailed, driving overall increased transport of latent heat and enhanced moisture transport, resulted in increased high-latitude precipitation (Huber et al., 2003; Zachos et al., 2008; Speelman 2010a).

The demise of the *Azolla* may be related to a crucial decrease in high-latitude precipitation, possibly caused by decreasing global temperatures in the middle Eocene (Zachos et al., 2008). A decrease in precipitation would likely have resulted in reducing the extent of continental wetlands and a reduction in freshwater discharge into the Arctic and Nordic Seas. A slight increase in surface-water salinities may have crossed the critical threshold of salinity tolerance of *Azolla*. In addition, a possible increase in the exchange of water masses between the North Atlantic, the Greenland-Norwegian Sea basins, and the Arctic Ocean, caused by subsidence of the ridges or/and sea-level rise, could have resulted in higher salinity Arctic and Norwegian-Greenland Sea surface Ocean waters. For example, the eastern part of the Greenland-Scotland Ridge sank beneath sea level in the early to middle Eocene (Thiede et al., 1996).

A cyclostratigraphical study on early Eocene tropical western Atlantic sediments (Demerara Rise, ODP Leg 207, site 1258) documented an ~800 kyr period of strong obliquity cycles during the middle part of magnetochron C22r (~50.1 to 49.4 Ma) and throughout the entire magnetochron C21r (Westerhold and Röhl, 2009). This obliquity pattern was interpreted to reflect a high-latitude signal, transferred to low latitudes via stronger wind-driven ocean circulation and intensification of high-latitude bottom-water formation. For the entire magnetochron C22n, which correlates to the main phase of the *Azolla* interval, no obliquity signal is detected (Westerhold and Röhl, 2009). This might be an indication that the connection from the Arctic Ocean and Norwegian-Greenland Sea to the Atlantic Ocean was indeed restricted at the time of the *Azolla* interval.

Considering the timing of the '*Azolla* phase', being associated with the onset of the Eocene cooling trend, the spatial extent (~ 30 million km<sup>2</sup>), duration (~1.2 Myrs), and carbon burial potential of *Azolla* (Chapter 1), this water fern may have played an important role in global carbon cycling.

## Acknowledgments

We thank L. Bik and N. Welters for their great support. We would like to thank J. van Tongeren in Utrecht and B.J. van Heuven in Leiden for technical support for the SEM work; and T. Brain in Kings College London for his extensive support for both TEM and SEM work during this study. The samples and accompanying data for *Azolla arctica* (Collinson et al., 2009; Chapter 5), were provided by the Integrated Ocean Drilling Program (IODP). We thank Statoil Hydro and the Canadian Geological Survey for providing samples for this study. We thank the Darwin Centre and Statoil Hydro for their financial support. JB thanks Arthur R. Sweet for fruitful discussions.

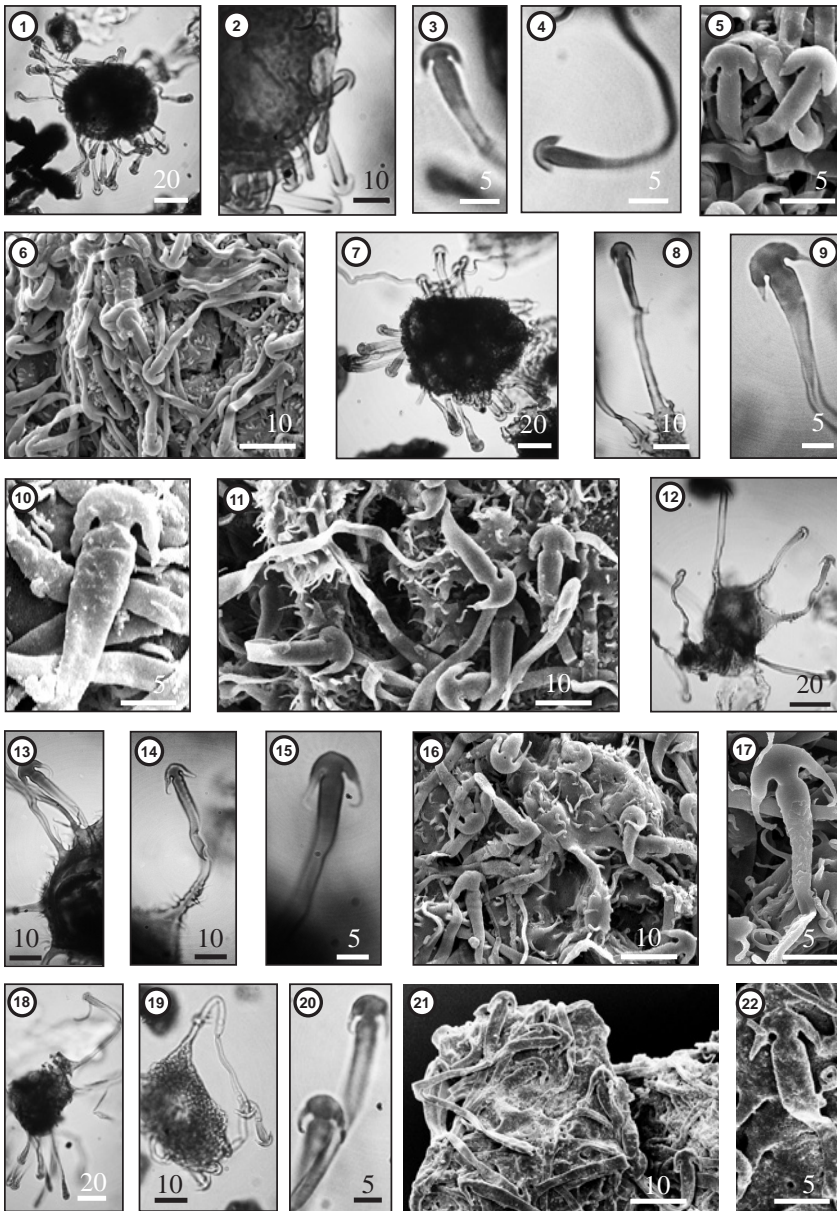


**Plate I.** Distinctive characteristics of the microspore massulae and their glochidia in *Azolla arctica* (1-6), *A. jutlandica* (7-11), *Azolla* sp. 1 (12-17) and *Azolla* sp. 2 (18-22). *A. arctica* – no hairs on lower stalk, narrow tips, fluke tips not recurved; *A. jutlandica* – hairs present on lower stalk, wide fluke and wide shaft; *Azolla* sp. 1 – hairs present on lower stalk, fluke tips recurved; *Azolla* sp. 2 – no hairs on lower stalk or massula surface (see Supplementary Table S-2 for more information).



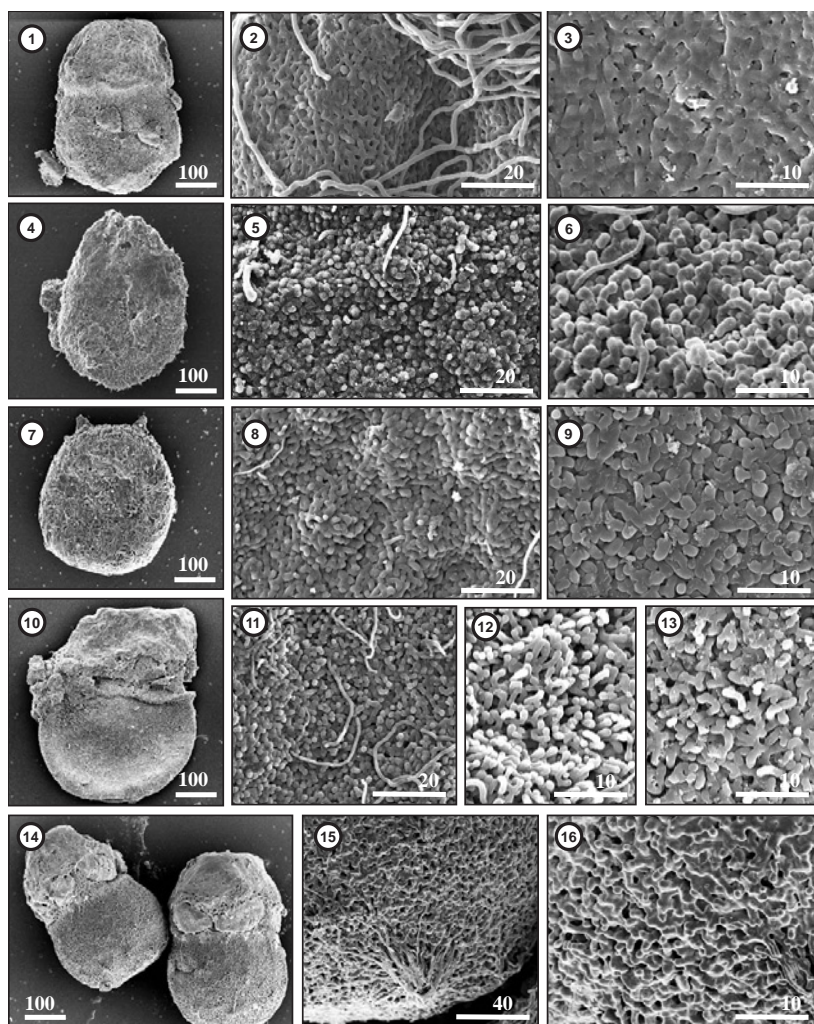


**Plate II.** Scanning electron microscope images of magaspore apparatuses (1,4,7,10,14) and megaspore walls (other numbers) of *Azolla arctica* (1-3), *Azolla jutlandica* (4-6), *Azolla* sp. 1 (7-9), *Azolla* sp. 2 (10-13) and *Azolla* sp. 3 (14-16) showing distinctive characteristics. *A. arctica* – wavy and undulating exoperine surface rugulate in several planes (forming a reticulum); *A. jutlandica* – exoperine surface scabrate to granulate to baculate or clavate, exoperinal masses fusing in a single plane (no reticulum); *Azolla* sp. 1 – exoperine surface with rounded rugulae (2  $\mu$ m in narrowest dimension), which often act as the muri for a very fine-scaled reticulum with lumina; *Azolla* sp. 2 – rounded rugulae (typically 1 $\mu$ m), which only occasionally act as the muri for a very fine-scaled reticulum; *Azolla* sp. 3 – 9 floats in two tiers, lowermost tier always visible, megaspore wall with large excrescences, exoperine surface with rounded rugulae and small papillae (less than 1  $\mu$ m).

## Supplementary Figure S-1

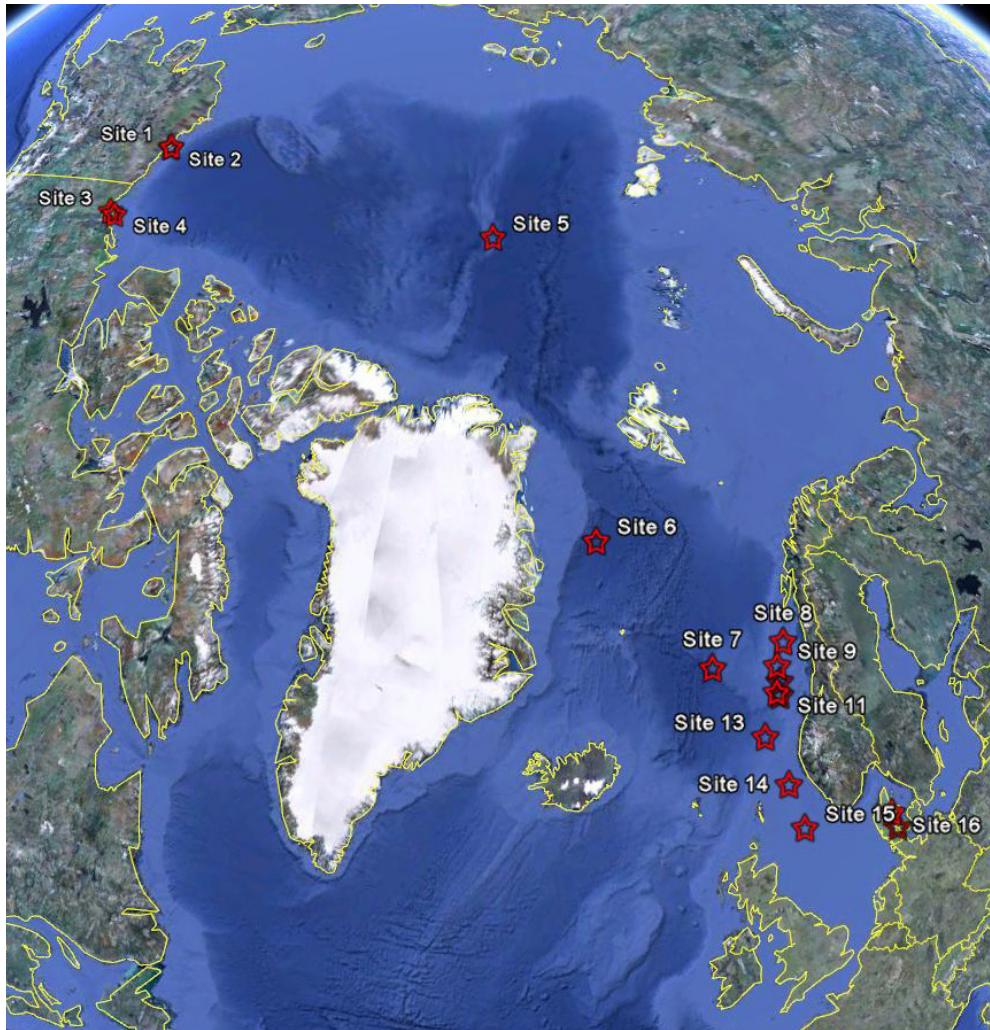


**Fig.S-1.** Study sites (modified from [www.google-earth.com](http://www.google-earth.com))



## Supplementary Table S-1

**Table S-1.** Site descriptions. ‡The *Azolla* material from site 5 (IODP 302-4A) has been fully documented in Collinson et al. (2009) and Chapter 5. \* The *Azolla* material from site 16 (Kirstinebjerg) has been fully documented in Collinson et al. (2010) and Chapter 6.

Area	Location	Site	Name (Operator)	Position	Azolla- bearing horizon	Sampling depth	Sample weight (g)	# mega- spores studied
Western Arctic	Northern Alaska	1	Sandpiper 1 (Shell)	70°35'4.73"N/ 149°5'48.82"W	1070-1097 mMD	1088-1097 mMD	16	19
		2	Northstar 1 (Amerada)	70°31'42.02"N/ 148°51'22.5"W	1088-1143 mMD	1088-1116 mMD	10	13
	Canadian BMB	3	Ellice I-48 (Chevron et al)	69°7'34.00" N/ 135°55'33.50"W	1910-2075 mMD	1910-1915 mMD & 1940-1945 mMD	23	19
		4	Upluk M-38 (Chevron sobe)	69°27'56.00"N/ 135°24'54.00"W	3182-3292 mMD	3237-3240 mMD	22	3
Central Arctic	Lomonosov Ridge	5‡	IODP 302- 4A	87°51'59.69"N/ 136°10'38.46"E	298.8-302.6 mbsf	298.9- 302.6 mbsf (with 10 cm spacing)	1 to 2	details in Chapter 5
Nordic Seas	Norwegian-Greenland Sea	6a 6b 6c 6d	ODP 151- 913B	75°29'21.12"N/ 6°56'48.48"W	674.8-717.6 mbsf	684.4 687.9 694.2 694.7 mbsf	13 13 13 14	6 4 0 6
		7a 7b 7c	ODP 104- 643A	67°42'54.00"N/ 1° 1'59.88"E	556.0-565.3 mbsf	563.7 564.7 564.8 mbsf	12 13 12	9 10 3
		8	6610/2-1S (Statoil)	66°48'48.73"N/ 10°30'26.70"E	as for sampling depth	1240 mMD	13	11
		9	6608/10-10 (Statoil)	66°4'17.90"N/ 8°10'11.40"E	as for sampling depth	1760 mMD	12	0
		10	6507/8-4 (Statoil)	65°23'17.18"N/ 7°23'59.65"E	as for sampling depth	1920 mMD	8	6
		11	6506/11-6 (Statoil)	65°1'26.24"N/ 6°25'10.71"E	as for sampling depth	2240 mMD	13	0
		12	6406/2-2 (Statoil)	64°49'46.35"/ 6°34'15.43"E	as for sampling depth	2370 mMD	15	18
		13	6302/6-1 (Statoil)	63°31'38.43"N/ 2°45'51.56"E	as for sampling depth	3180 mMD	12	12
	North Sea	14	30/2-1 (Statoil)	60°52'05.42"N/ 2°38'49.16"E	as for sampling depth	1860 mMD	14	0
		15	16/4-4 (Statoil)	58°31'47.81"N/ 2°8'59.69"E	as for sampling depth	2020 mMD	14	6
		16 *	Kirstinebjerg	56°23'7.00"N/ 10°3'0.00"E	~ 2.8 m thick horizon in outcrop	sample 2904	29	details in Chapter 6
		17	Kasmose	55°33'16.89"N/ 9°50'05.65"E	~ 2.8 m thick horizon in outcrop	sample 2903	25	0

## Supplementary Information - Note 1

### Biostratigraphy and correlation

*Western Arctic Basin sites: Northern Alaska and Canadian Beaufort Mackenzie Basin (sites 1-4, see Table S-1)*

The basal middle Eocene *Azolla* horizon has been recognized in more than 100 commercial wells in Northern Alaska and the Canadian Beaufort Mackenzie Basin (BMB), and is documented in an informal palynological zonal scheme (Bujak Research International, unpublished data). This zonal scheme is based on the last occurrences of dinocysts, fungi, pollen and spores and comprises zones from the Paleocene (T1) to the Oligocene (T6). In all wells, the basal middle Eocene *Azolla* horizon occurs in the same biostratigraphical position, namely in the palynological subzone T4a, which is characterized by the abundant occurrence of the dinocyst *Charlesdownia tenuivirgula*. This subzone belongs to zone T4 (middle Eocene), which is characterized by the abundant occurrence of the fungus *Pesavis tagaluensis*. The index dinocyst species that have stratigraphical importance for the basal middle Eocene succession in the Nordic Seas (Bujak and Mudge, 1994; Eldrett et al., 2004), are all absent due to the unusual freshwater conditions in the Arctic.

Furthermore, the Northern Alaskan wells include the uppermost Paleocene *Apectodinium* horizon, which corresponds to the upper part of zone T2 (latest Paleocene) and relates to the global PETM. Both the PETM and the *Azolla* horizon are characterized by a distinctive high-gamma curve in the Northern Alaskan wells. These markers are absent from the Canadian Beaufort Mackenzie Basin wells, probably due to the strong depositional influence of the Mackenzie delta. The uppermost Paleocene *Apectodinium* horizon and the basal middle Eocene *Azolla* horizon are the only chronostratigraphical correlations available that allow us to correlate from the Arctic to the Nordic latitudes.

*Central Arctic Ocean site: the Lomonosov Ridge (site 5, see Table S-1)*

The *Azolla* bearing horizon in core M0004-11X, drilled during the Arctic Coring Expedition (ACEX) or Integrated Ocean Drilling Program (IODP) Expedition 302, is bracketed by the same dinocyst events as the basal middle Eocene *Azolla* horizon in the Canadian BMB wells. The late Paleocene/early Eocene to middle Eocene dinocyst succession informally described for the Canadian BMB wells includes the following events: *Apectodinium* acme and *Glaphyrocysta ordinata* prior to the *Azolla* acme event and *Operculodinium* cf. *tiara* and *Cribroperidinium tenuitabulatum* following this event (Bujak Research International, unpublished data). As in the Canadian BMB wells, the age-diagnostic dinocyst markers of the Nordic Sea succession are absent from the ACEX cores and furthermore no palaeomagnetic data are available (Backman et al., 2006). However, correlation of the last abundant occurrence (LAO) of *Azolla* in the Arctic with the last abundant occurrence (LAO) of *Azolla* in ODP Hole 913B (Brinkhuis et al., 2006) is consistent with the current age model of the Paleogene ACEX cores (Backman et al., 2006; Brinkhuis et al., 2006).

### *Nordic Sea sites: Norwegian-Greenland Sea & North Sea (sites 6-17, see Table S-1)*

The main bioevents of the Eocene succession in the Norwegian-Greenland Sea have been calibrated against magnetostratigraphy. This magnetobiostratigraphic calibration is based on the composite section developed from Holes DSDP 338, ODP 104-643A and ODP 151-913B. Hence, site 6 (ODP cores 104-643A) and site 7 (ODP cores 151-913B) contain the *Azolla* bearing horizon, the age diagnostic dinocyst markers as well as paleomagnetic data. The last abundant occurrence (LAO) of *Azolla* in this composite section has been shown to coincide with the last consistent occurrence (LCO) of *Eatonicysta ursulae* and is directly calibrated against mid Chron C21r (Eldrett et al., 2004). The interval of abundant *Azolla* correlates with the last occurrence (LO) of *Charlesdowniea columna* (Brinkhuis et al., 2006), which is directly correlated to the top of Chron C22n (49 Ma) (Eldrett et al., 2004). Although the onset of the *Azolla* horizon has not been recovered, the low abundances of *Azolla* at the base of the core suggest that this level is close to the onset. This level corresponds to the LAO of *Eatonicysta ursulae* within Chron C22n (Brinkhuis et al., 2006).

The *Azolla*-bearing horizon at sites 8-15 has been recognized in commercial wells. Since these wells were studied by means of cutting samples, the *Azolla* interval can only be defined by last occurrence (LO), last consistent occurrence (LCO) or last abundant occurrence (LAO) of *Azolla*. In all these wells the last (abundant/consistent) occurrence of *Azolla*, is located within or at the top of the Ypresian and coincides with the LCO of *Eatonicysta ursulae* and LO of *Charlesdowniea columna*. Site 12 (site 6406/2-2) is an exception where the LCO of *E. ursulae* is positioned slightly below the LO/LCO of *Azolla*. Moreover at sites 10 (site 6507/8-4) and 14 (30/2-1) *C. columna* is not present at all. Further dinocyst events relevant for the age assessment of the *Azolla* interval are the LO of *E. ursulae* and *Drachodinium pachydermum* situated above the top of the Ypresian within the Lutetian (the latter dinocyst is only present in some of the wells). Furthermore, the LO of *Deflandrea oebisfeldensis* is situated well below the LO/LCO/LAO of *Azolla* and the LO of *Apectodinium augustum* is associated with the Top of the Thanetian (Late Paleocene). In addition, there is a lithological boundary in this interval, which is positioned between the Hordaland group (Lutetian age) and Rogaland group (Ypresian age). The Rogaland group has the Tare Formation or Balder Formation at the top. These formations are dominated by volcanic tuff and called Balder to the south and Tare to the north.

Sites 16 and 17 (Kirstinebjerg and Kasmose, respectively) are in outcrops. The *Azolla*-bearing horizon spans a ~2.8 m interval at both sites. At site 16, the *Azolla* bearing horizon spans the boundary between the *Areosphaeridium diktyoplokum* Zone and the *Dracodinium pachydermum* Zone (Heilmann-Clausen, 1988) and is positioned in the middle of Bed L2 of the Lillebælt Clay Formation (Heilmann-Clausen et al., 1985). The last occurrence of *C. columna* is positioned at the zonal boundary, which is defined by the first occurrence of *D. pachydermum* (Heilmann-Clausen, 1993). The LO of *E. ursulae* is situated within the *D. pachydermum* Zone (in the lower part of Bed L4).

## Age comparison of *Azolla* intervals between sites

At the Norwegian-Greenland Sea sites (sites 6 and 7) the LAO of *Azolla* coincides with the LCO of *E. ursulae* (Eldrett et al., 2004). This is consistent with the evidence from sites 8-15 where the LO/LCO/LAO of *Azolla* is associated with the LCO of *E. ursulae*. The LO of *E. ursulae* as well as the LO of *D. pachydermum* at sites 8-15 is well above the LO/LCO/LAO of *Azolla*, which is in agreement with the evidence from site Kristinebjerg (site 16), where the LO of *E. ursulae* and *D. pachydermum* is well above the LAO of *Azolla* (Heilmann-Clausen, 1988). At sites 6, 7 and 16-17 the *Azolla* interval has been shown to span the LO of *C. columna*. For sites 8-15, where a continuous record is missing, the LO of *C. columna* coincides with the LO/LCO/LAO of *Azolla* and LCO of *E. ursulae*.

Despite the absence of the age diagnostic dinocyst marker species of the Nordic Sea succession in the Arctic Ocean sediments (sites 1-5), an early middle Eocene age assessment is in line with the informal palynological zonal scheme established for the western Arctic Basin (sites 1-4) (Bujak Research International, unpublished data) and with the current age model of the ACEX core (site 5) (Backman et al., 2008).

In summary, the *Azolla* bearing horizon has been shown to be contemporaneous at the different sites in the Norwegian-Greenland Sea and North Sea based on the presence of significant age-diagnostic dinocysts markers. Correlation from the Norwegian Greenland Sea and North Sea sites to the Arctic Ocean sites is based on very little direct evidence. However, within the limits of the available evidence the Arctic *Azolla* appears to be of at least overlapping age.

## Supplementary Table S-2

<b>Table S-2.</b> Distinctive microspore massula characteristics of <i>Azolla arctica</i> , <i>Azolla jutlandica</i> , <i>Azolla</i> sp. 1 and <i>Azolla</i> sp. 2. There is no record of microspore massulae for <i>Azolla</i> sp. 3 (see explanation to Table S-3). Measured distances for features lettered (A) – (E) are shown in Fig. S-2.				
	<i>Azolla arctica</i>	<i>Azolla jutlandica</i>	<i>Azolla</i> sp. 1	<i>Azolla</i> sp. 2
Width of glochidia fluke (A)	4-6 $\mu\text{m}$	8-11 $\mu\text{m}$	8-9 $\mu\text{m}$	7-9 $\mu\text{m}$
Width of glochidia shaft (B)	2-2.5 $\mu\text{m}$	5-7 $\mu\text{m}$	3-4(5) $\mu\text{m}$	3-4 $\mu\text{m}$
Width of glochidia thread (C)	1 $\mu\text{m}$	2 $\mu\text{m}$	2 $\mu\text{m}$	2 $\mu\text{m}$
Length of glochidia flukes (D)	2-5 $\mu\text{m}$	6 $\mu\text{m}$	5 $\mu\text{m}$	5 $\mu\text{m}$
Length of glochidia fluke extensions (E)	0.5-1.5 $\mu\text{m}$	1.5-2.5 $\mu\text{m}$	4-6 $\mu\text{m}$	2-4 $\mu\text{m}$
Total length of glochidia (F)	22-30 $\mu\text{m}$ 45-85 $\mu\text{m}$	15-55 $\mu\text{m}$	30-75 $\mu\text{m}$	30-75 $\mu\text{m}$
Shape of glochidia fluke	rounded	typically broad, flat and blunt-ended	obtusely rounded	broad and flat to rounded to arrow head-shaped
Shape of glochidia fluke tips	not recurved	straight; occasionally recurved (inwards or outwards)	typically curved-recurved	sometimes recurved (inwards or outwards); sometimes straight; often with long thin extensions
Attachment of glochidia stalk to massula	Stalk width unchanged at attachment area	Stalk width widening slightly	Stalk expanding to wide attachment	Stalk expanding to wide attachment
Hairs on lower glochidia stalk (length)	absent	sometimes (2-5 $\mu\text{m}$ )	often (3-4) $\mu\text{m}$	absent
Hairs on massulae (length)	1-2(3) $\mu\text{m}$	2-5 $\mu\text{m}$	3-4 $\mu\text{m}$	absent
Structure massulae	spongy; reticulate in appearance; dense	spongy; reticulate in appearance (coarser than <i>A. arctica</i> ); dense	not reticulate in appearance; less dense	spongy; reticulate in appearance; dense
Length of laesurae	2/3 radius	1/3 radius	1/2 radius	1/2 radius

**Supplementary Figure S-2**

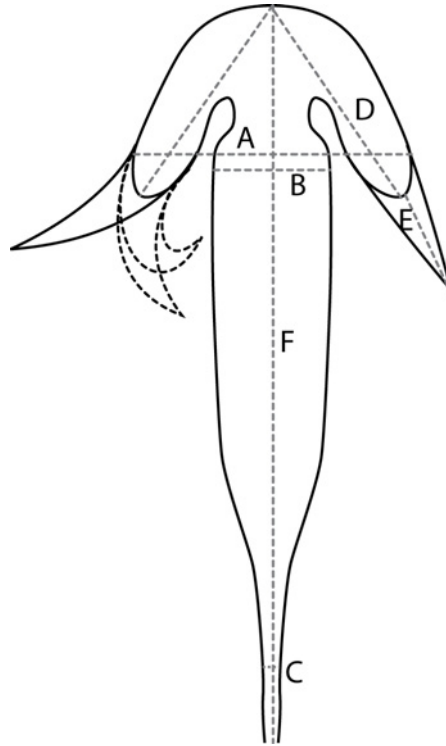


**Fig.S-2.** Illustration of glochidium morphology and terminology. A= width of glochidium fluke; B= width of glochidium shaft; C= width of lower part of glochidium stalk; D= length of glochidium fluke; E= length of glochidium fluke extension; F= total length of glochidium.

## Supplementary Information - Note 2

### Material and Methods

The samples studied are listed in Supplementary Table S-1. All samples were processed for palynology at the Laboratory of Palaeobotany and Palynology at Utrecht University using HCl (30%) and cold HF (40%) with no oxidation and sieving with a 15 and 250  $\mu\text{m}$  mesh (for details see Wood et al., 1996). *Lycopodium clavatum* tablets containing a known amount of spores were added to the samples to calculate the concentrations of *Azolla* massulae per gram of sediment (sites 5-7). Slide-mounted residues (size fraction between 15 and 250  $\mu\text{m}$ ) were examined under the light microscope. For percentage calculation of *Azolla* spp., peridinoid dinocysts, gonyaulacoid dinocysts, non-saccate pollen, bisaccate pollen and spores a minimum of 100 palynomorphs were counted (see Supplementary Table S-3). Pollen and spore identification was based on Moore et al. (1991). Dinocysts were identified following nomenclature cited in Fensome and Williams (2004); environmental interpretations followed Pross and Brinkhuis (2005), Sluijs et al. (2005), Sluijs et al. (2008), and Sluijs and Brinkhuis (2009). *Azolla* counts were based on complete and partial massulae; due to their spongy structure with pre-formed divisions, it is impossible to distinguish complete from partial massulae. Isolated glochidia were not counted. For percentage calculation of individual *Azolla* species, a total of 100 *Azolla* massulae was also counted for most samples. Some samples contained only a few massulae; in these cases the actual number of massulae counted is indicated in brackets below the percentages (see Supplementary Table S-3).

The > 250  $\mu\text{m}$  size fraction of the sample residues was studied under the dissecting microscope. Mesofossils encountered in these residues include wood, fusain, cuticles (together grouped as terrestrially-derived mesofossils) and *Azolla* remains (megaspore apparatuses and clusters of microspore massulae). The abundance of terrestrially-derived mesofossils is categorized as present (-), rare (+), frequent (++) and common (+++), see Supplementary Table S-3. A selection of megaspore apparatuses representative of the range of morphologies seen in the sample was picked and studied by scanning electron microscopy (SEM). The number of megaspore apparatuses studied per site is indicated in Supplementary Table S-1. Specimens studied by SEM were processed following the method described in Collinson et al. (2009) and Collinson et al. (2010).

The slide-mounted residues and mesofossil material studied are housed in the Laboratory of Palaeobotany and Palynology (Utrecht).



### Supplementary Information - Note 3

#### Palynomorph assemblage composition at the various study sites

In the western Arctic Basin (sites 1-4), the contribution of *Azolla* spp. to the total palynomorph assemblage ranges between 12-27%. Furthermore, these assemblages are rich in peridinioid dinocysts, dominated by the low-salinity tolerant *Senegalinium* spp., and pollen (many non-saccate forms). The amount of terrestrially-derived mesofossils is frequent to common (Supplementary Table S-3). At the Lomonosov Ridge in the central Arctic Basin (site 5) the monospecific assemblage of *Azolla arctica* contributes up to 90% to the total palynomorph assemblage. Furthermore, the palynomorph assemblage comprises a high abundance of peridinioid dinocysts (notably *Senegalinium* spp.) and intermediate amounts of pollen (many non-saccate forms). Terrestrially-derived mesofossils are extremely rare. Also at site 6 in the Norwegian-Greenland Sea, *Azolla* spp. is very abundant, contributing up to 70% of the total palynomorph assemblage. Moreover, the assemblage comprises high abundances of peridinioid dinocysts (high proportion of low-salinity tolerant forms such as *Cerodinium depressum*, *Deflandrea* spp., *Wetzeliiella* spp., and *Senegalinium* spp.), and intermediate amounts of pollen (both non-saccate and saccate forms). The amount of terrestrial derived mesofossils is small. Site 7 in the Norwegian-Greenland Sea contains small amounts of terrestrially-derived mesofossils and very little pollen (mainly saccate forms). The *Azolla* assemblage contributes up to 20% to the total palynomorph assemblage. Moreover, the assemblage contains a large amount of Gonyaulacoid dinocysts. Peridinioid dinocysts (high proportion of the low-salinity forms *Phthanoperidinium* spp. and *Wetzeliiella* spp.) occur in intermediate amounts. Sediments from sites 8-17 in the Norwegian Greenland Sea and North Sea generally comprise many Gonyaulacoid dinocysts and only few peridinioid dinocysts. Pollen and spores and also terrestrially-derived mesofossils only occur in small to intermediate amounts. *Azolla* spp. contributes between 1-30% to the total palynomorph assemblage and up to 50% at site 10 (for more details see Supplementary Table S-3).

Absolute abundances of *Azolla* are only derived for sites 5, 6 and 7, since all other sites concern commercial wells. The monospecific assemblage of *A. arctica* at site 5 contains by far the highest concentrations of *Azolla* reaching up to 350,000 massulae per gram. At sites 6 and 7 *A. arctica* reaches concentrations of up to 28,512 and 5,865 massulae per gram, respectively. *Azolla* sp. 1 reaches concentrations of up to 1,700 and 4,700 massulae per gram of sediment at site 6 and 7, respectively. *A. jutlandica*, with 66,529 massulae per gram, has the highest concentration of all *Azolla* species at site 6. *Azolla* sp. 2 shows the lowest concentrations with a maximum concentration of 1092 massulae per gram at site 6.

**Supplementary Table S-3**

Site	% <i>Azolla</i> spp.	% Peridinoid dinocysts	% Gonyaulacoid dinocysts	% Non-saccate pollen	% Bisaccate pollen	% Spores	Terrestrially-derived mesofossils	% <i>Azolla</i> massulae (total counts)				Megaspore apparatuses <sup>d</sup>				
								A. arctica	A. jutlandica	Azolla sp. 1	Azolla sp. 2	A. arctica	A. jutlandica	Azolla sp. 1	Azolla sp. 2	Azolla sp. 3
1	12	26 <sub>a</sub>	5	43	14	0	++	15		85		✓		✓ <sub>†</sub>		
2	27	12 <sub>a</sub>	0	48	12	1	+++	100				✓ <sub>†</sub>				✓
3	16	38 <sub>a</sub>	6	24	16	0	+++	4 (1)		96 (17)		✓				
4	16	54 <sub>a</sub>	2	16	12	0	+++	7 (1)		93 (14)						
5	10 to 90	5 to 50 <sub>a</sub>	0 to 15	5 to 30	0 to 10	0 to 10	-	100				✓ <sub>*</sub>				
6a	52	13 <sub>b</sub>	6	3	25	1	+	92		8		✓			✓ <sub>*</sub>	
6b	71	25 <sub>b</sub>	0	0	3	1	-	100				✓ <sub>*</sub>				
6c	11	73 <sub>a</sub>	5	0	11	0	-	34	59	7		d				
6d	28	24 <sub>b</sub>	4	14	28	2	-	97		1	2	✓			✓ <sub>*</sub>	
7a	16	28 <sub>c</sub>	50	3	3	0	+	62		38		✓ <sub>*</sub>				
7b	20	5 <sub>c</sub>	70	1	4	0	-	1		99				✓		
7c	13	14	63	4	6	0	+			100				✓		
8	3	7	83	2	5	0	+	83 (5)		17 (1)				✓		
9	3	3	70	10	8	6	+	92	8			d				
10	52	4	42	1	1	0	-		100				✓ <sub>*</sub>			
11	13	6	68	2	6	5	+	36	40	14	10		✓ <sub>†</sub>		✓	
12	7	9	66	10	8	0	+	44	33	16	7		✓	✓	✓	
13	19	8	53	1	19	0	++	10	90				✓	✓		
14	6	11	74	5	4	0	+	100 (3)				d				
15	30	11	48	2	9	0	++		100				✓	✓ <sub>*</sub>		
16	1	7	91	0	1	0			100				✓ <sub>*</sub>			
17	3	2	93	2	0	0			100							

**Table S-3** shows the relative abundance of *Azolla* spp., peridinoid dinocysts, gonyaulacoid dinocysts, non-saccate pollen, bisaccate pollen and spores relative to the total palynomorphs. a = high proportion of *Senegalinium* spp.; b = high proportion of *Cerodinium depressum*, *Deflandrea* spp. *Wetzeliiella* spp. and *Senegalinium* spp.; c = high proportion of *Phthanoperidinium* spp. and *Wetzeliiella* spp.. The amount of terrestrial derived mesofossils is categorized as present (-), rare (+), frequent (++) and common (+++). Relative abundances of *Azolla* massulae (massulae %) and occurrences of megaspore apparatuses are given for *Azolla arctica*, *Azolla jutlandica*, *Azolla* sp. 1, *Azolla* sp. 2 and *Azolla* sp. 3. For *Azolla* sp. 3 no microspore massulae were found, probably a consequence of the overall low abundance of this species, as indicated by the very small number of megaspore apparatuses recorded. Megaspore apparatuses with attached microspore massula(e) are indicated with\*; megaspore apparatuses that themselves were indeterminable, but had massula(e) attached that could be identified, are indicated with†. No microspore massulae have been found attached to the megaspore apparatuses of *Azolla* sp. 3, probably because there is no filusum over the megaspore, hence no hairs in which glochidia can become entwined. All megasporae from site 3 and 4 were covered by a surface deposit, which obscured their morphological details and made identification in most cases impossible. d = all sites yielded megasporae but in three cases these were not studied.



## References

- Akhmetiev, M.A., and Beniamovski, V.N., 2009, Paleogene floral assemblages around epicontinental seas and straits in Northern Central Eurasia: proxies for climatic and paleogeographic evolution, *Geologica Acta* 7, 297-309.
- Allen, S.G., Idso, S.B., Kimball, B.A., and Anderson, M.G., 1988, Interactive effects of CO<sub>2</sub> and environment on photosynthesis of *Azolla*, *Agricultural and Forest Meteorology* 42, 209-217.
- Altabet, M.A., and Francois, R., 1994, Sedimentary nitrogen isotopic ratio as a recorder for surface ocean nitrate utilization, *Global Biogeochemical Cycles* 8, 103-116.
- Andreasson, F.P., Schmitz, B., and Spiegler, D., 1996, Stable isotope composition ( $\delta^{18}\text{O}_{\text{CO}_2}$ ,  $\delta^{13}\text{C}$ ) of early Eocene fish-apatite from Hole 913B: an indicator of the early Norwegian-Greenland Sea paleosalinity. In Thiede, J., Myhre, A.M., Firth, J.V., Johnson, G.L., and Ruddiman, W.F. (Eds.), 1996, *Proceedings of the Ocean Drilling Program, Scientific Results 151*, Edinburgh (Integrated Ocean Drilling Program Management International, Inc.).
- Archer, D., 2005, The fate of fossil fuel in geologic time, *Journal of Geophysical Research* 110, C09S05.
- Backman, J., Moran, K., McInroy, D.B., Mayer, L.A., and the Expedition 302 Scientists, 2006, Arctic Coring Expedition (ACEX), *Proceedings of the Integrated Ocean Drilling Program 302*, Edinburgh (Integrated Ocean Drilling Program Management International, Inc.).
- Backman, J., Jakobsson, M., Frank, M., Sangiorgi, F., Brinkhuis, H., Stickley, C., O'Regan, M., Løvlie, R., Pälike, H., Spofforth, D., Gattacecca, J., Moran, K., King, J., and Heil, C., 2008, Age model and core-seismic integration for the Cenozoic Arctic Coring Expedition sediments from the Lomonosov Ridge, *Paleoceanography* 23, PA1S03, doi:10.1029/2007PA001476.
- Basinger, J.F., Greenwood, D.R., and Sweda, T., 1994, Early Tertiary vegetation of Arctic Canada and its relevance to paleoclimatic interpretation. In LePage, B.A., Williams, C.J and Yang, H. (Eds.), 1994, *The geobiology and ecology of metasequoia*, Kluwer Academic/Plenum Publisher, New York.
- Battarbee, R. W., and Kneen, M. J., 1982, The use of electronically counted microspheres in absolute diatom analysis, *Limnology and Oceanography* 27, 184-188.
- Batten, D.J., and Collinson, M.E., 2001, Revision of *Minerisporites*, *Azolla* and associated plant microfossils from deposits of the Upper Palaeocene and Palaeocene/Eocene transition of the Netherlands, Belgium and the USA, *Review of Palaeobotany and Palynology* 115, 1-32.
- Berner, R.A., 1984, Sedimentary pyrite formation: An update, *Geochimica and Cosmochimica Acta* 48, 605-615.
- Bertelsen, F., 1972, *Azolla* species from the Pleistocene of the central North Sea area, *Grana* 12, 131-145.

## References

- Bertelsen, F. 1974, Late Tertiary *Azolla* species from Rømø, SW Denmark. Danmark geologiske Undersøgelser, Årbog 1973, 15-25.
- Boulter, M.C., and Manum, S.B., 1989, The "Brito-Arctic Igneous Province" flora around the Palaeocene/Eocene boundary, Proceedings of the Ocean Drilling Programme Scientific Results 104, 663-680.
- Braun-Howland, E.B., and Nierzwicki-Bauer, S.A., 1990, *Azolla-Anabaena azollae* symbiosis: biochemistry, ultrastructure and molecular biology. In Rai, A.N. (Ed.), Handbook of symbiotic cyanobacteria 65, 118. Boca Raton, FL, USA.
- Brinkhuis, H., Schouten, S., Collinson, M.E., Sluijs, A., Sinninghe Damsté, J.S., Dickens, G.R., Huber, M., Cronin, T.M., Onodera, J., Takahashi, K., Bujak, J.P., Stein, R., van der Burgh, J., Eldrett, J.S., Harding, I.C., Lotter, A.F., Sangiorgi, F., van Konijnenburg-van Cittert, H., de Leeuw, J.W., Matthiessen, J., Backman, J., Moran, K., and the Expedition 302 Scientists, 2006, Episodic fresh surface-waters in the Eocene Arctic Ocean, Nature 441, doi:10.1038/nature04692.
- Bujak, J.P., and Mudge, D., 1994, A high resolution North Sea Eocene dinocyst zonation, Journal of the Geological Society of London 151, 449-462.
- Bunn S.E., and Boon P.I., 1993, What sources of organic carbon drive food webs in Billabongs: a study based on stable isotope analysis, Oecologia 96, 85-94.
- Carrapiço, F., 1991, Are bacteria the third partner of the *Azolla-Anabaena* symbiosis? Plant and Soil 137, 157-160.
- , 2006, Is the *Azolla-Anabaena* symbiosis a co-evolution case? Botany of the Kazan University, 23-27.
- Carrapiço, F., Costa, M.H., Costa, M.L., Teixeira, G., Frazao, A.A., Santos, M.C.R., and Baioa, M.V., 1996, The uncontrolled growth of *Azolla* in the Guadiana River, Aquaphyte Newsletter 16, 11.
- Cary P.R., Weerts P.G.J., 1992, Growth and nutrient composition of *Azolla pinnata* R. Brown and *Azolla filiculoides* Lamarck as affected by water temperature, nitrogen and phosphorus supply, light intensity and pH. Aquatic Botany 43, 163-180.
- Chambers, P.A., Lacoul, P., Murphy, K.J., Thomaz, S.M., 2008, Global diversity of aquatic macrophytes in freshwater, Hydrobiologia 595, 9-26.
- Cline J.D., Kaplan I.R., 1975, Isotopic fractionation of dissolved nitrate during denitrification in the eastern tropical north pacific Ocean, Marine Chemistry 3, 271-299.
- Collinson, M. E., 1980, A new multiple-floated *Azolla* from the Eocene of Britain with a brief review of the genus, Palaeontology 23, 213-229.
- Collinson, M. E., 1983, Palaeofloristic assemblages and palaeoecology of the lower Oligocene Bembridge Marls, Hamstead Ledge, Isle of Wight. Botanical Journal of the Linnean Society 86, 177-225.
- Collinson, M. E., 1991, Diversification of modern heterosporous pteridophytes. In Blackmore, S., Barnes S. H. (Eds.), Pollen and Spores, Patterns of Diversification. Systematics Association Special volume 44, 119-150.
- , 2001, Cainozoic ferns and their distribution, Brittonia 53, 173-235.

- , 2002, The ecology of Cainozoic ferns, *Review of Palaeobotany and Palynology*, 119, 51-68.
- Collinson, M.E., Barke, J., van der Burgh, J., and van Konijnenburg-van Cittert, J.H.A., 2009, A new species of the freshwater fern *Azolla* (Azollaceae) from the Eocene Arctic Ocean, *Review of Palaeobotany and Palynology*, 155, 1-14.
- Collinson, M.E., Barke, J., van der Burgh, J., van Konijnenburg-van Cittert, J.H.A., Heilmann-Clausen, C., Howard, L.E., and Brinkhuis, H., 2010, Did a single species of Eocene *Azolla* spread from the Arctic Basin to the southern North Sea? *Review of Palaeobotany and Palynology*, 159, 152-165.
- Dorofeev, P.I., 1955, Sarmatian plants from the river Tiligul and S. Bug. *Trudy Bot. Inst. Akad. Nauk. SSSR*, ser.1, 11, 144-160 (in Russian)
- Dorofeev, P.I., 1959, New species of *Azolla* Lam in Tertiary flora of USSR, *Botanicheski Zhurnal* 44, 1756-1763.
- Dorofeev, P.I., 1963, The Tertiary flora of Western Siberia, *Izd. Akad. Nauk. SSSR. Moscow and Leningrad*. 345 pp. (in Russian)
- Dorofeev, P.I., 1968, Oligocene flora of Transuralia, *Paleontological Journal* 2, 248-255.
- Dunham, D. G., and Fowler, K., 1987, Megaspore germination, embryo development and maintenance of the symbiotic association in *Azolla filiculoides* Lam, *Botanical Journal of the Linnean Society* 95, 43-53.
- Eldholm, O., Myhre, A.M., and Thiede, J., 1994, Cenozoic tectono-magnetic events in the North Atlantic: Potential palaeoenvironmental implications, *In*: Boulter, M. C., and Fisher, H.C., (Eds.), *Cenozoic plants and climates of the Arctic*, Springer-Verlag Berlin.
- Eldrett, J.S., Harding, I.C., Firth, J.V., and Roberts, A.P., 2004, Magnetostratigraphic calibration of Eocene-Oligocene dinoflagellate cyst biostratigraphy from the Norwegian-Greenland Sea, *Marine Geology*, 204, 91-127.
- Eldrett, J.S., Greenwood, D.R., Harding, I.C., and Huber, M., 2009, Increased seasonality through the Eocene to Oligocene transition in northern high latitudes: *Nature*, v. 459, doi:10.1038/nature08069.
- Estes R., and Hutchinson J.H., 1980, Eocene lower vertebrates from Ellesmere Island, Canadian Arctic Archipelago, *Palaeogeography, Palaeoclimatology, Palaeoecology* 30, 325– 347.
- Evrard, C., and van Hove, C., 2004, Taxonomy of the American *Azolla* species (Azollaceae): a critical review, *Systematics and Geography of Plants* 74, 301-318.
- Fensome, R.A., and Williams, G.L., 2004, The Lentin and Williams Index of fossil dinoflagellates *American Association of Stratigraphic Palynologists*, Houston, TX 42, 909.
- Field, M.H., 1999, Variations in *Azolla* section *Azolla* megaspore apparatus and their implications for paleotaxonomy and European Pleistocene biostratigraphy, *Review of Palaeobotany and Palynology* 105, 85-92.
- Florschütz, F., 1938, Die beiden *Azolla*-arten des Niederländischen Pleistozäns. *Recueil des Travaux Botaniques Neerlandais* 35, 932-945.



## References

- Florschütz, F., and Menedez Amor, J., 1960, Une Azolle fossile dans les Pyrénées Orientales, *Pollen et Spores* 2, 285-292.
- Fowler, K., 1975, Megaspores and massulae of *Azolla prisca* from the Oligocene of the Isle of Wight, *Palaeontology* 18, 483-507.
- Fowler, K., Stennett-Willson, J., 1978, Sporoderm architecture in modern *Azolla*. *Fern Gazette* 11, 405-412.
- Francis, J.E., 1988, A 50-million-year-old fossil forest from Strathcona Fiord, Ellsemere Island, Arctic Canada: Evidence for a warm polar climate, *Arctic* 41, 314-318.
- Friis, E.M., 1977, EM studies on Salviniaceae megaspores from the Middle Miocene Fæstøhøjt flora, Denmark, *Grana* 16, 113-128.
- Gächter R., Meyer J.S., Mares A., 1988, Contribution of bacteria to release and fixation of phosphorus in lake sediments, *Limnology and Oceanography* 33, 1542-1558.
- Garcia-Murillo, P., Fernandez-Zamudio, R., Cirujano, S., Sousa, A., Espinar, J.M., 2007, The invasion of Doñana National Park (SW Spain) by the mosquito fern (*Azolla filiculoides* Lam), *Limnetica* 26, 243-250.
- Gardenal, P., Morbelli, M.A., Giudice, G.E., 2007, Morphology and ultrastructure of heterosporous Filicophyta spores from north-west Argentina, *Grana* 46, 65-77.
- Glebovsky VY, Kaminsky VD, Minakov AN, Merkuriev SA, Childers VA, Brozena JM, 2006, Formation of the Eurasia Basin in the Arctic Ocean as inferred from geohistorical analysis of the anomalous magnetic field, *Geotectonics* 40, 263-281.
- Godfrey, R.K., Reinert, G.W., and Houk, R.D., 1961, Observations on microsporocarpic material of *Azolla caroliniana*, *American fern journal* 51, 89-92.
- Goodwin, P., Williams, R.G., Follows, M.J., Dutkiewicz, S., 2007, Ocean-atmosphere partitioning of anthropogenic carbon dioxide on centennial timescales. *Global Biogeochemical Cycles* 21, GB1012.
- Gradstein, F.M., Luterbacher, H.P., Ali, J.R., Brinkhuis, H., Gradstein, F.M., Hooker, J.J., Monechi, S., Ogg, J.G., Powell, J., Röhl, U., Sanfilippo, A., and Schmitz, B., 2004, The paleogene period. In Gradstein, F.M., Ogg, J.G., Smith, A.G. (Eds.), *A Geologic Time Scale*, Cambridge University Press, Cambridge, UK, pp. 396.
- Greenwood, D.R., and Basinger, J.F., 1993, Stratigraphy and floristics of Eocene swamp forests from Axel Heiberg Island, Canadian Arctic Archipelago, *Canadian Journal of Earth Sciences* 30, 1914-1923.
- , 1994, The paleoecology of high-latitude Eocene swamp forests from Axel Heiberg Island, Canadian High Arctic, *Review of Palaeobotany and Palynology* 81, 83-97.
- Greenwood D.R., and Wing S.L., 1995, Eocene continental climates and latitudinal temperature gradients, *Geology* 23, 1044-1048.
- Greenwood, D.R., Basinger, J.F., and Smith, R.Y., 2010, How wet was the Arctic Eocene rainforest? Estimates of precipitation from Paleogene Arctic macrofloras, *Geology* 38, 15-18, doi: 10.1130/G30218.1.
- Hall, J. W., and Swanson, N. P., 1968, Studies on fossil *Azolla*: *Azolla montana* a Cretaceous megaspore with many small floats, *American Journal of Botany* 55, 1055-1061.

- Hay, W.W., Eicher, D.L., and Diner, R., 1993, Physical oceanography and water masses in the Cretaceous Western Interior Seaway, *In* Caldwell, W.G.E., and Kauffman, E.G. (Eds.), *Evolution of the Western Interior Basin*. Geological Association of Canada. Special Publications 39, 297-318.
- Hayes J.M., Strauss H., and Kaufman A.J., 1999, The abundance of  $^{13}\text{C}$  in marine organic matter and isotopic fractionation in the global biogeochemical cycle of carbon during the past 800 Ma, *Chemical Geology* 161, 103-125.
- Hayes, J.M. 2001, Fractionation of carbon and hydrogen isotopes in biosynthetic processes, *Stable isotope geochemistry* 43, 225-277.
- Heilmann-Clausen, C., 1978, Undersøgelse af den fossile dinoflagellatflora i "Plastisk Ler" fra det nordlige lillebæltområde. Master's Thesis, Department of Earth Sciences, Aarhus University, 99 pp (unpublished).
- Heilmann-Clausen, C., 1988, The Danish Subbasin, Paleogene dinoflagellates, *Geologisches Jahrbuch. A* 100, 339-343.
- Heilmann-Clausen, C., 1993, Gradual morphological changes in some dinoflagellate cysts from the Eocene (Lower Tertiary) of the North Sea Basin. *Palynology* 17, 91-100.
- Heilmann-Clausen, C., 1996, The Ypresian-Lutetian transition in Denmark: A hemipelagic record of change in the North Sea Basin. *In* Molina, E. (Ed.), *Early Paleogene Stage Boundaries, Abstracts and field trip guides* 19. University of Zaragoza, Zaragoza, Spain.
- Heilmann-Clausen, C., Nielsen, O.B., and Gersner, F., 1985, Lithostratigraphy and depositional environments in the Upper Paleocene and Eocene of Denmark. *Bulletin of the Geological Society of Denmark* 33, 287-323.
- Heilmann-Clausen, C., Abrahamsen, N., Larsen, M., Piasecki, S. and Stemmerik, L., 2008. Age of the youngest Paleogene flood basalts in East Greenland. *Newsletters on Stratigraphy* 43, 55-63.
- Held, I.M., and Soden, B.J., 2006, Robust Responses of the Hydrological Cycle to Global Warming, *Journal of Climate* 19, 5686-5699.
- Hills, L., and Weiner, N., 1965, *Azolla geneseeana*, n. sp., and revision of *Azolla primaeva*. *Micropaleontology* 11, 255-261.
- Hoffman, G. L., and Stockey, R. A., 1994, Sporophytes, megaspores, and massulae of *Azolla stanleyi* from the Paleocene Joffre Bridge locality, Alberta, *Canadian Journal of Botany* 72, 301-308.
- Huber M., Sloan L.C., and Shellito C.J., 2003, Early Paleogene oceans and climate: a fully coupled modeling approach using the NCAR CCSM. *In* Wing S.L. et al. (Eds.), *Causes and consequences of globally warm climates in the early Palaeogene*, Special Papers Geological Society of America, 369, 25- 47.
- Idso, S.B., Allen, S.G., Anderson, M.G., and Kimball, B.A., 1989, Atmosphere  $\text{CO}_2$  enrichment enhances survival of *Azolla* at high temperatures, *Botany of the Kazan University* 29, 337-341.

## References

- Jahren, A.H., and Sternberg, L.S.L., 2003, Humidity estimate for the middle Eocene Arctic rain forest, *Geology* 31, 463-466, doi: 10.1130/0091-7613(2003)031<0463:HEFTME>2.0.CO;2.
- Jakobsson, M., Backman, J., Rudels, B., Nycander, J., Frank, M., Mayer, L., Jokat, W., Sangiorgi, F., O'Regan, M., Brinkhuis, H., King, J., and Moran, K., 2007, The early Miocene onset of a ventilated circulation regime in the Arctic Ocean, *Nature* 447, doi:10.1038/nature05924.
- Jain, R.K., Hall, J.W., 1969. A contribution to the early Tertiary fossil record of the Salviniaceae. *American Journal of Botany* 56,527-539.
- Janes, R., 1998a, Growth and survival of *Azolla filiculoides* in Britain I. Vegetative reproduction, *New Phytologist* 138, 367-375.
- , 1998b, Growth and survival of *Azolla filiculoides* in Britain II. Sexual reproduction, *New Phytologist* 138, p. 377-384.
- Kingston, H.M., and Haswell, S.J., 1997, Microwave enhanced chemistry: fundamentals, sample preparation and applications, American Chemical Society, Washington DC, USA.
- Knies, J., and Mann, U., 2002, Depositional environment and source rock potential of Miocene strata from the central Fram Strait: Introduction of a new computing tool for simulating organic facies variations, *Marine Petroleum Geology* 19, 811– 828.
- Knies, J., Mann, U., Popp, B.N., Stein, R., and Brumsack, H.J., 2008, Surface water productivity and paleoceanographic implications in the Cenozoic Arctic ocean, *Paleoceanography* 23, PA1S16.
- Koizumi, H., Kibe, T., Mariko, S., Ohtsuka, T., Nakadai, T., Mo, W., Toda, H., Seiichi, N., and Kobayashi, K., 2001, Effects of free-air CO<sub>2</sub> enrichment (FACE) on CO<sub>2</sub> exchange at the flood-water surface in a rice paddy field. *New Phytologist* 150, 231-239.
- Kouli, K., Brinkhuis, H, Dale, B., 2001, *Spiniferites cruciformis*: a freshwater dinoflagellate cyst? Review of Palaeobotany and Palynology 133, 273-286.
- Kurtz, A.C., Kump, L.R., Arthur, M.A., Zachos, J.C., and Paytan, A., 2003, Early Cenozoic decoupling of the global carbon and sulfur cycles, *Paleoceanography* 18 (4).
- Kuypers, M.M.M., Sliekers, A.O., Lavik, G., Schmid, M., Jorgensen, B.B., Kuenen, J.G., Sinninghe Damsté, J.S., Strous, M., and Jetten, M.S.M., 2003, Anaerobic ammonium oxidation by anammox bacteria in the Black Sea, *Nature* 422, 608-611.
- Kuypers, M.M.M., van Breugel, Y., Schouten, S., Erba, E. and Sinninghe Damsté, J.S., 2004, N<sub>2</sub>-fixing cyanobacteria supplied nutrient N for Cretaceous oceanic anoxic events, *Geology* 32, 853-856.
- Kvaček, Z., and Manum, S. B., 1993, Ferns in the Spitsbergen Palaeogene, *Palaeontographica B*. 230, 169-181.
- Laberg, J.S., Dahlgren, K.I.T., and Vorren, T.O., 2005, The Eocene–late Pliocene paleoenvironment in the Vøring Plateau area, Norwegian Sea -paleoceanographic implications, *Marine Geology* 214, 269- 285.

- Large, M.F., Braggins, J.E., 1993, Spore morphology of New Zealand *Azolla filiculoides* LAM. (Salviniaceae), New Zealand Journal of Botany 31, 419-423.
- Laskar, J., Robutel, P., Joutel, F., Gastineau, M., Correia, A. C. M., and Levrard, B. 2004, A long-term numerical solution for the insolation quantities of the Earth. Astronomy and Astrophysics 428, 261–285, doi: 10.1051/0004-6361:20041335
- Lawrence, K.T., Sloan, L.C., and Sewall, J.O., 2003, Terrestrial climatic response to precessional orbital forcing in the Eocene, Geological Society of America Special Papers 369, 65-77, doi: 10.1130/0-8137-2369-8.65.
- LePage, B.A., 2003, A new species of Thuja (Cupressaceae) from the late Cretaceous of Alaska: Implications of being evergreen in a polar environment, American Journal of Botany, 90, 167-174.
- Lumpkin, T.A., and Plucknett, D.L. 1980, *Azolla*: Botany, physiology, and use as a green manure, Economic Botany 34, 111-153.
- Lumpkin, T.A., and Plucknett, D.L., 1982, *Azolla* as a green manure: use and management in crop production, Westview tropical agriculture series 5, Westview Press, Boulder, Colorado.
- Mainwaring, P., 2008, Application of the Gatan X-ray Ultramicroscope (XuM) to the investigation of materials and biological samples, Microscopy Today 16, 14-17.
- Manabe, S., 1997, Early development in the study of greenhouse warming: The emergence of climate models, Ambio 26, 47– 51.
- Manum, S.B., Boulter, M.C., Gunnarsdottir, H., Rangnes, K., and Scholze, A., 1989, Eocene to Miocene palynology of the Norwegian Sea (ODP Leg 104). In Eldholm, O., Thiede, J., Taylor, E., et al. (Eds.), Proceedings of Ocean Drilling Program, Scientific Results 104, College Station, TX, 611–662.
- Marschner, H., 1995, Mineral Nutrition of Higher Plants (second edition), Academic Press, London (1995).
- Martin, A., 1976, Some structures in *Azolla* megaspores, and an anomalous form, Review of Palaeobotany and Palynology 21, 141-169.
- Mayo, S.C., Miller, P.R., Sheffield-Parker, J., Gureyev, T., and Wilkins, S.W., 2005, Attainment of <60nm resolution in phase-contrast x-ray microscopy using an add-on to an SEM. Proc. 8<sup>th</sup> Int. Conf. X-ray Microscopy, IPAP Conference Series 7, 343-345.
- McIntyre, D.J., 1991, Pollen and spore flora of an Eocene forest, eastern Axel Heiberg Island, N.W.T, In Christie, R.L., and McMillan, N.J. (Eds.), Tertiary Fossil Forests of the Geodeltic Hills, Axel Heiberg Island, Arctic Archipelago Geological Survey of Canada, Bulletin 403, 83-97.
- McIver, E.E., and Basinger, J.F., 1999, Early Tertiary floral evolution in the Canadian High Arctic, Annals of the Missouri Botanical Garden 86, 523-545.
- Metzgar, J.S., Schneider, H., and Pryer, K.M., 2007, Phylogeny and divergence time estimates for the fern genus *Azolla* (Salviniaceae), International Journal of Plant Sciences 168, 1045-1053.

## References

- Milankovitch, M., 1941, Kanon der Erdbestrahlung und seine Anwendung auf das Eiszeitenproblem: Royal Serbian Academy, Special Publication, v. 133, p. 1-633.
- Miller, K.G., Kominz, M.A., Browning, J.V., Wright, J.D., Mountain, G.S., Katz, M.E., Sugarman, P.J., Cramer, B.S., Christie-Blick N., and Pekar, S.F., 2005, The Phanerozoic record of global sea-level change, *Science* 310, 1293-1298.
- Miller, K.G., Wright, J.D., and Browning, J.V., 2005, Visions of ice sheets in a greenhouse world, *Marine Geology* 217, 215-231.
- Minagawa, M, and Wada, E., 1986, Nitrogen isotope ratios of red tide organisms in the East China Sea, a characterization of biological nitrogen fixation, *Marine Chemistry* 19, 245-259.
- Montoya, J.P., Holl, C.M., Zehr, J.P., Hansen, A., Villareal, T.A., and Capone, D.G., 2004, High rates of N<sub>2</sub> fixation by unicellular diazotrophs in the oligotrophic Pacific Ocean, *Nature* 430, 1027-1031.
- Moore, P. D., Webb, J. A., and Collinson, M. E., 1991, *Pollen Analysis* (second edition), Blackwell Scientific Publications, Oxford, UK.
- Moran, K., Backman, J., Brinkhuis, H., Clemens, S.C., Cronin, T., Dickens, G.R., Eynaud, F., Gattacceca, J., Jakobsson, M., Jordan, R.W., Kaminski, M., King, J., Koc, N., Krylov, A., Martinez, N., Matthiessen, J., McInroy, D., Moore, T.C., Onodera, J., O'Regan, M., Pälike, H., Rea, B., Rio, D., Sakamoto, T., Smith, D.C., Stein, R., St John, K., Suto, I., Suzuki, N., Takahashi, K., Watanabe, M., Yamamoto, M., Farrell, J., Frank, M., Kubik, P., Jokat, W., and Kristoffersen, Y., 2006, The Cenozoic palaeoenvironment of the Arctic Ocean, *Nature* 441, doi:10.1038/nature04800.
- Moretti, A., Siniscalco Gigliano, G., 1988, Influence of light and pH on growth and nitrogenase activity on temperate-grown *Azolla*. *Biology and Fertility of soils* 6, 131-136.
- Nikitin, P. A., 1948, Pliocene flora from the River Ob' in Tomsk Region. *Doklady Akademii Nauk SSSR* 61, 1103-1106. (in Russian).
- Nikitin, P. A., 1957, Pliocene and Quaternary floras from the Voronezh district. *Akademii Nauk. SSSR, Leningrad*. 200 pp. (in Russian).
- Nikitin, P. A., 1965, An Aquitanian seed floras from Lagernogo Sad (Tomsk). *Tomsk University, Tomsk*, 119 pp. (in Russian).
- Ogg, J.G., and Gradstein, F.M., 2008, *The Concise Geologic Time Scale*, Cambridge University Press, 177 pp.
- Onodera, J., Takahashi, K., and Jordan, R.W., 2008, Eocene silicoflagellate and ebridian paleoceanography in the central Arctic Ocean, *Paleoceanography* 23, PA1S15, doi:10.1029/2007PA001474.
- Pagani, M., Zachos, J.C., Freeman, K.H., Tipple, B., and Bohaty, S., 2005, Marked decline in atmospheric carbon dioxide concentrations during the Paleogene. *Science* 309, 600-603.
- Paillard, D., Labeyrie, L., and Yiou, P., 1996, Macintosh program performs time-series analysis: *Eos, Transactions, American Geophysical Union* 77, 379.

- Pälike, H., Spofforth, D.J.A., O'Regan, M., and Gattacceca, J., 2008, Orbital scale variations and timescales from the Arctic Ocean, *Paleoceanography* 23, PA1S10, doi: 10.1029/2007PA001490.
- Pearson, P.N., and Palmer, M.R., 2000, Atmospheric carbon dioxide concentrations over the past 60 million years, *Nature* 406, 695-699.
- Pearson, P.N., Ditchfield, P.W., Singano, J., Harcourt-Brown, K.G., Nicholas, C.J., Olsson, R.K., Shackleton, N.J., and Hall, M.A., 2001, Warm tropical sea surface temperatures in the Late Cretaceous and Eocene epochs, *Nature* 413, 481-487.
- Perkins, S.K., Peters, G.A., Lumpkin, T.A., and Calvert, H.E., 1985, Scanning electron microscopy of perine architecture as a taxonomic tool in the genus *Azolla* Lamarck. *Scanning electron microscopy* 4, 1719-1734.
- Peters, G.A., and Mayne, B.C., 1974, The *Azolla*, *Anabaena azollae* Relationship: *Plant Physiology* 53, 813-819.
- Peters, G.A., Toia, R.E. Jr., Evans, W.T., Crist, D.K., Mayne, B.C., and Poole, R.E., 1980, Characterizations and comparisons of five N<sub>2</sub>-fixing *Azolla*-*Anabaena* associations. I. Optimization of growth conditions for biomass increase and N content in a controlled environment. *Plant, Cell and Environment* 3, 261-269.
- Peters, G.A., and Meeks, J.C., 1989, The *Azolla*-*Anabaena* Symbiosis: Basic Biology, *Annual reviews in Plant Physiology and Plant Molecular Biology* 40, 193-210.
- Powers, L.A., Werne, J.P., Johnson, T.C., Hopmans, E.C., Sinninghe Damsté, J.S., and Schouten, S., 2004, Crenarchaeotal membrane lipids in lake sediments: A new Paleotemperature proxy for continental paleoclimate reconstruction? *Geology* 32, 613-616.
- Pross, J., and Brinkhuis, H., 2005, Organic-walled dinoflagellate cysts as paleoenvironmental indicators in the Paleogene; a synopsis of concepts, *Paläontologische Zeitschrift*. 79, 53-59.
- Punt, W., Hoen, P. P., Blackmore, S., Nilsson, S., and Le Thomas, A., 2007, Glossary of pollen and spore terminology, *Review of Palaeobotany and Palynology* 143, 1-81.
- Radionova, E.P., and Khokhlova, I.E., 2000, Was the North Atlantic connected with the Tethys via the Arctic in the early Eocene? Evidence from siliceous plankton, *GFF* 122, 133-134.
- Rai, V., and Rai, A.K., 1998, Growth behaviour of *Azolla pinnata* at various salinity levels and induction of high salt tolerance: *Plant Soil* 206, 79-84.
- Rai, V., Tiwari, S.P., and Rai, A.K., 2001, Effects of NaCl on nitrogen fixation of unadapted and NaCl adapted *Azolla pinnata*-*Anabaena azollae*. *Aquatic Botany* 71, 109-117.
- Raymo, M.E., and Nisancioglu, K., 2003, The 41 kyr world: Milankovitch's other unsolved mystery: *Paleoceanography*, 18, 1011, doi:10.1029/2002PA000791.
- Read, J., and Francis, J.E., 1992, Responses of some Southern Hemisphere tree species to a prolonged dark period and their implications for high-latitude Cretaceous and Tertiary floras, *Palaeogeography, Palaeoclimatology, Palaeoecology*, 99, 271-290.

## References

- Reid, J.D., Plunkett, G.M., and Peters, G.A., 2006, Phylogenetic relationships in the heterosporous fern genus *Azolla* (Azollaceae) based on DNA sequence data from three noncoding regions, *International Journal of Plant Sciences* 167, 529-538.
- Reuveni, J., Gale, J., and Zeroni, M., 1997, Differentiating day from night effects of high ambient CO<sub>2</sub> on the gas exchange and growth of *Xanthium strumarium* L exposed to salinity stress, *Annual Botany* 9, 191-196.
- Revelle, R., and Suess, H.E., 1957, Carbon dioxide exchange between atmosphere and ocean and the question of an increase of atmospheric CO<sub>2</sub> during the past decades, *Tellus* 9, 18-27.
- Richter, S.L., and LePage, B.A., 2004, A high-resolution palynological analysis, Axel Heiberg Island, Canadian High Arctic, *In* The Geobiology and Ecology of *Metasequoia*, LePage, B. A. Williams, C. J. and Yang, H. (Eds.) Kluwer Academic/Plenum Publishers, New York 137-158.
- Roberts, C.D., LeGrande, A.N., and Tripathi, A.K., 2009a, Climate sensitivity to Arctic seaway restriction during the early Paleogene, *Earth and Planetary Science Letters* 286, 576-585.
- Royer, D.L., Wing, S.L., Beerling, D.J., Jolley, D.W., Koch, P.L., Hickey, L.J., Berner, R.A., 2001, Paleobotanical evidence for near present day levels of atmospheric CO<sub>2</sub> during part of the Tertiary, *Science* 292, 2310-2313.
- Sah, R.N., Goyal, S.S., Rains, D.W., 1989, Interactive effects of exogenous combined nitrogen and phosphorus on growth and nitrogen fixation by *Azolla*, *Plant and Soil* 117, 1-8.
- Sahni, B., Rao, H.S., 1943. The silicified flora of the Deccan Intertrappean Series, part IV. *Azolla intertrappea* sp. nov. Proceedings of the 21<sup>st</sup> Indian Science Congress Bombay (1934), 318-319.,
- Sangiorgi, F., Brumsack, H.J., Willard, D. A., Schouten, S., Stickley, C.E., O'Regan, M., Reichart, G.J., Sinninghe Damsté, J.S. and Brinkhuis H., 2008a, A 26 million year gap in the central Arctic record at the greenhouse-icehouse transition: Looking for clues, *Paleoceanography* 23, PA1S04, doi:10.1029/2007PA001477, 2008.
- Sangiorgi, F., van Soelen, E.E., Spofforth, D.J.A., Pälike, H., Stickley, C.E., St. John, K., Koç, N., Schouten, S., Sinninghe Damsté, J.S., and Brinkhuis, H., 2008b, Cyclicity in the middle Eocene central Arctic Ocean sediment record: Orbital forcing and environmental response, *Paleoceanography* 23, PA1S08, doi:10.1029/2007PA001487.
- Saunders, R.M.K., and Fowler, K., 1992, A morphological taxonomic revision of *Azolla* Lam. Section *Rhizosperma* (Mey.) Mett. (Azollaceae). *Botanical Journal of the Linnean Society* 109, 329-357.
- Saunders, R.M.K., and Fowler, K., 1993, The supraspecific taxonomy and evolution of the fern genus *Azolla* (Azollaceae), *Plant Systematics and Evolution* 184, 175-193.
- Schofield, E.K., Colinvaux, P.A., 1969, Fossil *Azolla* from the Galapagos Islands, *Bulletin of the Torrey Botanical Club* 96, 623-628.



- Schouten, S., Klein Breteler, W.C.M., Blokker, P., Schoot, N., Rijpstra, W.I.C., Grice, K., Baas, M., and Sinninghe Damsté, J.S., 1998, Biosynthetic effects on the stable carbon isotopic compositions of algal lipids: Implications for deciphering the carbon isotopic biomarker record, *Geochimica et Cosmochimica Acta* 62, 1397–1406.
- Schouten, S., Hopmans, E.C., Schefuß, E., and Sinninghe Damsté, J.S., 2002, Distributional variations in marine crenarchaeotal membrane lipids: a new tool for reconstructing ancient sea water temperatures? *Earth and Planetary Science Letters* 204, 265–274.
- Schubert, C.J., Calvert, S.E., and Stein, R., 2001, Tracking nutrient and productivity variations over the last deglaciation in the Arctic Ocean, *Paleoceanography* 16, 199– 211.
- Scotese, C.R., Gahagan, L.M., Larson, R.L., 1988, Plate tectonic reconstructions of the Cretaceous and Cenozoic ocean basins, *Tectonophysics* 155, 27–48.
- Serreze, M.C., Barrett, A.P., Slater, A.G., Woodgate, R.A., Aagaard, K., Lammers, R.B., Steele, M., Moritz, R., Meredith, M., and Lee, C.M., 2006, The large-scale freshwater cycle of the Arctic: *Journal of Geophysical Research* 111, C11010, doi:10.1029/2005JC003424.
- Shellito, C.J., Lamarque, J.F., and Sloan, L.C., 2009, Early Eocene Arctic climate sensitivity to pCO<sub>2</sub> and basin geography, *Geophysical Research Letters* 36, C11010, doi:10.1029/2005JC003424.
- Skipski, V.P., Smolowe, A.F., Sullivan, R.C., and Barclay, M., 1965, Separation of lipid classes by thin-layer chromatography, *Biochimica et biophysica acta* 196, 386–396.
- Sloan, L.C., and Huber, M., 2001, Eocene oceanic responses to orbital forcing on precessional time scales, *Paleoceanography* 16, 101–111.
- Sluijs, A., Pross, J., and Brinkhuis, H., 2005, From greenhouse to icehouse; organic-walled dinoflagellate cysts as paleoenvironmental indicators in the Paleogene, *Earth-Science Reviews* 68, 281–315.
- Sluijs, A., Schouten, S., Pagani, M., Woltering, M., Brinkhuis, H., Sinninghe Damsté, J.S., Dickens, G.R., Huber, M., Reichert, G.J., Stein, R., Matthiessen, J., Lourens, L.J., Pedentchouk, N., Backman, J., Moran, K. and the Expedition 302 Scientists, 2006, Subtropical Arctic Ocean temperatures during the Palaeocene/Eocene thermal maximum, *Nature* 441, 610– 613.
- Sluijs, A., Röhl, U., Schouten, S., Brumsack, H.J., Sangiorgi, F., Sinninghe Damsté, J.S., and Brinkhuis, H., 2008, Arctic late Paleocene–early Eocene paleoenvironments with special emphasis on the Paleocene-Eocene thermal maximum (Lomonosov Ridge, Integrated Ocean Drilling Program Expedition 302), *Paleoceanography* 23, 1–17.
- Sluijs, A., and Brinkhuis, H., 2009, A dynamic climate and ecosystem state during the Paleocene-Eocene Thermal Maximum – inferences from dinoflagellate cyst assemblages at the New Jersey Shelf, *Biogeosciences* 6, 1755–1781.
- Smith, A. R., Pryer, K. M., Schuettpelz, E., Korall, P., Schneider, H., and Wolf, P. G., 2006, A classification for extant ferns, *Taxon* 55, 705–731.

## References

- Snead, R. G., 1969, Microfloral diagnosis of the Cretaceous-Tertiary boundary, Central Alberta, Research Council of Alberta Bulletin 25, 1-148.
- Speelman, E.N., Reichart, G.J., de Leeuw, J.M., Rijpstra, W.I.C., Sinninghe Damsté, J.S., 2009a, Biomarker lipids of the freshwater fern *Azolla* and its fossil counterpart from the Eocene Arctic Ocean, Organic Geochemistry. Organic Geochemistry 40, 628-637.
- Speelman, E.N., van Kempen, M. L., Barke, J., Brinkhuis, H., Reichart, G.J., Smolders, A. J. P., Roelofs, J. G. M., Sangiorgi, F., de Leeuw, j., Lotter, A.F., Sinninghe Damsté, J. S., 2009b, The Eocene Arctic *Azolla* bloom: environmental conditions, productivity and carbon drawdown, Geobiology 7, 155-170, doi: 10.1111/j.1472-4669.2009.0195.x.
- Speelman, 2010a, Thesis Chapter 4, Modeling the influence of a reduced equator-to-pole sea surface temperature gradient on the distribution of water isotopes in the Eocene (ISBN: 978-90-5744-192-9).
- Speelman, 2010b, Thesis Chapter 6, Reconstruction of Eocene Arctic hydrology using proxy data and isotope modeling (ISBN: 978-90-5744-192-9).
- Stein, R., Boucsein, B., and Meyer, H., 2006, Anoxia and high primary production in the Paleogene central Arctic Ocean: First detailed records from Lomonosov Ridge: Geophysical Research Letters 33, L18606, doi:10.1029/2006GL026776.
- Stickley, C.E., Koç, N., Brumsack, H.J., Jordan, R.W., and Suto, I., 2008, A siliceous microfossil view of middle Eocene Arctic paleoenvironments: A window of biosilica production and preservation, Paleoceanography 23, PA1S14, doi:10.1029/2007PA001485.
- Sun, M.Y., Wakeham, S.G., 1994, Molecular evidence for degradation and preservation of organic matter in the anoxic Black Sea Basin, Geochimica et Cosmochimica Acta 58, 3395-3406.
- Sweet, A. R., Hills, L. V., 1976, Early Tertiary species of *Azolla* subg. *Azolla* sect *Krematospora* from western and arctic Canada, Canadian Journal of Botany 54, 334-351.
- Teixeira, G., Glen, R., Carrapiço, 2000, Megaspore apparatus ultrastructure in *Azolla pinnata* R. Br. from South Africa. Garcia de Orta, Ser. Bot. 16, 33-37.
- Thiede, J., Myhre, A.M., Firth, J.V., Johnson, G.L., and Ruddiman, W.F., 1996, Introduction to the North Atlantic-Arctic gateways: plate tectonic-paleoceanographic history and significance, Proceedings of the Ocean Drilling Program, Scientific Results 151.
- Tripathi, A., Backman, J., Elderfield, H., Ferretti, P., 2005, Eocene bipolar glaciation associated with global carbon cycle changes, Nature 436, 341-346.
- Trivedi, B.S., Verma, C.L., 1971, Contributions to the knowledge of *Azolla indica* sp. nov. from the Deccan Intertrappean Series M.P. India, Palaeontographica B 136, 71-82.
- Vajda, V., McLoughlin, S., 2005, A new Maastrichtian-Paleocene *Azolla* species from Bolivia, with a comparison of the global record of coeval *Azolla* microfossils, Alcheringa 29, 305-329.
- van Bergen, P. F., Collinson, M. E., and de Leeuw, J. W., 1993. Chemical composition and ultrastructure of fossil and extant salvinealean microspore massulae and megaspores. Grana 1993, Supplement 1, 18-30.

- van Cappellen, P., and Ingall, E.D., 1994, Benthic phosphorus regeneration, net primary production, and ocean anoxia: A model of the coupled marine biogeochemical cycles of carbon and phosphorus, *Paleoceanography* 9, 677-692.
- van Hove, C., and Lejeune, A., 2002, The *Azolla-Anabaena* symbiosis: Proceedings of the Royal Irish Academy 102B, 23-26.
- van Kempen, M.M.L., Smolders, A.J.P., Bögeman, G.M., and Roelofs, J.G.M., under review, Long term effects of salt stress on the growth, nutrient content and amino acid composition of the *Azolla filiculoides* Lam.- *Anabaena azollae* Stras. Association.
- Waddell, L.M., and Moore, T.C., 2008, Salinity of the Eocene Arctic Ocean from oxygen isotope analysis of fish bone carbonate, *Paleoceanography* 23, PA1S12, doi:10.1029/2007PA001451.
- Wagner, G.M., 1997, *Azolla*: a review of its biology and utilization, *Botanical Review* 63, 1-26.
- Westerhold, T., and Röhl, U., 2009, High resolution cyclostratigraphy of the early Eocene – new insights into the origin of the Cenozoic cooling trend, *Climate of the Past* 5, 309-327.
- Wood, G.D., Gabriel, A.M., and Lawson, J.C., 1996, Palynological techniques - processing and 906 microscopy, in Jansonius, J., and McGregor, D.C. (Eds.), *Palynology: Principles and 907 Applications*, American Association of Stratigraphic Palynologists Foundation, 908 Dallas, TX, 1, 29-50.
- Yapp, C.J., 2004,  $\text{Fe}(\text{CO}_3)\text{OH}$  in goethite from a mid-latitude North American Oxisol: Estimate of atmospheric  $\text{CO}_2$  concentration in the early Eocene "climatic optimum," *Geochimica et Cosmochimica Acta*, 68, 935-947.
- Zachos, J.C., Pagani, M., Sloan, L.C., Thomas, E., Billups, K., 2001, Trends, rhythms, and aberrations in global climate 65Ma to present. *Science* 292, 686-693.
- Zachos, J.C., Dickens, G.R., and Zeebe, R.E., 2008, An early Cenozoic perspective on greenhouse warming and carbon-cycle dynamics, *Nature* 451, doi:10.1038/nature06588.
- Zeebe RE, Wolf-Gladrow D (Eds.), 2001,  $\text{CO}_2$  in seawater: equilibrium, kinetics, isotopes, Elsevier Oceanography Series 65.
- Zhou, Z., 1983, Quaternary record of *Azolla pinnata* from China and its sporoderm ultrastructure, *Review of Palaeobotany and Palynology* 39, 109-129.
- Zimmerman, W.J., 1985, Biomass and pigment production in three isolates of *Azolla* II. response to light and temperature stress, *Annals of Botany* 56, 701-709.



## **Algemene inleiding en samenvatting**

Enorme aantallen resten van de zoetwatervaren *Azolla* karakteriseren sedimenten uit het vroeg midden Eoceen (~ 49 Ma) in de centrale Arctische Oceaan (Lomonosov Rug), geboord tijdens de zgn. *Arctic Coring Expedition* (ACEX), ook wel *Integrated Ocean Drilling Program*, IODP, Expeditie 302 genoemd (Backman et al., 2006; Brinkhuis et al., 2006). Het samen voorkomen van restanten van verschillende levensfasen, incl. reproductieve delen van *Azolla*, en het ontbreken van landplant resten in de ACEX sedimenten, suggereert dat deze drijvende zoetwater varens *in situ* groeiden en zich vermenigvuldigden op de oppervlakte wateren van de toenmalige Arctische Oceaan (Brinkhuis et al., 2006). Deze en soortgelijke bevindingen impliceren de episodische aanwezigheid van aanhoudende zoete oppervlaktewater condities, en daaraan gekoppelde sterke gelaagdheid van het water, en mogelijk afwezigheid van zuurstof (anoxia) in de waterkolom en/of in het bodemwater (Brinkhuis et al., 2006; Stein et al., 2006; Onodera et al., 2008; Stickley et al., 2008; Waddell en Moore, 2008). *Azolla* resten waren reeds sporadisch bekend uit vroeg midden Eocene sedimenten van brede gebieden van de Barentsz-, Labrador- en Noorwegen-Groenland zeeën, en zelfs uit de noordelijke delen van de Noordzee, incl. Denemarken (Brinkhuis et al., 2006). De distributie van deze midden Eocene *Azolla* resten suggereert in eerste instantie dus een Noordelijk brongebied, mogelijk de toenmalige Arctische Oceaan; de voorkomens in nabijgelegen zeeën zouden het resultaat zijn van transport (cf. Brinkhuis et al., 2006). Dit proefschrift gaat dieper in op de palaeobotanische, geografische en palaeomilieu aspecten van de '*Azolla* fase', en de omvang, de oorzaak en gevolgen van dit unieke fenomeen.

## Wat is *Azolla*?

*Azolla*, ook bekend als de kroosvaren, is een relatief kleine watervaren, met een wereldwijde distributie van gematigde tot tropische klimaten (Van Hove en Lejeune, 2002). *Azolla* behoort tot de Divisie van de Pteridophyta (varens) en is het enige geslacht in de familie Azollaceae. Zeven moderne soorten *Azolla* zijn bekend, verdeeld in twee taxonomische secties: de sectie *Euazolla* omvat de soorten *A. filiculoides*, *A. rubra*, *A. mexicana*, *A. caroliniana*, en *A. microphylla*, terwijl de sectie *Rhizosperma* de soorten *A. pinnata* en *A. nilotica* omvat (Saunders en Fowler, 1993; van Hove en Lejeune, 2002). Meer dan vijftig fossiele soorten *Azolla* zijn beschreven; de oudste dateren uit het midden tot laat Krijt (Collinson, 1980, 2001, 2002).

## Morfologie

*Azolla* is een drijvende plant, die zelden groter wordt dan 3 tot 4 cm (met uitzondering van de soort *A. nilotica*, die kan groeien tot 15 cm of meer). De plant bestaat uit veervormig vertakte, horizontaal drijvende stengels, die wortels aan de onderkant dragen. Aan de bovenzijde dragen ze kleine, afwisselend geplaatste, overlappende bladeren (figuur 1,

bladzijde 11). Elk blad is verdeeld in twee lobben, de dikkere dorsale lob is doorgaans boven water, en bevat chlorofyl, terwijl de dunnere ventrale lob zich gedeeltelijk onder water bevindt, en kleurloos tot wat bruinig is, en drijfvermogen biedt (Wagner, 1997; Van Hove en Lejeune, 2002). Onder bepaalde voorwaarden, bv fosforgebrek, zeer hoge instraling, of lage wintertemperatuur, kan de kleur van de bladeren veranderen van groen naar rood, veroorzaakt door de productie van anthocyanen (rood plantaardig pigment) in het fotosynthetische weefsel. Roodheid van de bladeren maakt de plant resistent tegen licht beschadiging van het fotosynthetische weefsel (Janes, 1998a).

De morfologie en fysiologie van *Azolla* is zeer plastisch, waardoor deze zoetwaterplant in een zeer breed scala van habitats voor kan komen. Drie fenotypen worden geïdentificeerd (Janes, 1998a):

(i) de *overlevings-vorm* is typerend voor de rode (winter) planten. De planten zijn klein, vertakken nauwelijks en groeien zeer langzaam.

(ii) de *koloniserende-vorm* groeit het snelst en is te vinden tijdens het voorjaar en de zomer. Deze vorm is kenmerkend voor planten in open water waar de ruimte niet beperkend is. Planten zijn groen, compact en groeien plat op het wateroppervlak (tot een monolaag).

(iii) De *mat-vorm*. Deze vorm is te vinden in cm-dikke matten (groter dan een monolaag) van midden tot einde van de zomer. Planten zijn groen en met elkaar verstrengeld. In deze matten zijn de groeipercentsages lager dan bekend voor de koloniserende vorm, maar uitgebreide vorming van sporangia is gebruikelijk.

Deze drie fenotypen kunnen snel in elkaar overgaan, binnen een paar weken, als de externe omstandigheden zijn veranderd (Janes, 1998a).

## Groei en voortplanting

De geringe omvang van *Azolla* maakt een snelle groei en de kolonisatie van waterlichamen door middel van ongeslachtelijke voortplanting mogelijk (Saunders en Fowler, 1993). Verdubbeling van de biomassa kan binnen 5 dagen optreden (Janes, 1998a). Ongeslachtelijke voortplanting is veruit de meest voorkomende manier van reproductie en bestaat uit vermenigvuldiging met eenvoudige deling van de bladeren (Wagner, 1997). De geslachtelijke (sexuele) voortplantingscyclus is ingewikkelder (figuur 2, bladzijde 13). *Azolla* is een zgn heterospore varen, wat inhoudt dat het twee verschillende soorten sporen, micro- en megasporen, produceert, die zich ontwikkelen in de micro- en megasporangia. Deze sporangia zijn ontwikkeld in afzonderlijke micro- en megasporocarpes, binnen individuele planten (Saunders en Fowler, 1993). De megasporocarpes produceren elk een enkel megasporangium, voorzien van één megaspore-apparaat die bestaat uit distaal een megaspore en proximaal een aantal zogenaamde 'drijflichamen' (men dacht in het verleden dat deze functioneren als luchtzakken ten behoeve van het drijvend vermogen van de megaspore, maar dit blijkt is niet het geval). Het megaspore-apparaat is meestal



bedekt met een laag verstrengelde draden (*filosum*). De microsporocarpn produceren tot 130 microsporangia, elk met 32 of 64 microsporen samengeklonterd in 3-10 sponsachtige fragmenten, *massulae* genaamd (Wagner, 1997; Van Hove en Lejeune, 2002). Na volgroeing van de microsporangia breken deze open en komen de massulae in het water. Door middel van hun haar-achtige aanhangsels (*glochidia*), verstrengelen deze met het filosum van de megasporocarpn. Samen zinken ze naar de bodem, tot ontkieming volgt (Janes, 1998b). Het is nog niet goed duidelijk welke milieuomstandigheden *Azolla* aanzetten om zich seksueel voort te planten. Verhoogde plantdichtheid, relatief hoge fosfaatconcentraties, en ongunstige temperaturen in de winter zijn factoren die verondersteld worden betrokken te zijn bij het stimuleren van seksuele voortplanting bij *Azolla* (Janes, 1998a, b).

### De *Azolla-Anabaena*-Bacteria-symbiose

Moderne *Azolla* soorten worden gekarakteriseerd door een permanente endosymbiotische prokaryotische gemeenschap (cyanobacteriën, speciaal het blauwwier *Anabaena azollae*), die leven in een holte in de dorsale lob van het blad (Peters en Mayne, 1974; Carrapiço, 1991). Tijdens de levenscyclus van *Azolla* worden de symbionten overgedragen van de moederplant naar de nieuwe sporofyt. Deze symbiose wordt gezien als een co-geëvolueerd systeem (Carrapiço, 2006). *Anabaena azollae* levert *Azolla* organische stikstof voor de groei. In ruil daarvoor biedt de *Azolla* aan *Anabaena* een beschermde omgeving en een vaste bron van koolstof (Wagner, 1997). Daarom is stikstof-limitatie niet aan de orde binnen *Azolla*.

### Milieufactoren die de groei van de *Azolla* beïnvloeden

Ondanks het relatief onafhankelijk zijn van externe bronnen van organische stikstof, heeft *Azolla* wel alle andere essentiële voedingsstoffen nodig. Fosfor is de meest belangrijke en vaak beperkende voedingsstof voor de *Azolla* groei. De drempelwaarde van fosfaat voor de *Azolla* groei is 0,03 mmol L<sup>-1</sup> (Wagner, 1997). Hoge fosforconcentraties in het water kunnen leiden tot ongebreidelde bloei van *Azolla* (Carrapiço et al., 1996). De optimale luchttemperatuur voor *Azolla* varieert tussen 18 en 28 °C. Sommige soorten kunnen echter overleven binnen een zeer breed luchttemperatuurbereik van -5 tot 35 °C. De optimale fotoperiode wordt geschat op 20 uur (Wagner, 1997). Met betrekking tot temperatuur versus daglengte, is vooral de minimum temperatuur bepalend als belangrijkste factor voor de relatieve groeisnelheid van *Azolla*. CO<sub>2</sub> heeft een positief effect op de omvang van de door *Azolla* geproduceerde biomassa (Allen et al., 1988; Idso et al., 1989). De laatste auteurs hebben aangetoond dat hogere concentraties van CO<sub>2</sub> in de atmosfeer (340 ppm tot 640 ppm) *Azolla* niet negatief beïnvloeden; in tegendeel, de planten floreren bij temperaturen boven 30 °C met verhoogd CO<sub>2</sub>. Het optimale pH-bereik voor *Azolla* groei ligt tussen 4,5 en 7, maar *Azolla* kan overleven binnen 3,5-10 pH. De respons van *Azolla* op de pH wordt echter sterk bepaald door andere omgevingsfactoren zoals licht, temperatuur, en beschikbaar oplosbaar ijzer (Wagner, 1997).

*Azolla* is een zoetwatervaren, en een verhoogd zoutgehalte van het water (saliniteit) doet de productie van biomassa aanzienlijk afnemen. Voor bestaande soorten *Azolla* is

aangetoond dat deze saliniteits-waarden van 5 ‰ kunnen verdragen (Van Kempen et al., in review). Bij hogere saliniteiten wordt de wortelgroei en dus water- en nutriëntenopname ernstig negatief beïnvloed wat uiteindelijk resulteert in de dood van de planten (Van Kempen et al., in review).

## **De Eocene Arctische ‘*Azolla* fase’**

De oudste *Azolla* fossielen zijn bekend uit het midden en laat Krijt als complete, reproducerende planten, en als tal van verspreide megaspore-apparaten, losse megasporen en massulae. Deze vondsten staan altijd in verband met een sedimentaire facies typisch voor zoetwater systemen, inclusief meren en vennen (Collinson, 2001, 2002). Het massaal voorkomen van overblijfselen van *Azolla* in Eocene mariene afzettingen in sub-Arctische en Noordelijke randzeeën, voornamelijk gevonden in commerciële olie en gas exploratie boringen, is verrassend en uniek. Er zijn aanwijzingen dat deze ‘*Azolla* fase’ zich mogelijk ~synchroon in alle noordelijke randzee locaties voordoet (Bujak en Mudge, 1994; Eldrett et al., 2004). Met name de beëindiging van deze fase wordt op grote schaal gebruikt als stratigrafische marker in industriële boringen en ontsluitingen, gekalibreerd aan magnetochron C21r (~ 49 Ma; Eldrett et al., 2004) offshore Groenland. Tot nu toe zijn er geen studies die aandacht hebben geschonken aan de omvang, de oorzaak en gevolgen van dit unieke fenomeen.

Pas in 2004, toen enorme aantallen *Azolla* resten werden gevonden in even oude micro-gelamineerde (gelaagde) centrale Arctische Oceaan (Noordelijke IJszee) sedimenten (figuur 3, bladzijde 14) tijdens de ACEX expeditie, werd de aandacht gevestigd op de mogelijke palaeoecologische en palaeoceanografische implicaties van dit fenomeen (Brinkhuis et al., 2006; Moran et al., 2006; Backman et al., 2006). De aanwezigheid van volwassen megasporen met- en zonder aangehechte massulae van *Azolla*, de enkele, kleine groepen en grote clusters van *massulae*, en losse megasporen die waarschijnlijk abortief geweest zijn, geven allemaal aan dat het hoogst onwaarschijnlijk is dat deze associatie getransporteerd is van nabijgelegen landmassa's. Dit wordt sterk ondersteund door de relatieve schaarste van terrestrische palynomorfen (pollen en sporen) en extreem lage (<0,1) waarden van de BIT (vertakte en isoprenoïde tetraether) index, een maat voor de hoeveelheid van door de rivier getransporteerde terrestrische organische stof ten opzichte van mariene organische stof. Alle aanwijzingen suggereren sterk dat *Azolla in situ* groeide en reproduceerde in de Noordelijke IJszee. Dit is alleen mogelijk als het oppervlaktewater van de centrale Noordelijke IJszee zoet (en warm) genoeg was om deze *in situ* groei en reproductie van *Azolla* mogelijk te maken. De wijdverbreide, even oude *Azolla* houdende sedimenten in de noordelijke randzeeën werden verondersteld het resultaat te zijn van transport vanuit de Noordelijke IJszee, door periodieke uitstroom van zoetwater (Brinkhuis et al., 2006).

## **De Eocene Arctische Oceaan; palaeogeografie en palaeoceanografie**

Tijdens het vroege midden Eoceen was de Noordelijke IJszee (Arctische Oceaan) een vrijwel volledig ingesloten bekken (figuur 4, bladzijde 15). De uitwisseling tussen de

Noordelijke IJszee en de wereldwijde oceanen was waarschijnlijk beperkt tot de zeestraat tussen Noorwegen en Groenland, omdat de verbinding met de Tethysche Oceaan via de Straat van Turgay was opgehouden te bestaan (Radionova en Khokhlova, 2000; Akhmetiev en Beniamovski, 2009). Bovendien was de uitwisseling tussen de Arctische en Noord-Atlantische Oceaan via de zeestraat tussen Groenland en Noorwegen waarschijnlijk beperkt tot alleen het oppervlakte water (Jakobsson et al., 2007). De Noorwegen-Groenland Zee bestond uit een aantal geïsoleerde deelstroomgebieden gescheiden door een mid-oceanische rug, en de Jan Mayen en Groenland-Senja breukzones. Verder werd de Noorse en Groenland Zee gescheiden van de Noord-Atlantische Oceaan door de Groenland-Schotland Rug. Ten gevolge hiervan was de ventilatie van intermediair en diep water beperkt, en de regionale uitwisseling van oppervlaktewater was slecht (Eldholm et al., 1994).

### Het Eocene Arctische milieu en klimaat

Tijdens het vroege Eoceen was de Aarde in broeikas modus met atmosferische CO<sub>2</sub>-concentraties van meer dan 2000 ppm (Pearson en Palmer, 2000; Pagani et al., 2005). Hoge breedte graden waren gekarakteriseerd door hoge temperaturen en de Arctische landmassa's waren bebost, zelfs op breedtegraden van 75-80° N (McIver en Basinger, 1999). Een mozaïek van plantengemeenschappen kenmerkte het landschap in het Canadese Noordpoolgebied, gedomineerd door moerassen en bossen (Francis, 1988; Greenwood en Basinger, 1994; McIntyre, 1991; McIver en Basinger, 1999). Droog gelegen zones van de moerassen werden vaak bezet door een climax bos van bladverliezende coniferen, waarin *Metasequoia* en/of *Glyptostrobus* de dominante taxa waren. Op beter gedraineerde plaatsen tussen de moerassen groeiden hardhout angiosperme bossen (Greenwood en Basinger, 1993; Greenwood en Basinger, 1994), gedomineerd door *Carya* (McIver en Basinger, 1999). Hoger gelegen gebieden werden waarschijnlijk hoofdzakelijk bedekt door een mix van hardhout angiospermen en groenblijvende coniferen, gedomineerd door *Picea* (McIntyre, 1991; McIver en Basinger, 1999; Richter en Lepage, 2004).

De dominantie van bladverliezende vegetatie wijst op milde en vochtige zomerse omstandigheden en verklaart ook enigszins de tolerantie van het gebrek aan zonlicht gedurende de winter duisternis op deze hogere breedtegraden (Basinger et al., 1994). Veldwaarnemingen en jaarringmetingen van het Strathcona fjord Eoceen fossiel bos (ongeveer 50 Ma) op Ellesmere Island geven aan dat het klimaat grote seizoensfluctuaties kende, en warm was, naast overvloedige regenval gedurende het groeiseizoen (Francis, 1988). De samenstelling van het vroege Paleogene fossiele bos van het Arctisch gebied suggereert een gemiddelde jaarlijkse temperatuur van 12-15° C, warmste maand gemiddelde temperaturen van > 25° C, en koudste maand gemiddelde temperaturen van 0-4° C (Basinger et al., 1994; Greenwood et al., 2010). De temperatuur op aarde bereikte een lange termijn maximum tijdens de Vroege Eoceen Climatic Optimum (EECO) tussen 51 en 53 Ma. Het EECO werd gevolgd door een 17 Mjr durende trend naar koudere omstandigheden, die bekend staat als de broeikas-ijskast overgang (Zachos et al., 2001). De timing van de 'Azolla fase' (~49 Ma) valt samen met het begin van de afkoeling.

## Het kader van dit proefschrift

Dit proefschrift is een onderdeel van een multidisciplinair onderzoek in het kader van het Darwin Centre of Biogeosciences, het DARWIN *Azolla* project. Het overkoepelende doel van dit project is om informatie te verzamelen over de potentiële rol van *Azolla* als moderator van de wereldwijde nutriënten-cycli in het Eoceen, en/of die rol, in combinatie met de geologische en oceanografische evolutie van de Arctische Oceaan, instrumenteel was voor de initiële afkoeling van de aarde na het EECO temperatuuroptimum. Dit proefschrift richt zich op de palaeobotanische, palaeoecologische, en palaeoceanografische aspecten van het *Azolla* fenomeen.

In **Hoofdstuk 2** onderzoeken we de mogelijke gevolgen van de overvloedige en wijdverbreide vroeg midden Eocene Arctische *Azolla* bloei op de regionale en mondiale nutriënten cycli. Verder beoordelen we de mogelijke gevolgen van de aanhoudende *Azolla* bloei op de atmosferische  $p\text{CO}_2$ . Flux berekeningen wijzen op een opslag van koolstof van ~ 0,9 tot 3,5 gigaton koolstof 103 in het noordpoolgebied tijdens het *Azolla* interval die zouden kunnen hebben geresulteerd in een 55 tot 470 ppm opname van atmosferische  $p\text{CO}_2$  onder Eocene condities. Dit geeft aan dat de langdurige Arctische *Azolla* bloei een significant effect op de globale atmosferische  $p\text{CO}_2$  niveaus gehad kan hebben, via opslag van organische stof.

De fluctuaties in aantallen *Azolla*-resten in de Arctische midden Eoceen ACEX kernen laten een cyclische distributie zien die al eerder in verband is gebracht met mogelijk orbitaal-gemoduleerde episodische oppervlaktewater verzoeting. In **Hoofdstuk 3 en 4** passen we een geïntegreerde micropalaeontologische en cyclostratigraphische studie toe om de potentieel onderliggende mechanismen van de verzoetings-cycli, en het uiteindelijke verdwijnen van *Azolla* op ~ 48,1 Ma, te evalueren. Onze resultaten laten zien dat robuuste cyclische veranderingen in de absolute en relatieve hoeveelheden van alle belangrijke aquatische en terrestrische palynomorph groepen twee duidelijke periodiciteiten kennen: een dominante ~1,2 m cyclus, die we aan obliquiteits-veranderingen (~40 ka) koppelen, en een zwakkere ~0,7 m cyclus, die wij verwijzen naar de precessie (~21 ka) cyclus. In **Hoofdstuk 3** laten we zien dat cycli in de *Azolla* hoeveelheden schommelen met de obliquiteits frequentie. Piek hoeveelheden zijn geassocieerd met periodes van verhoogde regenval en afwatering naar zee, vermoedelijk in verband met verhoging van de plaatselijke temperaturen in de zomer tijdens obliquiteits maxima. In **Hoofdstuk 4** wordt aanvullend onderzoek gepresenteerd van de gehele palynologische associatie, inclusief organische dinoflagellatencysten, en in combinatie met studie van silicieuze microfossielen (kiezelhoudende microfossielen) van dezelfde ACEX kern. De gegevens wijzen erop dat gedurende de gehele obliquiteits cyclus de oppervlakte wateren gelaagd waren tijdens het groeiseizoen, met een zoete oppervlaktelaag. Echter, tijdens obliquiteits minima, leidde een lichte stijging in het oppervlaktewater zoutgehalte en een minder stabiele gelaagdheid van de wateren waarschijnlijk tot sterk verminderde *Azolla* hoeveelheden. Het precessie signaal op deze hoge breedtegraden wordt gerelateerd aan lange afstandstransport vanaf het omringende vasteland en aan sterke seizoensfluctuaties. De cyclisch fluctuerende afwatering van zoetwater naar zee blijkt zich na het verdwijnen van *Azolla* (~48,1 Ma) op dezelfde

wijze voort te zetten. Waarschijnlijk was slechts een kleine verandering in zoutgehalte van de oppervlaktewateren verantwoordelijk voor de beëindiging van de 'Azolla fase'.

Gecorreleerde *Azolla*-houdende lagen in het midden Eoceen van alle noordelijke zeeën werden verondersteld het resultaat te zijn van transport via periodieke uitvloeiing van de Arctische Oceaan. Met het oog op deze hypothese was het essentieel om te bepalen of het bij de voorkomens in de Noordelijke IJzee en de noordelijke randzeeën om één en dezelfde soort gaat. Daarom wordt in eerste instantie in **Hoofdstuk 5** de Noordelijke IJzee *Azolla* soort beschreven als een nieuwe soort: *Azolla arctica*. Deze soort wordt gekarakteriseerd door een volledig ontwikkeld megaspore-apparaat met aangehechte microspore massulae, alsmede door geclusterde en verspreide microsporen massulae. In **Hoofdstuk 6** bestuderen we de *Azolla* associaties met dezelfde ouderdom van een van de meest zuidelijke gebieden van *Azolla* voorkomen in de Noordzee, de Lillebælt kleiformatie, vertegenwoordigd in een Deense ontsluiting (Heilmann-Clausen et al., 1985). De Deense sedimenten kennen een uitstekende biochrono-stratigrafie, die in staat te stelt te correleren naar de internationale geologische tijdschaal. Bovendien levert het uitstekend bewaard gebleven materiaal, met megaspore-apparaten en microspore massulae, die een gedetailleerde vergelijking met alle kenmerken van *Azolla arctica* toestaan. Verrassend leiden meerdere macromorfologische en ultrastructurele eigenschappen tot het onderscheiden van een andere, nieuwe soort, hier beschreven als *Azolla jutlandica*. In tegenstelling tot de verwachtingen gebaseerd op dezelfde ouderdom van deze associaties, komen tegelijkertijd verschillende soorten *Azolla* voor, verspreid van de Noordelijke IJzee tot de zuidelijke Noordzee. Na de kenmerken en variatie van de ruimtelijk gescheiden Arctische en de Deense *Azolla* soorten te hebben vastgesteld, volgt verder onderzoek naar wat meer fragmentarisch en minder rijk materiaal uit boorkernen van tussenliggende locaties. In **Hoofdstuk 7** worden de resultaten gepresenteerd van dertien locaties langs een gradiënt van noord naar zuid tussen de Noordelijke IJzee en zuidelijke Noordzee, en vier locaties in de westelijke Noordelijke IJzee, van het vroeg midden Eocene *Azolla* interval. Onze resultaten tonen aan dat minstens vijf verschillende soorten van de snel groeiende *Azolla* voorkwamen in en rond de Noordelijke IJzee tot de Noordelijke randzeeën tijdens hetzelfde, vroeg midden Eocene tijdsinterval. Warme klimaten, hoge regenval hoeveelheden en de daarmee samenhangende afvoer van zoetwater naar de zeeën, gecombineerd met de afgesloten palaeogeografie van de Arctische en de Noorse–Groenlandse zee zijn gezamenlijk verantwoordelijk voor een ten minste episodisch extreem laag zoutgehalte van de oppervlaktewateren en gelijktijdige sterke gelaagdheid van de waterkolom. Op sommige locaties zijn er aanwijzingen voor *in situ* groei van *Azolla*, op andere plaatsen zijn de associaties waarschijnlijk het gevolg van vervoer vanaf nabijgelegen continenten. De ruimtelijke omvang (~30 miljoen km<sup>2</sup>), duur (~1,2 Mjr), ouderdom, en de bijbehorende aspecten waaronder toegenomen koolstof opslag en afkoeling van het klimaat suggereren dat de 'Azolla-fase' een belangrijke rol in de wereldwijde koolstofcyclus heeft gespeeld.





# Acknowledgements

During my Bachelor's studies I participated in a course on the *Environmental Changes in the Sub-Arctic* that took place in an incredibly beautiful and remote place, *Abisko*, in Northern Sweden. During this course Peter Rosén introduced us to the palaeo-world and we got the opportunity to take part in his research, drilling sediment cores from a lake on Mount *Njulla*. This was the spark that I got interested in palaeoecology. After returning home, I decided to enroll in more courses on palaeoecology and climate change at the University of Amsterdam in the group of Bas van Geel and Henry Hooghiemstra at the Institute of Biodiversity and Ecosystem Dynamics (IBED). What started only with a course, in the end resulted in staying for my entire Master's studies at this group. Besides all the things they taught me and the great support I received, we also spent some nice moments together. Therefore I'd like to thank all the people in this research group and especially Bas for his great supervision, enthusiasm and trust.

After I finished my studies I was very lucky to be accepted as a PhD student and to be able to continue in this field of research. For all the opportunities, support, great experience and fun moments that I had during the four years of my PhD I'd like to thank a lot of people at the university and those who are out in the real world :).

First of all I'd like to thank Henk Brinkhuis and Andy Lotter, my promotors, for giving me this great opportunity and for their support. Henk, thanks a lot for all your efforts, supervision and for giving me the opportunity to participate in many conferences and meetings, where I met many interesting people. The best memories I have from the Urbino summer school, where we had a great introduction to palaeoclimatology and besides that, we had a great time in this beautiful small Italian village, playing water polo, frisbee, enjoying the Italian kitchen and dancing. Andy, thanks a lot for your support and help, correcting my manuscripts, always taking time for my questions and for keeping me on the right track (also time management-wise). Special thanks also goes to my two co-promotors Han van Konijnenburg-van Cittert and Johan van der Burgh. You have been a great support for me during the past four years (and still are), introducing me to the world of palaeobotany, and figuring out together how we could distinguish the various species of *Azolla*. Han, thanks for always being there for me and helping me with your incredible skill to manage everything at the same time, even me :). Without you things wouldn't have gone so smoothly and efficiently. Johan, thanks for all your efforts, help, discussions and good advice! Above that, I was impressed by your techniques of hand-sectioning these tiny little pieces of *Azolla* with a scalpel. It was great to experience how the 'old-school methods' are still working so efficiently and how valuable they still are. All this work wouldn't have been possible without the hard work, great help and enthusiasm of Margaret Collinson. Together we spent many days, evenings and weekends working with the great result of three manuscripts. Thanks also for hosting us in London and the nice time Han and I were having.



## Acknowledgements

Furthermore, there are a number of other people that have greatly supported me with my research. Special thanks goes to Francesca; thanks for all your support, help, discussions and time you spent on correcting my manuscripts and for the great time in Norway! Timme, thanks a lot for all your help at the microscope, with the interpretation of the results, and for correcting the various versions of the manuscript. Thank you, Gert-Jan, for taking the time to sit down with me to restructure my manuscript, to critically but constructively think over the results, and for helping me writing the rebuttal-letters. Frits, Luc and especially Hemmo, thanks a lot for taking the time to help me with the cyclostratigraphy and for the fruitful discussion we had. I'd like to thank the whole *Azolla* research team (or A-Team how Frits called us on the first IODP-meeting) for the great collaboration, especially the other two PhD students involved in this multidisciplinary research, Eveline and Monique.

In the past four years I had great help, interest and fun moments from many people at the LPP. First of all I'd like to thank you Leonard for saving my life uncountable times, helping me wherever you could (and even more) but most of all for your great friendship. Being part of the AIO-gang together with Emi, Peter S., Maarten, Micha, Nina, Freddy, Emmy, Sander, Peter B, Cornelia, Gianluca, Adriana and the adopted ones especially Bas and Adam, we kept up the good spirits with table tennis, frisbee, squash, the famous AIO-dinners, dancing, drinking and eating, a great weekend on Schier and so on. Thank you guys; you were all there for me, supporting me and cheering me up whenever I got the blues. I had an incredible time with you!!!!!!

Furthermore, I'd like to thank Natasja and Jan for their great support in the lab and at the SEM, Marjolein for the many uncountable things you did for me and Zwier for helping me find the right literature. I would also like to thank all the other people from our department for their support, help and interest: Oliver, Appy, Walter, Wim S., Wolfram, Rike, Henk V., Boris, Hans and Roel, and all students, especially Maud who was also involved in the *Azolla* project.

Thanks also to the people at the Geochemistry department and from Strat-Pal for their help and for an enjoyable time.

During my PhD I had the opportunity to spend some weeks in Canada, working together with David and Catherine Greenwood, who warmly welcomed me in their home and besides giving me great support with my work, making my stay very enjoyable. Callum, their son, was even taking care of my daily workout on the trampoline. Thanks Callum for having lots of fun! During the second part of my stay I visited the Geological Survey in Canada and was warmly welcomed to stay with Art and Alberta Sweet, where I had a wonderful time. Art, thanks a lot for our very fascinating and inspiring talks and for the many moments of laughing.

There are also lots of people not related to my work that have supported me the past years. First of all I'd like to thank my parents and my dear brother. Danke, dass ihr mich immer unterstützt habt bei all meinen Entscheidungen und dass ihr mich immer ermutigt habt um meine Ziele zu verwirklichen. Mein Bruderherz, mein grosses Vorbild...Du bist der beste! ... ook jij Marielle, dankje voor je steun, interesse en vele leuke momenten. And Jamie... my little nephew... looking forward to spending more time with you.

The ones that committed themselves to take over my defense in case I'll decide to faint are Mascha and Peter, my paranymphs. Mascha, dankje dat je er altijd voor mij bent geweest (zelfs toen ik in Australië zat), voor talloze gezellige avonden en voor al je hulp bij het zoeken naar een baan. Dankje voor je lieve vriendschap! Peter, ook aan jou heb ik altijd heel veel steun gehad. Dankje dat je altijd een luisterend oor voor mij had, maar vooral voor alle leuke momenten buiten de uni (vooral op de dansvloer ;) ).

I'd like to thank my friends Anna, Elsemiek, Boogy, Luz, Maite, Luisa, Claudia, Steffen, Merel, Carla, Injoo and my housemates, especially Igor and Maarten for always being there for me, supporting me with food donations (thanks Igor!!) and for lots of nice moments.

I wouldn't have survived the last and most difficult period without you liefje. You are the master queen of support, feeding me delicious greek cuisine, giving me raki to prevent me from getting a cold or just to calm me down when exceptionally I was stressed and distracting me with practicing silly dancing. Thank you Eleni for always being there for me. Από 'δὼ και πέρα θα `ναι μόνο σεξ, ναρκωτικά και rock n `roll!



## Curriculum Vitae

Judith Barke was born in Mayen, Germany, on April 28, 1979. She completed her secondary school at the *Freie Waldorfschule Aachen* in Germany. In 2000, she started her Bachelor's degree in Biology at the University of Groningen in the Netherlands. As an undergraduate, she specialized in ecology, marine biology and oceanography and graduated *with honors* in 2004. As part of her undergraduate studies she spent one semester at the University of Umeå in Sweden, where she participated in courses on the environmental changes in the sub-Arctic and applied population ecology. During her Master's degree at the University of Amsterdam she specialized in the field of palaeoecology and climate change. She conducted one literature essay on the effect of UV-radiation on photosynthetic organisms and two internships within the field of palaeoecology. In her first internship she reconstructed the impact of humans on the landscape in northern Sweden during the last Millennium, applying pollen assemblage analysis. For her second internship she went to the University of Queensland in Australia. There she applied benthic foraminiferal assemblage analyses and stable isotope analyses to reconstruct the environmental changes in the Torres Strait, Gulf of Papua region, during the past ~6000 years. This resulted in a *cum laude* Master's graduation in August 2006. In September 2006 she started her PhD at the University of Utrecht in the groups of *Palaeoecology* and *Biomarine Sciences* within a multi-disciplinary project, partially funded by the Darwin Center for Biogeosciences. Under supervision of Prof. Dr. André Lotter, Prof. Dr. Henk Brinkhuis, Prof. Dr. Han van Konijnenburg-van Cittert, and Dr. Johan van der Burgh she studied the palaeobotany and palaeoecology of the freshwater fern *Azolla*. The results of this research are presented in this thesis.